**UNIVERSIDAD DE SALAMANCA**

CENTRO DE INVESTIGACIÓN DEL CÁNCER

INSTITUTO DE BIOLOGÍA MOLECULAR Y CELULAR DEL CÁNCER (IBMCC, USAL-CSIC)

# Role of platelet C3G in vesicle trafficking and spreading. Involvement in hemostasis and platelet-mediated inflammation

MEMORIA PARA OPTAR AL GRADO DE DOCTOR PRESENTADA POR

**Cristina Fernández Infante**

Bajo la dirección de la Doctora

**Carmen Guerrero Arroyo**

Salamanca, 2023

Dra. **CARMEN GUERRERO ARROYO**, Catedrática del Departamento de Medicina, Instituto de Biología Molecular y Celular del Cáncer (IBMCC, Universidad de Salamanca).

**CERTIFICA:**

Que Dña. **Cristina Fernández Infante**, graduada en Farmacia por la Universidad de Salamanca, ha realizado bajo su dirección el trabajo de Tesis Doctoral que lleva por título "**Role of platelet C3G in vesicle trafficking and spreading. Involvement in hemostasis and platelet-mediated inflammation**", y considera que éste reúne originalidad y contenidos suficientes para que sea presentado ante el Tribunal correspondiente y optar al Grado de Doctor por la Universidad de Salamanca.

Y para que conste, y a los efectos oportunos, expide el presente certificado en Salamanca a 24 de abril de 2023.

Fdo. Dra. Carmen Guerrero Arroyo

Directora de la Tesis

Dña Cristina Fernández Infante ha realizado esta tesis doctoral siendo beneficiaria de un contrato predoctoral de la Junta de Castilla y León (*ayudas destinadas a financiar la contratación predoctoral de personal investigador cofinanciadas por el Fondo Social Europeo*) durante el periodo de julio de 2018 a junio de 2022.

Este trabajo se ha enmarcado dentro de los proyectos del Plan nacional I+D+I: "*Función de C3G en el desarrollo tumoral y en la patofisiología del hígado. Implicación de C3G plaquetario en la angiogénesis y en enfermedades hepáticas y cardiovasculares*" (SAF2016-76588-C2-2-R) y "*New functions for C3G in tumor progression, liver physiology and megakaryocyte and platelet biology. Contribution of platelet C3G to pathological neoangiogenesis and liver damage*" (PID2019-104143RB-C21), financiados por los Ministerios de Economía y Competitividad y de Ciencia en Innovación, respectivamente, y por el Fondo Europeo de Desarrollo Regional (FEDER), y de los proyectos "*Papel de C3G en la regulación de la función plaquetaria: Implicaciones en angiogénesis y aplicación al diagnóstico y tratamiento de la enfermedad trombótica*" (SA017U16) y "*Papel de C3G en tumores hematopoyéticos y en angiogénesis mediada por plaquetas. Evaluación de su uso como diana terapéutica*" (SA078P20), financiados por el Programa de apoyo a proyectos de investigación de la Consejería de Educación de la Junta de Castilla y León y por el Fondo Europeo de Desarrollo Regional (FEDER), *"a way of making Europe"*.

*A mis padres,*

*por su valentía, coraje y resiliencia*

*‘‘Un viaje de mil millas comienza con el primer paso’’*

*Lao-Tse*

# THESIS SUMMARY

C3G is a guanine nucleotide exchange factor (GEF) for several members of the Ras family of GTPases, such as Rap1, R-Ras, or TC21, and of the Rho family, such as TC10. GTPases are proteins that act as molecular switches, cycling between a GTP-bound state (active conformation) and a GDP-bound state (inactive conformation), resulting in rapid switching of signaling pathways. This cycle is regulated by GEF proteins, which promote the exchange of GDP for GTP, triggering the activation of the GTPase, and by GAP proteins, which catalyze the hydrolysis of GTP into GDP. C3G participates in most cellular processes, such as proliferation, adhesion and migration, apoptosis or cell-cell interaction, among others. Previous results from the group have revealed a role for C3G in platelet function, through its GEF activity. Thus, C3G regulates Rap1b activation, induced by most platelet agonists, through the PKC-Src, ERK-Shp2, P2Y12-PI3K, and $TXA_2$ pathways. C3G also modulates pathologic megakaryopoiesis in response to thrombopoietin (TPO) or 5-fluorouracil treatment, by regulating the TPO-Mpl pathway in megakaryocytes. Finally, a series of evidences indicated that C3G could control the release of platelet α-granule content, since C3G regulates the secretion of angiogenic factors. C3G overexpression in platelets causes retention of VEGF, SDF-1, and TSP-1 within them, leading to a proangiogenic secretome that promotes tumor growth and metastasis. Likewise, the absence of C3G triggers the release of VEGF-1 and SDF-1 and the retention of TSP-1, which also results in a secretome that promotes angiogenesis.

In this Thesis work, we have studied the role of C3G in (i) hemostasis, (ii) platelet spreading on substrate, (iii) secretion of platelet granules and (iv) platelet-mediated inflammation. For this, we have used two transgenic mouse models that overexpress C3G (tgC3G) or a mutant form in which C3G lacks the catalytic domain (tgC3GΔCat), specifically in megakaryocytes (MKs) and platelets, and a C3G knockout mouse model (C3G-KO), in which C3G is specifically deleted in these cell types. In the first place, we have corroborated in C3G-KO platelets, the participation of C3G in the PKC-Rap1 pathway, which regulates the second wave of thrombin-induced Rap1 activation. In addition, we have determined that PKCδ would be the PKC isoform that controls C3G in this system. Thus, C3G-KO platelets showed defective inside-out signaling, presenting alterations in the activation of the integrin αIIbβ3, responsible for platelet aggregation, and in the exposure of P-selectin on the surface. C3G would also modulate secondary hemostasis, regulating phosphatidylserine (PS) translocation. Indeed, C3G-KO platelets displayed defective PS translocation, resulting in decreased thrombin generation upon tissue factor (TF) stimulation. However, the absence of C3G promoted a procoagulant secretome that compensated for the faulty translocation of PS, generating normal thrombin levels. In contrast, C3G overexpression induced an anticoagulant secretome and did not affect PS translocation, suggesting that low levels of C3G are necessary but sufficient to induce PS translocation.

In the second part of this work, we have examined the role of C3G in outside-in signaling, specifically, in platelet spreading and clot retraction. Previous results of the group have described that C3G positively modulates platelet spreading on poly-L-lysine, independently of its GEF function. In this work we describe that the role of C3G in spreading is controlled by PKC and Src and is substrate dependent. Specifically, C3G would modulate platelet spread on poly-L-lysine, collagen/CRP, fibronectin, and vitronectin, but not on fibrinogen, laminin, or osteopontin,

independently of its GEF domain. These differences can be partially explained by the defects in the expression of αV and β1 integrins observed in C3G-KO platelets.

C3G regulates platelet spreading by modulating remodelling of the actin cytoskeleton, but not of microtubules. In addition, we have shown that C3G is associated with the formation of lamellipodia, but not filopodia, through the activation of Rac1 GTPases. In addition, C3G interacted with proteins related to actin cytoskeleton dynamics, such as β-actin, the Arp2/3 complex, VASP, and Abi-1. The C3GΔCat mutant also interacted with Arp2 and β-actin and induced Rac1 activation, which is consistent with the spreading results and suggests that the role of C3G in actin cytoskeleton remodeling is independent of Rap1. Thus, C3G would modulate the formation of lamellipodia through the control of the Rac1/WAVE/Arp2/3 pathway.

C3G is also involved in the formation of focal adhesion complexes (FA) on platelets, through its interaction with talin, p130Cas, c-Cbl, vinculin, and FAK, in response to thrombin. C3G regulated the number of FA during platelet spreading on CRP and fibronectin; however, both overexpression and deletion of C3G induced increased FA formation, indicating that C3G would up- and down-regulate different components during FA formation. In fact, C3G differentially modulated the phosphorylation of paxillin, c-Cbl and p130Cas on fibronectin and CRP. In addition, C3G-KO platelets exhibited a significant delay in clot retraction, further supporting a role for C3G in outside-in signaling.

In the third part of the Thesis, we have explored the role of C3G in the secretion of platelet granules. Previous results from the group demonstrated that C3G controls the release of angiogenic factors, such as VEGF, SDF-1 and TSP-1, which are contained in α-granules. Indeed, deletion of C3G in platelets resulted in increased cargo release. The role of C3G in granule secretion appears to be specific to α-granules, not affecting δ-granules or lysosomes. This increased secretion of α-granules observed in C3G-KO platelets was not caused by alterations in the number of granules, indicating that C3G would act as a secretion brake.

In platelets, granule secretion is controlled by SNARE proteins. Under resting conditions, C3G-KO platelets showed lower levels of P-selectin, as well as v-SNAREs (vesicle SNAREs) VAMP-7 and VAMP-8, all of them located in α-granules. However, after thrombin stimulation the levels (measured as fluorescence signal) increased, suggesting that the absence of C3G could promote granule fusion, prior to exocytosis (compound exocytosis). In fact, a high percentage of VAMP-7 α-granules from C3G-KO platelets showed a peripheral distribution pattern, that is, granules close to the plasma membrane (PM), which was not observed in C3G-wt platelets, where the granules preferentially concentrated in the center of the platelet. This abnormal α-granule distribution observed in C3G-KO platelets is possibly due to the actin cytoskeleton defects detected in these platelets.

C3G regulates α-granule secretion through RalA activation, which is dependent on C3G GEF activity. However, we did not observe any effect of C3G on Rab27b activation, consistent with its lack of involvement in the regulation of δ-granules. Additionally, C3G interacted with VAMP-8, Syntaxin 11, SNAP23 and Munc18-b, all of which involved in the association between v-SNAREs and t-SNAREs to form the trans-SNARE complex, but not with components of the exocystic complex. These interactions were not detected in tgC3GΔCat platelets, suggesting that they

would be mediated by the C3G catalytic domain (GEF). C3G overexpression caused deficient formation of the trans-SNARE complex, while the opposite phenotype was observed in C3G-KO platelets. C3G would modulate the formation of the trans-SNARE complex through its positive role in the formation of the VARP/VAMP-7/Arp2/3 complex, which prevents the uncontrolled secretion of α-granules and the remodeling of the actin cytoskeleton. All of this explains why the absence of C3G in platelets promoted a kiss-and-run phenotype, in which platelets show a decrease in the exposure of P-selectin on the surface, due to a lack of incorporation of the α-granule membrane into the PM, accompanied by a marked increase in secretion, after platelet stimulation.

Finally, we have shown that the role of C3G in granule secretion is not platelet-specific, but that C3G also modulated granule secretion in the PC12 cell line. Overexpression of an active C3G mutant induced slower NPY secretion, whereas absence of C3G triggered the opposite phenotype. However, C3G positively regulated the number of vesicles docked to the PM, as well as the number of exocytic events. Thus, C3G mutants showed the opposite phenotype in PC12 cells to that of platelets; ie, overexpression of the active C3G mutant caused increased secretion, whereas C3G silencing promoted decreased secretion. This contradictory phenotype could be explained by the different functionality of the VARP-VAMP-7 interaction in platelets and in neurons. In neurons, VARP positively regulates VAMP-7, inducing the trans-SNARE complex, while, in platelets, the VAMP-7-VARP interaction promotes the opposite effect.

All these results support the notion that C3G regulates granule secretion through the modulation of the trans-SNARE complex formation and Ral activation, both processes dependent on its GEF activity.

In the last part of the Thesis, we have examined the role of C3G in platelet-mediated inflammation. Platelets are important regulators of the immune response through their role in leukocyte activation, mediated by the formation of platelet-leukocyte aggregates (PLA) and the secretion of inflammatory factors contained in their α-granules. C3G modulated PLA formation, following thrombin stimulation, through regulation of P-selectin and CD40L exposure on the platelet surface. Specifically, C3G promoted the interaction between platelets and neutrophils (NE) and B lymphocytes, but not with T lymphocytes or monocytes. In addition to favoring platelet-NE interaction, C3G also modulated NE activation, finding a higher NETosis in tgC3G platelets, after thrombin stimulation, and a lower NETosis in C3G-KO platelets. In addition, the absence of C3G resulted in increased secretion of PF4, IL-1α, CX3CL1, among others, while C3G overexpression showed the opposite phenotype, that is, retention of inflammatory factors, consistent with what was observed in the secretion of angiogenic and coagulation factors. However, it seems that the platelet secretome did not influence the formation of NETosis, with P-selectin exposure being the most important factor.

C3G also modulated *in vivo* the progression of colitis induced by DSS (Dextran Sodium Sulfate) treatment. Indeed, the absence of C3G significantly accelerated DSS-induced colitis symptoms, in contrast to *in vitro* experiments. C3G-KO mice suffered significant weight loss accompanied by diarrhea and bloody stools and increased bacterial dissemination.

Consistently, the absence of C3G also induced increased PLA formation, specifically with NE, but not with monocytes or lymphocytes, accompanied by increased NE counts in peripheral blood. These results suggest that platelet C3G could act as a protector against ulcerative colitis.

In conclusion, in this work we present evidence of a role for C3G in the modulation of platelet spreading through the regulation of lamellipodia formation via its participation in the Rac1/WAVE2/Arp2/3 pathway, which is independent of its GEF function. In addition, C3G would regulate the secretion of α-granules by modulating the formation of the trans-SNARE and the VARP/VAMP-7/Arp2/3 complexes, as well as the activation of Ral, in a Rap1-dependent manner. Finally, we present preliminary results, both in vitro and in vivo, on a novel role of the C3G protein in the platelet-mediated inflammatory response, through the regulation of PLA formation, with NE and B lymphocytes, and the release of inflammatory factor

# RESUMEN

C3G es un factor de intercambio de nucleótidos de guanina (GEF) para varios miembros de la familia Ras de GTPasas, como Rap1, R-Ras o TC21, y de la familia Rho, como TC10. Las GTPasas son proteínas que actúan como interruptores moleculares, alternando entre un estado unido a GTP (conformación activa) y un estado unido a GDP (conformación inactiva), lo que da lugar a una rápida conmutación de las vías de señalización. Este ciclo está regulado por las proteínas GEF, que promueven el intercambio de GDP por GTP, desencadenando la activación de la GTPasa, y por proteínas GAP, que catalizan la hidrólisis del GTP a GDP. C3G participa en la mayoría de los procesos celulares, como proliferación, adhesión y migración, apoptosis o interacción célula-célula, entre otros. Resultados previos del grupo han revelado un papel de C3G en la función plaquetaria, a través de su actividad GEF. Así, C3G regula la activación de Rap1b, inducida por la mayoría de agonistas plaquetarios, a través de las vías PKC-Src, ERK-Shp2, P2Y12-PI3K y $TXA_2$. C3G también modula la megacariopoyesis patológica en respuesta al tratamiento con trombopoyetina (TPO) o 5-fluorouracilo, mediante la regulación de la vía TPO-Mpl en los megacariocitos. Por último, una serie de evidencias indicaban que C3G podría controlar la liberación del contenido de gránulos $\alpha$ plaquetarios, ya que C3G regula la secreción de factores angiogénicos. La sobreexpresión de C3G en las plaquetas provoca la retención de VEGF, SDF-1 y TSP-1 en su interior, lo que da lugar a un secretoma proangiogénico que promueve el crecimiento tumoral y la metástasis. Asímismo, la ausencia de C3G desencadena la liberación de VEGF-1 y SDF-1 y la retención de TSP-1, lo que resulta también en un secretoma que promueve la angiogénesis.

En este trabajo de Tesis, hemos estudiado el papel de C3G en (i) la hemostasia, (ii) la extension plaquetaria sobre sustrato o *spreading*, (iii) la secreción de gránulos plaquetarios y (iv) la inflamación mediada por plaquetas. Para ello, hemos utilizado dos modelos de ratón transgénicos que sobreexpresan C3G (tgC3G) o una forma mutante en la que C3G carece del dominio catalítico (tgC3GΔCat) específicamente en megacariocitos (MK) y plaquetas, y un modelo de ratón *knockout* para C3G (C3G-KO), con deleción específica en estos mismos tipos celulares. En primer lugar, hemos corroborado en plaquetas C3G-KO, la participación de C3G en la vía PKC-Rap1, ruta que regula la segunda oleada de activación de Rap1 inducida por trombina. Además, hemos determinado que PKCδ sería la isoforma de PKC que controla a C3G. Así, las plaquetas C3G-KO muestran una señalización *inside-out* defectuosa, presentando alteraciones en la activación de la integrina αIIbβ3, responsable de la agregación plaquetaria, y en la exposición de la P-selectina en superficie. C3G también modularía la hemostasia secundaria, regulando la translocación de fosfatidilserina (PS). De hecho, las plaquetas C3G-KO mostraron una translocación defectuosa de PS que resultó en una menor generación de trombina tras la estimulación con factor tisular (TF). Sin embargo, la ausencia de C3G resultó en un secretoma procoagulante que compensó la translocación defectuosa de PS, generando niveles normales de trombina. Por el contrario, la sobreexpresión de C3G indujo un secretoma anticoagulante y no afectó a la translocación de PS, lo que sugiere que niveles bajos de C3G son necesarios pero suficientes para inducir la translocación de PS.

En la segunda parte de este trabajo, hemos examinado la función de C3G en la señalización *outside-in*, concretamente en la extensión (*spreading*) plaquetaria y la retracción del coágulo.

Resultados anteriores del grupo han descrito que C3G modula positivamente el *spreading* plaquetario sobre poli-L-lisina de forma independiente de su función GEF. En este trabajo describimos que la función de C3G en el *spreading* está controlada por PKC y Src y es dependiente de sustrato. Específicamente, C3G modularía la extension plaquetaria sobre poli-L-lisina, colágeno/CRP, fibronectina y vitronectina, pero no sobre fibrinógeno, laminina u osteopontina, de forma independiente de su dominio GEF. Estas diferencias se pueden explican parcialmente por los defectos en la expresión de las integrinas αV y β1 observados en las plaquetas C3G-KO.

C3G regula el *spreading* plaquetario modulando la remodelación del citoesqueleto de actina, pero no de los microtúbulos. Además, hemos demostrado que C3G está asociado a la formación de lamellipodios, pero no de filopodios, a través de la activación de la GTPasa Rac1. C3G interaccionó con proteínas relacionadas con la dinámica del citoesqueleto de actina como β-actina, el complejo Arp2/3, VASP y Abi-1. Además, el mutante C3GΔCat también interaccionó con Arp2 y β-actina e indujo la activación de Rac1, lo que concuerda con los resultados de *spreading* y sugiere que el papel de C3G en la remodelación del citoesqueleto de actina es independiente de Rap1. Así pues, C3G modularía la formación de lamelipodios a través del control de la vía Rac1/WAVE/Arp2/3.

C3G también participa en la formación de los complejos de adhesión focal (FA) en las plaquetas, a través de su interacción con talina, p130Cas, c-Cbl, vinculina y FAK, en respuesta a trombina. C3G reguló el número de FA durante la extensión plaquetaria sobre CRP y fibronectina; sin embargo, tanto la sobreexpresión como la deleción de C3G indujeron un aumento de la formación de FA, indicando que C3G regularía positiva y negativamente distintos componentes durante la formación de las FA. De hecho, C3G moduló diferencialmente la fosforilación de paxilina, c-Cbl y p130Cas sobre fibronectina y CRP. Además, las plaquetas C3G-KO presentaron un retraso significativo en la retracción del coágulo, lo que apoya aún más el papel de C3G en la señalización *outside-in*.

En la tercera parte de la Tesis, hemos explorado el papel de C3G en la secreción de gránulos plaquetarios. Resultados previos del grupo demostraron que C3G controla la liberación de factores angiogénicos, como VEGF, SDF-1 y TSP-1, los cuales están contenidos en gránulos $\alpha$. De hecho, la deleción de C3G en las plaquetas dio lugar a una mayor liberación de carga. El papel de C3G en la secreción de gránulos parece ser específico de los granulos $\alpha$, no afectando a granulos $\delta$ o lisosomas. Esta mayor secreción de gránulos $\alpha$ observada en las plaquetas C3G-KO no está causada por alteraciones en el número de granulos, lo que indica que C3G actuaría como un freno de la secreción.

En plaquetas, la secreción de gránulos está controlada por las proteínas SNARE. En condiciones de reposos, las plaquetas C3G-KO mostraron niveles más bajos de P-selectina, así como de las v-SNARE (SNARE de vesícula) VAMP-7 y VAMP-8, todas ellas contenidas en gránulos $\alpha$. Sin embargo, tras estimulación con trombina los niveles (medidos como señal de fluorescencia) aumentaron, lo que sugiere que la ausencia de C3G podría promover la fusión de gránulos, previo a la exocitosis (exocitosis compuesta). De hecho, un alto porcentaje de granulos $\alpha$ VAMP-7 de las plaquetas C3G-KO mostraron una distribución periférica, es decir, gránulos próximos a la membrana plasmática (PM), que no se observó en las plaquetas C3G-wt, donde

los gránulos se concentran preferentemente en el centro de la plaqueta. Esta distribución anómala de los gránulos $\alpha$ observada en las plaquetas C3G-KO se debe posiblemente a los defectos en el citoesqueleto de actina detectados en estas plaquetas.

El papel de C3G en la regulación de la secreción de gránulos $\alpha$ está mediado por la activación de RalA, que depende de su actividad GEF. Sin embargo, no observamos ningún efecto de C3G en la activación de Rab27b, de acuerdo con su falta de implicación en la regulación de los gránulos $\delta$. Adicionalmente, C3G interaccionó con VAMP-8, Sintaxina 11, SNAP23 y Munc18-b, todas ellas implicadas en la asociación entre v-SNARE y t-SNARE para formar el complejo trans-SNARE, pero no con componentes del complejo exocístico. Estas interacciones no se detectaron en las plaquetas tgC3GΔCat, lo que sugiere que estarían mediadas por el dominio catalítico (GEF) de C3G. La sobreexpresión de C3G provocó una formación deficiente del complejo trans-SNARE, mientras que en las plaquetas C3G-KO se observó el fenotipo opuesto. C3G modularía la formación del complejo trans-SNARE a través de su papel positivo en la formación del complejo VARP/VAMP-7/Arp2/3, el cual previene la secreción descontrolada de gránulos $\alpha$ y la remodelación del citoesqueleto de actina. Todo ello explica que la ausencia de C3G en plaquetas promueva un fenotipo *kiss-and-run,* donde las plaquetas muestran una disminución de la exposición de P-selectina en superficie, debido a una falta de incorporación de la membrana de los gránulos $\alpha$ a la PM, acompañado con un marcado aumento de la secreción tras la estimulación plaquetaria.

Finalmente, hemos demostrado que el papel de C3G en la secreción de gránulos no es específico de las plaquetas, sino que C3G también moduló la secreción en la línea celular PC12. La sobreexpresión de un mutante activo de C3G indujo una secreción más lenta de NPY, mientras que la ausencia de C3G desencadenó el fenotipo opuesto. Sin embargo, C3G reguló positivamente el número de vesículas acopladas a la PM, así como el número de eventos exocíticos. Por tanto, los mutantes de C3G mostraron en las células PC12 el fenotipo opuesto al de las plaquetas; es decir, la sobreexpresión del mutante activo de C3G provocó una mayor secreción, mientras que el silenciamiento de C3G promovió una menor secreción. Este fenotipo contradictorio podría explicarse por la diferente funcionalidad de la interacción VARP-VAMP-7 en plaquetas y en neuronas. En las neuronas VARP regula positivamente a VAMP-7 induciendo el complejo trans-SNARE, mientras que en las plaquetas la interacción VAMP-7-VARP promueve el efecto contrario.

Todos estos resultados apoyan la noción de que C3G regula la secreción de gránulos a través de la modulación de la formación del complejo trans-SNARE y la activación de Ral, procesos ambos dependientes de su actividad GEF.

En la última parte de la Tesis, hemos examinado el papel de C3G en la inflamación mediada por plaquetas. Las plaquetas son importantes reguladores de la respuesta inmunitaria a través de su papel en la activación de los leucocitos, mediado por la formación de agregados plaqueta-leucocito (PLA) y la secreción de factores inflamatorios contenidos en sus gránulos $\alpha$. C3G moduló la formación de PLA, tras la estimulación con trombina, a través de la regulación de la exposición de P-selectina y CD40L en la superficie plaquetaria. En concreto, C3G promovió la interacción entre plaquetas y neutrófilos (NE) y linfocitos B, pero no con linfocitos T o monocitos. Además de favorecer la interacción plaqueta-NE, C3G también moduló la activación de los NE,

encontrándose una mayor NETosis en plaquetas tgC3G, tras estimulación con trombina, y una menor NETosis en plaquetas C3G-KO. Además, la ausencia de C3G resultó en una mayor secreción de PF4, IL-1α, CX3CL1, entre otros, mientras que la sobreexpresión de C3G mostró el fenotipo opuesto, es decir, la retención de factores inflamatorios, en consonancia con lo observado en la secreción de factores angiogénicos y de coagulación. Sin embargo parece ser que el secretoma de las plaquetas no influyó en la formación de NETosis, siendo la exposición de P-selectina el factor más importante.

C3G también moduló *in vivo* la progresión de colitis inducida por tratamiento con DSS (Dextrán Sulfato Sódico). De hecho, la ausencia de C3G aceleró significativamente los síntomas de la colitis inducida por DSS, en contraste con los experimentos *in vitro*. Los ratones C3G-KO sufrieron una pérdida de peso significativa acompañada de diarrea y sangre en las heces y una mayor diseminación bacteriana. En concordancia, la ausencia de C3G también indujo una mayor formación de PLA, específicamente con NE, pero no con monocitos o linfocitos, acompañado de un incremento de NE en sangre periférica. Estos resultados sugieren que C3G plaquetario podría actuar como un protector de la colitis ulcerosa.

En conclusión, en este trabajo presentamos evidencias de un papel de C3G en la modulación de la extensión plaquetaria a través de la regulación de la formación de lamellipodia por su participación en la vía Rac1/WAVE2/Arp2/3 de forma independiente de su función GEF. Además, C3G regularía la secreción de gránulos $\alpha$ modulando la formación de los complejos trans-SNARE y VARP/VAMP-7/Arp2/3, así como la activación de Ral, de forma dependiente de Rap1. Por último, presentamos resultados preliminares, tanto *in vitro* como *in vivo* sobre una nueva función de la proteína C3G en la respuesta inflamatoria mediada por plaquetas, a través de la regulación de la formación de PLA, con NE y linfocitos B, y la liberación de factores inflamatorios.

# LIST OF ABBREVIATIONS

| | |
|---|---|
| **5-FU** | 5-Fluorouracilo |
| **aa** | Amino Acids |
| **AC** | Adenylate Cyclase |
| **ADP** | Adenosine Diphosphate |
| **AF** | Alexa Fluor |
| **AIR** | Autoinhibitory region |
| **ATP** | Adenosine Triphosphate |
| **APC** | Allophycocyanin |
| **a.u.** | Arbitrary Units |
| **AUC** | Area Under the Curve |
| **BB** | Binding Buffer |
| **BIS** | Bisindolylmaleimide |
| **BM** | Bone Marrow |
| **BSA** | Bovine Serum Albumin |
| **C3G** | Crk SH3-domain-binding guanine-nucleotide-releasing factor |
| **$Ca^{2+}$** | Calcium |
| **CAT** | Catalytic |
| **CAT** | Calibrated Automated Thrombography |
| **cDNA** | Complementary DNA |
| **cPKC** | Conventional PKC |
| **CRP** | Collagen Related Peptide |
| **CT** | Control |
| **$C_T$** | Threshold Cycle |
| **Da** | Dalton |
| **DAG** | Diacylglycerol |
| **DIC** | Differential Interference Contrast Microscopy |
| **DMEM** | Dulbeco's Modified Eagle's Medium |
| **DMSO** | Dimethyl Sulfoxide |
| **dNTP** | Deoxyribonucleotide triphosphate |
| **DSS** | Dextran Sulfate Sodium |
| **DTS** | Dense Tubular System |
| ***E. coli*** | *Escherichia coli* |
| **ECL** | Enhanced Chemiluminescence |
| **ECM** | Extracellular Matrix |
| **ETP** | Endogenous Thrombin Potential |
| **F-actin** | Filamentous actin |
| **FACS** | Fluorescence-Activated Cell Sorting |
| **FA** | Focal Adhesions |
| **FBS** | Fetal Bovine Serum |
| **FcR** | Fc receptor |
| **FHL** | Familial Hemophagocytic Lymphohistiocytosis |
| **FITC** | Fluorescein |
| **FSC** | Forward scatter |
| **G-actin** | Globular actin |
| **GAP** | GTPase Activating Proteins |
| **GDP** | Guanosine Diphosphate |
| **GEF** | Guanine nucleotide Exchange Factor |
| **GFP** | Green Fluorescence Protein |

| | |
|---|---|
| **GP** | Glycoprotein |
| **GPCR** | G-protein-coupled receptors |
| **GST** | Glutathione S-Transferase |
| **GTP** | Guanosine Triphosphate |
| **HRP** | Horseradish Peroxidase |
| **IBD** | Inflammatory bowel disease |
| **IgG** | Immunoglobulin G |
| **IL-** | Interleukin- |
| **$IP_3$** | Inositol triphosphate |
| **IPTG** | 0.2 mM isopropyl-β-D-1-thiogalactopyranoside |
| **KO** | Knockout |
| **LV** | Large dense core Vesicles |
| **Mϕ** | Macrophages |
| **MAPK** | Mitogen-Activated Protein Kinase |
| **MFI** | Mean Fluorescence Intensity |
| **MK** | Megakaryocyte |
| **MLB** | Modified Lysis Buffer |
| **mRNA** | Messenger RNA |
| **MRB** | Modified Ringer Buffer |
| **MW** | Molecular Weight |
| **nPKC** | Novel PKC |
| **NE** | Neutrophil |
| **NET** | NE Extracellular Trap |
| **NFDM** | Non-Fat Dried Milk |
| **NO** | Nitric Oxide |
| **NPF** | Nucleation-Promoting Factor |
| **NTD** | N-Terminal Domain |
| **NSF2** | N-ethylmaleimide-sensitive factor 2 |
| **NPY** | Neuropeptide Y |
| **Oligo(dT)** | Oligo (deoxythymine) |
| **o/n** | Overnight |
| **OCS** | Open Canalicular System |
| **P** | Proline |
| **PBS** | Phosphate Saline Buffer |
| **PCR** | Polymerase Chain Receptor |
| **PE** | Phycoerythrin |
| **PEI** | Polyethylenimine |
| **PF4** | Platelet Factor 4 |
| **PFA** | Paraformaldehyde |
| **$PGI_2$** | Prostaglandin $I_2$ |
| **Pi** | Inorganic Phosphate |
| **PI3k** | Phosphoinositide 3-Kinase |
| **$PIP_2$** | Phosphatidylinositol-(4,5)-bisphosphate ( |
| **PKA** | Protein kinase A |
| **PKC** | Protein kinase C |
| **PKG** | Protein kinase G |
| **PLA** | Platelet leukocyte aggregate |
| **PLA** | Phospholipase A |
| **PLC** | Phospholipase C |
| **PM** | Plasma Membrane |
| **PMA** | 4 beta-Phorbol-12-myristate-13-acetate |
| **PRP** | Platelet Rich Plasma |

| | |
|---|---|
| **PS** | Phosphatidylserine |
| **PVDF** | Polyvinylidene Fluoride |
| **qPCR** | Quantitative PCR |
| **RB** | Rinfer Buffer |
| **RBC** | Red Blood Cell |
| **RBD** | Rap-Binding Domain |
| **REM** | Ras Exchange Motif |
| **RFP** | Red Fluorescence Protein |
| **rpm** | Revolutions per minute |
| **RPMI** | Roswell Park Memorial Institute |
| **RT** | Room Temperature |
| **RT-PCR** | Reverse Transcription-PCR |
| **SC** | Subcomplex |
| **SD** | Standard Deviation |
| **SDS** | Sodium Dodecyl Sulfate |
| **SDS-PAGE** | Sodium Dodecyl Sulfate-Polyacrylamide Gel Electrophoresis |
| **SEM** | Standard Error of the Mean |
| **SH3-b** | Sh3-binding |
| **SNAP** | Synaptosome Associated Protein |
| **SNARE** | Soluble N-ethylmaleimide-sensitive factor Attachment Protein Receptor |
| **SSC** | Side Scatter |
| **Stx** | Syntaxin |
| **SV** | Small Vesicles |
| **t-** | Target |
| **$T_C$** | Cytotoxic T lymphocyte |
| **TF** | Tissue factor |
| **Tg** | Transgenic |
| **$T_H$** | Helper T lymphocyte |
| **TH** | Thrombin |
| **TIRFM** | Total internal reflection fluorescence microscopy |
| **TLR** | Toll-like receptors |
| **tPA** | Tissue plasminogen activator |
| **TPO** | Thrombopoietin |
| **TTBS** | Tween Tris-Buffered Saline |
| **$TXA_2$** | Thromboxane $A_2$ |
| **uPA** | Urokinase-type Plasminogen Activator |
| **v-** | Vesicle |
| **VAMP** | Vesicular Associated Membrane Protein |
| **vWF** | Von Willebrand factor |
| **WAS** | Wiskott-Aldrich syndrome |
| **wt** | Wild-type |

# TABLE OF CONTENTS

# INTRODUCTION

# 1. C3G

C3G (Crk SH3-domain-binding guanine-nucleotide-releasing factor), also known as RapGEF1 or GRF2, is a guanine nucleotide exchange factor (GEF) for several members of the Ras family of GTPases, such as Rap1, R-Ras and TC21 (Gotoh *et al.*, 1995; Gotoh *et al.*, 1997; Ohba *et al.*, 2000). C3G also produces a marginal stimulation of Rap2, N-Ras, H-Ras and RalA, although with lower efficiency than their GEFs, Epac, Sos1 and RalGDS, respectively (Popovic *et al.*, 2013). In addition, C3G also acts as a GEF of TC10, a GTPase of the Rho family (Gotoh *et al.*, 1997; Chiang *et al.*, 2006).

C3G is ubiquitously expressed in human and fetal tissues, although at higher levels in heart, skeletal muscle and placenta. In contrast, lung and liver tissue express low levels of C3G (Guerrero *et al.*, 1998).

## 1.1. C3G structure

C3G is a protein of 1077 amino acids (140 kDa), encoded by the *RAPGEF1* gene (NM_005312), which has multiple well-differentiated functional and structural domains: a N-terminal domain (NTD), a central proline-rich region or SH3-binding (SH3-b) domain, and the catalytic GEF region (Manzano *et al.*, 2021a) (**Figure I-1**).

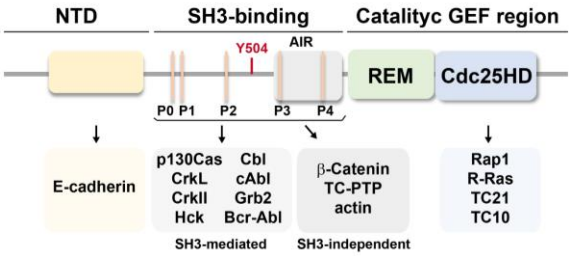


**Figure I-1. C3G structure**. C3G domains are represented: NTD: amino terminal region containing an E-cadherin-binding domain; SH3-binding (SH3-b) domain containing five proline-rich sequences (P0-P4) and the autoinhibitory region (AIR); the catalytic GEF region, formed by the Cdc25 homology domain (Cdc25HD) and the Ras Exchange Motif (REM) domain. The proteins that interact with the NTD and SH3-b domains are indicated, as well as the GTPases activated by the catalytic domain. P: proline.

The C-terminal region of C3G harbors the catalytic domain, which is responsible for the GEF function, and is conserved among all GEFs of the Ras family. This region includes a Cdc25 homology domain (Cdc25HD), homologous to the *S. cerevisiae* Cdc25 protein (Martegani *et al.*, 1992), and a REM (Ras Exchange Motif) domain, which contributes to the exchange reaction (Bos *et al.*, 2007).

The SH3-b domain is located in the central region of the protein and contains five proline rich sequences (P0-P4) that follow the Pro-Pro-X-X-Pro-X-Lys/Arg consensus sequence (Knudsen *et al.*, 1994). The SH3-b region interacts with the SH3 domains of adaptor proteins, such as Crk (Matsuda *et al.*, 1992) and p130Cas (Kirsch *et al.*, 1998), and tyrosine kinases including c-Abl (Radha *et al.*, 2007) and Bcr-Abl (Gutierrez-Berzal *et al.*, 2006), among others (Maia *et al.*, 2013). The central region also interacts with proteins that lack SH3 domains, such as β-catenin or actin (Martin-Encabo *et al.*, 2007; Dayma *et al.*, 2012). In addition, recent results from our group

unveiled the existence of an autoinhibitory region (AIR) in the SH3-binding domain. The AIR region binds to Cdc25HD, blocking the activation of the protein. Crk binding to AIR disrupts the inhibition mechanism (Carabias *et al.*, 2020). Of note, two missense mutations (Y554H and M555K) in the AIR region, described in non-Hodgkin´s lymphomas, interfere with the AIR-Cdc25HD interaction, resulting in a hyperactive protein (Carabias *et al.*, 2020).

Finally, the N-terminal region includes an E-cadherin-binding domain, through which C3G modulates E-cadherin recruitment during the initial steps of junction formation (Hogan *et al.*, 2004). The NTD also modulates the catalytic activity of C3G through its binding to the REM domain (Carabias *et al.*, 2020).

## 1.2. C3G as a GEF

Ras and Rho proteins belong to the Ras superfamily of monomeric GTPases, which regulate several cellular processes, including proliferation, differentiation, and vesicular trafficking. GTPases act as molecular switches, cycling between a GTP-bound state (active conformation) and a GDP-bound state (inactive conformation), resulting in a rapid switch of signaling pathways (Figure I-2). Active GTPase interacts with its effectors, triggering downstream signaling.

GEFs, such as C3G, promote the GDP to GTP exchange and hence, the activation of the GTPase. After a stimulus, the GEF binds to the GTPase in its GDP conformation, inducing the release of GDP and its replacement by GTP, due to its higher concentration in the cytoplasm. The hydrolysis of GTP to GDP is catalyzed by GAPs (GTPase Activating Proteins), resulting in the inactivation of the GTPase.

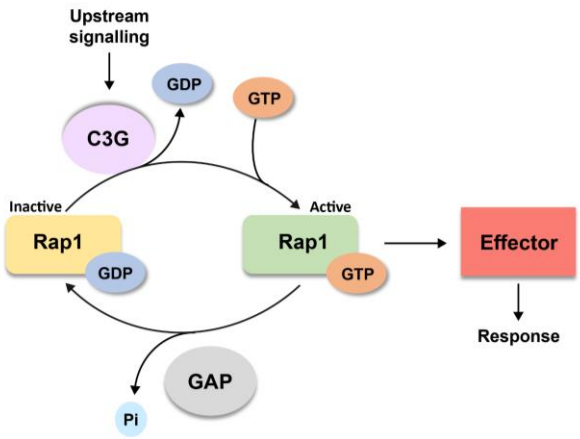


Figure I-2. **The GTPase activation cycle.** GTPases cycle between two conformational states: inactive conformation when bound to GDP, and active conformation or GTP-bound state, capable of activating effector proteins. The exchange of GDP to GTP is regulated by GEFs, whereas the hydrolysis of GTP to GDP is catalyzed by GAPs. GEF: Guanine Nucleotide Exchange Factor; GAP: GTPase Activating Protein; GTP: guanosine triphosphate; GDP: guanosine diphosphate; Pi: inorganic phosphate.

## 1.3. C3G functions

C3G plays an essential role in a wide variety of cellular processes such as cell differentiation, proliferation, adhesion and migration, apoptosis or cell-cell interaction, among others (Radha *et al.*, 2011). The main functions of C3G are depicted in Figure I-3.

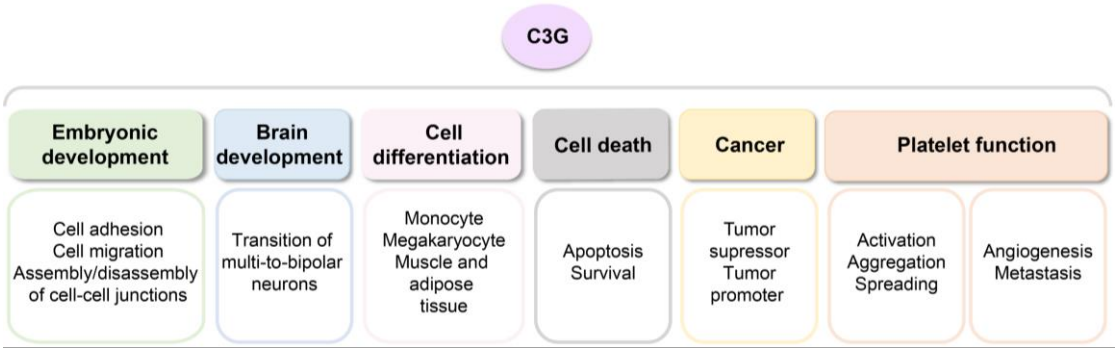


**Figure I-3. C3G functions.** Schematic representation of C3G functions in different processes: embryonic and brain development, cell differentiation and death, cancer and platelet function.

Some of these functions are mediated by its catalytic activity, leading to GTPase activation. However, C3G can also act as an adapter protein, performing functions independently of its GEF domain, through protein-protein interactions involving its polyproline and N-terminal regions.

C3G is essential for mouse embryonic development, due to its crucial role in cell adhesion. In fact, the constitutive C3G knockout mouse ($C3G^{-/-}$) dies before embryonic day 7.5 (Ohba *et al.*, 2001), showing defects in the nervous system and vasculature (Voss *et al.*, 2003; Voss *et al.*, 2006).

### 1.3.1. Role of C3G in cell differentiation

C3G regulates cell differentiation of monocytes, adipocytes, skeletal muscle and pluripotent stem cells (Radha *et al.*, 2011; Sasi Kumar *et al.*, 2015; Vishnu *et al.*, 2021), and participates in the maturation of the vascular system (Voss *et al.*, 2003). In the nervous system, C3G regulates differentiation and migration of neural precursors, controls the size of the cerebral cortex precursor population and is essential for the multipolar to bipolar transition of neurons (Voss *et al.*, 2006; Shah *et al.*, 2016; Manzano *et al.*, 2021b). Moreover, C3G overexpression induces neurite outgrowth and enhances differentiation of PC12 cells induced by NGF or serum deprivation (Schonherr *et al.*, 2010). C3G also regulates the differentiation of human neuroblastoma cells independently of its GEF function (Radha *et al.*, 2008).

Regarding this role in differentiation, our group has demonstrated a role for C3G in megakaryopoiesis, using a mouse model with transgenic expression of human C3G in megakaryocytes (tgC3G). C3G overexpression enhances megakaryocyte (MK) differentiation, modulates their migration to the vascular niche and increases proplatelet formation. However, this increased MK differentiation does not correlate with increased platelet levels (Ortiz-Rivero *et al.*, 2018). Similarly, C3G obliteration in MKs (C3G-KO mouse model) does not trigger differences in MK maturation or platelet number under physiological conditions. However, increased platelet levels were observed in tgC3G and C3G-KO mice upon thrombopoietin (TPO) injection (Ortiz-Rivero *et al.*, 2018; Hernandez-Cano *et al.*, 2022). In tgC3G mice this is mediated by the participation of C3G in the TPO-Mpl pathway in MKs. In C3G-KO mice, this increase is explained by the involvement of platelet C3G in c-Cbl-mediated Mpl degradation, resulting in increased plasma TPO levels (Hernandez-Cano *et al.*, 2022). Therefore, C3G uses several mechanisms to regulate megakaryopoiesis and platelet production under pathological conditions.

### 1.3.2. Role of C3G in cancer

Over the past few years, numerous studies have demonstrated a role for C3G in cancer, where C3G can act as a tumor promoter or suppressor depending on the cellular context, tumor type and stage. There are several studies supporting a tumor suppressor activity for C3G; in NIH3T3 cells, C3G suppresses malignant transformation induced by the overexpression of *sos, ras, dbl, raf1* and *R-ras* oncogenes (Guerrero *et al.*, 1998; Guerrero *et al.*, 2004), which is mediated by its SH3-b domain (Guerrero *et al.*, 2004). In addition, lower levels of C3G have been observed in squamous cell carcinoma (Okino *et al.*, 2006) and similarly, C3G downregulation has been associated to increased migration and invasion in breast cancer (Dayma & Radha, 2011), hepatocellular carcinoma (Sequera *et al.*, 2020) and glioblastoma (Manzano *et al.*, 2021a; Manzano *et al.*, 2021b).

On the other hand, C3G acts as a tumor promoter in non-small cell lung cancer, where C3G is overexpressed (Hirata *et al.*, 2004). In addition, the *RAPGEF1* gene shows somatic demethylation in patients with colon, gastric and ovarian cancer, which is associated with increased expression (Samuelsson *et al.*, 2011). C3G is also crucial for the growth and progression of papillary thyroid carcinoma (De Falco *et al.*, 2007), colorectal carcinoma (Priego *et al.*, 2016) and hepatocellular carcinoma (Sequera *et al.*, 2020).

Some of the actions of C3G in cancer are mediated through its role in apoptosis, as it has been described in myelomonocytic cells (Shivakrupa *et al.*, 2003), neuroblastoma cells (Radha *et al.*, 2008) or chronic myeloid leukemia cells (Maia *et al.*, 2009), although C3G also regulates apoptosis in non-tumor cells (Gutierrez-Uzquiza *et al.*, 2010).

### 1.3.3. Role of C3G in actin cytoskeleton dynamics and vesicle trafficking

Several publications have demonstrated a role for C3G in actin cytoskeleton remodelling, independently on its catalytic activity. Indeed, C3G and phospho-C3G colocalize with F-actin, and disruption of actin cytoskeleton impairs phosphorylation of C3G at the plasma membrane (PM) (Radha *et al.*, 2004; Martin-Encabo *et al.*, 2007). Furthermore, C3G modulates filopodia formation in epithelial cell lines (Radha *et al.*, 2007) and regulates the stabilization of microtubules (Dayma & Radha, 2011).

Moreover, C3G colocalizes with focal adhesion proteins, such as Abl, p38αMAPK, c-Cbl, p130Cas, Abi1, FAK and paxillin (Maia *et al.*, 2013). In fact, overexpression of a C3G dominant-negative mutant disrupts actin cytoskeleton remodeling and focal adhesion formation (Sasi Kumar *et al.*, 2015).

There is also some evidence for a role of C3G in vesicular trafficking; thus, in muscle and adipocyte tissue, C3G GEF activity modulates TC10-mediated GLUT4 vesicle exocytosis induced by insulin, through its association with CrkII and c-Cbl (Chiang *et al.*, 2001; Chiang *et al.*, 2006). In addition, C3G expression rescues the defects in vesicular trafficking induced by the expression of a dominant negative form of NSF2 (N-ethylmaleimide-sensitive factor 2) in *Drosophila* (Laviolette *et al.*, 2005).

## 2. Platelet

Platelets are small, anucleate cell fragments of approximately 2-5 µm in size with an irregular shape. Platelets are produced by MKs in the bone marrow (BM) during the thrombopoiesis, from where they are released into the blood stream. This process is regulated by TPO and consists of the fragmentation of proplatelets, previously formed from mature MKs. The half-life of platelets in the blood circulation is 5 days in mice and 7 days in humans. After this time they are degraded in the spleen, liver or lung (Thon & Italiano, 2010).

Depending on their age, two different platelet populations can be found in peripheral blood: reticulated or immature platelets and old or mature platelets (Hoffmann, 2014). Reticulated platelets are newly released from the BM; they are larger, more reactive, and have more RNA and higher levels of surface activation markers than mature platelets. Indeed, the number of reticulated platelets reflects the activity of megakaryopoiesis in the BM (Bongiovanni *et al.*, 2022; Hamad *et al.*, 2022).

Despite their small size, platelets are highly organized cells, rich in distinguishable structural elements, including a delimited PM, skeletal components (microtubules and actin filaments), the open canalicular system (OCS), the dense tubular system (DTS) and various organelles, such as mitochondria and three different types of granules (Fitch-Tewfik & Flaumenhaft, 2013) (Figure I-4).

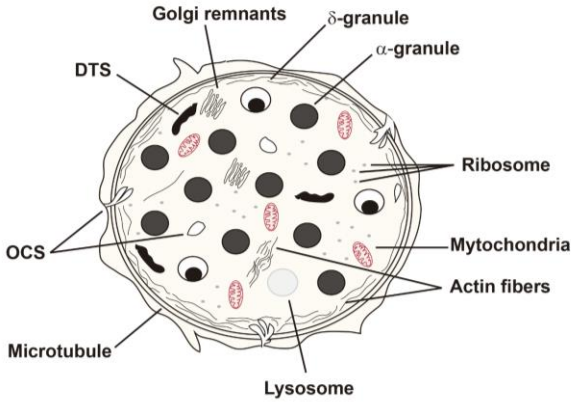


**Figure I-4. Platelet structure.** Schematic representation of platelet organelles. The three different platelet-granules (α-granules, δ-granules and lysosomes), mitochondria, ribosomes, Golgi remnants, actin fibres, microtubules, the Dense Tubular System (DTS) and the Open Canicular System (OCS) are represented. Based on (Fitch-Tewfik & Flaumenhaft, 2013).

The platelet OCS consists of cytoplasmatic invaginations with a composition of phospholipids and surface glycoprotein receptors, similar to those of the PM. Its main function is to transport proteins both in and out of platelets. Upon platelet stimulation, the granules fuse with the OCS or PM and release their content (Selvadurai & Hamilton, 2018). Furthermore, the OCS serves as an extensive membrane reservoir that helps platelet adhesion to different surfaces and facilitates the formation of actin structures, such as filopodia or lamellipodia (White & Escolar, 1991; Thon & Italiano, 2012). Platelets also have a DTS, which is a closed-channel network that functions as an intracellular calcium store (Fitch-Tewfik & Flaumenhaft, 2013).

Three different types of granules can be found in platelets: α-granules, δ-granules (also known as dense granules) and lysosomes, with α-granules and δ-granules being the main storage granules. α-granules are the largest (200–500 nm) and most abundant (40-80 per platelet) granules in platelets. They are derived from the trans-Golgi network and have a spherical shape with a dark central core. There is evidence that α-granule population is not uniform, and that different subpopulations can be distinguished according to their shape (spherical, multivesicular or tubular granules (Heijnen & van der Sluijs, 2015)), cargo type (differential packaging of pro-angiogenic and anti-angiogenic factors, von Willebrand factor (vWF) or fibrinogen (Sehgal & Storrie, 2007; Italiano *et al.*, 2008)) or response to agonists (differential release of pro-angiogenic and anti-angiogenic factors after thrombin or ADP stimulation (Italiano *et al.*, 2008; Peters *et al.*, 2012)). However, this is controversial because other authors describe that the cargo distribution in the α-granules is random and that the segregation observed by immunofluorescence is caused by segregation within each granule (Kamykowski *et al.*, 2011; Whiteheart, 2011).

α-granules contain a wide variety of soluble and membrane-associated proteins (more than 300 factors, some of them described in **Table-I-1**), which are involved in the regulation of different processes, such as hemostasis, coagulation, angiogenesis, inflammation or metastasis (Maynard *et al.*, 2007; Thon & Italiano, 2012; Gremmel *et al.*, 2016).

**Table I-1. Description of the factors contained in α-granules, indicating their function.** TF: tissue factor.

| Type | Examples |
|---|---|
| Membrane proteins | P-selectin, CD40L, αIIbβ3, GPVI |
| Coagulant factors | TF, PF4, Factor V, Factor IX, Factor XII, Factor XIII, prothrombin |
| Anticoagulant factors | Anti-thrombin, TF pathway inhibitor, Serpin E1, plasminogen |
| Adhesion proteins | Fibrinogen, vWF |
| Chemokines | CXCL1 (GRO-α), PF4, CXCL5 (ENA-78), CXCL-7, CXCL8 (IL8), CCL2, CXCL16, CCL3 (MIP-1α), CCL5 (RANTES), pentraxin-3, IL-1α, CX3CR1, IL-6 |
| Angiogenic factors | TSP-1, VEGF, bFGF, endostatin, PDGF |
| Immune mediators | Complement C3 precursor, complement C4 precursor |
| Growth factors | EGF, HGF, IGF, TFG-β, GM-CSF, HB-EGF |

There are 3 to 8 δ-granules per platelet, which are smaller than α-granules (250 nm). They are recognized because they have an opaque spherical structure surrounded by an empty space. They contain high concentrations of ADP and ATP, uracil and guanine nucleotides, $Ca^{2+}$, potassium and bioactive amines (serotonin and histamine) (Gremmel *et al.*, 2016).

Finally, lysosomes have enzymes, such as collagenase, elastase, glucosidase or galactosidase, all of which are active in acidic environments (Bentfeld-Barker & Bainton, 1982; Gremmel *et al.*, 2016).

Platelets also have an organized cytoskeleton responsible of platelet shape. There are three cytoskeletal components in platelets: actin cytoskeleton, microtubules and spectrin-based membrane skeleton (Thon & Italiano, 2012). This will be explained in depth in **Section 2.7.**

As mentioned before, platelets are known to contribute to hemostasis and thrombosis but also have been implicated in angiogenesis, inflammation or metastasis (Franco *et al.*, 2015).

## 2.1. Platelet function in hemostasis

Hemostasis is the first step of wound healing; it prevents blood loss when the integrity of the vascular endothelium is disrupted (Figure I-5). The hemostatic process is divided into primary hemostasis, secondary hemostasis and fibrinolysis (Arnout *et al.*, 2006). Platelets are the main modulators of hemostasis.

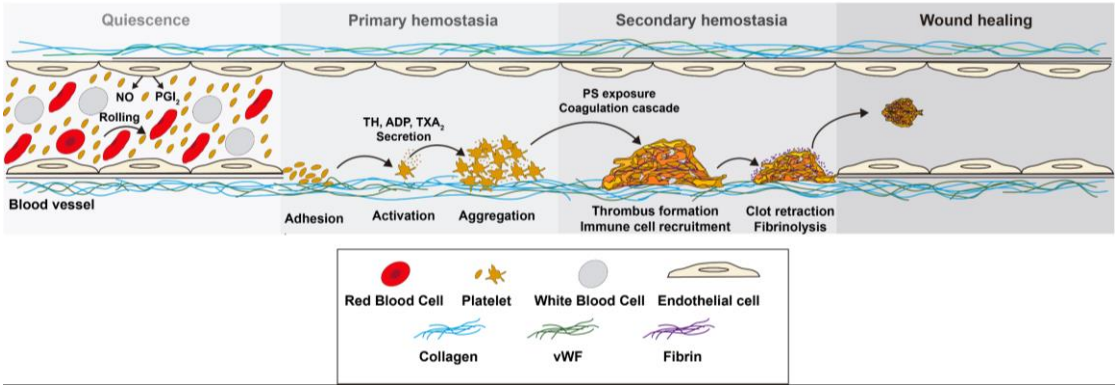


**Figure I-5. Platelets and hemostasis.** Schematic representation of the hemostatic process, showing its different phases. In physiological conditions, platelets are maintained in a round, quiescent state. When the vascular wall is disrupted, platelets interact with ECM components, such as collagen or vWF, which induces their activation and aggregation (primary hemostasis). During secondary hemostasis, platelets release factors and expose phosphatidylserine (PS) on their surface, triggering the coagulation cascade and thrombus formation. Finally, during fibrinolysis the clot is retracted and reabsorbed. ECM: extracellular matrix; TH: thrombin; vWF: von Willebrand factor; $TXA_2$: thromboxane $A_2$; NO: nitric oxide; $PGI_2$: prostaglandin $I_2$. Based on (Montague *et al.*, 2020).

Under physiological conditions, platelets are in a resting state and circulate close to the vascular endothelium. Healthy endothelium releases inhibitory mediators, such as prostaglandin $I_2$ ($PGI_2$) or nitric oxide (NO), which inhibit platelet activation (Smolenski, 2012).

### 2.1.1. Primary hemostasis

After a vascular injury, the endothelium is disrupted, resulting in the exposure of molecules from the subendothelial matrix, such as collagen, vWF, fibronectin or laminin. Although platelets have multiple integrin receptors that can adhere to fibronectin or laminin, vWF seems to be the primary ligand for platelet recruitment (Arnout *et al.*, 2006).

In the initial steps of primary hemostasis, collagen and vWF bind to platelet receptors, α2β1 or glycoprotein (GP) VI, and GPIb-IX-V, respectively, triggering platelet adhesion to the damaged area. Platelet adhesion induces the activation of different signaling pathways involved in actin cytoskeleton remodeling and platelet secretion. As a result, platelets extend over the damaged area and release some hemostatic factors, such as ADP or thromboxane $A_2$ ($TXA_2$). This rapid granule secretion amplifies platelet activation and induces the recruitment of more platelets to the damaged area (Golebiewska & Poole, 2015; Pryzdial *et al.*, 2018).

Platelet activation is followed by platelet aggregation, which produces an accumulation of platelets leading to plug formation. The main receptor involved in platelet aggregation is the platelet-specific integrin αIIbβ3. In resting platelets, integrin αIIbβ3 is in an inactive or low affinity conformation, in which it cannot interact with its primary ligand, fibrinogen. Platelet

activation induces a conformational change in the integrin, favouring its interaction with fibrinogen (Pryzdial *et al.*, 2018).

Platelets form aggregates through fibrinogen bridges due to the ability of fibrinogen to bind to different receptors at the same time (Ma *et al.*, 2007; Broos *et al.*, 2011). To facilitate plug formation, platelets induce thrombus contraction. Platelet contractile forces, generated by myosin and transmitted by the actin cytoskeleton and integrins, are transduced through a network to fibrinogen/vWF-bound platelets (Samson *et al.*, 2017).

### 2.1.2. Secondary hemostasis or coagulation

Once the initial plug is formed, the coagulation cascade triggers a thrombin-mediated-fibrin network that strengthens the plug (Pryzdial *et al.*, 2018). This process is known as secondary hemostasis. Secondary hemostasis is classified into intrinsic (contact activation) and extrinsic (tissue factor related) pathways (Figure I-6). Both are activated by the exposure of the extracellular matrix (ECM), and consist of a series of proteolytic events, mainly located on the surface of activated platelets, which converge in the activation of factor X. Following factor X activation, prothrombin is converted to thrombin, which cleaves fibrinogen to fibrin (Green, 2006; Pryzdial *et al.*, 2018).

The extrinsic pathway begins with the exposure of tissue factor (TF, also known as factor III) and its interaction with factor VII, leading to its activation into factor VIIa, which activates factor X into factor Xa. The intrinsic pathway leads to the activation of factor XII into XIIa, induced by blood contact with the subendothelial collagen. Following factor XIIa activation, different factors are activated (XIa, IXa) resulting in the activation of factor X.

Finally, factor Xa activates factor V, forming the prothrombinase complex. Prothrombin is converted to thrombin by factor Xa on platelet surface and catalyzes the cleavage of fibrinogen to form insoluble fibrin. Fibrin stabilizes the plug by forming a thrombus that serves as a temporary matrix for the wound (Figure I-6) (Pryzdial *et al.*, 2018; Rodrigues *et al.*, 2019).

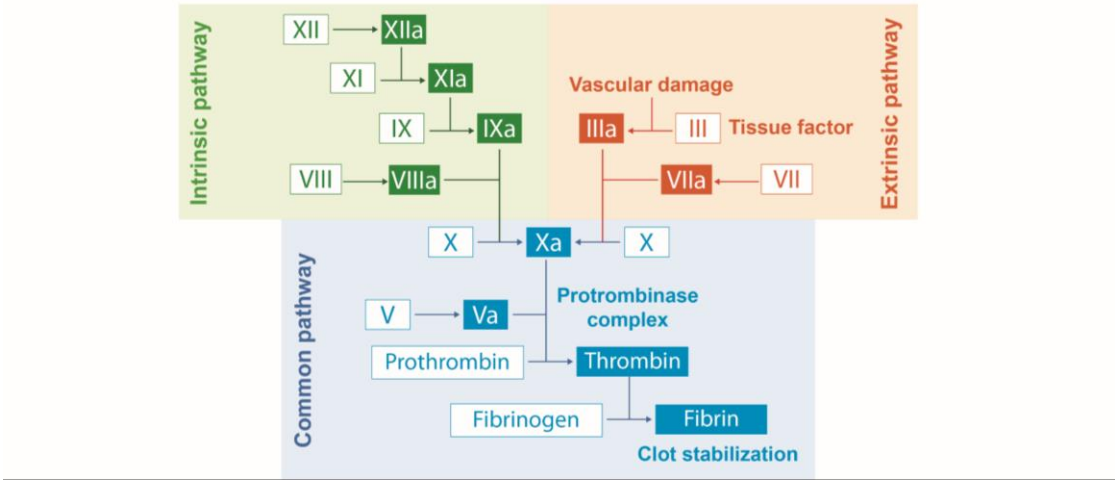


**Figure I-6. Secondary hemostasis.** Schematic representation of the coagulation cascade, indicating the components of the different pathways: intrinsic (green), extrinsic (orange) and the common pathway (blue) in which both converge to stabilize the clot. Color filled boxes indicate active factors.

To strengthen the plug, activated platelets transduce their contractile forces to fibrin networks to bind the edges of the endothelium and produce effective wound healing. Clot retraction begins with the contraction of fibrin, which increases clot density, and decreases clot size due to the extrusion of the plasma volume (Pryzdial *et al.*, 2018; Nurden, 2022).

Platelets play an essential role in clot stabilization, providing their surface for the activation of coagulation complexes (modulated by the exposure of procoagulant phospholipids) and are themselves a reservoir of coagulation factors (Factor V, Factor XII, TF, prothrombin, among others) (Golebiewska & Poole, 2015).

Platelet PM is made up of phospholipids, cholesterol and glycolipids. The most important phospholipid in coagulation is phosphatidylserine (PS). Platelet activation is accompanied by a flip-flop movement of anionic phospholipids, such as PS, which results in their exposure on the platelet surface. This procoagulant exposure provides a surface for the binding and activation of coagulant factors, leading to amplification of thrombin generation (Kholmukhamedov & Jobe, 2019). Two different subtypes of platelets have been described, based on their response to activation and their location within the thrombus: procoagulant platelets and aggregating platelets. Aggregating platelets are situated in the core of the thrombus, while procoagulant platelets are located at the edges (Kholmukhamedov & Jobe, 2019; Nechipurenko *et al.*, 2019).

Both types of platelets have different functions, shapes and characteristics. Aggregating platelets show activation of integrin αIIbβ3 and P-selectin exposure; they have an irregular shape with pseudopods and secrete molecules, such as ADP or serotonin. In contrast, procoagulant platelets present a greater PS exposure, are balloon-shaped and their secretion is related to inflammatory factors and microparticles (Jurk & Kehrel, 2005; Kholmukhamedov & Jobe, 2019; Chu *et al.*, 2021). Other authors separate these groups into four: (i) aggregating platelets and (ii) secretory platelets, distinguished by exposure of activated integrin αIIbβ3 or P-selectin, respectively; (iii) procoagulant platelets and (iv) coated platelets, both expose PS on their surface, but while coated platelets serve as anchor points for fibrin formation, procoagulant platelets provide the surface for thrombin formation (**Figure I-7**) (van der Meijden & Heemskerk, 2019).

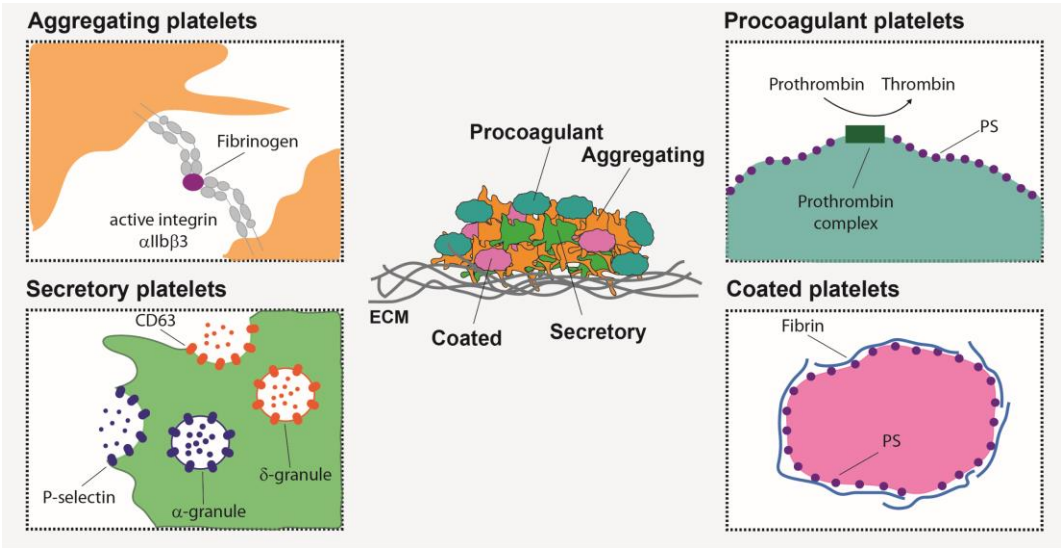

**Figure I-7. Platelets subtypes after stimulation.** Schematic representation of platelet heterogeneity in response to activation. Four different subtypes of platelets are distinguished: aggregating, secretory, procoagulant and coated platelets. ECM: extracellular matrix; PS: phosphatidylserine. Based on (van der Meijden & Heemskerk, 2019).

### 2.1.3. Fibrinolysis

In fibrinolysis, the final stage of hemostasis, clots are reabsorbed by plasmin-mediated destruction of fibrin and the fibrinogen network. The primary fibrinolytic protease, plasmin, is produced when tissue plasminogen activator (tPA) or urokinase-type plasminogen activator (uPA) converts plasminogen to plasmin (Cesarman-Maus & Hajjar, 2005; Kanji *et al.*, 2021).

## 2.2. Role of platelets in inflammation

Platelets are the regulators of the immune response, playing a crucial role in immune surveillance and inflammation during infection. On the one hand, platelet Toll-like receptors (TLRs) can interact with pathogens, triggering the secretion of pro-inflammatory factors that facilitate their clearance (Repsold & Joubert, 2021). On the other hand, platelets can activate leukocytes by direct interactions through platelet receptors or indirectly through the secretion of immunomodulatory factors (Finsterbusch *et al.*, 2018).

Activated platelets can adhere to the inflamed endothelium through GPVI-collagen or vWF-GPIbα/IX/V interactions, among others, promoting the release of inflammatory factors from endothelial cells, such as CCL2 or CXCL8, triggering leukocyte recruitment (May *et al.*, 2007). Then, platelets form complexes with leukocytes (termed platelet-leukocyte aggregates or PLAs), promoting their recruitment and extravasation to sites of inflammation and the release of pro-inflammatory factors from leukocytes. Platelets mainly interact with monocytes and neutrophils (NEs); however, they can also bind to macrophages (Mϕ), lymphocytes, natural killer cells, and even eosinophils (Koupenova *et al.*, 2018; Ebermeyer *et al.*, 2021) through P-selectin-PSGL-1, CD40-CD40L or GPIβ-α-Mac1 interactions (**Figure I-8**) (May *et al.*, 2007). PLA formation induces a wide variety of pro-inflammatory functions in leukocytes, including the release of pro-inflammatory cytokines, the production of reactive oxygen species, phagocytosis or endothelial adhesion (Thomas & Storey, 2015).

Specifically, platelet interaction with monocytes causes monocyte differentiation (Fu *et al.*, 2021). In addition, platelet interaction with B lymphocytes induces their proliferation and antibody production, whereas platelets can attenuate the immunosuppressive responses of $T_H$ (helper T) cells and enhance proliferation and cytotoxicity of $T_C$ (cytotoxic T) cells (Li, 2008). Finally, platelet interaction with NEs is critical, both for initiating the immune response and for the formation of NE extracellular traps (NETs), which are extracellular DNA fibers, comprising histones and neutrophil antimicrobial proteins, through which pathogens are captured and neutralized. This process is known as NETosis (Stark, 2019; Ebermeyer *et al.*, 2021).

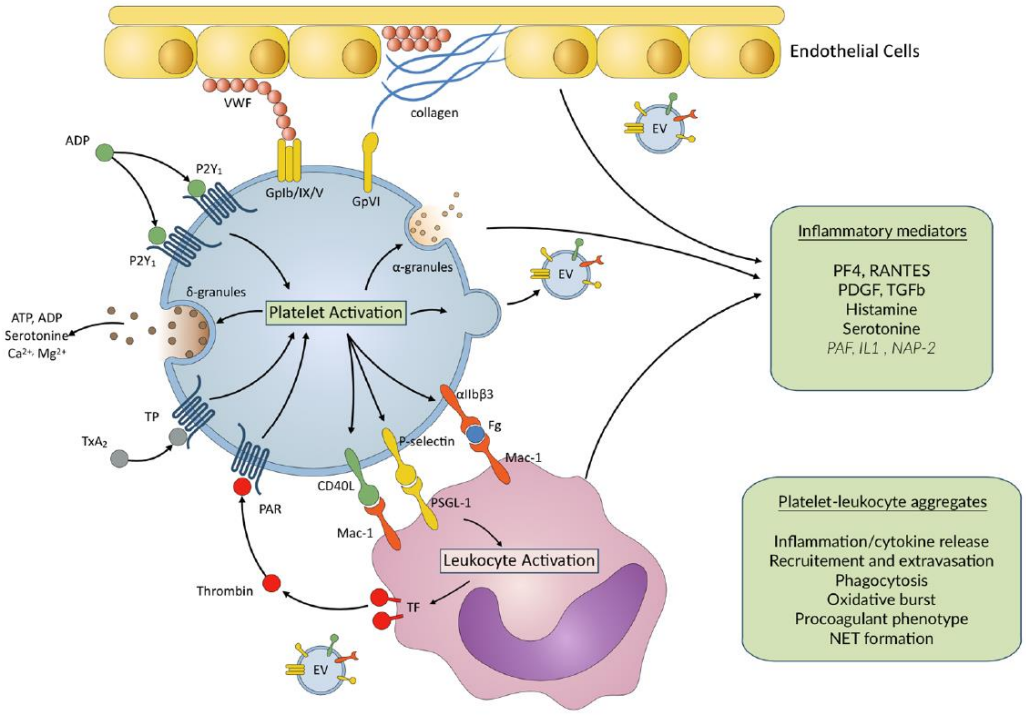


**Figure I-8. Schematic representation of platelet-leukocyte interactions.** Platelets interact with inflamed endothelium (via GPIb/IX/V-VWF and GPVI-collagen interactions) and with leukocytes (through P-selectin-PSGL-1, CD40L-CD40/Mac1 and αIIbβ3-fibrinogen-Mac1 interactions). Platelets also secrete inflammatory mediators, such as PF4, RANTES, PDGF, histamine or serotonin among others. Fg: fibrinogen; EV: extracellular vesicle; NET: NE extracellular trap; PF4: platelet factor 4; PDGF: platelet derived growth factor; TF: tissue factor (Mansour *et al.*, 2020).

Supporting PLA formation, active platelets secrete a large number of inflammatory mediators, such as chemokines or interleukins, contained in their α-granules. The effect of the different inflammatory factors is described in Table-I-2. Briefly, platelet factor 4 (PF4, also known as CXCL4) promotes the release of pro-inflammatory cytokines from leukocytes, NE activation, monocyte differentiation and phagocytosis. CCL5 (or RANTES) induces eosinophil, monocyte and Mϕ recruitment, consolidating their attachment to the endothelium (Manne *et al.*, 2017).

**Table I-2. Description of the inflammatory factors contained in platelet α-granules, indicating their receptor and their function.** LE: leukocyte; M: monocyte; NE: neutrophil; Mϕ: macrophage; TL: T lymphocyte; BL: B lymphocyte.

| Mediator | Interactors | Effect | Reference |
|---|---|---|---|
| CCL2 (MCP-1) | CCR2 | M and Mϕ recruitment | (Deshmane *et al.*, 2009) |
| CCL3 (MIP-1α) | CCR1, CCR3 and CCR5 | Recruitment of M and Mϕ, release of pro-inflammatory mediators | (Maurer & von Stebut, 2004) |
| CCL5 (RANTES) | CCR1, CCR3 and CCR5 | Eosinophile, M, Mϕ chemotaxis | (Manne *et al.*, 2017) |
| CCL7 (MCP3) | CCR2 | M and Mϕ recruitment | (Jonnalagadda *et al.*, 2012) |
| CCL8 (MCP3) | CCR5 | M and Mϕ recruitment | (Jonnalagadda *et al.*, 2012) |
| CXCL1 | CXCR2, CXCR1 | M and NE recruitment | (Gleissner *et al.*, 2008) |
| CXCL4 (PF4) | CXCR3 | Release of pro-inflammatory factors from LE, phagocytosis, chemotaxis, generation of ROS and NE activation | (Thomas & Storey, 2015). |
| CXCL5 (ENA-78) | CXCR2 | Mϕ activation | (Bakogiannis *et al.*, 2019) |

| Mediator | Interactors | Effect | Reference |
|---|---|---|---|
| CXCL7 (NAP-2) | CXCR1, CXCR2 | NE recruitment | (Gleissner *et al.*, 2008) |
| CXCL16 | CXCR6 | LE recruitment | (Bakogiannis *et al.*, 2019) |
| IL-1 | IL-1 receptor | LE mobilization | (Collado *et al.*, 2018) |
| TGF-β | TGF-β receptor | TL differentiation, BL and Mϕ phenotype regulation | (Morrell *et al.*, 2014) |
| PDGF | PDGFR | M and Mϕ differentiation | (Morrell *et al.*, 2014) |
| Pentraxin-3 | - | Block of NE recruitment | (Inoue *et al.*, 2012) |

Interestingly, there is a crosstalk between platelets and leukocytes. Not only do platelets modulate the inflammatory response, but leukocytes also regulate hemostasis (Margetic, 2012).

## 2.3. Signaling pathways in platelets

In platelets, the interaction of the agonist with its receptor initiates intracellular signaling pathways (inside-out) that lead to cytoskeleton remodelling, integrin αIIbβ3 conformational change and granule secretion.

Platelet activation is mediated by several agonists, such as thrombin, ADP or $TXA_2$, which engage G-protein-coupled receptors (GPCRs) located on platelet surface. In the cytoplasmic part of the membrane, these GPCRs interact with heterotrimeric G proteins formed by an α subunit (which binds GDP or GTP) and a βϒ heterodimer. After agonist-GPCR interaction, GPCR triggers the exchange of GDP to GTP in the Gα subunits, inducing their dissociation from the Gβϒ heterodimer. This dissociation causes the interaction of G subunits with downstream effectors (Pradhan *et al.*, 2017).

The function of the different GPCRs depends on their associated G protein, which are classified according to their α subunit. There are four families of Gα subunits, based on their structural and functional characteristics: Gαs, Gαi, Gαq, Gα12. Whereas Gαi, Gαq, and Gα12 subunits are related to platelet activation, Gαs regulates platelet inhibition through its coupling with the $PGI_2$ receptor (IP) (**Figure I-9**) (Offermanns, 2000).

Upon activation, Gαq-coupled GPCRs activates phospholipase Cβ (PLCβ). PLCβ catalyzes the hydrolysis of phosphatidylinositol-(4,5)-bisphosphate ($PIP_2$) to diacylglycerol (DAG) and inositol triphosphate ($IP_3$), which activates protein kinase C (PKC) and stimulates the release of calcium from the DTS, both triggering Rap1 activation. An example of this type of receptor is the thrombin receptor (Offermanns *et al.*, 1997; Offermanns, 2000).

Stimulation of GPCRs coupled to Gαi subunits induces the activation of phosphoinositide 3-kinase (PI3K), which triggers the activation of p38MAPKs (p38 mitogen-activated protein kinases). p38MAPKs induce the activation of phospholipase A (PLA), which releases arachidonic acid from the PM to generate $TXA_2$. In addition, Gαi subunits inhibit the production of cAMP by adenylyl cyclase (AC). An example of this type of receptor is the ADP receptor, P2Y12 (Woulfe, 2005).

Activation of GPCRs couples to Gα12 subunits in platelets, such as the $TXA_2$ receptor (TP), stimulates activation of RhoA GTPase, which regulates platelet shape change through

reorganization of the actin cytoskeleton. Stimulation of Gα12 subunits could also activate the PI3K pathway (Woulfe, 2005).

Finally, Gαs-coupled receptors, such as the aforementioned $PGI_2$ receptor, stimulate AC, increasing cAMP production, which suppresses platelet function (Li *et al.*, 2010).

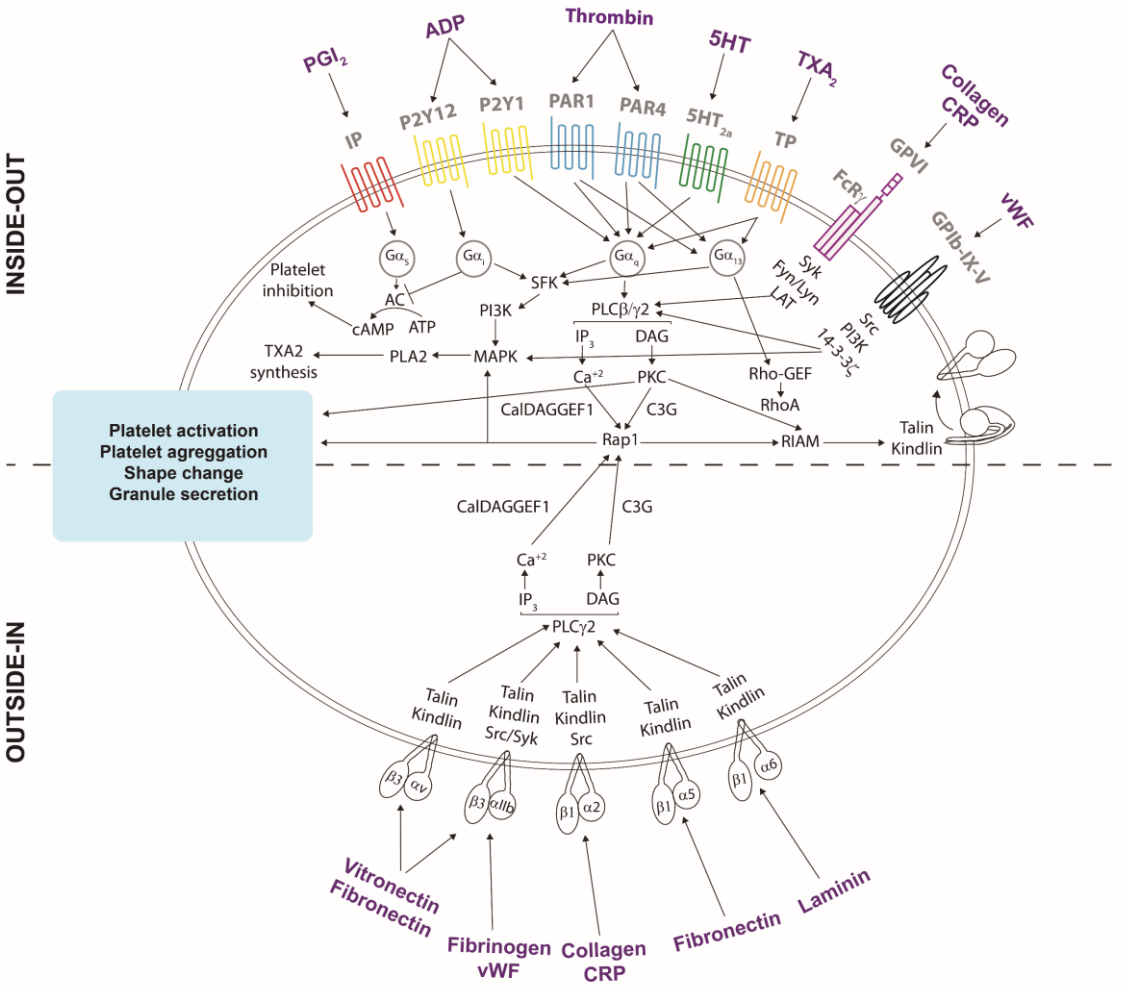


**Figure I-9. Main signaling pathways in platelets.** Agonists interact with their receptors and induces downstream signaling that modulates platelet activation and aggregation, shape change and granule secretion. Inside-out signaling and outside-in signaling are represented. CRP: Collagen related peptide; 5HT: serotonin; SFK: Src family of kinases. See the text for a description of other components.

Platelets also express on their surface the GPIb-IX-V complex formed by four glycoproteins: GPIbα, GPIbβ, GPIX, and GPV. After activation of the complex by vWF, 14-3-3ζ binds to the cytoplasmic domain of GPIbα and activates the Src kinase and PI3K pathways. In addition, the activation of the GPIb-IX-V complex induces the activation of PLCγ2, which catalyzes the hydrolysis of $PIP_2$ to DAG and $IP_3$, triggering Rap1 activation (Estevez & Du, 2017). Platelets also express GPVI on the platelet surface, which is the major receptor for collagen. GPVI is coupled to a disulphide-linked Fc receptor (FcR) γ-chain, and after its activation initiates a Syk-dependent signaling, ending in PLCγ2 activation (Watson *et al.*, 2005).

In basal conditions, integrins are maintained in a low-affinity state in which the extracellular ectodomain is in a closed conformation. Activation of the integrins triggers a conformational

change to a form with higher affinity for the ligands. Activation of integrins can occur by signaling pathways induced by agonist-GPCR interaction (known as inside-out signaling) or through binding to ECM ligands (known as outside-in signaling) (Estevez *et al.*, 2015) (**Figure I-9**).

Platelets express different integrins that bind to different ECM components, such as α2β1 (collagen), α5β1 (fibronectin), α6β1 (laminin), and αvβ3 (vitronectin, fibronectin) among others, although the main platelet integrin (and the most expressed) is αIIbβ3. Platelets express ≈80,000 αIIbβ3 copies on their surface. Integrin αIIbβ3 can bind to different ligands, such as fibrinogen, fibrin, vWF or fibronectin, although fibrinogen is the main ligand (Durrant *et al.*, 2017).

Outside-in integrin αIIbβ3-mediated signaling modulates platelet spreading, further granule secretion, stable thrombus formation and clot retraction, through regulation of the cytoskeletal machinery, including actin polymerization, cytoskeleton reorganization and force sensing/transmission (Li et al., 2010; Durrant et al., 2017).

## 2.4. Rap1 GTPase in hemostasis and its regulation

### 2.4.1. Rap1 GTPase regulation in platelets

Rap GTPases are small GTPases of the Ras family that are ubiquitously expressed (Bos, 1998). There are five Rap GTPases in platelets: Rap1a, Rap1b, Rap2a, Rap2b, Rap2c, with Rap1b being the most abundant (Stork & Dillon, 2005). As mentioned above, GEFs promote the GTP-bound state of GTPases (active conformation). C3G was the first GEF of Rap1 identified (Stork & Dillon, 2005). In addition to C3G, there are other GEFs of Rap1b in platelets, such as CalDAG-GEFI (in mice) (Crittenden *et al.*, 2004), CalDAG-GEFIII and PDZ-GEF1 (in humans) (Schultess *et al.*, 2005) (**Figure I-10**).

CalDAG-GEFI, also known as RasGRP2, is the predominant GEF of Rap1b in platelets and MKs (Stefanini & Bergmeier, 2016). CalDAG-GEFI contains binding sites for $Ca^{2+}$ and DAG and catalyzes the activation of different members of the Ras family, in particular Rap1 and Rap2. Unlike the other members of the RasGRP family, CalDAG-GEFI is found mainly in the cytoplasm and upon activation translocates to the PM (Stefanini & Bergmeier, 2010; Canault & Alessi, 2020). CalDAG-GEFI is involved in Rap1 activation in response to agonists that trigger an increase in intracellular calcium concentration (Stefanini *et al.*, 2009).

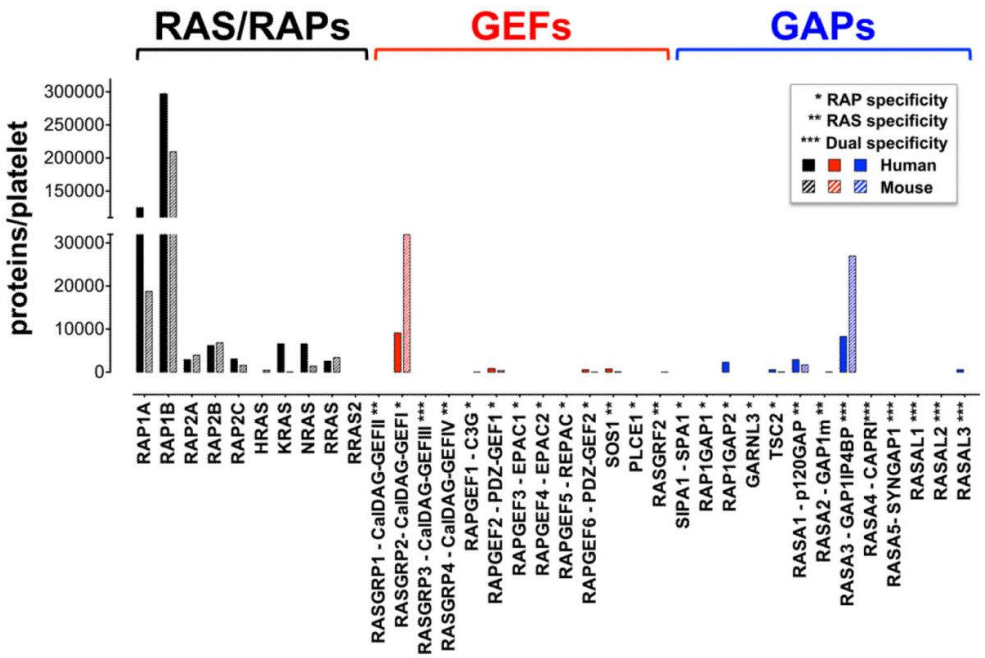


**Figure I-10. Expression of Ras/Rap proteins and their GEFs and GAPs in human and mouse platelets.** Expression levels of the indicated proteins based on the quantitative proteomic analysis in human and mouse platelets (Stefanini & Bergmeier, 2016).

In platelets, there are different GAPs for Rap1: RAP1GAP2, RASA1, RASA2, RASA3 and RASAL3, but the most abundant is RASA3 (Figure I-10) (Stefanini & Bergmeier, 2016). RASA3 belongs to the GAP1 family and in its structure we can find two C2 domains (that bind $Ca^{2+}$ and lipids), a central GAP catalytic domain and a C-terminal PH (pleckstrin homology) domain, linked to a Btk motif (named PH/Btk) (Schurmans *et al.*, 2015).

RASA3 acts as a negative regulator of platelet activation, by antagonizing the activation of Rap1 by CALDAG-GEFI. Bermeier's group described a balance between CalDAG-GEFI and RASA3 in Rap1 activation. In resting platelets, RASA3 is activated to prevent Rap1 activation, thus, maintaining platelets in a resting state. Upon platelet activation, CalDAG-GEFI activates Rap1b, which through ADP secretion from δ-granules and its interaction with P2Y12 receptor, initiates activation of the PI3K-pathway, which inhibits RASA3 (Stefanini *et al.*, 2015).

Another protein involved in Rap1b activation is VASP, a member of a conserved family of actin regulatory proteins. VASP knockout platelets present lower levels of Rap1b activation and higher adhesion to collagen (Aszodi *et al.*, 1999; Benz *et al.*, 2016). Benz *et al*. described a ternary complex formed by VASP-CrkL-C3G that acts in parallel to CalDAG-GEFI to regulate Rap1b activation in platelets (Benz *et al.*, 2016).

It has been described that protein kinase A (PKA) negatively regulates Rap1b activation through two different pathways. On the one hand, PKA directly phosphorylates Rap1, as well as its GEFs and GAPs. Phosphorylation of Rap1 triggers its translocation to the cytosol and hence, its inactivation. Phosphorylation of CalDAG-GEFI also leads to its inactivation, whereas PKA-mediated RASA3 phosphorylation induces its activation, thus preventing Rap1b activation (Stefanini *et al.*, 2015). On the other hand, PKA phosphorylates VASP, which abrogates the formation of the ternary complex VASP-CrkL-C3G (Benz *et al.*, 2016).

### 2.4.2. Rap1 GTPase function in platelets

Rap1b GTPase plays a crucial role in platelet function, regulating platelet adhesion and aggregation through activation of the integrin αIIbβ3 (Shattil *et al.*, 1998). Rap1b also regulates platelet secretion of δ- and α-granules, platelet spreading and clot retraction (Zhang *et al.*, 2011). Indeed, Rap1b is activated by most platelet receptors in response to ADP, collagen, thrombin or PMA (Phorbol 12-Myristate 13-Acetate) (Chrzanowska-Wodnicka *et al.*, 2005).

Rap1 activation in response to thrombin depends on the stimulation conditions. Thus, after stimulation under non-aggregating conditions, Rap1-GTP levels rapidly reach peak activation and are maintained over time, while under aggregating conditions, Rap1-GTP levels decrease rapidly after peaking, due to its translocation from the PM to the cytoskeleton (**Figure I-11**) (Franke *et al.*, 2000).

Rap1 activation occurs in two different phases in response to thrombin (**Figure I-11**). In the first wave Rap1 is activated by CalDAG-GEFI through a pathway involving intracellular $Ca^{2+}$ generated by PLC activity. The second wave, which is calcium-independent, involves the activation of PKC and induces a slower Rap1 activation (Franke *et al.*, 2000).

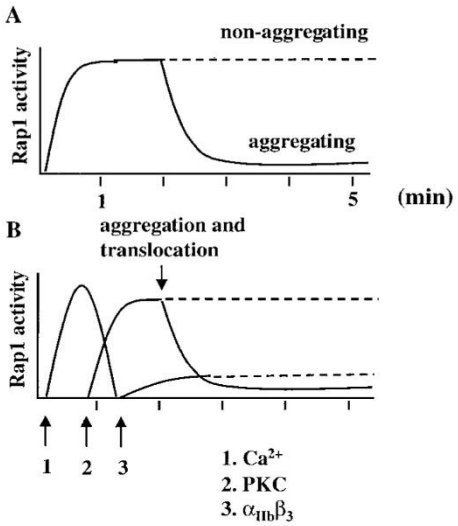


**Figure I-11. Thrombin-induced Rap1 activation in platelets. (A)** Schematic representation of Rap1 activation and inactivation in response to thrombin under non-aggregating and aggregating conditions. **(B)** Model of sequential activation of Rap1 induced by $Ca^{2+}$ (first wave) or PKC (second wave). This second wave is partially dependent on integrin αIIbβ3 (Franke *et al.*, 2000).

The first evidence that GEFs other than CalDAG-GEFI might regulate Rap1 in platelets came from the observation that CalDAG-GEFI knockout platelets, which exhibit impaired aggregation in response to most platelet agonists, display normal aggregation in response to PMA or elevated thrombin concentrations (**Figure I-12**). Similarly, CalDAG-GEFI knockout platelets show no defects in P-selectin and integrin αIIbβ3 activation, in response to high thrombin concentrations (Crittenden *et al.*, 2004).

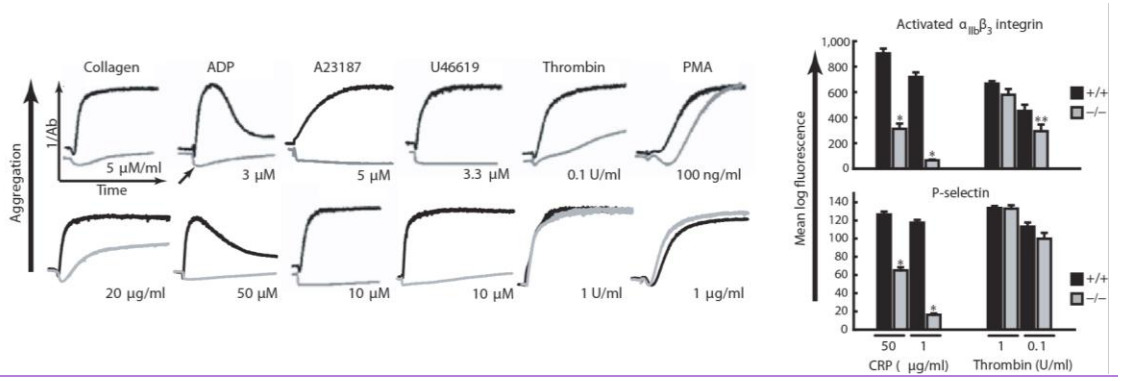


**Figure I-12. CalDAG-GEFI knockout platelets show normal aggregation and activation in response to high dose thrombin or PMA.** Left panel: aggregation assay, using CalDAG-GEFI knockout (grey) and wildtype (black) platelets, in response to collagen, ADP, A23187, U46619, thrombin and PMA. CalDAG-GEFI knockout platelets display impaired aggregation in response to most agonists, except high thrombin concentration and PMA. Right panel: Analysis of integrin αIIbβ3 activation and P-selectin exposure in CalDAG-GEFI knockout (grey) and wildtype (black) platelets, in response to different concentrations of CRP (collagen related peptide) and thrombin. CalDAG-GEFI knockout platelets present no defects in integrin αIIbβ3 activation and P-selectin exposure in response to high dose thrombin. A23187: Calcium ionophore; U46619: $TXA_2$ analogue. (Crittenden *et al.*, 2004).

The existence of a PKC-dependent pathway, alternative to CalDAG-GEFI, for the activation of Rap1 in platelets was confirmed by Cifuni *et al*., who demonstrated that CalDAG-GEFI and PKC are independent pathways used by thrombin to activate Rap1 in platelets (Cifuni *et al.*, 2008). This would suggest the existence of a GEF for Rap1, downstream PKC, distinct from CalDAG-GEFI.

Although the role of Rap1b GTPase in platelet homeostasis is not debatable, its involvement in platelet spreading its quite controversial. Using a systemic Rap1b knockout mouse model, Chrzanowska-Wodnicka and co-workers described that Rap1 is essential for platelet spreading (Chrzanowska-Wodnicka *et al.*, 2005). In the same line, Zhang *et al*., using a platelet-specific Rap1b knockout mouse model, found defective P-selectin exposure, δ-granule secretion, spreading on fibrinogen and clot retraction in Rap1b-knockout platelets (Zhang *et al.*, 2011). In contrast, using platelet-specific single and double Rap1a/Rap1b knockout platelets, Stefanini *et al*. established that Rap1b does not modulate platelet spreading. Specifically, while single Rap1a and Rap1b knockout platelets spread normally on fibrinogen, double Rap1a/1b knockout platelets show lower spread area and abnormal morphology, suggesting that each isoform could compensate for the loss of the other. However, Rap1b knockout platelets show significant reduced α-granule secretion and defective Rac1 activation at early points during the activation process. Furthermore, these defects in α-granule secretion are displayed only in response to GPVI, but not PAR4 stimulation (Stefanini *et al.*, 2018).

## 2.5. C3G regulates platelet aggregation and activation through the modulation of multiple pathways

Given that C3G expression has been detected in both human and mouse platelets (Rowley *et al.*, 2011), and based on the evidence of the existence of a GEF other than CalDAG-GEFI that would activate Rap1 downstream PKC, our group began to study the role of C3G in platelet function.

Using transgenic mouse models that overexpress full-length C3G (tgC3G) or a mutant form in which C3G lacks the catalytic domain (tgC3GΔCat), specifically in MKs and platelets, we demonstrated that C3G regulates platelet function. TgC3G platelets show increased platelet activation and aggregation accompanied by decreased bleeding time. Consistently, tgC3GΔCat platelets present impaired platelet activation and aggregation and higher bleeding times. Furthermore, we identified C3G as the Rap1 GEF responsible for Rap1 activation by PKC, since the inhibition of PKC with bisindolylmaleimide (BIS) completely abrogated the increased platelet activation induced by the transgenic expression of C3G (Gutierrez-Herrero *et al.*, 2012).

In addition, our group demonstrated that in response to thrombin and PMA, platelet C3G is phosphorylated in Tyr residues by a mechanism involving PKC and Src (Gutierrez-Herrero *et al.*, 2020). Furthermore, C3G is activated by p38/ERK MAPKs through two different pathways. On the one hand, p38/ERK induces $TXA_2$ synthesis, which, after its release, interacts with its receptor triggering C3G phosphorylation by Src. On the other hand, p38/ERK inhibits Shp2 phosphatase, which is involved in C3G dephosphorylation and inactivation. Moreover, C3G regulates $TXA_2$ synthesis through inhibition of $PLA_2$ phosphorylation. Finally, C3G also participates in the ADP-P2Y12-PI3K pathway that activates Rap1 (Gutierrez-Herrero *et al.*, 2020) (Figure I-13).

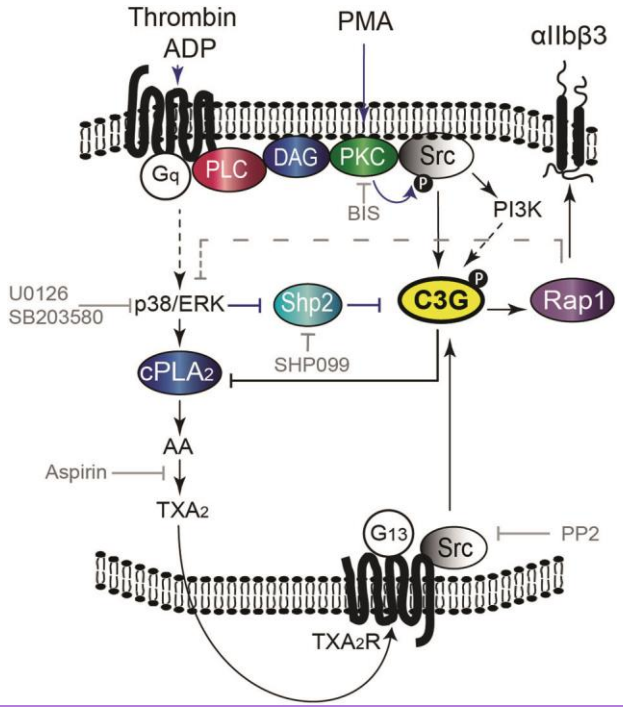


**Figure I-13. C3G modulates platelet activation and aggregation by regulating major signaling pathways.** C3G participates in the second wave of Rap1 activation after thrombin stimulation. C3G is phosphorylated in tyrosine residues through PKC-Src pathway. C3G phosphorylation is also regulated by p38/ERK through the inhibition of Shp2 tyrosine phosphatase, or the production of $TXA_2$. C3G participates in the PI3K-Rap1 pathway activated by ADP and regulates $TXA_2$ synthesis through a negative feedback loop involving the inhibition of $PLA_2$. Inhibitors of different components of the pathways are indicated in grey (Gutierrez-Herrero *et al.*, 2020).

## 2.6. PKC function in platelets

Several studies have demonstrated that PKC proteins play an essential role in platelet function. PKC proteins are a family of serine/threonine kinases that include twelve isoforms divided into three groups based on their structure: conventional, novel and atypical (Nishizuka, 1986; 1988; Harper & Poole, 2010).

Conventional or classical PKC (cPKC) isoforms include PKCα, βI, βII and γ, which contain a tandem C1 domain capable of binding to DAG, and a $Ca^{2+}$ binding C2 domain. Novel PKC (nPKC) isoforms (PKCθ, δ, η and ε) lack the ability to bind $Ca^{2+}$ but preserve a functional C1 domain (Harper & Poole, 2010). The C1 domain is also activated by phorbol esters such as PMA and is responsible for the translocation of PKC to the PM. Finally, atypical isoforms are PKCζ , ι, λ and μ, which are insensitive to $Ca^{2+}$ and to DAG, and only respond to PS (Harper & Poole, 2010).

Human platelets express cPKC α and β and nPKC δ, η and θ, whereas mouse platelets express cPKC α and β and nPKC δ, η, ε and θ (Harper & Poole, 2010). Several studies, using knockout mouse models and specific inhibitors have revealed some of the functions of each PKC isoform in platelets (**Table I-3**).

PKCα positively regulates platelet function by modulating platelet activation and aggregation through integrin αIIbβ3 activation. However, it does not modulate platelet spreading (Konopatskaya *et al.*, 2009). In contrast, although the role of PKCβ is less studied, it has been associated with platelet spreading (Buensuceso *et al.*, 2005; Gilio *et al.*, 2010).

As for nPKCs, they can positively or negatively regulate platelet function, although there are some discrepancies in the literature (Harper & Poole, 2010). Pula and co-workers reported that PKCδ does not regulate δ-granule secretion or integrin αIIbβ3 activation, and that it plays a negative role in platelet aggregation (Pula *et al.*, 2006). However, Chari *et al*. have described a dual role for PKCδ in granule secretion and platelet aggregation depending on the stimulus; a negative role in GPVI signaling and a positive role in PAR signaling (Chari *et al.*, 2009). On the other hand, Nagy and co-workers described that PKCθ has a positive role in granule secretion and platelet aggregation at low-dose agonists (Nagy *et al.*, 2009), while Hall *et al*. described opposite functions for PKCθ in α-granule secretion and integrin αIIbβ3 activation, that is, a negative role in aggregation and δ-granule secretion (Hall *et al.*, 2008; Gilio *et al.*, 2010). Finally, PKCε exhibits a positive role in δ-granule secretion and platelet aggregation (Pears *et al.*, 2008).

**Table I-3. Role of different PKC isoforms in platelets.** The effect of knockout mouse models for each PKC isoforms in integrin αIIbβ3 activation, granule secretion, platelet aggregation and spreading is indicated. ↓: decrease; ↑: increase; =: no effect; -: not studied; C: after GPVI (collagen) stimulation; P: after PAR (thrombin) stimulation; g: granule.

| Knocked out protein | Integrin αIIbβ3 activation | α-g secretion | δ-g secretion | Platelet aggregation | Spreading | Reference |
|---|---|---|---|---|---|---|
| **α** | ↓ | ↓ | ↓ | ↓ | = | (Konopatskaya *et al.*, 2009) |
| **β** | - | - | - | - | ↓ | (Buensuceso *et al.*, 2005; Gilio *et al.*, 2010) |
| **δ** | - | ↑C<br>↓P | ↑C<br>↓P | ↑C<br>↓P | - | (Chari *et al.*, 2009) |

| Knocked out protein | Integrin αIIbβ3 activation | α-g secretion | δ-g secretion | Platelet aggregation | Spreading | Reference |
|---|---|---|---|---|---|---|
| | = | - | = | ↑ | ↓ | (Pula *et al.*, 2006) |
| θ | ↓ | ↓ | ↓ | - | - | (Nagy *et al.*, 2009) |
| | ↑ | ↑ | = | = | ↓ | (Hall *et al.*, 2008) |
| ε | - | - | ↓ | ↓ | = | (Pears *et al.*, 2008) |

Finally, it has been reported that PKCα and PKCδ can be phosphorylated on tyrosine residues by Src kinases in human platelets (Murugappan *et al.*, 2005; Hall *et al.*, 2007).

One of the main functions of PKC in platelets is the regulation of granule secretion. Although an increase in intracellular $Ca^{2+}$ is enough to induce granule secretion, PKCs amplify calcium response. In addition, PKCs regulate the interactions of platelet SNARE proteins through phosphorylation. In particular, PKCs phosphorylate Munc18 and inhibit its interaction with syntaxins (Stx), thereby enhancing platelet secretion (Reed, 2004). Moreover, PKCs also phosphorylate Stx4 and SNAP23, modulating their interaction and promoting exocytosis (Chung *et al.*, 2000).

## 2.7. Cytoskeleton remodelling in platelets

Several studies have described a crucial role of the cytoskeleton in platelet function. Under resting conditions it maintains the platelets with a discoid shape, while after platelet activation it rapidly remodels to form different structures, such as filopodia or lamellipodia. In addition, the platelet cytoskeleton facilitates granule secretion and stabilizes platelet aggregates and thrombi (Aslan & McCarty, 2013; Bender & Palankar, 2021). There are two main cytoskeletal components in platelets: the actin cytoskeleton and the microtubules (Thon & Italiano, 2012).

### 2.7.1. Microtubules

Microtubules are made up of lateral-associated protofilaments formed by heterodimers of α- and β-tubulin (Cuenca-Zamora *et al.*, 2019). Platelets express α, β and γ-tubulin (the latter participating in the initiation of polymerization), with β-tubulin being the most abundant (Rowley *et al.*, 2011). Under resting conditions, microtubules form a marginal ring (known as microtubule coil), which is necessary to maintain the discoid shape of the platelet (Schwer *et al.*, 2001). After platelet activation, the microtubule coil centralizes to allow for a change in shape and spreading (Cuenca-Zamora *et al.*, 2019). Microtubules not only regulate platelet shape, but also modulate granule secretion and platelet aggregation (Berry *et al.*, 1989). However, other studies describe that the actin cytoskeleton and not the microtubules, is the one that regulates δ-granule secretion (Ge *et al.*, 2012).

### 2.7.2. Actin cytoskeleton

Platelets contain a large amount of actin, which is involved in platelet shape. Following platelet activation, there is an increase in actin polymerization (F-actin *versus* G-actin), which triggers the elongation and organization of actin filaments (Bearer *et al.*, 2002).

In response to platelet activation, the cytoskeleton undergoes a series of morphological changes: initial spherification, attachment, spreading and finally contraction. Once the platelets adhere, they begin to spread and form filopodia and lamellipodia (Cerecedo, 2013).

Filopodia and lamellipodia differ in their actin organization and their function. While filopodia are fine protrusions containing barbed-end parallel actin filaments and are important in sensing the environment, lamellipodia are short or branched orthogonal actin networks, essential for wound sealing (Cerecedo, 2013; Bender & Palankar, 2021).

### 2.7.2.1. Actin polymerization

Actin is an ATPase, with ATP hydrolysis being the main regulator of the balance between G- and F-actin. G-actin polymerizes to F-actin to form actin fibers which area organized into two interlaced protofilaments that compose a double helix. Actin filaments are polar, i.e., they have two different ends: a barbed (or +) end and a pointed (or -) end. ATP-bound G-actin monomers are incorporated into the barbed end, whereas F-actin depolymerization occurs when ADP-actin monomers dissociate from the pointed end (Dominguez, 2009).

Actin fiber formation can be spontaneous or facilitated by actin nucleators and actin elongators. F-actin polymerization is divided into two steps: nucleation (a new filament is formed) and elongation (incorporation of G-actin monomers into the barbed end of the filament) (Krause & Gautreau, 2014). Spontaneous nucleation begins with the formation of an F-actin nucleus by the association of three actin monomers; the filament is then elongated by the incorporation of G-actin. Spontaneous filament formation is kinetically unfavourable because actin dimer is unstable (Goley & Welch, 2006; Krause & Gautreau, 2014). Several actin nucleators (such as formins or Arp2/3 complex) and actin elongators (ENA/VASP) facilitate F-actin formation (**Figure I-14**) (Krause & Gautreau, 2014). Furthermore, while profilin participates in actin elongation, through recruitment of actin to the barbed end, cofilin regulates actin depolymerization, by binding to actin monomers and inhibiting nucleotide exchange. Hence, both proteins regulate actin turnover (Pollard, 2016).

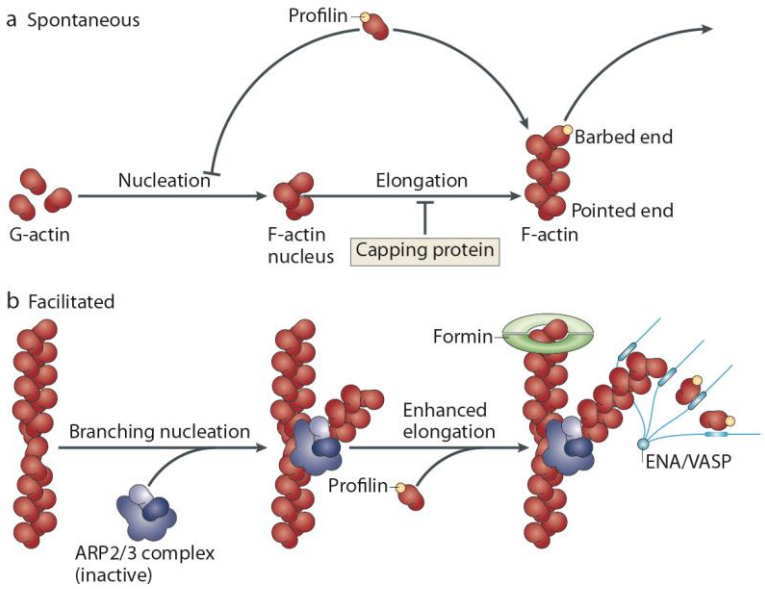

**Figure I-14. Actin polymerization process.** Schematic representation of the two modes of actin fiber formations: **(a)** spontaneous, in which three G-actin monomers bind to form an F-actin nucleus and then elongate; and **(b)** facilitated, in which actin nucleators, such as Arp2/3 complex, create a new actin filament from a pre-existing one and whose elongation is mediated by formin and VASP proteins (Krause & Gautreau, 2014).

The role of proteins related to the cytoskeleton, based on studies on knockout models, is summarized in Table I-4 and will be explained below.

**Table I-4. Role of different actin-related proteins.** The effect of their knockouts on integrin αIIbβ3 activation, granule secretion, platelet aggregation, platelet spreading and clot retraction is indicated. ↓: decreased; ↑: increased; =: no effect; -: no studied; d: debatable; g: granule.

| Knocked out protein | Integrin αIIbβ3 activation | α-g secretion | δ-g secretion | Platelet aggregation | Spreading | Clot retraction | Reference |
|---|---|---|---|---|---|---|---|
| **Arp2** | ↓ | ↓ | = | ↓ | ↓ | ↓ | (Paul *et al.*, 2017) |
| **VASP** | ↑ | - | - | ↑ | - | - | (Aszodi *et al.*, 1999) |
| **WASP** | d | - | - | - | ↓ | ↓ | (Tsuboi *et al.*, 2006; Shcherbina *et al.*, 2010) |
| **Rac1** | ↓ | ↓ | ↓ | ↓ | ↓ | ↓ | (McCarty *et al.*, 2005; Flevaris *et al.*, 2009; Pleines *et al.*, 2009) |
| **Cdc42** | - | d | d | ↑ | d | - | (Pleines *et al.*, 2010) |
| **RhoA** | ↓ | ↓ | ↓ | ↓ | = | ↓ | (Pleines *et al.*, 2012) |

### Actin nucleators and their role in platelets

The Arp2/3 complex is the major actin nucleating molecular machine and is made up of seven subunits: Arp2, Arp3, ArpC1, ArpC2, ArpC3, ArpC4 and ArpC5. Arp2 and Arp3 mimic the barbed end of an actin filament, creating a new filament from the side of an existing (mother) filament in a Y-branch configuration with a regular 70 ° branch angle (Goley & Welch, 2006; Molinie & Gautreau, 2018). The Arp2/3 complex needs to be activated by nucleation-promoting factors (NPFs). When the Arp2/3 complex is in an inactive conformation, Arp2 and Arp3 subunits are separated, whereas after activation by NPFs or ATP, these subunits bind and mimic the barbed end of the filament (Figure I-15) (Molinie & Gautreau, 2018).

The Arp2/3 complex plays an essential role in platelet function. Specifically, deletion of Arp2 in platelets triggers alterations in cytoskeletal remodelling, affecting lamellipodia formation, F-actin polymerization during platelet spreading, and platelet shape. In addition, Arp2 knockout platelets show defective integrin αIIbβ3 activation and α-granule secretion, but normal platelet aggregation and δ-granule secretion (Paul *et al.*, 2017).

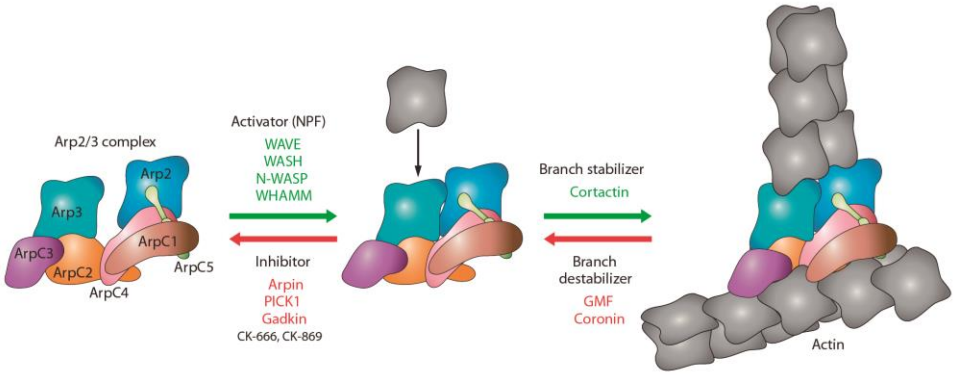


**Figure I-15. Conformational changes in the Arp2/3 complex.** Schematic representation of the inactive Arp2/3 complex (left), its active conformation (middle) and the newly formed branched filament (right). The activators or NPFs (in green), the inhibitors (in red) and the branch stabilizer (cortactin) and destabilizers (GMF and coronin) are indicated. CK-666 is the Arp2/3 inhibitor used in research. NPF: nucleation-promoting factor (Molinie & Gautreau, 2018).

There are four different families of NPFs in the human genome: WAVE, N-WASP, WASH, and WHAMM, based on their structure and function (Rotty *et al.*, 2013). These different NPF families serve various purposes: the WAVE family is associated to lamellipodia formation, while the N-WASP and WASH families are related to filopodia formation and endosomes, respectively (Miki *et al.*, 1998; Duleh & Welch, 2010). Finally, the WHAMM family is involved in ER to Golgi trafficking (Krause & Gautreau, 2014; Molinie & Gautreau, 2018). Yet, some studies have demonstrated that in the absence of an specific NPF other NPF families can act in its place; e.g., N-WASP can promote lamellipodia formation in the absence of WAVE (Veltman *et al.*, 2012).

The WAVE family is widely studied in platelet function. Platelets express three WAVE isoforms: WAVE1, WAVE2 and WAVE3, all of them involved in the reorganization of the actin cytoskeleton, following integrin-mediated aggregation (Oda *et al.*, 2005). All WAVE isoforms are found in a stable complex with ABI, CYFIP, NAP1 and BRK1 proteins (Molinie & Gautreau, 2018). WAVE proteins are located at the edge of the lamellipodia and constitute the main effector of Rac GTPases. In platelets WAVE2 has a predominant location in the lamellipodia, while WAVE1 and WAVE3 are located in dots throughout the cell (Oda *et al.*, 2005).

The N-WASP family (consisting of the ubiquitous N-WASP and the hematopoietic WASP) has also been studied in platelets, because WASP mutations are associated with Wiskott-Aldrich syndrome (WAS) (Imai *et al.*, 2003), which triggers thrombocytopenia and defects in integrin αIIbβ3 outside-in signaling (Shcherbina *et al.*, 2010). N-WASP proteins are effectors of Cdc42 GTPase in filopodia formation. Some studies revealed that WASP is required for outside-in signaling, with WASP-defective platelets showing defects in spreading and clot retraction (Shcherbina *et al.*, 2010). However, other studies demonstrated normal Arp2/3 activation in platelets lacking WASP, with normal filopodia and lamellipodia formation and no defects in platelet spreading (Falet *et al.*, 2002). In addition, there is also controversy on the role of WASP in inside-out platelet signaling. Some authors describe a role of WASP in integrin αIIbβ3 activation (Tsuboi *et al.*, 2006), while others claim that WASP does not participate in this process (Shcherbina *et al.*, 2010).

### Actin elongators and their role in platelets

VASP, a member of the ENA/VASP family of proteins, is an actin elongator that protects the barbed ends from being capped, and recruits profiling-bound G-actin to promote actin polymerization. VASP is located at the edge of lamellipodia and the tip of filopodia (Krause & Gautreau, 2014). There is conflicting information about the role of VASP in platelet function. In one report, VASP was described to play a positive role in platelet function, promoting platelet aggregation through Rap1 activation (Aszodi *et al.*, 1999). However, using VASP knockout platelets, another study showed that VASP negatively modulates P-selectin exposure and integrin αIIbβ3 activation (Hauser *et al.*, 1999). A more recent report has described that VASP modulates Rap1 function via VASP-CrkL-C3G in parallel to the CalDAG-GEFI pathway (Benz *et al.*, 2016). VASP function in platelets is negatively regulated by its phosphorylation by PKA and PKC on Ser157 and by PKG on Ser329 (Harper & Poole, 2010; Benz *et al.*, 2016).

## 2.7.2.2. GTPases involved in actin cytoskeleton remodelling

The Rho family of GTPases is the main regulators of cytoskeleton remodelling. Within this family, RhoA, Cdc42 and Rac1 are important players in platelet function (Aslan & McCarty, 2013). Each of these GTPases has a defined role: RhoA is associated with contraction, stress fiber formation and microtubule stabilization; Cdc42 is related to filopodia formation and Rac1 with the formation of lamellipodia (Figure I-16) (Elvers, 2016).

RhoA is the most highly expressed Rho isoform in platelets. It regulates actomyosin contractility, so that the platelet returns to its spherical shape after platelet activation. RhoA has a complex regulation in platelets. Thus, after initial activation, integrin αIIbβ3 signaling inhibits it to allow platelet spreading, but at later stages RhoA is activated again to stabilize thrombi and promote clot retraction (Goggs *et al.*, 2015). In addition to platelet shape, RhoA also regulates platelet aggregation, platelet secretion and integrin αIIbβ3 activation after GPCR stimulation (Pleines *et al.*, 2012).

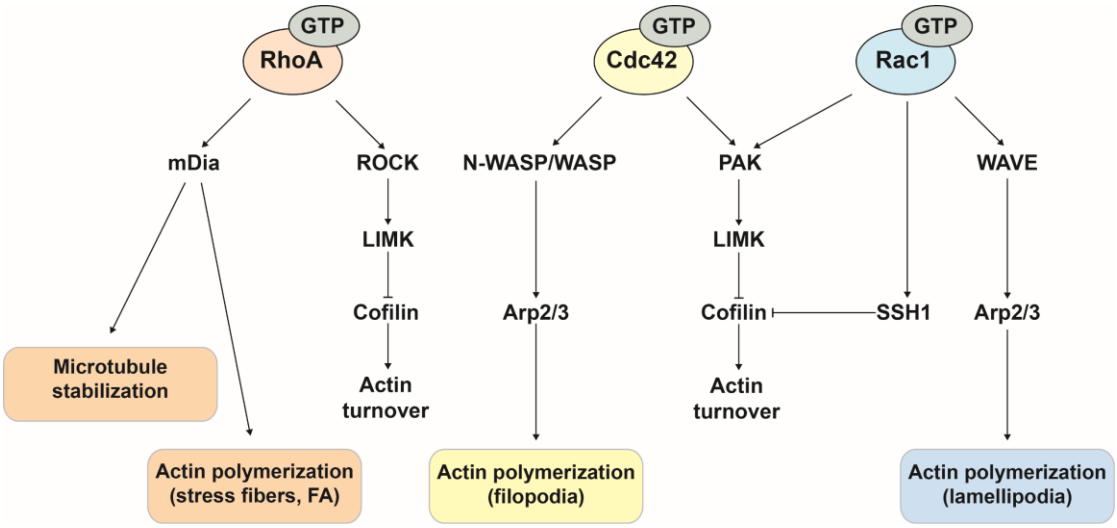


**Figure I-16. Schematic representation of signaling downstream of Rho GTPases**. The different effectors of RhoA, Cdc42 and Rac1 are indicated. Activated RhoA interacts with NPF mDia to stabilize microtubules and to induce actin polymerization to form stress fibers and focal adhesions. Cdc42-GTP interacts with NPF N-WASP/WASP to activate the Arp2/3 complex during filopodia formation. Activated

Rac1 stimulates NPF WAVE to activate the Arp2/3 complex and form lamellipodia. All of them induce the activation of LIMK, thus inhibiting cofilin, RhoA through ROCK and Rac1/Cdc42 through PAK. FA: focal adhesion; NPF: nucleation-promoting factors.

In platelets, the most predominant Rac isoform is Rac1, which is essential for platelet function. Rac1 regulates the WAVE/Arp2/3 pathway, leading to lamellipodia formation during spreading (McCarty *et al.*, 2005). In addition, Rac1 is involved in integrin αIIbβ3 activation, granule secretion and thrombi stabilization (Pleines *et al.*, 2009). Although the regulation of clot retraction is associated with RhoA GTPases, Flevaris and co-workers demonstrated that Rac1 also controls this process (Flevaris *et al.*, 2009). There is a crosstalk between Rac1 and Rap1 in platelets; while Rac1 regulates Rap1 activation through modulation of PLCγ2, Rap1 also regulates Rac1 through activation of its GEFs, Vav2 and Tiam1 (Stefanini *et al.*, 2012). The participation of Rap1 and Rac1 in a common pathway regulating cell spreading, has also been described in v-Abl-transformed NIH3T3 fibroblasts (Lee *et al.*, 2008).

Cdc42 is commonly associated with filopodia formation; however, its role in platelets is still unclear due to conflicting results. Some authors describe Cdc42 as a critical player during filopodia formation (Akbar *et al.*, 2011), while others observed that Cdc42 knockout platelets form normal filopodia during platelet spreading (Pleines *et al.*, 2010). Similarly, the role of Cdc42 in platelet secretion is controversial; Pleines *et al*. point to a negative role, while Akbar and co-workers detailed that it positively modulates platelet secretion.

#### 2.7.2.3. Role of C3G in the remodelling of the actin cytoskeleton in platelets

Previous results from our group suggest that C3G may play a role in platelet spreading. Indeed, C3G overexpression triggers increased spreading capacity on poly-L-lysine. Furthermore, this role could be independent on its catalytic activity, since C3GΔCat overexpression also increases spreading (Martin-Granado *et al.*, 2017). Its involvement in spreading suggests a role for C3G in the remodeling of the actin cytoskeleton in platelets.

## 2.8. Focal adhesion in platelet function

Focal adhesions (FAs) are large structures that connect the actin cytoskeleton to the ECM via integrin clusters and scaffold proteins that mediate outside-in signaling (Ivaska, 2012). The formation of FAs is triggered by cell adhesion to specific ligands of the ECM via integrin receptors, inducing the recruitment of scaffold proteins and cytoskeletal components (Romer *et al.*, 2006). FAs are made up of proteins that connect the actin cytoskeleton directly to integrins, or indirectly through adapters (Ciobanasu *et al.*, 2013). Additionally, proteins that form FAs can be divided into three different groups: i) structural proteins: actin, VASP, vinculin, talin, paxillin or α-actinin; ii) enzymatic proteins (kinases): Abl, focal adhesion kinase (FAK) or Src; iii) adapters: p130Cas, Crk or DOCK180 (Lo, 2006).

In platelets, FAs participate in both inside-out and outside-in integrin signaling. During outside-in signaling, integrin αIIbβ3 is activated by its interaction with ECM components. FAK is then recruited by talin and autophosphorylated creating docking sites for Src. Src, in turn, phosphorylates FAK creating binding sites for various proteins, such as paxillin, p130Cas, Syk, PI3K, PLCγ, etc (Mitra *et al.*, 2005; Tapial Martinez *et al.*, 2020). Talin, kindlin and vinculin link

integrin to the actin cytoskeleton. Additionally, talin and kindlin are also involved in inside-out signaling by controlling the conformational change of the extracellular domain of the integrin αIIbβ3 (Huang *et al.*, 2019). The role of FA proteins in platelet function has been widely studied. FAK plays an important role in platelet adhesion and spreading on fibrinogen, however it does not regulate inside-out signaling, which is instead controlled by Pyk2 kinase (Guidetti *et al.*, 2019). Surprisingly, vinculin does not regulate either platelet function or platelet adhesion (Mitsios *et al.*, 2010).

Additionally, previous results from the group unveiled a role of C3G in FA formation and maturation in K562 cell line. In fact, C3G acts as a positive regulator of cell adhesion, however the overexpression and its absence have an inhibitory effect in the expression of FA proteins (Maia *et al.*, 2009).

## 2.9. Platelet secretion

Platelet secretion plays an important role in the regulation of hemostasis, thrombosis, angiogenesis or inflammation. There is controversy about the content released after platelet activation. Some authors describe that the cargo released depends on the agonist (Italiano *et al.*, 2008; Italiano & Battinelli, 2009; Chatterjee *et al.*, 2011), while others state that there are no functional patterns in platelet secretion and that agonists only influence the kinetics and extent of the secretion (van Holten *et al.*, 2014).

### 2.9.1. Granule secretion

Upon platelet activation, which involves changes in platelet shape, granules centralize and fuse with the OCS, releasing their content into its channels, or with the PM (Gremmel *et al.*, 2016). Prior to fusion to PM/OCS, the granules can be fused together (so-called compound fusion) (Eckly *et al.*, 2016). Granule secretion is controlled by Soluble N-ethylmaleimide-sensitive factor Attachment protein REceptors (SNAREs). SNAREs are classified based on their location: v-SNAREs (vesicle-SNAREs) located on granules or t-SNAREs (target-SNAREs) situated on PM/OCS. Both SNAREs associate to form a complex that links the two membranes prior fusion. Multiple proteins regulate SNARE function, such as Sec/Munc18 proteins, Rab GTPases, Munc13 proteins or the exocyst complex (Joshi & Whiteheart, 2017).

The exocytosis process can be divided into five different steps: 1) targeting, when the vesicles are transported to the PM; 2) tethering/docking, in which the vesicles are in contact with the PM and initial association of SNARE proteins occurs; 3) priming, characterized by the formation of the trans-SNARE complex and, 4) fusion, in which the vesicle membrane and PM are fused and cargo is released (**Figure I-17**).

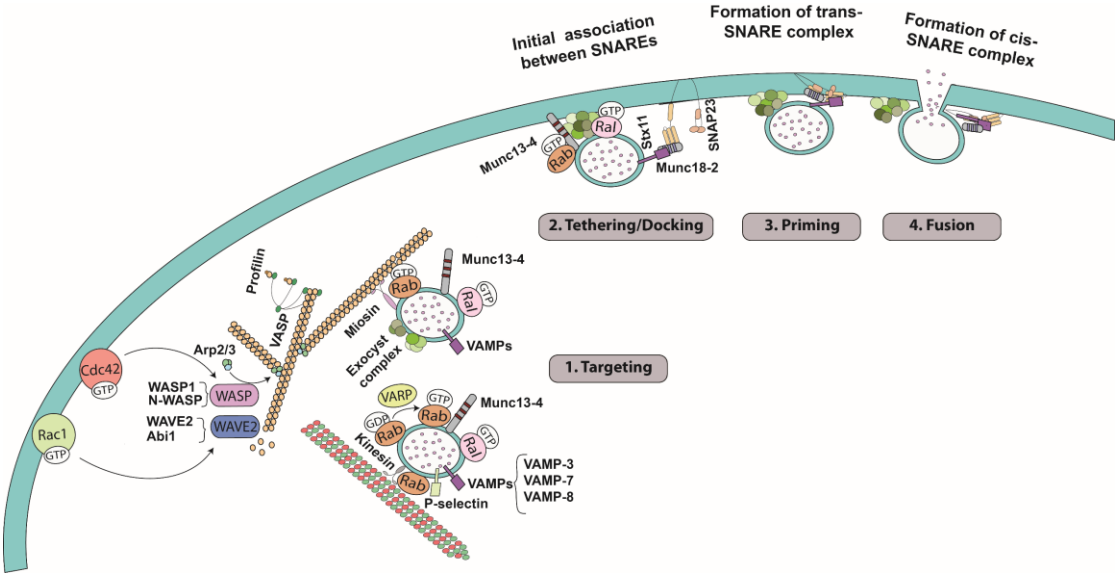


**Figure I-17. Schematic diagram of granule secretion in platelets, highlighting the different steps: targeting, tethering/docking, priming and fusion.** SNARE: Soluble N-ethylmaleimide-sensitive factor (NSF) Attachment protein REceptor, VAMP: Vesicle Associated Membrane Protein.

### Targeting

Granules are transported to the PM via microtubules and the actin cytoskeleton (Rendu & Brohard-Bohn, 2001). Vesicle transport is regulated by Rab GTPases through their interaction with effectors that controls actin motor proteins, such as myosin and kinesin, or microtubule-interacting proteins, such as dynein (Fukuda, 2013).

There are 40 Rab members expressed in platelets, with Rab27b being the most abundant isoform. Rab27b is associated with the packing and secretion of δ-granules but not α-granules, and its absence triggers impaired aggregation and bleeding diathesis in mice (Tolmachova *et al.*, 2007). Other Rab isoforms have been studied in platelets; thus, while Rab4 is associated with α-granule secretion (Shirakawa *et al.*, 2000), Rab28/32 are associated to δ-granules (Aguilar *et al.*, 2019). In addition, Rab GTPases also modulate other exocytic steps, such as tethering and docking, through interaction with their Munc13 effector proteins (Chicka *et al.*, 2016).

Molecular motors also have a crucial role in platelet function. Indeed, Kinesin 1 knockout platelets show impaired aggregation and altered α-granule and δ-granule secretion (Adam *et al.*, 2018).

### Tethering/Docking

After targeting to the PM, vesicles begin to bind to their target membranes via tethering/docking factors, such as the exocyst complex, Munc13 and Munc18 proteins (Hong & Lev, 2014). According to some authors, the initial contact of the granules with the PM occurs in two different steps: tethering and docking, defining tethering when the vesicles are between 1-25 nm from the PM, while in the docked vesicles there is no separation between the two membranes (Gracheva *et al.*, 2010). However, there is no agreement on the limits of those steps, nor the proteins related to each step.

The exocyst complex is a conserved octameric complex that regulates polarized secretion and initial contact between vesicles and PM. Exocyst complex consists of two different subcomplexes (SC): SCI, formed by Sec3 (EXOC1), Sec5 (EXOC2), Sec6 (EXOC3) and Sec8 (EXOC4); and SCII, made up of Sec10 (EXOC5), Sec15 (EXOC6), Exo70 (EXOC7) and Exo84 (EXOC8). Individual SCs can associate granules to PM independently, however interaction between the two SCs stabilizes tethering. After vesicle tethering, Sec3 leaves the PM, while the other subunits remain (**Figure I-18**) (Nishida-Fukuda, 2019). The role of the Sec6 subunit in platelets has been studied. Sec6 knockout platelets present defects in platelet aggregation, granule secretion and integrin αIIbβ3 activation under GPVI stimulation (Walsh *et al.*, 2021).

The exocyst complex is targeted to the PM by Ral GTPases. Indeed, Sec5 and Exo84 are Ral effectors (Walsh *et al.*, 2019). In platelets there are two Ral isoforms, RalA and RalB. Initially, Ral GTPases were associated with δ-granule secretion (Mark *et al.*, 1996), however, recent studies in RalA/B double knockout platelets revealed that RalA/B deletion has no effect on δ-granule secretion, but triggers a defect in P-selectin exposure, albeit with normal cargo release. This phenomenon is called kiss-and-run exocytosis (Wersall *et al.*, 2018), and will be explained below (see **Figure I-19**). The exocyst complex is also regulated by Rab, TC10 and Cdc42 GTPases (Nishida-Fukuda, 2019; Rossi *et al.*, 2020).

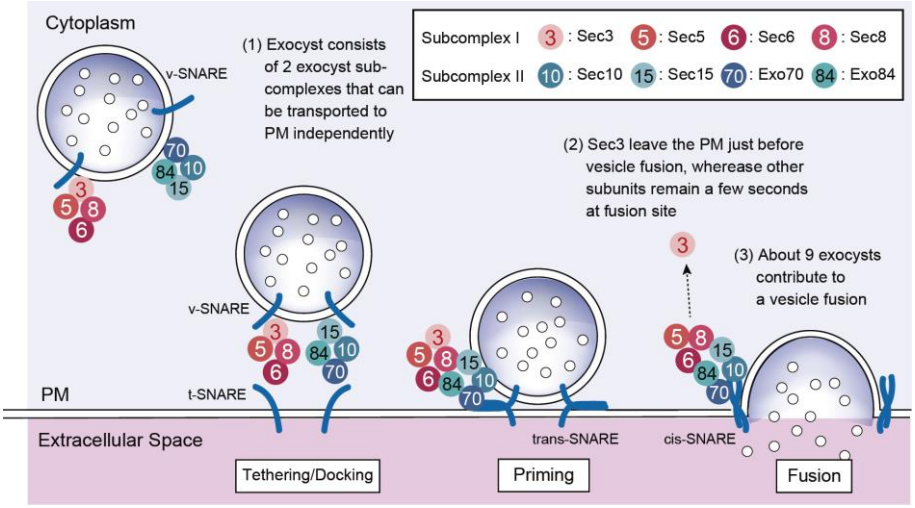


**Figure I-18. Assembly model of the exocyst complex during granule exocytosis**. The vesicle arrives at the PM with the individual subcomplexes separated. During priming, both subcomplexes fuse and stabilize vesicle tethering. Sec3 is released before fusion, whereas the other subunits remain for a few seconds. PM: plasma membrane; SNARE: Soluble N-ethylmaleimide-sensitive factor Attachment protein REceptor; v-SNARE: vesicle-SNARE; t-SNARE: target-SNARE (Nishida-Fukuda, 2019).

Munc13 proteins are a family of exocytosis regulators that have multiple $Ca^{2+}$ and PS-binding domains. There are four Munc13 isoforms, with Munc13-4 being the most abundant (Rowley *et al.*, 2011). Munc13-4 is a Rab27 effector that bridges vesicles and PM/OCS in a calcium-dependent manner, facilitating membrane fusion (Chicka *et al.*, 2016). Consistently, Munc13-4 knockout platelets show impaired granule secretion and defective integrin αIIbβ3 activation and platelet aggregation (Savage *et al.*, 2013; Cardenas *et al.*, 2018). Mutations in Munc13-4 are related to the familial hemophagocytic lymphohistiocytosis (FHL) type 3 disorder characterized, indeed, by defects in platelet granule secretion, among others (Nakamura *et al.*, 2015).

Other tethering/docking regulators are the members of the Sec/Munc family, which regulate fusion events through interaction with SNARE proteins. Thus, Munc18 regulates the trafficking of t-SNARES Stxs to their target membrane and its activation. Indeed, Munc18 keeps Stx proteins in a closed conformation until their interaction with Munc13 proteins, which catalyze the transition of Stx to an open conformation and favors association between SNAREs. There are three Sec/Munc isoforms in platelets, but only Munc18-b (also known as STXBP2 or Munc18-2) regulates platelet secretion. In addition, Munc18-b also modulates platelet aggregation and thrombus formation (Cardenas *et al.*, 2019). Consistently, Munc18-b mutations cause FHL type 5 syndrome (zur Stadt *et al.*, 2009).

### Priming

Priming is achieved by partial association of v-SNAREs with t-SNAREs (Li *et al.*, 2016). Specifically, three coiled-coil domains on t-SNAREs engage a single coiled-coil domain on a v-SNARE forming a 4-helix bundle that constitutes the trans-SNARE complex, which drives membrane deformation and fusion (**Figure I-18**). In addition, Munc13 interacts with Munc18 and allows t-SNARE Stx to interact with the other exocytic SNARE proteins (Ma *et al.*, 2011). After that, Munc18 directly interacts with the trans-SNARE complex to stabilize it and facilitate membrane fusion (Cardenas *et al.*, 2019).

Vesicle-Associated Membrane Proteins (VAMPs) are the major group of v-SNAREs. Platelets contain different VAMP isoforms, with VAMP-8 (also called endobrevin) and VAMP-7 (known as TI-VAMP or synaptobrevin) being the most abundant. VAMP-8 knockout platelets show impaired granule secretion and defective thrombus formation (Graham *et al.*, 2009). Furthermore, the absence of VAMP-7 induces defects in granule secretion and in platelet spreading (Koseoglu *et al.*, 2015). In addition, VAMP-3 isoform is related to endocytosis (Lowenstein, 2017).

Regarding t-SNAREs, platelets express both Stxs and SNAPs (Synaptosome Associated Proteins) proteins, of these, Stx11 and SNAP23 play a crucial role in platelet secretion. Indeed, ablation of SNAP-23 in platelets induces defects in granule secretion and platelet aggregation (Williams *et al.*, 2018), while absence of Stx11 triggers defects in granule secretion with normal integrin αIIbβ3 activation. Consistently, mutations in the *STX11* gene are associated with FHL type 4 syndrome (Ye *et al.*, 2012). Stx11 is associated with all granules, while Stx8 is associated with δ-granules (Golebiewska *et al.*, 2015).

### Fusion

Once the trans-SNARE complex is assembled, its C-terminal region further zippers up to provide energy to the membranes and induces fusion and cargo release. Membrane fusion involves the apposition of two membranes, which requires removal of the hydration layers, local membrane bending, merging of the two proximal leaflets, and formation of the fusion pore (Nishida-Fukuda, 2019). After membrane fusion, the SNARE complex changes its conformation to a cis-SNARE or a low-energy state (Sudhof & Rothman, 2009) (**Figures I-17 and I-18**).

Opening a fusion pore is not sufficient to ensure normal exocytosis, known as fuse and collapse. Once the pore is formed, it dilates and expands, leading to a fuse and collapse

exocytosis (also known as full-fusion), which involves vesicle membrane incorporation. Alternatively, the pore can reseal and the vesicle recycles, triggering a kiss-and-run phenotype (An *et al.*, 2021) (Figure I-19). Kiss-and-run exocytosis is often considered to release the vesicle cargo slowly and partially; however, kiss-and-run exocytosis can also open a large pore, ensuring a rapid and complete cargo release. This suggests that kiss-and-run events can secrete cargo just as fast as fuse and collapse events (Wu *et al.*, 2014).

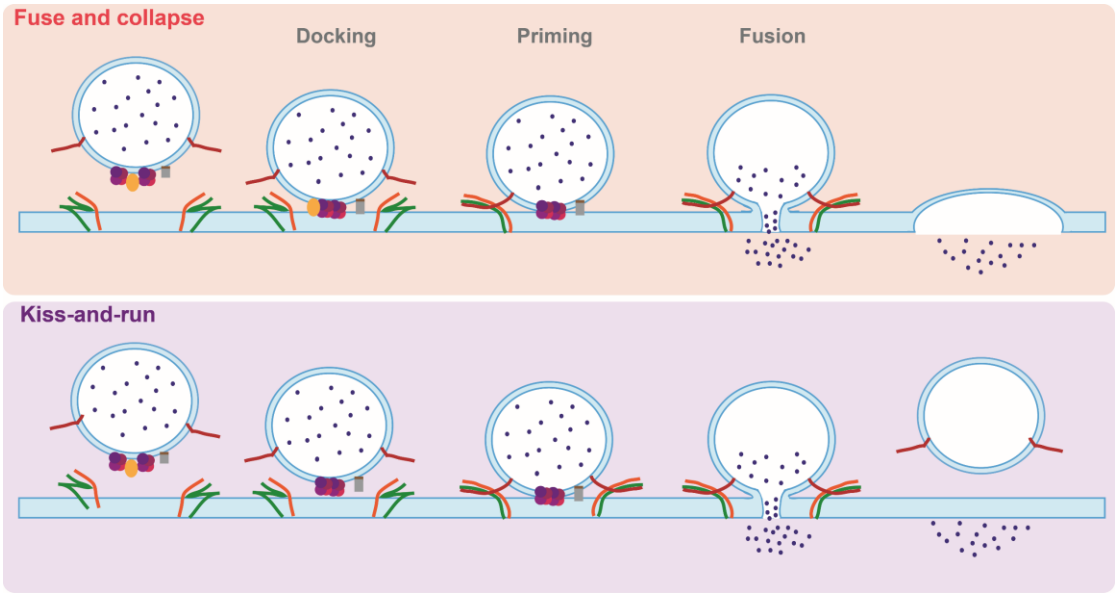


**Figure I-19. Scheme of the different exocytosis models: fuse and collapse and kiss-and-run.** Upper panel: representation of fuse and collapse exocytosis, where the vesicle membrane is fused to the PM. Lower panel: kiss-and-run exocytosis, where the cargo is released but the membrane is recycled. PM: plasma membrane.

Pore expansion is regulated by several proteins, such as the exocyst complex, which couples vesicle tethering and fusion through interaction with SNAREs. Multiple exocyst complexes are needed to promote the correct formation and spatial organization of SNARE complexes during fuse and collapse exocytosis (An *et al.*, 2021). On the other hand, the trans-SNARE complex regulates whether the cargo is released by transient (kiss-and-run) exocytosis, or by full-fusion, which involves irreversibly dilatation of the pore (Wu *et al.*, 2017). Furthermore, the formation of a large number of SNARE complexes is essential for pore expansion, whereas one or two SNARE complexes can open but not expand the pore, making it transient (Mion *et al.*, 2022). However, the number of complexes is not the limiting factor, nor is their dynamics or cargo release (Sharma & Lindau, 2018), but rather the restricted mobility of the SNARE complexes, which prevents the release of the complex needed for pore expansion. Indeed, four trans-SNARE complexes with restricted mobility promote the rapid formation of fusion pores but fail to expand and reclose them (Sharma & Lindau, 2018).

The role of granule secretion-related proteins in platelets has been revealed using knockout mouse models (Table I-5).

**Table I-5. Role of different proteins related to granule secretion in platelets, indicating the effect of their knockout in integrin αIIbβ3 activation, granule secretion, platelet aggregation and spreading.** ↓: decreased; ↑: increased; =: no effect; -: no studied; C: after GPVI (collagen) stimulation; P: after PAR (thrombin) stimulation; g: granule; Stx: Syntaxin.

| Knocked-out protein | Integrin αIIbβ3 activation | α-g secretion | δ-g secretion | Platelet aggregation | Spreading | Reference |
|---|---|---|---|---|---|---|
| **Rab27** | - | = | ↓ | ↓ | - | (Tolmachova *et al.*, 2007) |
| **Rab4** | - | ↓ | = | - | - | (Shirakawa *et al.*, 2000) |
| **Rab32/38** | ↓ | = | ↓ | ↓ | - | (Aguilar *et al.*, 2019) |
| **Munc13-4** | ↓ | ↓ | ↓ | ↓ | - | (Savage *et al.*, 2013; Cardenas *et al.*, 2018) |
| **Sec6** | ↓C ↑P | ↓ | ↓C ↑P | ↓ | - | (Walsh *et al.*, 2021) |
| **RalA/B** | = | Kiss-and-run | = | = | - | (Wersall *et al.*, 2018) |
| **Munc18-b** | ↓ | ↓ | ↓ | - | - | (Al Hawas *et al.*, 2012; Cardenas *et al.*, 2019) |
| **VAMP-7** | - | ↓ | ↓ | ↓ | ↓ | (Koseoglu *et al.*, 2015) |
| **VAMP-8** | - | ↓ | ↓ | ↓ | - | (Graham *et al.*, 2009) |
| **SNAP23** | ↓ | ↓ | ↓ | ↓ | - | (Williams *et al.*, 2018) |
| **Stx8** | = | = | ↓ | ↓ | - | (Golebiewska *et al.*, 2015) |
| **Stx11** | = | ↓ | ↓ | ↓ | - | (Ye *et al.*, 2012) |

In addition to the SNARE complex, VAMP-7, VARP and Arp2/3 form a complex that negatively regulates granule secretion in platelets. VARP traps VAMP-7 and Arp2/3 under resting conditions to prevent uncontrolled secretion and actin cytoskeleton remodelling. Upon stimulation, VAMP-7 and Arp2/3 are released, triggering trans-SNARE complex formation and actin cytoskeleton reorganization, respectively (Figure I-20) (Koseoglu *et al.*, 2015). Indeed, Schäfer and co-workers described that VARP interacts with the SNARE-domain of VAMP-7 keeping it in a closed conformation (Schafer *et al.*, 2012). In contrast, VARP positively regulates VAMP-7 in neurons (Burgo *et al.*, 2009).

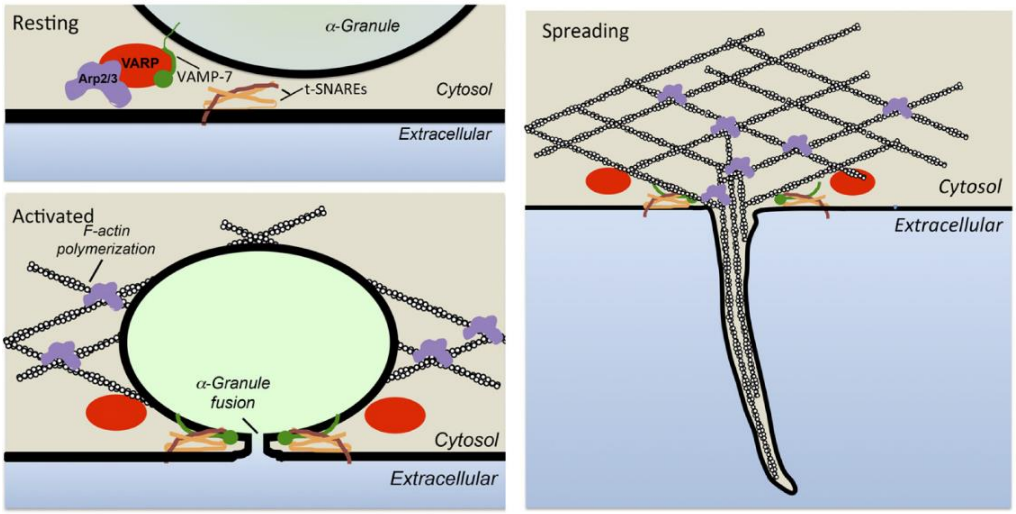


**Figure I-20. Schematic representation of the role of the VARP/VAMP-7/Arp2/3 complex in platelets.** Under resting conditions VARP binds to VAMP-7 and Arp2/3, keeping the granule exocytosis machinery and actin polymerization in an inactive state (top, left). Upon stimulation, VAMP-7 and Arp2/3 are released to form the trans-SNARE complex (bottom, left) and to promote actin remodelling (right), respectively (Koseoglu *et al.*, 2015).

### 2.9.2. Role of the platelet cytoskeleton in granule secretion

The platelet cytoskeleton is also involved in granule secretion. It inhibits granule release in the resting platelets, but facilitates granule secretion during platelet activation (Gremmel *et al.*, 2016). The cytoskeleton directs the centralization of the granules in the platelets, providing the contractile force that facilitates the release of the granule contents through the OCS (Flaumenhaft *et al.*, 2005). In fact, SNARE proteins, such as VAMP-8, Stx1, Stx4 and SNAP23, interact with actin (Woronowicz *et al.*, 2010). The membrane required for the formation of actin structures, such as filopodia or lamellipodia, can be derived from evagination of the OCS or from the granule membrane, which is incorporated after its secretion (Flaumenhaft *et al.*, 2005). Consistently, during platelet spreading VAMP-7 granules localize to the periphery to provide their membrane for spreading, whereas VAMP-3 and VAMP-8 granules localize to the granulomere, triggering secretion (Peters *et al.*, 2012). Indeed, the absence of VAMP-7 promotes defective platelet spreading (Koseoglu *et al.*, 2015).

### 2.9.3. C3G role in platelet secretion

C3G is believed to have a role in α-granule release, as it regulates the secretion of angiogenic factors. Indeed, C3G overexpression in platelets causes the retention of VEGF, SDF-1 and TSP-1 inside the platelet, both at rest and under thrombin stimulation (Martin-Granado *et al.*, 2017). Similarly, the absence of C3G also regulates the secretion of angiogenic factors, since C3G-KO platelets release more VEGF and SDF-1 and retain TSP-1 upon platelet stimulation (Hernandez-Cano *et al.*, 2022). Consistently, previous results from our group demonstrated an interaction between C3G and VAMP-7 in resting and thrombin-stimulated platelets (Martin-Granado *et al.*, 2017), suggesting that the defects in the secretion of angiogenic factors observed in transgenic C3G and C3G-KO platelets could be related to a putative role of C3G in the regulation of the secretory machinery.

# OBJECTIVES/
# OBJETIVOS

# OBJECTIVES

Our group has previously demonstrated the participation of C3G in key aspects of platelet function. Using transgenic mouse models that overexpress the complete human C3G gene, or a mutant form that lacks the catalytic domain, specifically in MKs and platelets, we have described that C3G participates in platelet activation and aggregation. In addition, C3G also regulates platelet spread on poly-L-lysine independently of its GEF activity.

Based on this, the general objective of this work is to deepen into the role of C3G in platelet function, using, in addition to our transgenic models, a knockout mouse model, in which C3G is specifically deleted in MKs and platelets. For this, the following specific objectives have been addressed:

1. To study the effect of C3G deletion on primary hemostasis.

2. To determine the role of C3G in secondary hemostasis.

3. To analyze the role of C3G in platelet spreading, identifying the signaling pathways involved.

4. To examine the participation of C3G in granule secretion, and in the regulation of the secretory machinery.

5. To study the contribution of C3G to platelet-mediated inflammation.

# OBJETIVOS

Nuestro grupo ha demostrado previamente la participación de C3G en aspectos clave de la función plaquetaria. Utilizando modelos de ratón transgénicos que sobreexpresan el gen humano C3G completo, o una forma mutante que carece del dominio catalítico, específicamente en MK y plaquetas, hemos descrito que C3G participa en la activación y agregación plaquetaria. Además, C3G también regula la extensión plaquetaria sobre poli-L-lisina de forma independiente de su actividad GEF.

En base a ello, el objetivo general de este trabajo es profundizar en el papel de C3G en la función plaquetaria, utilizando, además de nuestros modelos transgénicos, un modelo de ratón knockout, en el que C3G está específicamente deleccionado en MKs y plaquetas. Para ello, se han abordado los siguientes objetivos específicos:

1. Estudiar el efecto de la deleción de C3G en la hemostasia primaria.

2. Determinar el papel de C3G en la hemostasia secundaria.

3. Analizar el papel de C3G en la extensión plaquetaria, identificando las vías de señalización implicadas.

4. Examinar la participación de C3G en la secreción de gránulos y en la regulación de la maquinaria secretora.

5. Estudiar la contribución de C3G a la inflamación mediada por plaquetas.

# MATERIALS & METHODS

# 1. Mouse models and genotyping

We have used three different C3G mouse models in this work, two transgenic models for C3G (tgC3G and tgC3GΔCat) and a C3G knockout model, Rapgef1$^{flox/flox}$;PF4-Cre$^{+/-}$ (hereinafter C3G-KO), together with their corresponding wild-type counterparts, wtC3G, wtC3GΔCat and Rapgef1$^{flox/flox}$;PF4-Cre$^{-/-}$ (hereinafter C3G-wt), respectively. In addition, we have used a platelet-specific conditional SNAP23 knockout mouse (SNAP23-KO) with their corresponding wild-type counterpart (SNAP23-wt) (Williams *et al.*, 2018). All mice used in these studies were 8-13 weeks old, unless otherwise specified.

TgC3G mice express human full-length C3G, while tgC3GΔCat express a mutant form lacking the catalytic domain (specifically the last 439 bp of the gene). In both cases, C3G is expressed under the control of PF4 gene promoter, which is specific for megakaryocytes and platelets (Gutierrez-Herrero *et al.*, 2012). For tgC3G, two different lines (named 2C1 and 6A6) were used. For tgC3GΔCat, 8A3 line was used.

In the C3G-KO mouse model, C3G is deleted specifically in megakaryocytes and platelets (Gutierrez-Herrero *et al.*, 2020). This is due to the floxing of the intronic regions between exons 17 and 21 of the *RAPGEF1* gene with LoxP sites (Shah *et al.*, 2016) and the expression of the Cre recombinase under the PF4 promoter (Tiedt *et al.*, 2007) in these animals.

All animal procedures were performed under isoflurane anesthesia (Vetfluorane®, Virbac), and all efforts were done to minimize suffering. This study was performed in strict accordance with the EU Directive 2010/63/EU for animal experimentation, including the "three R's" rule. The protocols were approved by the Committee on the Ethics of Animal Experimentation of the University of Salamanca (ID: 297 and 639) and the Department of Agriculture, Livestock and Rural Development, Regional Government of Castilla y León, Spain.

To genotype, a tail-section of the mice at the time of weaning (≈21 days) was digested in 0.5 ml Tail Lysis Buffer [100 mM Tris pH 8.0, 5 mM EDTA pH 8.0, 200 mM NaCl and 0.2% SDS] supplemented with 6.25 μl (≈100 μg) proteinase K (Recombinant PCR Grade, Roche) at 55 °C overnight (o/n). DNA was isolated from the supernatant by precipitation with 5 M NaCl and ethanol, following the protocol described in (Miller *et al.*, 1988).

The primers used for genotyping of each mouse model are described in **Table M-1**.

**Table M-1. Primers used for the genotyping of the mouse models used in this work, indicating their purpose, name, and sequence.**

| Mouse model | Characteristics | Primer | Sequence |
|---|---|---|---|
| tgC3G and tgC3GΔCat | C3G and C3GΔCat overexpression | A1 | 5'-ACCACATGGCAGTCAAACTCACAGC-3' |
| | | C1 | 5'- TCTTCTGCCTTTGAGACCTGGAAGC-3' |
| Rapgef1xPF4-Cre | Conditional and Rapgef1 alleles | C3G-KO-LoxF | 5'-AGCCTGTTGGCAAGTTTGG-3' |
| | | C3G-KO-LoxR | 5'-CTGATGGAGAACCTAGCTGTGG-3' |
| | PF4-Cre and wild type alleles | PF4-prom-F | 5'-CCCATACAGCATACCTTTTG-3' |
| | | PF4-prom-Cre-R | 5'-TGCACAGTCAGCAGGTT-3' |

# 2. Cell lines

In this work we have used adherent cell lines, HEK-293T and PC12, which are described in **Table M-2**.

**Table M-2. Cell lines used in this work, indicating ATCC reference, origin, cell type, and culture medium used.**

| Cell line | ATCC Ref. | Organism | Tissue | Culture Medium |
|---|---|---|---|---|
| HEK-293T | CRL-3216 | Human | Embryonic Kidney | DMEM |
| PC12 | CRL-1721 | Rat | Pheochromocytoma | DMEM |

HEK-293T cells were cultured in Dulbecco's modified Eagle's medium (DMEM, Gibco) supplemented with 10% Fetal Bovine Serum (FBS, Gibco), 2 mM Glutamine (Gibco), 100 U/ml Penicillin (Gibco) and 100 µg/ml Streptomycin (Gibco).

PC12 cells were grown in DMEM medium supplemented with 10% Horse Serum (Gibco), 5% FBS, 2 mM Glutamine, 1% MEM Non-Essential Amino Acids (Gibco), 100 U/ml Penicillin and 100 µg/ml Streptomycin. PC12 cells were grown in plates previously coated with 50 µM Type I Collagen (StemCell) in 20 mM acetic acid.

All cell cultures were maintained at 37 °C in a humidified 5% $CO_2$/95% air incubator. Cells were collected by trypsinization with 0.25% Trypsin-EDTA (Gibco). To count cells, Beckman Coulter Z2 particle counter was used. Cells were stored in cryogenic storage vials in complete media with 10% dimethyl sulfoxide (DMSO). Cell suspensions were progressively frozen: at -80 °C for at least 4 h and finally at -180 °C in a liquid nitrogen freezer.

## 2.1. Transient transfection of HEK-293T cells

To examine the possible interaction between C3G and proteins of the secretory machinery and cytoskeleton remodeling, we performed transient transfection in HEK-293T. We used a full-length C3G DNA construct in combination with DNA constructs of the proteins of interest, all of which are described in **Table M-3**.

HEK-293T cells (1 x $10^6$) were seeded in 100 mm culture dishes. The following day, cells were transfected using the cationic polymer PEI (Polyethylenimine linear 25K, Polisciences Inc.). The transfection mix [750 µl NaCl 150 mM, 3 µg of each DNA and 15 µl PEI (1 mg/ml, pH 7.0)] was incubated for 30 min at room temperature (RT) to promote the formation of the DNA:PEI complexes, then added to the cell cultures and incubated for 48 h at 37 °C.

**Table M-3. DNA constructs used in this work for transient transfection in HEK-293T cells**. The name, vector type, cloned DNA, tag and supplier are indicated.

| Construct name | Vector | Cloned DNA | Tag | Provided by |
|---|---|---|---|---|
| pCEFLHA-C3G | pCEFLHA | Full-length human C3G (aa 4-1077) | HA | (Carabias *et al.*, 2020) |
| pcDNA-HA-CrkL | pcDNA-HA | Human CrkL | HA | |
| pEGFP-VAMP-7 (1-220) | pEGFP-C3 | Human VAMP-7 | EGFP | Addgene #42316 |
| pEGFP-VAMP-8 | pEGFP-C3 | Human VAMP-8 | EGFP | Addgene #42311 |

| Construct name | Vector | Cloned DNA | Tag | Provided by |
|---|---|---|---|---|
| pEGFP-VAMP-3 | pEGFP-C3 | Human VAMP-3 | EGFP | Addgene #42310 |
| pEGFP-VARP | pEGFP-C3 | Human VARP | EGFP | Addgene #42312 |
| pEGFP-SNAP23 | pEGFP-C3 | Human SNAP23 | EGFP | Addgene #101914 |
| mEmerald-ARP3-N-12 | mEmerald-N1 | Human Arp3 | mEmerald | Addgene #54979 |
| tdTomato-VASP-5 | tdTomato | Mouse VASP | tdTomato | Addgene #58141 |
| RFP-Abi1 | RFP | Human Abi1 | RFP | Dr. Machesky (Beatson, UK) |
| pCDNA-CFP-C4-WAVE2 | pcDNA-CFP | Human WAVE2 | EGFP | This work |
| pEGFP-C3-Sec3 | pEGFP-C3 | Human Sec3 | EGFP | Addgene #53755 |
| pEGFP-C3-Exo70 | pEGFP-C3 | Human Exo70 | EGFP | Addgene #53761 |
| mEmerald-WASP1-C-14 | mEmerald-N1 | Human WASP1 | mEmerald | Addgene #54314 |

## 2.2. Lentiviral infection of PC12 cells

### 2.2.1. Lentivirus production

HEK-293T cells were used for the production of lentiviral particles. For that, cells were transfected with three viral plasmids: i) pLenti-GFP o pLVTHM lentiviral plasmids (containing the insert); ii) psPAX2: packaging plasmid containing the *Gag*, *Pol*, *Rev* and *Tat* genes; iii) pMD2.G: VSV-G envelope expressing plasmid, containing the VSV-G gene (G glycoprotein), which facilitates the formation of the lentiviral particles.

HEK-293T ($5 \times 10^5$) cells were seeded in 100 mm culture dishes 24 h before transfection. The transfection mix was composed of 500 µl NaCl 150 mM, 9 µg pLenti-GFP or pLVTHM constructs, 3 µg pMD2.G, 5 µg psPAX2 and 60 µl PEI (1 mg/ml pH 7.0). The mix was incubated for 30 min at RT and then added to cells. The next day, the medium was replaced with complete DMEM medium. To obtain the lentiviral particles, culture medium was collected 48, 56 and 72 h post-transfection and centrifuged 5 min at 300 x *g*. Then, medium was filtered and supplemented with 4 µg/µl polybrene before use.

### 2.2.2. Lentivirus infection

The day before infection, $2 \times 10^5$ PC12 cells were seeded. The next day cells were starved for 5 h (DMEM + 2% Horse Serum + 1% FBS) prior to infection with the medium previously filtrated and supplemented with 4 µg/µl polybrene.

Selective medium (2 µg/µl blasticidine) was added 24 h post-infection to pLenti mutants, and 1 month later EGFP-positive cells were selected by Fluorescence-Activated Cell Sorting (FACS).

The lentiviral constructs used to overexpress or silence C3G are indicated in **Table M-4**.

**Table M-4. Constructs used in lentiviral transfection, indicating the lentiviral vector, plasmid type in terms of expression, insert and source.**

| Construct name | Vector | Plasmid Type | Cloned DNA | Tag | Reference |
|---|---|---|---|---|---|
| pLenti-GFP-C3G-127h | pLenti-C-mEGFP-IRES-BSD | Overexpression | Human Full-length C3G | mEGFP | (Carabias *et al.*, 2020) |
| pLenti-GFP-C3G-127h-Y554H | pLenti-C-mEGFP-IRES-BSD | Overexpression | Human Full-length C3G mutated Y554 to H554 | mEGFP | (Carabias *et al.*, 2020) |
| pLVTHM-C3Gi | pLVTHM | shRNA | CCACTATGATCCCGACTAT | EGFP | (Ortiz-Rivero *et al.*, 2018) |

### 2.3. Nucleofection of PC12 cells

PC12 cells were nucleofected following the manufacturer's instructions of Amaxa® Cell Line Nucleofector® Kit V. Briefly, 5 x $10^4$ PC12 cells were plated in 6-well plates the day before. Cells were collected, centrifuged for 5 min at 300 x *g* and resuspended in complete Nucleofector Solution [5 mM KCl, 120 mM $Na_2HPO_4/NaH_2PO_4$ pH 7.2, 25 mM Sodium Succinate, 25 mM Mannitol] supplemented with 15 µM $MgCl_2$. DNA (25 µg) was added and cell/DNA suspension was transferred to the cuvette and treated with Nucleofector® Program U-029. After nucleofection, 500 µl of warmed complete DMEM was added to the cuvette and cell suspension was transferred to 12-well plates. DNA used for nucleofection is listed in **Table M-5**.

**Table M-5. Plasmid used in nucleofection, indicating plasmid type, insert, tag and supplier.**

| Construct name | Vector | DNA cloned | Tag | Provided by |
|---|---|---|---|---|
| NPY-td-Orange2 | pEGFP-N1 | Human Neuropeptide-Y | tandem mOrange2 | Addgene #83497 |

## 3. Antibodies

### 3.1. Primary antibodies used for flow cytometry

**Table M-6** contains the fluorochrome-conjugated antibodies used for flow cytometry.

**Table M-6. Fluorochrome-conjugated antibodies used for flow cytometry, indicating its fluorochrome, target and the assay in which they were used**. Supplier, product reference and working dilution are also specified. Ref: reference.

| Antibody | Fluorochrome | Target | Assay | Supplier/Ref. | Dilution |
|---|---|---|---|---|---|
| Anti-Mouse CD41 | FITC | Mouse Integrin αIIb | Platelet-leukocyte aggregate formation | BioLegend (33903) | 1:100 |
| Anti-Mouse CD41 | PE | Mouse Integrin αIIb | Platelet-leukocyte aggregate formation | BD Pharmigen (558040) | 1:100 |
| Anti-Mouse CD41 | APC | Mouse Integrin αIIb | Platelet activation | eBiosciences (17-0411-82) | 1:100 |
| Anti-Mouse CD62P | FITC | Mouse P-selectin | α-granule secretion | BD Pharmigen (553744) | 1:30 |
| Anti-Mouse αIIbβ3 (JON/A clone) | PE | Activated αIIbβ3 integrin | Platelet activation | Emfret (M023-2) | 1:30 |
| Anti-Fibrinogen | AF488 | Activated αIIbβ3 integrin | Platelet activation | Molecular Probes (F13191) | 1:30 |
| Anti-Mouse CD9 | FITC | Platelet tetraspanin protein | Platelet aggregation | BioLegend (124808) | 1:100 |

| Antibody | Fluorochrome | Target | Assay | Supplier/Ref. | Dilution |
|---|---|---|---|---|---|
| Anti-Mouse CD9 | PE | Platelet tetraspanin protein | Platelet aggregation | BioLegend (124806) | 1:100 |
| Anti-Mouse CD63 | APC | Mouse LAMP3 | δ-granule secretion | BioLegend (143906) | 1:100 |
| Annexin V | APC | Membrane phosphatidylserine | Phosphatidylserine exposure | BD Pharmigen (550474) | 1:20 |
| Pyronin-Y | - | RNA and DNA | RNA determination | Across Organics (411863010) | 0.5 µg/ml |
| Hoechst 33342 | - | DNA | RNA determination | Molecular Probes (H1399) | 10 µg/ml |
| Anti-Mouse GPVI | FITC | type I transmembrane glycoprotein | Receptor expression | Emfret (M011-1) | 1:50 |
| Anti-Mouse CD61 | PE | Mouse Integrin β3 | Receptor expression | eBiosciences (12-0611-81) | 1:50 |
| Anti-Mouse CD42b | FITC | Mouse Integrin Ib | Receptor expression | Emfret (R300) | 1:50 |
| Anti-mouse CD154 (CD40L) | PE | CD40 ligand | CD40L exposure | BioLegend (157003) | 1:50 |
| Anti-Mouse CD45 | PE/Cy5 | Leukocyte common antigen | Platelet-leukocyte aggregate formation | BioLegend (103110) | 1:100 |
| Anti-Mouse Ly-6G/Ly-6C (Gr-1) | APC | Glycosylphosphatidylinositol-linked protein | Netosis | BioLegend (108412) | 1:150 |
| Anti-Mouse Ly-6G/Ly-6C (Gr-1) | FITC | Glycosylphosphatidylinositol-linked protein | Platelet-leukocyte aggregate formation | BioLegend (108405) | 1:100 |
| Anti-Mouse Mac1 (CD11b) | PE | Mac-1 α subunit | Platelet-leukocyte aggregate formation | BioLegend (101207) | 1:100 |
| Anti-Mouse CD115 (CSF-1R) | PE | Single pass type I membrane protein | Platelet-leukocyte aggregate formation | BioLegend (135505) | 1:100 |
| Anti-Mouse CD45R/B220 | FITC | CD45R, also known as B220 | Platelet-leukocyte aggregate formation | BioLegend (103205) | 1:100 |
| Anti-Mouse CD3 | APC | CD3, also known as T3 | Platelet-leukocyte aggregate formation | BioLegend (100235) | 1:100 |
| Phalloidin-iFluor 488 Reagent | AF488 | Actin filaments (F-actin) | F-actin levels | Abcam (ab176753) | 1:3000 |
| SYTOX™ Green Nucleic Acid Staining | - | Double-stranded DNA | NETs formation | Thermo Fisher (S7020) | 1 µM |

## 3.2. Primary antibodies used for Immunoprecipitation, Immunofluorescence, and Western blot

The antibodies and dyes used in this study for immunoprecipitation, immunofluorescence and western blot are listed in **Table M-7**.

**Table M-7. Primary antibodies and fluorescent molecules used in this work.** Target, host, supplier and product reference, working dilution and type of assay are indicated. Ref: reference; IF: immunofluorescence; IP: immunoprecipitation; WB: western blot.

| Antibody | Target | Host | Supplier/Ref. | Dilution |
|---|---|---|---|---|
| β-actin (AC-15) | β-actin | Mouse | Sigma-Aldrich (A5441) | 1:1000 (WB) |

| Antibody | Target | Host | Supplier/Ref. | Dilution |
|---|---|---|---|---|
| β-tubulin (2-28-33) | β-tubulin | Mouse | Sigma-Aldrich (T5293) | 1:1000 (WB) |
| Abi-1 (B-12) | aa 273 to 309 of human Abi1 | Mouse | Santa Cruz Biotechnology (sc-271180) | 1:1000 (WB) |
| Arp2 (B-6) | C-terminus of human Arp2 | Mouse | Santa Cruz Biotechnology (sc-376698) | 1:50 (IF), 1:50 (IP), 1:1000 (WB) |
| Arp3 (A-10) | aa 41 to 77 of human Arp3 | Mouse | Santa Cruz Biotechnology (sc-376625) | 1:1000 (WB) |
| c-Cbl | C-terminus of human c-Cbl | Rabbit | Cell Signalling (2747) | 1:1000 (WB) |
| Cdc42 | Cdc42 | Rabbit | Proteintech (10155-1-AP) | 1:1000 (WB) |
| Crk-L (C-20) | C-terminus of human Crk-L | Rabbit | Santa Cruz Biotechnology (sc-319) | 1:1000 (WB) |
| C3G (1008-5) | SH3b-RemCat domains of human C3G | Rabbit | (Guerrero *et al.*, 1998) | 1:100 (IF) |
| C3G (G-4) | aa 1-300 of human C3G | Mouse | Santa Cruz Biotechnology (sc-17840) | 1:100 (IF), 1:50 (IP), 1:1000 (WB) |
| C3G (C-19) | C-terminus of human C3G | Rabbit | Santa Cruz Biotechnology (sc-869) | 1:50 (IP), 1:1000 (WB) |
| C3G (F-5) | C-terminus of human C3G | Mouse | Santa Cruz Biotechnology (sc-376992) | 1:1000 (WB) |
| DAPI | Double-stranded DNA | - | Sigma (10236276001) | 5 µg/µl |
| Exo70 (D-6) | C-terminus of human Exo70 | Mouse | Santa Cruz Biotechnology (sc-365825) | 1:1000 (WB) |
| FM™1-43 Dye | Plasma membrane (PM) | - | Thermo Fisher (T3163) | 10 µM (IF) |
| GFP (B-2) | GFP | Mouse | Santa Cruz Biotechnology (sc-9996) | 1:100 (IP), 1:1000 (WB) |
| HA | HA | Rabbit | Abcam (ab137838) | 1:400 (IP), 1:2500 (WB) |
| HA.11 (16B12) | HA | Mouse | Covance (MMS-101R) | 1:50 (IP), 1:1000 (WB) |
| Hoechst 33342 | Double-stranded DNA | - | Sigma (10236276001) | 5 µg/ml (IF) |
| Munc18-b | aa 1 to 593 of mouse Munc18-2 | Rabbit | Synaptic System (116 102) | 1:150 (IF), 1:1000 (WB) |
| N-WASP (C-1) | aa 18 to 49 of human N-WASP | Mouse | Santa Cruz Biotechnology (sc-271484) | 1:1000 (WB) |
| NE Elastase (F-1) | aa 211 to 267 of human NE Elastase | Rabbit | Santa Cruz Biotechnology (sc-271484) | 1:100 (IF) |
| Phalloidin-iFluor 488 Reagent | Actin filaments (F-actin) | - | Abcam (ab176753) | 1:3000 (IF) |
| Phalloidin-iFluor 647 Reagent | Actin filaments (F-actin) | - | Abcam (ab176759) | 1:3000 (IF) |
| Phospho-Cbl (E-10) | pTyr 700 of human c-Cbl | Mouse | Santa Cruz Biotechnology (sc-377571) | 1:150 (IF) |
| Phospho-Paxillin (Tyr118) | pTyr 118 of human Paxillin | Rabbit | Invitrogen (44-722G) | 1:250 (IF) |

| Antibody | Target | Host | Supplier/Ref. | Dilution |
|---|---|---|---|---|
| Phospho-p130Cas (Tyr410) | Synthetic peptide corresponding to p130Cas (phospho Y410) | Rabbit | Invitrogen (PA5-104930) | 1:150 (IF) |
| Phospho-VASP (Ser157) | pSer157 of human VASP | Rabbit | Cell Signalling (3111) | 1:2000 (WB) |
| P-selectin (C-20) | C-terminus of human P-selectin | Goat | Santa Cruz Biotechnology (sc-6941) | 1:150 (IF) 1:1000 (WB) |
| RAB27B | Rab27b | Rabbit | Proteintech (13412-1-AP) | 1:1000 (WB) |
| Rac1 | Rac1 | Mouse | Cytoskeleton (ARC03) | 1:500 (WB) |
| RALA | RalA | Mouse | Proteintech (67093-1-Ig) | 1:1000 (WB) |
| Rap1/Krev-1 (121) | C-terminus of human Rap1 | Rabbit | Santa Cruz Biotechnology (sc-65) | 1:1000 (WB) |
| RhoA (67B9) | RhoA | Rabbit | Cell Signalling (2117) | 1:1000 (WB) |
| Sec3/EXOC1 | Sec3 | Rabbit | Proteintech (11690-1-AP) | 1:2000 (WB) |
| Sec5/EXOC2 | Sec5 | Rabbit | Proteintech (12751-1-AP) | 1:2000 (WB) |
| Sec10 (C-4) | N-terminus of human Sec10 | Mouse | Santa Cruz Biotechnology (sc-514802) | 1:1000 (WB) |
| SNAP 23 | aa 196 to 211 of human SNAP23 | Rabbit | Synaptic Systems (111-202) | 1:200 (IF), 1:50 (IP), 1:2000 (WB) |
| SYBL1 (158.2) | Human VAMP-7 | Mouse | Abcam (ab36195) | 1:100 (IF) |
| Stx11 | aa 1 to 15 of mouse syntaxin 11 (Stx11) | Rabbit | Synaptic Systems (110-113) | 1:200 (IF), 1:1000 (WB) |
| Talin (C-9) | aa 1 to 300 of human Talin | Mouse | Santa Cruz Biotechnology (sc-365875) | 1:1000 (WB) |
| TI-VAMP (H-55) | Human VAMP-7 | Rabbit | Santa Cruz Biotechnology (sc-67060) | 1:200 (IF), 1:1000 (WB) |
| Endobrevin (VAMP-8) | aa 1 to 75 of rat VAMP-8 | Mouse | Synaptic System (104 303) | 1:200 (IF), 1:1000 (WB) |
| Anti-ANKRD27 (VARP) | C-terminus of human VARP | Rabbit | Origene (TA342941) | 1:1000 (WB) |
| VASP (A-11) | aa 271 to 360 of human VASP | Mouse | Santa Cruz Biotechnology (sc-46668) | 1:100 (IF), 1:750 (WB) |
| WAVE1 (E-2) | aa 179 to 210 of human WAVE1 | Mouse | Santa Cruz Biotechnology (sc-271507) | 1:1000 (WB) |
| WAVE2 (C-6) | aa 177 to 206 of human WAVE2 | Mouse | Santa Cruz Biotechnology (sc-373889) | 1:100 (IF), 1:500 (WB) |

## 3.3. Secondary antibodies used for Immunofluorescence and Western blot

**Table M-8** provides information on the secondary antibodies that were employed in this work.

**Table M-8. Secondary antibodies used in this work.** The antibody target, host-species, supplier and reference, assay, and working dilution used are listed. Ref: reference; IF: immunofluorescence; WB: western blot.

| Antibody | Target | Host | Supplier/Ref. | Assay | Dilution |
|---|---|---|---|---|---|
| Anti-Mouse IgG HRP-linked | Anti-Mouse | Sheep | GE HealthCare (NXA931) | WB | 1:5000 |
| Anti-Rabbit IgG HRP-linked | Anti-Rabbit | Goat | Santa Cruz Biotechnology (sc-2004) | WB | 1:5000 |
| Anti-Mouse IgG Dylight 800 | Anti-Mouse | Goat | Thermo Fisher (35521) | WB | 1:5000 |
| Anti-Mouse IgG Dylight 680 | Anti-Mouse | Goat | Thermo Fisher (35518) | WB | 1:5000 |
| Anti-Rabbit IgG Dylight 680 | Anti-Rabbit | Goat | Thermo Fisher (35568) | WB | 1:10000 |
| Anti-Rabbit IgG Dylight 800 | Anti-Rabbit | Goat | Thermo Fisher (SA5-10036) | WB | 1:10000 |
| Anti-Goat AF680 IgG (H+L) | Anti-Goat | Donkey | Thermo Fisher (A-21084) | WB | 1:10000 |
| AF405 IgG (H+L) | Anti-Mouse | Goat | Thermo Fisher (A31553) | IF | 1:400 |
| AF647 IgG (H+L) | Anti-Mouse | Goat | Thermo Fisher (A21236) | IF | 1:800 |
| AF568 IgG (H+L) | Anti-Rabbit | Goat | Thermo Fisher (A11036) | IF | 1:800 |
| Cy™3 AffiniPure Donkey Anti-Goat IgG (H+L) | Anti-Goat | Donkey | Jackson Immunoresearch (705-165-147) | IF | 1:200 |

# 4. Platelet purification

## 4.1. Blood collection and platelet isolation

For platelet purification, blood was obtained by cardiac puncture from the left ventricle of mice anesthetized with 2% isoflurane (Vetfluorane®, Virbac). Blood was collected in tubes containing sodium citrate as an anticoagulant (Sarstedt 41.1352.005). To obtain platelet rich plasma (PRP), anticoagulated blood was centrifuged for 4 min at 100 x *g*, and the supernatant was again centrifuged for 5 min at 100 x *g*. Platelets were isolated by centrifuging PRP for 5 min at 1300 x *g*. Platelets were resuspended in Tyrode's Hepes Buffer [134 mM NaCl, 0.34 mM $Na_2HPO_4$, 2.9 mM KCl, 12 mM $NaHCO_3$, 20 mM HEPES [4-(2-hydroxyethyl)-1-piperazineethanesulfonic acid] pH 7.4 and 5 mM glucose] and allowed to rest at RT for at least 30 min. After isolation, platelet number was equalized using Beckman Coulter Z2 particle counter.

For platelet activation and aggregation assays, blood was obtained from the submandibular plexus. Blood was collected in tubes containing heparin (Sarstedt 41.1393.005), previously diluted in 800 µl of Tris-Buffered Saline (TBS) [10 mM Tris pH 7.3, 150 mM NaCl].

For *in vivo* experiments, blood was collected from the submandibular plexus in sodium citrate tubes (**Section 19**).

## 4.2. Platelet activation

Platelets were stimulated with different agonists and conditions depending on the assay. **Tables M-9** and **M-10** and **Figure M-1** show the different agonists and inhibitors used in this work.

**Table M-9. Agonists used for platelet activation.** Agonist, target molecule, assay, working conditions, supplier and product reference are described. Ref: reference.

| Agonist | Target | Assay | Conditions | Supplier/Ref. |
|---|---|---|---|---|
| Thrombin | PAR4 receptor | Flow cytometry | 0.2, 0.5 and 1 U/ml, 15 min at RT | Sigma (T7513) |
| | | Western blot | 0.5 U/ml, 1 min at 900 rpm 37 °C | |
| | | GTPase activation assays | 0.2 and 1 U/ml, 1 min at RT | |
| | | Clot retraction | 1 U/ml, 3 h at 37 °C | |
| | | Platelet secretome | 0.2 U/ml, 1 min at 1100 rpm 37 °C | |
| | | δ-granule secretion | 0.2, 0.5 and 1 U/ml, 10 min at 1100 rpm 37 °C | |
| | | Lysosome secretion | 0.2, 0.5 and 1 U/ml, 20 min at 37 °C | |
| Phorbol 12-Myristate 13-Acetate (PMA) | Protein Kinase C (PKC) | Flow cytometry | 0.2, 2, 5 and 10 µM, 15 min at RT | Sigma (91585) |
| | | Rap1 activation assays | 0.2 and 2 µM, 5 min at RT | |
| | | Platelet spreading | 0.2 µM, 5 min at RT | |
| Adenosine 5'-diphosphate (ADP) | P2Y12 receptor | Flow cytometry | 10 µM, 15 min at RT | Sigma (A4386) |
| Collagen related peptide (CRP-XL, hereinafter CRP) | GPVI GPα2β2 | Flow cytometry | 1, 2, 5 and 10 µM, 15 min at RT | Peptide Synthetics |
| | | Rap1 activation assays | 2, 5 and 10 µM, 5 min at RT | |

**Table M-10. Inhibitors used for platelet inhibition.** The name of the inhibitor, its target, the assay in which were used, the supplier and working conditions are described. WB: Western blot.

| Inhibitor | Target | Assay | Conditions | Supplier/Ref. |
|---|---|---|---|---|
| Cytochalasin D | Actin polymerization | Spreading assays | 10 µM, 40 min at RT | Sigma (C8273) |
| Latrunculin | Actin polymerization | Spreading assays | 10 µM, 40 min at RT | Dr. Miguel Vicente (IBMCC) |
| 1A-166 | Rac1 | Spreading assays | 50 µM, 30 min at RT | Dr. Xosé Bustelo (IBMCC) |
| PP2 | Src | Spreading assays | 10 µM, 5 min at RT | Selleckchem (S7008) |
| H89 dihydrochloride hydrate | Protein kinase A (PKA) | WB | 50 µM, 30 min at RT | Sigma (B1427) |
| Bisindolylmaleimide I, Hydrochloride (BIS) | Protein kinase C (PKC) | WB, Flow cytometry<br>Spreading assays | 5 µM, 5 min at RT | Sigma (203291) |
| Go6976 | PKCα and PKCβ | Flow cytometry | 1 µM and 2 µM, 30 min at RT | Selleckchem (S7119) |
| PKC-theta inhibitor | PKCθ | Flow cytometry | 20 µM and 40 µM, 30 min at RT | MedChemExpress (1321924-70-2) |
| Vtx27 | PKCθ and PKCδ | Flow cytometry | 100 µM and 200 µM, 30 min at RT | Selleckchem (S6577) |

Figure M-1 shows a schematic representation of the main inside-out and outside-in signaling pathways involved in the activation of integrin αIIbβ3 during platelet activation, spreading and clot retraction, indicating the targets of all agonists and inhibitors used in this work.

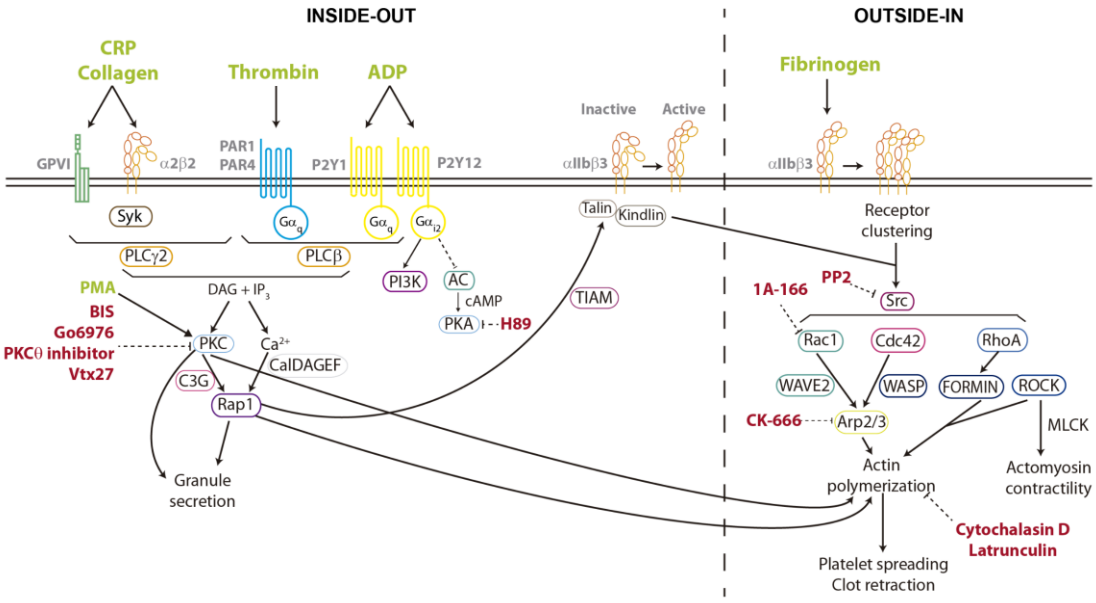


**Figure M-1. Schematic representation of the main pathways involved in platelet activation, spreading and clot retraction, indicating all agonists and inhibitors used.** Agonists (CRP, collagen, thrombin, ADP, PMA, Fibrinogen) are indicated in green. Inhibitors (BIS, Go6976, PKCθ inhibitor, Vtx27, H89, PP2, 1A-166, CK-666, Cytochalasin D, Latrunculin) are indicated in red. ADP: Adenosine 5'-diphosphate; AC: adenylate cyclase; CRP: collagen related peptide; BIS: Bisindolylmaleimide; MLCK: myosin light chain kinase; PKA: protein kinase A; PKC: protein kinase C; PLC: phospholipase C; PMA: Phorbol 12-Myristate 13-Acetate.

### 4.3. Isolation of platelet releasates

Platelets were activated with 0.2 U/ml thrombin for 5 min at 1100 rpm at 37 °C (Table M-9). After activation, platelet releasates were obtained by centrifuging 10 min at 2500 x *g* at 4 °C. Platelet secretomes were kept at -80 °C until needed.

## 5. Thrombin generation

Platelets play an important role in thrombin generation, the last step of the coagulation cascade. After PS exposure, different factors are activated forming the prothrombinase complex, which transforms prothrombin to thrombin (Pryzdial *et al.*, 2018).

Thrombin generation measurements were conducted by calibrated automated thrombography (CAT). PRP (60 µl) was mixed with 20 µl of different trigger solutions, denoted PPPLow (mixture of 1 pM TF and 4 pM phospholipids); MP reagent (4 pM phospholipids) or PRP reagent (1 pM TF), and subsequently coagulation was initiated by the addition of 20 µl FluCa buffer containing a fluorescent substrate (Z-Gly-Gly-Arg-AMC) and $CaCl_2$.

All measurements were performed per duplicate. To correct for differences in plasma color, each plasma measurement was calibrated against the same plasma mixed with 20 µl thrombin

calibrator (Thrombinoscope BV), also per duplicate. The fluorescence of AMC (7-amino-4 methylcoumarin) was measured using a Fluoroskan Ascent (Thermo Scientific, Waltham, MA, USA) equipped with a 390 nm excitation and 460 nm emission filter set. The dedicated Thrombinoscope software (Thrombinoscope BV) was used to calculate: lag time, endogenous thrombin potential (ETP) or AUC, peak, and time to peak (ttPeak) (Figure M-2).

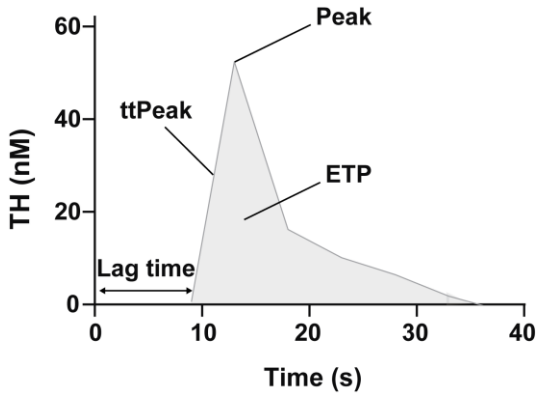


**Figure M-2. Schematic representation of the analysis of thrombin generation by CAT.** Lag time (time it takes to start generating thrombin), ttPeak (time to reach the thrombin peak), Peak (thrombin peak) and ETP (endogenous thrombin potential or AUC). TH: thrombin; AUC: area under the curve.

To evaluate the effect of platelet C3G on thrombin generation we used platelet secretomes from the different genotypes as a trigger solution. For that, platelets (1 x $10^8$) were stimulated with thrombin and releasates were isolated as described in Section 4.3.

# 6. Clot retraction

Clot retraction begins after fibrin formation and triggers the reduction of wound size. Moreover, the volume reduction of the clot allows for reperfusion in the case of thrombosis, and retraction of the wound edges facilitates healing (Jansen & Hartmann, 2021).

PRP was adjusted to 5 x $10^8$ platelets/ml, which were subsequently stimulated with 1 U/ml thrombin to initiate coagulation. Clot retraction was monitored for 3 h at 37 °C, taking photographs at 30 min intervals. The clot area was analyzed with FIJI Software (National Institutes of Health, USA) and the retracted volume and clot weight were measured at the end of the experiment.

# 7. Flow cytometry assays

## 7.1. Platelet activation

P-selectin is a transmembrane protein of platelet α-granules, which is exposed on the surface after platelet activation. Thus P-selectin is a marker for both platelet activation and α-granule secretion (Andre, 2004). On the other hand, although platelets express different integrins, integrin αIIbβ3 is the most specific, being highly expressed. In resting conditions, integrin αIIbβ3 is maintained in a low affinity state. Platelet stimulation causes an inside-out signaling triggering a conformational change in this integrin, from a low affinity state to a high affinity state.

Consequently, integrin αIIbβ3 is widely considered a marker of platelet activation (Durrant *et al.*, 2017).

Thus, to determine platelet activation, we monitored the exposure of P-selectin (CD62P) and the level of the active form of integrin αIIbβ3 presented on platelet surface by flow cytometry. For that, we used FITC-labeled Rat anti-mouse CD62P and PE-labeled JON/A (Rat anti-mouse αIIbβ3) antibodies (**Table M-6**), respectively. In some cases, AF488-labeled fibrinogen was used, which binds selectively and with high affinity to the active conformation of integrin αIIbβ3. The αIIb (CD41) subunit of platelet integrin was used as a platelet marker, which was detected with the APC-labeled anti-mouse CD41 antibody (**Table M-6**).

Blood (50 µl), collected as described in **Section 4.1**, was washed and resuspended in 700 µl Tyrode's Hepes Buffer. Washed blood (30 µl) was incubated with anti-CD62P-FITC, anti-αIIbβ3 (JON/A)-PE and anti-CD41-APC antibodies, for 15 min at RT in the presence of different agonists and inhibitors. BD Accuri™ C6 cytometer (Becton Dickinson) was used to analyze the data after collecting 30000 CD41-positive events. The agonists and inhibitors used are listed in **Table M-9** and **Table M-10**.

## 7.2. Platelet aggregation

Aggregation studies were based on the technique described by (De Cuyper *et al.*, 2013). This technique consists of splitting the blood into two populations and labeling the platelets of each population with anti-CD9 antibodies conjugated with different fluorochromes, since the CD9 platelet marker does not intervene in the platelet aggregation process. In this case, we used anti-CD9-PE and anti-CD9-FITC antibodies (**Table M-6**). Once the populations were labeled separately, they were pooled and activated under aggregation conditions. Positive events for both markers are considered aggregates.

For this analysis, 50 µl of blood, obtained as detailed in **Section 4.1**, were used. Blood was washed with Tyrode's Hepes Buffer, centrifuged for 5 min at 1300 x *g* and resuspended in the same buffer. Washed blood was then separated into two populations and each one was incubated with its corresponding antibody (anti-CD9-PE or anti-CD9-FITC) for 15 min at RT and darkness. After 5 min centrifugation at 2500 x *g* to remove the excess of antibody, blood was resuspended in Tyrode's Hepes Buffer and both populations were mixed. The mixture was incubated with the agonists at 37 °C, while shaking at 900 rpm. The aggregation reaction was stopped at different times (0, 1, 2, 5 and 10 min) by addition of 450 µl 0.5% formaldehyde in 1X PBS (Phosphate-Buffered saline). Analysis was then performed using BD Accuri™ C6 cytometer, acquiring 10000 platelets, identified according to forward and side scatter profiles (FSC/SSC). The agonists used are listed in **Table M-9**.

## 7.3. Analysis of the exposure of other proteins on the platelet surface

### 7.3.1. CD63

CD63 was used as a marker for the determination of δ-granule secretion by flow cytometry. CD63 is a transmembrane protein that localizes into the δ-granule membrane. After fusion with the platelet membrane, it is exposed on the platelet surface (Nishibori *et al.*, 1993).

Washed blood (30 µl), obtained as indicated in **Section 4.1**, was incubated with anti-CD63-APC and anti-CD41-FITC antibodies (**Table M-6**) for 15 min at RT in the presence of 0.5 U/ml thrombin and 2 mM $Ca^{2+}$. CD41-positive (10000) events were collected using a BD Accuri™ C6 cytometer.

### 7.3.2. Receptors

For analysis of the levels of surface receptors GPVI, GPIIIa (ITGB3 or integrin β3), GP1BA and GPIIb (ITGA2B or integrin αIIb), washed blood (50 µl) was incubated with anti-GPVI-FITC, anti-CD61-PE or CD42b-PE and anti-CD41-APC antibodies, respectively (**Table M-6**) for 15 min at RT. Mean fluorescence intensity (MFI) of 30000 platelets, identified according to FSC/SSC, was analyzed using a BD Accuri™ C6 cytometer.

### 7.3.3. Phosphatidylserine

PS is a phospholipid that is found exposed on the platelet surface of activated procoagulant platelets. In the last stage of coagulation, PS facilitates the assembly of the intrinsic tenase complex (factor (F)VIIIa; FIXa; FX) and prothrombinase complex (FVa; FXa; prothrombin), contributing to thrombin generation (Kholmukhamedov & Jobe, 2019). Platelets that expose PS upon platelet activation are called procoagulant platelets.

To study PS exposure, washed platelets were isolated from blood obtained by cardiac puncture, as previously explained in **Section 4.1**. Platelets were stimulated with 1 U/ml thrombin and with different concentrations of collagen related peptide (CRP; 2, 5 and 10 µg/ml), in the presence of anti-CD41-FITC antibody and Annexin V-APC (**Table M-6**) at RT and darkness. After 15 min, platelets were washed with Binding Buffer [0.1 M HEPES (pH 7.4), 1.4 M NaCl, 25 mM $CaCl_2$] and analyzed by flow cytometry on BD Accuri™ C6 cytometer, collecting 20000 CD41-positive events.

### 7.3.4. CD40L

CD40 ligand, also known as CD40L, is a type II transmembrane protein belonging to the TNF (Tumor Necrosis Factor) superfamily. CD40L ensures the interaction between platelets and the immune system (Cognasse *et al.*, 2022).

Washed blood (30 µl), obtained as described in **Section 4.1**, was incubated with anti-CD40L-PE and anti-CD41-FITC antibodies (**Table M-6**) for 15 min at RT in the presence of different concentrations of thrombin (0.5 and 1 U/ml). Then, we analyzed the percentage of CD40L exposure in 20000 CD41-positive events by flow cytometry on BD Accuri™ C6 cytometer.

## 7.4. Quantification of F-actin levels

To determine F-actin levels, washed platelets were isolated from blood obtained by cardiac puncture, as previously explained in **Section 4.1**. Platelets were stimulated with 0.2 and 1 U/ml thrombin and fixed with 2% paraformaldehyde (PFA) for 15 min at RT. After washing twice, platelets were permeabilized with 0.2% Triton X-100 and were blocked with 1% bovine serum albumin (BSA) for 30 min. Platelets were stained with Phalloidin-AF488 for 30 min at RT and

darkness. Finally, diluted samples were analyzed in BD Accuri™ C6 cytometer, acquiring 10000 platelets identified according to their FSC/SSC features.

## 7.5. Determination of platelet maturity

In blood circulation, two different platelet populations can be found, reticulated or immature platelets and old or mature platelets. Reticulated platelets are released from the megakaryocyte cytoplasm and can be identified by its higher amount of RNA, in comparison with old platelets (Bongiovanni *et al.*, 2022; Hamad *et al.*, 2022).

For total RNA determination, platelets from 15 µl of blood were isolated. In order to prevent Pyronin Y binding to DNA, platelets were first incubated with Hoechst 33342 for 45 min at 37 °C, prior to incubation with Pyronin Y for 15 min at 37 °C. Samples were diluted and analyzed in BD Accuri™ C6 cytometer, analyzing the MFI of Pyronin Y signal in 10000 platelets, identified according to FSC/SSC.

## 7.6. Platelet-leukocyte aggregate (PLA) formation

PLAs play a crucial role in inflammation. Platelet activation and simultaneous degranulation enable platelets to interact with leukocytes through different receptors. This interaction is facilitated via soluble factors. The most significant leukocyte receptors involved in direct interactions include PSGL-1, CD40, and Mac-1 (integrin M2, CD11b/CD18), which interact respectively with platelet ligands P-selectin (CD62P), CD40L and GPIβ/α (Finsterbusch *et al.*, 2018).

PLA formation assays were based on the technique described in (Finsterbusch *et al.*, 2018), which consists on measuring the CD41 MFI inside the gate of CD45-positive population, considered as leukocytes.

For the determination of complexes formed by PLAs, whole blood was obtained by cardiac puncture as indicated in **Section 4.1** and lysed with Red Cell Lysis Buffer [RBC: 155 mM $NH_4Cl$, 10 mM $KHCO_3$, 0.1 mM EDTA pH 7.4] (1:9 v/v). The mixture was shaked for 15 min at RT before centrifugation at 500 x *g* for 5 min. The pellet was resuspended in Tyrode's Hepes Buffer and incubated with anti-CD45-PE/Cy5 (leukocyte marker) and anti-CD41-FITC (platelet marker) antibodies (**Table M-6**) for 15 min at RT in the presence of 0.5 or 1 U/ml thrombin. The analysis of PLA formation was performed by flow cytometry in a BD Accuri™ C6 cytometer, analyzing the MFI of CD41-FITC in the CD45-positive population (**Figure M-3**).

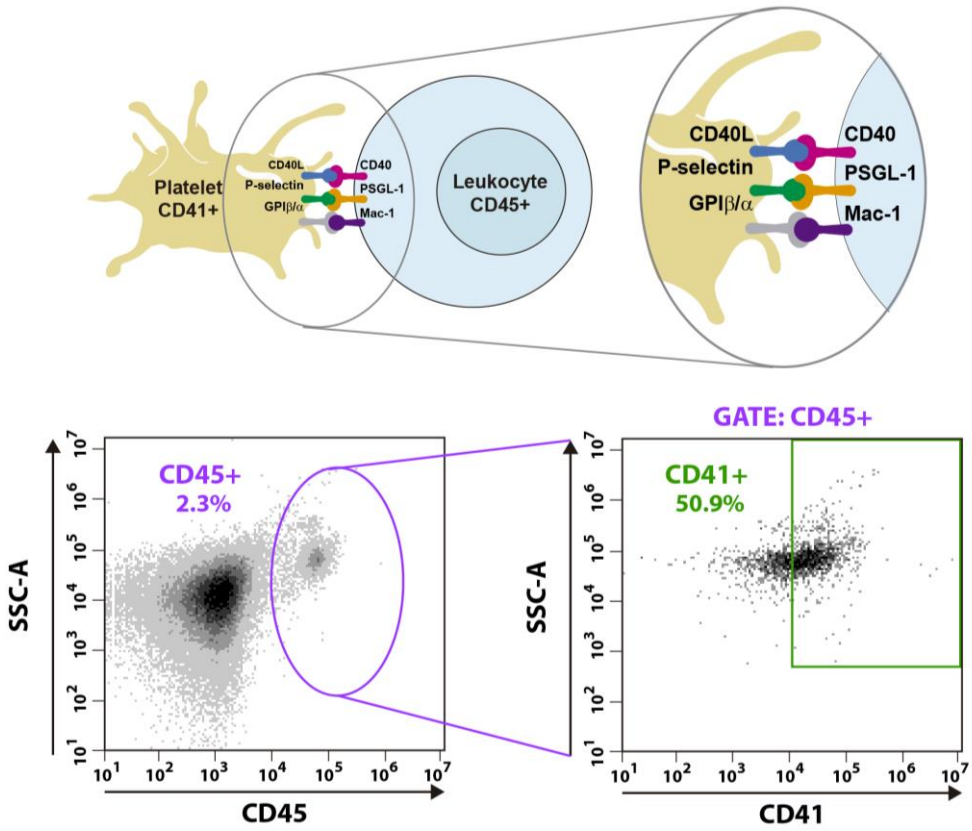


**Figure M-3. Measurement of PLA formation.** Schematic representation of the interaction between platelets and leukocytes, describing the different ligands/receptors involved (CD40L/CD40; P-selectin/PSGL-1; GPIβ/α/Mac-1). Panels show the gating strategy to determine platelet-leukocyte aggregates. CD41-MFI was measured in the CD45-positive population. MFI: mean fluorescence intensity.

To evaluate whether the PLA formation is regulated by P-selectin or CD40L, lysed blood was resuspended in Tyrode's Hepes Buffer and incubated with anti-CD40L-PE or anti-CD62P-FITC (Table M-6) antibodies in the presence of 1 U/ml thrombin for 15 min at RT. After washing twice, blood was stained with anti-CD45-PE/Cy5 (leukocyte marker) and anti-CD41-FITC/PE (platelet marker) antibodies (Table M-6) for 15 min at RT. PLA formation was analyzed as indicated above (Figure M-3).

To determine the type of leukocyte involved in PLAs we analyzed specific markers for monocytes, NEs and lymphocytes (Figure M-4), using the following antibodies: anti-CD45-PE/Cy5 + anti-CD115-PE to label monocytes; anti-CD45-PE/Cy5 + anti-Ly6G-FITC to label NEs; or anti-CD45-PE/Cy5 + anti-CD11b-PE to label lymphocytes (in this case CD11b-negative cells); all of them in combination with anti-CD41-FITC or anti-CD41-APC (platelet marker) (Table M-6). These markers were chosen because they are not involved in platelet-leukocyte interaction.

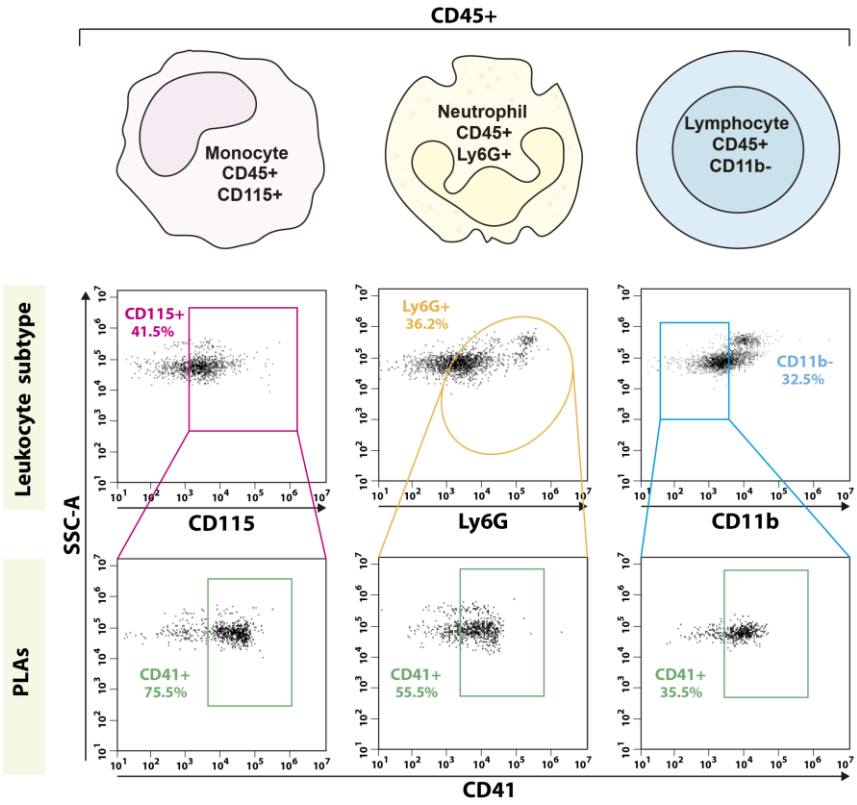


**Figure M-4. Measurement of platelet aggregate formation with leukocyte subtypes.** The drawings illustrate the different types of leukocytes and their markers. Panels show the different gating strategy used to determine platelet hetero-aggregates with distinct leukocyte subtypes. The following markers were used: CD115 (monocyte marker), Ly6G (NE marker), CD11b (marker to exclude cells other than lymphocytes) and CD41 (platelet marker). PLA: platelet leukocyte aggregate.

To ascertain the type of lymphocyte that was involved in PLAs, we used the following antibodies: anti-CD45-PE/Cy5 + anti-B220-FITC to label B lymphocytes and anti-CD45-PE/Cy5 + anti-CD3-APC to label T lymphocytes, all of them in combination with anti-CD41-FITC or anti-CD41-APC (platelet marker) (Table M-6). As before, these markers were chosen because they are not involved in platelet-leukocyte interaction.

## 7.7. Quantification of NET formation

NETs are formed after NE activation, releasing DNA structures in order to neutralize pathogens during the innate immune response (Kaplan & Radic, 2012). To examine the effect of platelets on NE activation, we used SYTOX Green assay, which is a DNA binding that detects NEs undergo NETosis but not early apoptosis.

For the analysis of NE activation after thrombin stimulation, we measured the percentage of NETs formed. To this end, washed blood was lysed as described in Section 7.6 and incubated with anti-Gr1-APC antibody (NE marker) and SYTOX Green (Acid Nucleic Stain) (Table M-6) for 60 min at 37 °C in presence of 0.5 or 1 U/ml thrombin. The presence of NETs was quantified by flow cytometry in a BD Accuri™ C6 cytometer, analyzing the percentage of SYTOX Green-positive events in the Gr1-APC-positive population (5000 events).

# 8. Microscopy assays

## 8.1. Determination of platelet morphology by transmission electron microscopy

Platelet morphology and granularity were analyzed by transmission electron microscopy. Platelets were isolated as described in **Section 4.1** and fixed with Fixation Buffer [2% glutaraldehyde, 1.6% PFA in 0.1 M Phosphate Buffer pH 7.4] for 30 min at RT. Platelets were washed with 0.1 M Phosphate Buffer (pH 7.4), included in warm 2% agarose in $dH_2O$ at 50 °C for 5 min and then let them cold. After being divided into multiple pieces, the blocks were incubated in the Fixation Buffer for 30 min. Then, they were washed and taken to the Microscopy Service of the University of Salamanca (Nucleus) for examination by electron microscopy using a Tecnai Spirit Twin 120 kV transmission Electron microscope.

## 8.2. Detection of protein colocalization by confocal microscopy

To detect protein-protein interactions in platelets, we performed colocalization assays using a confocal microscope. After stimulation, platelets were fixed with 8% PFA 1:1 (v/v) for 15 min at RT before being seeded onto glass coverslips pre-coated with poly-L-lysine for at least 50 min at RT. Attached platelets were washed twice with PBS and then permeabilized with 0.2% Triton X-100 for 10 min. After washing twice, platelets were blocked with 1% BSA o/n at 4 °C. Coverslips were incubated with the primary antibodies (**Table M-7**) for 2 h at RT and washed twice again before incubating with secondary antibodies for 1 h at RT in darkness (**Table M-8**). After that, platelets were stained with Phalloidin-AF488 (**Table M-7**) to visualize actin filaments. Coverslips were mounted with ProLong™ Diamond Antifade Mountant (Thermo Scientific) onto slides. Between the different steps three washes with 1X PBS were performed, except for the final step where three additional washes with MilliQ water were done.

Images were captured using a Leica TCS SP8 confocal microscope system with a 100x/1.4 Oil Plan-ApoChromat Ph1 immersion objective and an extra 12X digital zoom. Images were processed with Leica LAS X Software using Lightning process. After that, images were processed and analyzed with ImageJ/FIJI Software (Schindelin *et al.*, 2012). Protein colocalization studies were performed using Coloc2 plug-in, analyzing Pearson's correlation coefficient (Dunn *et al.*, 2011).

Protein distribution was analyzed using Plot Profile Tool. Two different distribution patterns were established: (i) membrane/periphery pattern, when higher MFI values were presented in the edges, and (ii) central pattern, when MFI values were distributed across the diameter, as described in **Figure M-5**.

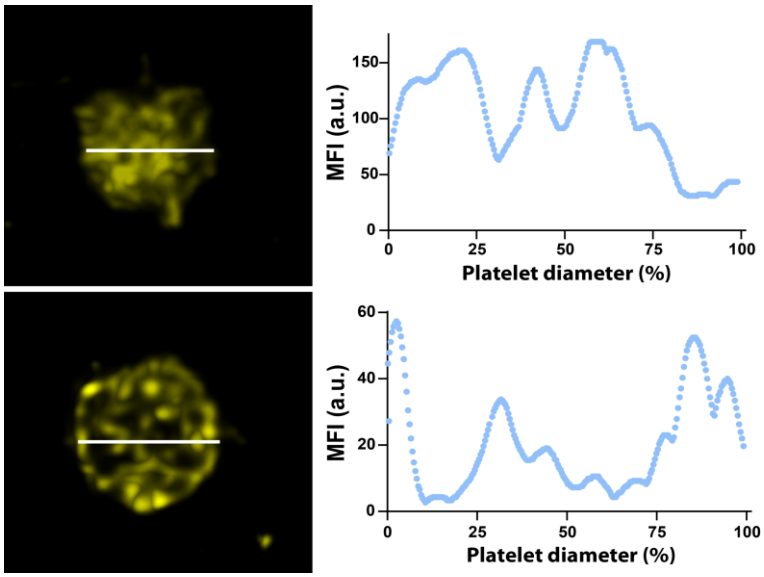


**Figure M-5. Protein distribution analysis using Plot Profile Plug-in.** Representative images of the strategy used to analyze protein distribution along platelets, and their corresponding graphs. We measured MFI of the protein of interest across the platelet diameter. The plot profile tool displays a two-dimensional graph of the MFI of the pixels across the platelet diameter. To correct differences each platelet diameter was represented as percentage, considering the center as a value of 50% and both ends of the periphery of platelets as values of 0% and 100%. To avoid variability, in all measurements the diameter was traced as a horizontal line in the central part of the platelet, as represented in the figure. MFI: mean fluorescence intensity; a.u.: arbitrary units.

## 8.3. Analysis of granule exocytosis of PC12 cells by TIRFM: Detection of single-vesicle exocytosis by NPY secretion

Total internal reflection fluorescence microscopy (TIRFM) is based on the idea that an electromagnetic field with the same frequency as the excitation light, known as the evanescent wave, is generated in the liquid at the solid-liquid interphase when excitation light is completely reflected in a transparent solid (cover glass). The most notable application of TIRFM is single-molecule experiments such as exocytic events, revealing information about fluctuation or distribution.

When visualizing single events prior to exocytosis, the fluorescently charged vesicles appear to glow as they enter the evanescent field. Eventually, as they fuse with the PM, the signal rapidly decreases, as the fluorescently labeled content spills out the cell (Fish, 2009; Martin-Fernandez *et al.*, 2013).

PC12 cells contain a large number of vesicles, small vesicles (SV) that contain acetylcholine and large dense core vesicles (LV) that contains monoamines. NPY (Neuropeptide Y) is commonly used as a marker for exocytosis since it is packaged into secretory granules.

PC12 cells were nucleofected with 25 µg of tdOrange-NPY plasmid (**Table M-5**), as described in **Section 2.3**. 48-h post-transfection, 3 x $10^5$ cells were seeded at a density of 0.75 x $10^5$ cells/ml on 25-mm cover glasses (Deckgläser) previously coated with poly-L-lysine and type I collagen. After 72 h, the culture medium was replaced with Ringer Buffer [RB: 130 mM NaCl, 3 mM KCl, 5 mM $CaCl_2$, 1.5 mM $MgCl_2$, 10 mM glucose and 10 mM HEPES pH 7.4].

Cover glasses were mounted into AttoFluor™ Cell Chambers (ThermoFisher) in the THUNDER Image Live Cell 12899 SP8 Leica inverted microscope system equipped with a 100x/1.47 Oil Plan-ApoChromat Ph1 immersion objective type TIRFM system. PC12 cells were stimulated by replacing the RB with high KCl Modified Ringer Buffer [MRB: 37 mM NaCl, 56 mM KCl, 5 mM $CaCl_2$, 1.5 mM $MgCl_2$, 10 mM glucose and 10 mM HEPES pH 7.4] and maintained at 37 °C.

All TIRFM images were acquired at the same intensity and at the same grade of penetrance and were taken every 0.3 s (~3 frames/sec) for 30 s. Before measuring total fluorescence in the evanescent field and the fluorescence of individual vesicles, the background was corrected by measuring the MFI in a region outside the cells and in a region without a vesicle inside the cell, and those measurements were subtracted from the fluorescence of the vesicles.

To analyze the TIRFM imaging data, we selected single exocytic events that underwent a rapid increase in fluorescence intensity. We started to study the MFI, 4 frames before the exocytic event until it disappears. To differentiate between fusion events and vesicle movement, we focused on fluorescence changes just before the fluorescent signal decay; thus, while vesicle mobility causes the MFI to progressively decrease to background levels, a fusion event causes a rapid transitory increase in MFI.

We normalized the MFI to the exocytic event, which is considered 100%. Then, we studied the kinetics of NPY secretion; normally the intensity value of the peak frame (exocytic event) decays rapidly to values lower than those of the first frames (Figure M-6). We monitored the kinetics of the tdOrange-NPY secretion manually, and the granule number, area of granules and the number of exocytic events was quantified with ImageJ software.

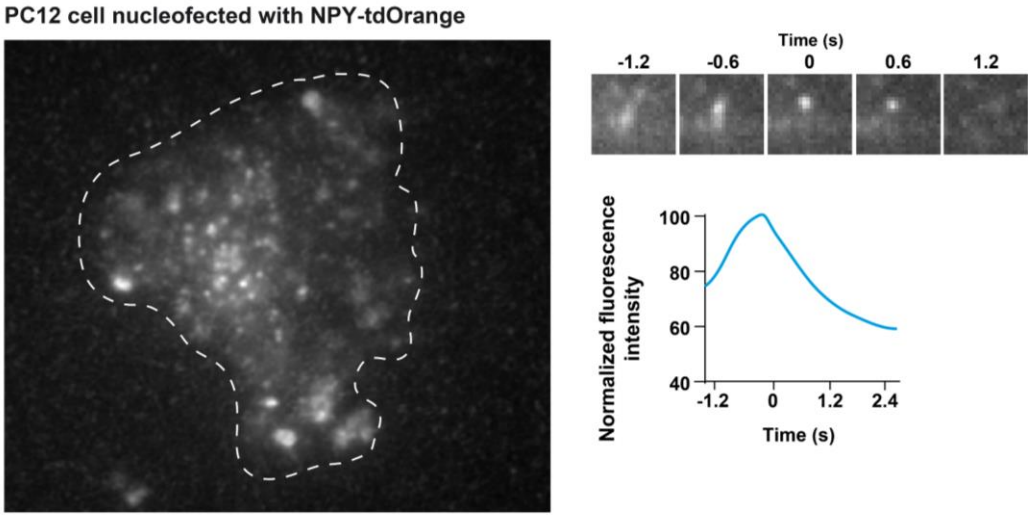


**Figure M-6. Analysis of NPY-tdOrange secretion in PC12 cells after KCl stimulation.** Left: Representative TIRFM image of PC12 cells nucleofected with NPY-tdOrange. To assess granule secretion, MFI of individual NPY-tdOrange positive granules was measured. Right: Example of NPY secretion kinetics. MFI: mean fluorescence intensity; NPY: Neuropeptide Y.

## 9. AF488-labeled fibrinogen endocytosis assay

The labeled fibrinogen endocytosis assay allows determination of the endocytic capacity of platelets by immunofluorescence. Platelets were incubated with 5 µM AF488-labeled fibrinogen (**Table M-6**) for different times (0, 5, 15 and 30 min) at 37 °C. Then platelets were fixed with 8% PFA and seeded on poly-L-lysine-treated coverslips. Attached platelets were permeabilized with 0.2% Triton X-100 and blocked with 1% BSA. After labeling with Phalloidin-AF647 (**Table M-7**) to visualize actin filaments, preparations were mounted and images were obtained with a Leica TCS SP8 confocal microscope system using a 100x/1.4 Oil Plan-ApoChromat Ph1 immersion objective and an extra 12X digital zoom.

## 10. FM1-43 staining assay

To monitor the dynamics of granule release, we used the dye FM1-43 (N-(3-Triethylammoniumpropyl)-4-(4-(Dibutylamino) Styryl) Pyridinium Dibromide), which has a high affinity for membranes. After staining, when vesicles undergo exocytosis in dye-free medium, FM1-43 molecules dissociate from the membrane, thus fluorescence is lost (Amaral *et al.*, 2011). The FM1-43 signal only remains in recycled vesicles, i.e., in those undergoing kiss-and-run secretion, but is lost in full collapse exocytosis (Kavalali & Jorgensen, 2014; Henkel *et al.*, 2019).

Platelets ($1 \times 10^7$) were incubated with 10 µM FM1-43 (**Table M-7**) at 37 °C for 30 min. The excess of FM1-43 was removed by centrifuging at 1300 x *g* for 5 min. Stained platelets were then plated in a µ-Slide 8-well plate (Ibidi). Decrease in signal (dye release) from synaptic vesicles was monitored by fluorescence imaging. Platelets were recorded every 1.3 s at 37 °C and 5% $CO_2$ with a Leica TCS SP8 confocal microscope with a 100x/1.4 Oil Plan-ApoChromat Ph1 immersion objective and an extra 10X digital zoom.

Granule exocytosis analysis was performed by measuring intensities of the same granule tracked along successive frames. Two different secretion patterns were established: (i) kiss-and-run, when FM1-43 MFIs are maintained over time (a subtle decrease was observed due to dye bleaching), indicating retention of FM1-43 in the vesicle; (ii) full collapse exocytosis, in which FM1-43 MFI is decreased due to rapid diffusion of the dye to the PM (**Figure M-7**).

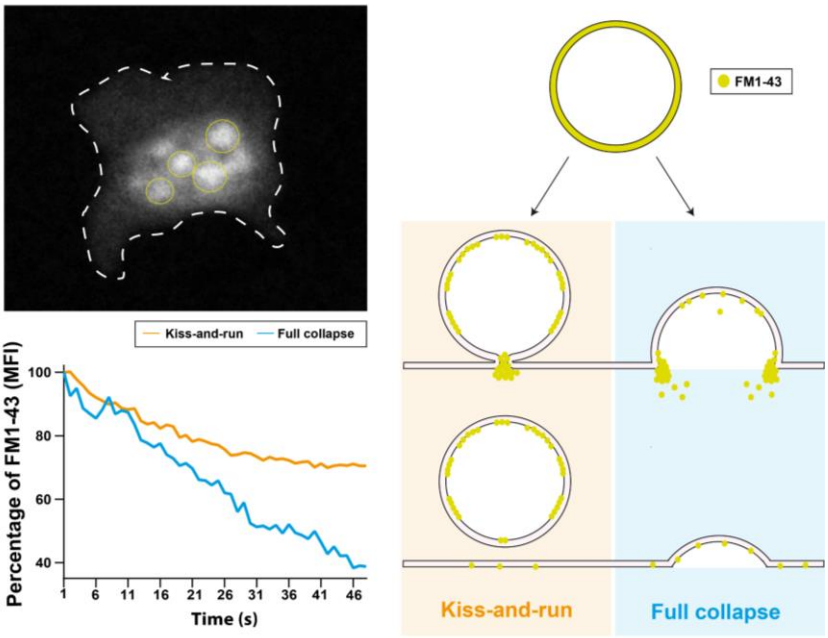


**Figure M-7. Granule exocytosis analysis based on FM1-43 intensity measurement.** To assess granule secretion, MFI of individual FM1-43-stained granules from spread platelets on Ibidi plates was measured. Upper left: representative image of a spread platelet stained with FM1-43, surrounding the granules by green circles. Lower left and right: Graphs and schematic representation of the two different FM1-43 MFI kinetic patterns established: (i) kiss-and-run, where MFIs are maintained over time; (ii) full collapse pattern, where MFI values rapidly decrease. MFI: mean fluorescence intensity.

## 11. Quantification of NETosis by spectrophotometry and immunofluorescence

After blood lysis, as described in **Section 7.6**, NEs were isolated with anti-Gr1-APC antibodies using a FACS Aria, and then allowed to rest at 37 °C for 1 h in RPMI (Roswell Park Memorial Institute, Gibco). On the other hand, platelets were isolated and allowed to rest for at least 1 h at RT. NEs (4 x $10^4$) were co-incubated, in 90 µl Tyrode's Hepes buffer, with 5 x $10^8$ resting or thrombin-activated (0.2 U/ml for 5 min at 1100 rpm) platelets, or with thrombin-induced secretomes (obtained as described in **Section 4.3**), in opaque 384-well plates (Greiner) and stained with 5 µM SYTOX Green. NET fluorescence (ex: 488 ± 5 nm; em: 523 ± 10 nm) was measured on an Infinite M200 Pro2 plate reader every 10 min for 12 h at 37 °C. Stimulation with 300 nM PMA was used as a positive control of NET formation.

In addition, we performed platelet-NE cocultures. Freshly isolated NEs (5 x $10^5$) were resuspended in 200 µl RPMI, seeded in poly-L-lysine coated coverslips and maintained at 37 °C for 2 h. NEs were incubated with either, resting platelets, thrombin-activated platelets or thrombin-induced secretomes for 2 h at 37 °C. As a positive control, NEs were stimulated with 100 nM PMA.

Cells were fixed in 4% PFA in PBS for 15 min at RT and permeabilized with 0.2% Triton X-100. Then, cells were blocked with 1% BSA in PBS at 4 °C o/n and, after that, incubated with anti-mouse NE elastase (**Table M-7**) for 1 h at RT. After three washes, AF647 donkey anti-mouse IgG (**Table M-8**) was added for 60 min at RT and DNA was stained with Hoechst 33342 (**Table M-7**).

Finally, preparations were mounted with Prolong™ Diamond Antifade Mountant. NETosis was analyzed by fluorescence, using a Leica SP8 confocal microscope.

According to (Lelliott *et al.*, 2019), NEs can be classified in three different groups: i) Healthy NEs with lobulated nucleus and intact membrane; ii) Decondensed DNA NEs with an intact membrane but large, diffuse DNA staining and; iii) NEs starting NETosis, which are NEs that have lost their membrane integrity, so that their DNA and elastase have spread beyond the cell boundaries (**Figure M-8**).

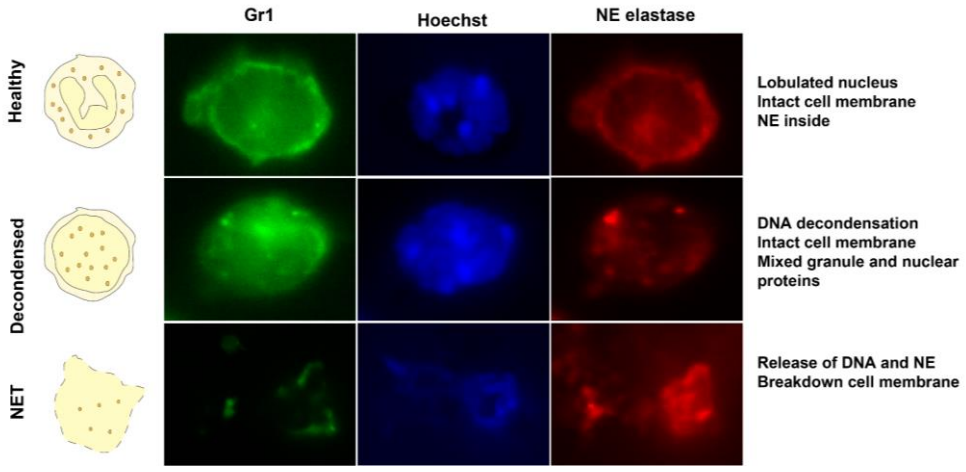


**Figure M-8. Analysis of NETosis by immunofluorescence.** To assess the effect of platelets in NETosis, NEs were incubated either with resting, thrombin-activated platelets or thrombin-induced secretomes and then fixed and staining with Hoechst 33342 and NE elastase. Images and schematic representation of the three different categories or steps of NETosis established. NE: neutrophil; NET: NE extracellular traps; Gr1: NE marker.

## 12. Platelet adhesion and spreading

To analyze platelet spreading, coverslips were coated with different substrates described in **Table M-11** o/n at 4 °C. Platelets were treated with different inhibitors and agonists (**Tables M-9 and M-10**) and added to coated coverslips previously blocked with 1% BSA for 1 h at RT. Then, they were allowed to spread at 37 °C at various times (0, 5, 15, and 30 min), fixed with 4% PFA, permeabilized with 0.2% Triton X-100, blocked with 1% BSA and stained with phalloidin-AF488 and anti-tubulin + AF568 antibodies (**Table M-7**) to visualize the actin cytoskeleton and microtubules, respectively. The images were obtained with a Leica TCS SP8 confocal microscope with a 100X objective and an extra 12X digital zoom. Platelet area, perimeter and circularity were analyzed with FIJI software (Schindelin *et al.*, 2012).

**Table M-11. Substrates used in adhesion and spreading studies, indicating their target, work concentration, supplier and product reference (Ref.)**.

| Substrate | Target (GPVI and integrins) | Concentration | Supplier/Ref. |
|---|---|---|---|
| Poly-L-lysine hydrobromide | Negatively charged ions of the cell membrane | 0.1 mg/ml | Sigma (P6282) |
| Type I Collagen | GPVI, α2β2 | 100 µM | Stem cell (07001) |
| CRP | GPVI, α2β2 | 50 µM | Peptide Synthetics |
| Fibrinogen | αIIbβ3, αVβ3, αXβ2, αMβ2 | 100 µM | Sigma (F3879) |

| Substrate | Target (GPVI and integrins) | Concentration | Supplier/Ref. |
|---|---|---|---|
| Fibronectin | αIIbβ3, α5β1, αVβ3, αVβ6, αVβ1, α8β1 | 100 µM | Sigma (F1141) |
| Laminin | α3β1, α6β1, α6β4, α7β1, α1β1, α2β1, α10β1 | 50 µM | Roche (11243217001) |
| Osteopontin | α4β7, α4β1, α9β1, α8β1, α5β1, αVβ1, αVβ6, αVβ3, αVβ5 | 20 µM | Sigma (O2260) |
| Vitronectin | αIIbβ3, α8β1, αVβ3, αVβ5 | 5 µM | Advanced BioMatrix (5051) |

Platelets were classified according to their shape (Figure M-9), following the workflow developed by (Pike *et al.*, 2021), using the Ilastik Software (Berg *et al.*, 2019) and the KNIME software (Berthold *et al.*, 2009; Stoter *et al.*, 2013).

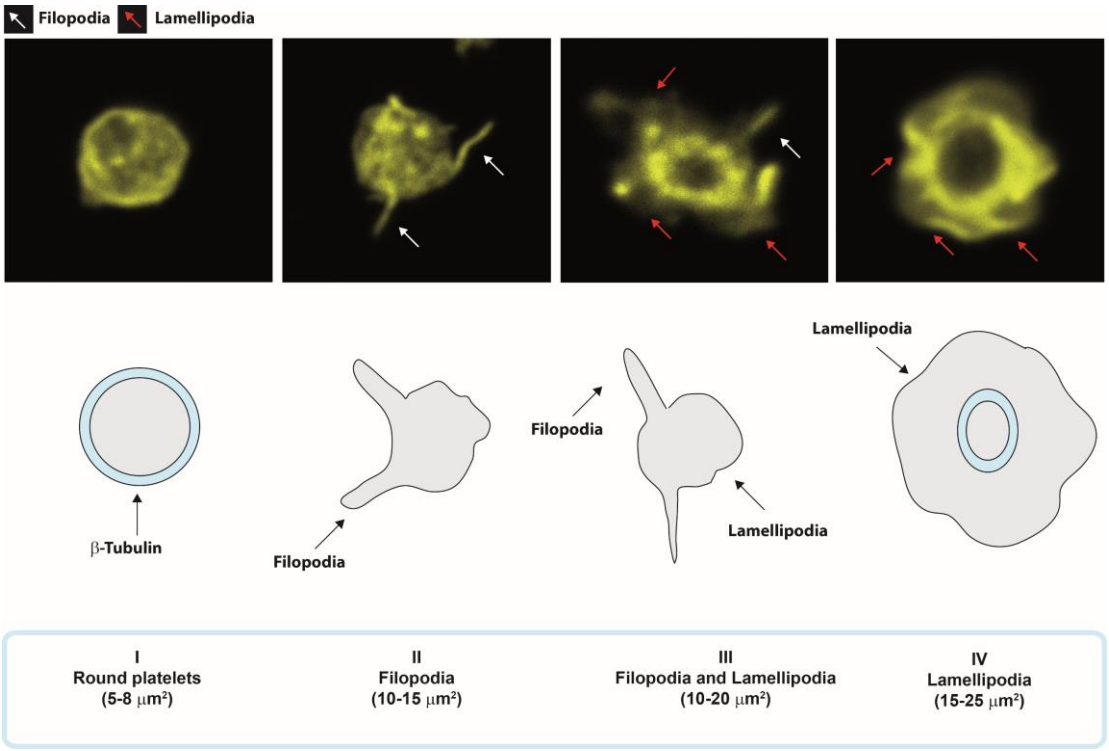


**Figure M-9. Platelet classification based on their shape during platelet spreading**. To analyze spreading, platelets were classified according to the formation of actin structures. Four groups were established: I) round platelets (before spreading); II) platelets that form filopodia; III) intermediate state of spreading, in which platelets have both filopodia and lamellipodia; IV) fully spread platelets, where only lamellipodia are found. White arrows indicate filopodia and red arrows indicate lamellipodia.

To analyze the levels of F-actin during platelet spreading, platelets were allowed to spread at 37 °C at various times (0, 5, 15, and 30 min), fixed with 4% PFA, permeabilized with 0.2% Triton X-100, blocked with 1% BSA and stained with phalloidin-AF488 (Table M-7). The images were obtained with a Leica TCS SP8 confocal microscope with a 100X objective and an extra 12X digital zoom, without modification in the intensity of phalloidin signal.

To monitor cytoskeletal dynamics in real time, 1 x $10^5$ platelets were seeded in µ-Slide 8-well plates (Ibidi). Platelets were recorded for 5 min at 37 °C and 5% $CO_2$ using differential interference contrast (DIC), to assess platelet morphology, with a Nikon Eclipse TE2000-E microscope coupled to a video camera Hamamatsu Orca-er and processed with Metamorph® software. Images were acquired every 10 s and then stacked and processed using Fiji software

(Schindelin *et al.*, 2012). To determine platelet adhesion, we monitored the time it takes to adhere to the IbiTreat plates (**Figure M-10**), setting the adhesion point where platelets flatten and begin to form filopodia.

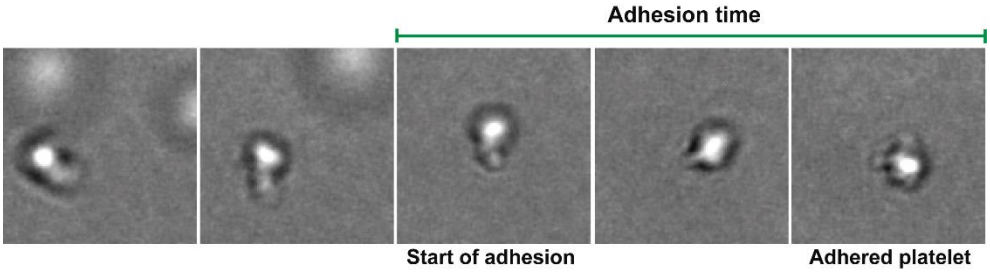


**Figure M-10. Criteria to study platelet adhesion to IbiTreat plates**. The starting point of platelet adhesion was established when the platelet begins to make filopodia and the end point was considered when the platelet flattened.

Platelets in steady state, or after 0.2 U/ml thrombin stimulation, were adjusted to 1.5 x $10^6$, seeded on coverslips pre-treated with poly-L-lysine and let adhere for 30 min; for the timelapse of platelet adhesion, platelets (1.5 x $10^6$) in steady state or after 0.2 U/ml thrombin stimulation were seeded on coverslips pretreated with CRP or fibrinogen and let adhere for 5, 15 and 30 min. Finally, the number of adhered platelets was quantified with ImageJ software.

# 13. Immunodetection of proteins by Western blot

## 13.1. Protein sample preparation and protein quantification

### 13.1.1. Preparation of HEK-293T lysates

HEK-293T (1 x $10^6$) cells were washed twice with cold PBS before lysing with Modified Lysis Buffer [MLB; 20 mM Tris-HCl pH 7.5, 150 mM NaCl, 0.5% Triton X-100] supplemented with 1 mM $Na_3VO_4$, 25 mM NaF, 1 mM PMSF, 1X cOmplete protease inhibitor cocktail (Roche) for 10 min on ice. Lysates were clarified by centrifuging at 16000 x *g* for 10 min at 4 °C. Supernatants were transferred into a new tube and kept at -80 °C.

### 13.1.2. Preparation of platelet lysates

For immunoprecipitation assays, platelets were lysed in 120 µl 1X RIPA [100 mM Tris pH 7.5, 100 mM NaCl, 1% Triton X-100, 1 mM EDTA, 0.1% Sodium Deoxycholate, 0.1% SDS, 1 mM $Na_3VO_4$, 25 mM NaF, 1 mM PMSF, 1X cOmplete protease inhibitor cocktail (Roche)].

For GTPase activation assays platelets were lysed in an equal volume of 2X modified RIPA buffer [100 mM Tris pH 7.5, 400 mM NaCl, 5 mM $MgCl_2$, 2% Igepal, 20% Glycerol, 1 mM PMSF, 1X cOmplete protease inhibitor cocktail (Roche)] for 10 min on ice and supernatant collected by centrifugation at 16000 x *g* for 10 min at 4 °C.

For monitor the protein distribution after platelet activation, platelets were lysed in an equal volume of 2X modified RIPA buffer. Lysates were centrifuged at 16000 x *g* for 10 min at 4 °C. The

supernatants were considered as the cytosolic fraction, while the pellets were considered as the membrane fraction. Membranes were directly resuspended in 12 µl of Laemmli Buffer 2X.

To analyze the levels of phosphorylated proteins, platelets were lysed directly in 2X Laemmli Buffer [100 mM Tris pH 6.8, 20% Glycerol, 2% SDS, 2% β-Mercaptoethanol, 2% Bromophenol Blue] and boiled for 10 min at 100 °C. In order to have the same protein concentration in each sample, number of platelets was previously adjusted, as described in **Section 4.1**.

Bradford assay (Bradford, 1976) was used to determine protein concentration. Briefly, 1 µl of sample was added to 200 µl of Bradford reagent [0.25 mg/ml Coomassie Brilliant Blue G-250, 25% Methanol, 42.5% orthophosphoric acid] and 800 µl MilliQ water. The mixture was incubated at RT for 5 min and the absorbance shift of Coomassie Brilliant Blue G-250 induced by protein binding (from 465 nm to 595 nm) was measured on a spectrophotometer. To determine protein concentration, absorbance values were extrapolated using a standard curve made with different known concentrations of BSA.

After protein determination, supernatants containing the desired amount of protein were mixed with the same volume of 2X Laemmli Buffer. Samples were boiled at 100 °C for 5 min. Denatured protein samples were stored at -80 °C.

## 13.2. SDS-polyacrylamide gel electrophoresis

Proteins were separated using SDS-polyacrylamide gel electrophoresis (SDS-PAGE). The concentration of polyacrylamide depends on the molecular weight (MW) of the target protein; in this study, we used gels with acrylamide concentrations ranging from 7.5% to 15%.

The electrophoresis was carried out in Running Buffer [25 mM Tris-HCl pH 8.3, 250 mM Glycine] at constant voltage. To identify protein sizes, PageRuler™ Plus Prestained Protein Ladder (Thermo Fisher) was used.

## 13.3. Protein transfer to PDVF membranes

After electrophoresis, proteins were transferred to Immobilon-P PVDF membranes (Merck Millipore) by wet transfer using the Mini Trans Blot® Cell System (Bio-Rad). Membranes were previously activated with methanol. The transfer was performed in Transfer Buffer [66 mM Tris-HCl pH 8.3, 386 mM Glycine, 0.1% SDS, 20% Methanol] at 0.3 A (constant amperage) for 2 h at 4 °C.

To reduce non-specific protein binding, membranes were blocked with 5% non-fat dried milk (NFDM) in TTBS [10 mM Tris pH 7.3, 150 mM NaCl, 0.5% Tween-20] for 1 h at RT or o/n at 4 °C. For determination of phospho-proteins, membranes were incubated with 5% BSA in TTBS.

## 13.4. Immunodetection

After blocking, membranes were incubated with primary antibodies (**Table M-7**) in 2% BSA in TTBS for 2 h at RT or o/n at 4 °C on rotation. After that, membranes were washed with TTBS,

and incubated with secondary antibodies (Table M-8) for 1 h at RT in 5% NFDM in TTBS in darkness. Finally, excess of secondary antibody was removed by washing with TTBS.

For detection by immunofluorescence, membranes were incubated with fluorochrome-conjugated secondary antibodies (Table M-8) and signal was detected using Odyssey Infrared Imaging System (LI-COR). For detection by chemiluminescence, membranes were incubated with HRP-conjugated secondary antibodies (Table M-8) and proteins detected using the reagents of the commercial Clarity™ Western ECL Blotting Substrates kit (Bio-Rad).

## 14. Analysis of platelet granule content secretion

To quantify the protein content in the releasate after platelet activation, secretome from thrombin-activated platelets (3 x $10^8$) was obtained as indicated in Section 4.3. Platelet releasates (30 µl) were mixed with 10 µl 4X Laemmli Buffer and loaded into a 10% SDS-polyacrylamide gel. Proteins were detected by gel staining with Colloidal Blue [5% aluminum sulfate-(14-18)-hydrate, 0.02% Coomassie G-250, 20% ethanol and 2% ortho-phosphoric acid (85%)].

The release of the content of the different platelet granules (Figure M-11) was monitored as described below.

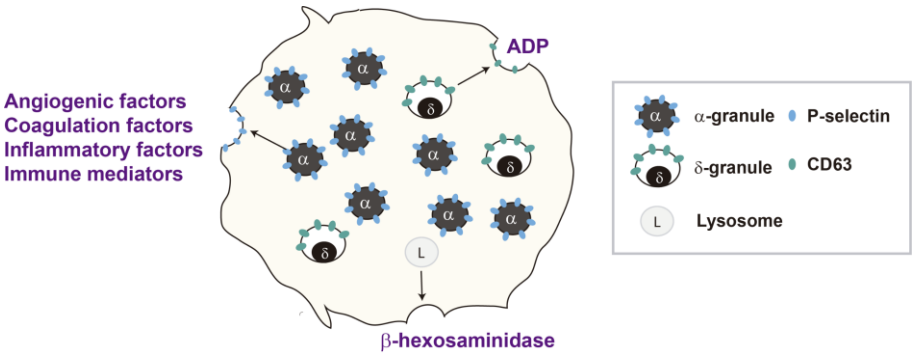


**Figure M-11. Schematic representation of the different platelet granules (α-granules, δ-granules and lysosomes) and their content**. Different factors were measured to analyze α-granule secretion, whereas ADP was monitored to study δ-granule secretion and β-hexosaminidase was examined as a lysosome secretion marker.

### 14.1. Analysis of α-granule secretion

To examine the composition of α-granule content we used the commercial Proteome Profiler Mouse Angiogenesis Array kit (ARY015 R&D), which contains antibodies against different angiogenic, coagulation and inflammatory factors. Secretome from thrombin-stimulated platelets (8 x $10^8$) was collected as described in Section 4.3. Platelet releasate (700 µl) was mixed with different reagents for protein biotinylation, following the manufacturer's instructions. Protein-antibody complexes were identified by peroxidase-conjugated streptavidin (HRP) reaction and subsequently revealed by chemiluminescence, whose signal was quantified with ImageJ.

### 14.2. Analysis of δ-granule secretion

δ-granule secretion was determined by monitoring by bioluminescence the amount of ATP released, using the commercial CellTiter Glo 2.0 kit (Promega G9241). For this purpose, PRP, obtained as described in **Section 4.1**, was adjusted to 9 x $10^6$ platelets and stimulated with different concentrations of thrombin (0.2, 0.5 and 1 U/ml) for 10 min at 37 °C under aggregating conditions. Platelets were centrifuged 1 min at 650 x *g* and 15 µl of secretome were mixed with 15 µl of the reagent and added to opaque 384-well plates (Greiner) for 40 min at 37 °C. Bioluminescence was measured with an integration time of 0.75 s on a Tecan Infinite M200 Pro2 plate reader.

### 14.3. Analysis of lysosome secretion

To analyze the release of cargo from lysosomes, the release of β-hexosaminidase was measured. Platelets (6 x $10^6$) were stimulated with different concentrations of thrombin (0.2, 0.5 and 1 U/ml) for 20 min at 37 °C. Platelet releasate was isolated after centrifuging 1 min at 650 x *g*. Total sample controls were generated by lysing unstimulated platelets with 1% Triton X-100. Secretome (20 µl) was incubated with the same volume of 5 mM 4-NAG (4-Nitrophenyl N-acetyl-β-D-glucosaminidase) in Citrate Phosphate Buffer [80 mM $Na_2HPO_4$, 60 mM citric acid, pH 4.2) for 1 h at 37 °C in a 96-well plate (Corning). The reaction was stopped by adding 0.1 M NaOH and the absorbance was read at 405 nm on a Tecan Infinite M200 Pro2 plate reader.

## 15. Analysis of PC12 secretion

To quantify the protein content in the releasate after PC12 stimulation, PC12 cells (1.5 x $10^5$) were plated in a 12-well plate (Corning). Next day, PC12 cell were starved for 5 h at 37 °C (DMEM + 2% Horse Serum + 1% FBS). Then, medium was replaced by MRB and cells were stimulated for 1 h at 37 °C. Medium was collected and centrifuged at 300 x *g* for 5 min at 4 °C to eliminate death cells and debris. Finally, the protein in the medium was quantified by Bradford assay (Bradford, 1976).

## 16. GTPase activation assays

Detection of the activation of different GTPases was performed by pull-down assay, based on the interaction between the active state of the GTPases (GTP-bound) and their effectors described in **Table M-12**. For that, fusion proteins that include the specific effector domains fused to GST (glutathione-S-transferase) were used. Specific binding of GST to glutathione-sepharose beads allowed purification of effector-GTPase complexes and quantification of active GTPase levels.

**Table M-12. GST-fusion proteins used in this work for GTPase activation assays.** The name and description of the construct containing the effector domain, the plasmid from which they are derived and the target GTPase are described. In addition, the provider is indicated.

| Name | Plasmid | Description | Target | Provided by |
|---|---|---|---|---|
| GST-RalBP1 | pGEX4T3 | Contains amino acids 397–518 of human RalBP1 | Activated Ral GTPase | Dr. A. Poole (Bristol Univ., UK) |
| GST-RalGDS-RBD | pGEX4T3 | Contains amino acids 701–852 of human RalGDS | Activated Rap1 GTPase | Generated previously in our laboratory |
| GST-PAK-PBD | pGEX4T3 | Contains amino acids 67–150 of human PAK | Activated Rac and Cdc42 GTPases | Dr. X. Bustelo (IBMCC, Spain) |
| GST-Rhoketin-RBD | pGEX4T3 | Contains amino acids 7–89 of human Rhoketin | Activated Rho GTPase | Dr. X. Bustelo (IBMCC, Spain) |
| GST-Slac2b | pGEX4T3 | Contains amino acids 1–78 of human Slac2b | Activated Rab27 GTPases | Dr. R. Hirakawa (Tohoku Univ., JP) |

## 16.1. Expression and purification of GST-fusion proteins

Fusion proteins were produced in *E. coli* strain BL21(DE3)T1, which were grown in Terrific Broth medium (Tartoff & Hobbs, 1987) supplemented with 100 µg/ml ampicillin. Cultures were maintained at 37 °C and shaking (190 rpm) until reaching an optical density at 600 nm of ~0.6. Protein expression was induced with 0.2 mM isopropyl-β-D-1-thiogalactopyranoside (IPTG) at 37 °C for 3 h under shaking. In the case of pGEX4T3-GST-Slac2b protein, it was co-expressed with GroES/L chaperones (Noguchi *et al.*, 2015), supplementing the medium with 50 µg/ml spectinomycin and inducing the expression at 15 °C o/n. Bacteria were collected by centrifugation at 11900 x *g* for 20 min at 4 °C, and resuspended in 100 ml PBS supplemented with 0.1% (v/v) Triton X-100 to favor their lysis.

Bacteria were lysed on ice by sonication with VibraCell® VCX750 Ultrasonic Cell Disrupter at 25% amplitude by applying pulses of 50 s, with 10 s between each pulse, for 6 min. Cell debris were discarded by centrifuging at 39000 x *g* for 30 min at 4 °C, and supernatants were sonicated again to break the DNA and avoid viscosity.

GST-fusion proteins were purified using glutathione-agarose affinity columns (ABT), previously equilibrated in Binding Buffer [BB: 20 mM Tris, 150 mM NaCl, pH 7.5]. Sample supernatant was loaded twice in the column, which, was subsequently washed with Washing Buffer [20 mM Tris, 150 mM NaCl, 0.1% Triton X-100, pH 7.5] and with BB. The GST-fusion protein was eluted in Elution Buffer [50 mM Tris, 150 mM NaCl, 10 mM reduced glutathione, pH 7.5] and fractions were collected manually. Protein was extensively dialyzed against BB to remove reduced glutathione. Finally, the protein was concentrated by ultracentrifugation and its concentration was measured. Purified GST-fusion protein samples were kept at -80 °C until being used.

## 16.2. GTPase activation assays in platelets

Platelets (2 x $10^8$) were stimulated at RT with different agonists (**Table M-9**), except for Ral assays in which platelets were stimulated under stirring conditions at 37 °C. After that, platelets were lysed for 10 min at 4 °C with the same volume of 2X RIPA Modified Buffer (**Section 12.1.2.**) or, in the case of Ral assays, with 2X Lysis Buffer [20% Glycerol, 2% NP-40, 400 mM NaCl, 50 mM HEPES pH 7.4, 20 mM $MgCl_2$], supplemented with 20 µg of the different fusion proteins (**Table**

M-12). Then, samples were clarified by centrifugation (16000 x *g*, 15 min, 4 °C). Subsequently, lysates were incubated for 2 h in rotation at 4 °C with glutathione-sepharose resin (Glutathione-Sepharose 4 fast Flow, Amersham Bioscience), previously washed with 1X modified RIPA buffer. Next, 3 washes with 1X modified RIPA lysis buffer were performed and the pellet was resuspended in 20 µl of 2X Laemmli Buffer. Proteins were denatured at 100 °C for 5 min. Protein complexes were separated by SDS-PAGE and GTPases detected by western blot with specific anti-Rap1, anti-RalA, anti-Rac1, anti-Cdc42, anti-RhoA or anti-Rab27b antibodies (Table M-7). The amount of total GTPase protein present in the platelet lysate was determined from a 20 µl lysate sample, taken prior to incubation with the GST-fusion protein.

# 17. Co-immunoprecipitation assays

To detect proteins that interact with C3G we performed co-immunoprecipitation assays. We used two different models: HEK-293T cells and platelets.

In HEK-293T cells, we transfected the cells with plasmids harboring HA- or GFP-tags and performed the immunoprecipitation with antibodies against them. For the analysis in platelets, immunoprecipitation was performed with anti-C3G, anti-SNAP23 or anti-Arp2 antibodies. In both cases, immunocomplexes were purified with Protein G Agarose Resin 4 Rapid Run® (ABT), which has a high affinity for IgG.

## 17.1. Co-immunoprecipitation assay in HEK-293T

Typically, 1 x $10^6$ co-transfected HEK-293T cells were lysed as described in Section 13.1.1. Protein lysate (500 µg) was incubated with anti-HA or anti-GFP antibodies (Table M-7) for 1 h at 4 °C with gentle rotation. The immunocomplexes were purified by incubation for 2 h at 4 °C with 20 µg protein G agarose resin. To quantify the amount of protein present in the lysates, 20 µl of lysate sample was taken prior to incubation with primary antibodies.

## 17.2. Co-immunoprecipitation assay in platelets

Platelets were lysed as previously detailed in Section 13.1.2. After clarification, lysates were incubated o/n at 4 °C under gentle shaking with primary antibodies anti-C3G (C3G-G4 or C3G-C19), anti-Arp2, or anti-SNAP23 (Table M-7). The next day, 20 µl of lysate were kept as a total protein control and the rest of the sample was incubated with 20 µg protein G agarose resin for 2 h at 4 °C under rotation conditions. To remove unbound proteins, three washes were performed with 1X RIPA Buffer.

Finally, the same volume of 2X Laemmli Buffer was added to the agarose beads and samples were boiled at 100 °C for 10 min. Immunocomplexes were separated by SDS-PAGE and detected with the specific antibodies detailed in Table M-7.

## 18. Analysis of F/G actin ratio

To study cytoskeletal remodeling, we measured the amount of actin filaments formed by monitoring the F/G actin ratio. This ratio reflects the amount of filamentous actin (F-actin) content versus free globular-actin (G-actin) content (Stocker *et al.*, 2018).

Platelets (5 x $10^6$) were activated with different amounts of thrombin and immediately lysed with an equal volume of Lysis Buffer [100 mM Tris-HCl (pH 7.4), 10 mM EDTA, 2 mM $MgCl_2$ and 2% Triton X-100] supplemented with protease and phosphatase inhibitors [2 mM $NaV_3O_4$, 5 mM NaF] and kept on ice for 10 min. Lysates were ultra-centrifuged at 100000 x *g* for 1 h at 4 °C to separate Triton-X-100-soluble G-actin from Triton-X-100-insoluble F-actin. Supernatant containing G-actin was collected, and the F-actin pellets were solubilized with an equal volume of 8 M urea.

Fractions and total protein (lysate prior to ultra-centrifugation) were separated by SDS-PAGE and immunoblotted as previously described. F-actin, G-actin and total actin were detected with an anti-β-actin antibody (**Table M-7**). F-actin content was defined as the ratio of F-actin in total actin. F/G actin ratios after stimulation were calculated as the fold change over unstimulated samples and relativized against total protein.

## 19. Dextran Sulfate Sodium (DSS)-colitis induced model

Dextran Sulfate Sodium (DSS) is a water-soluble negatively charged sulfated polysaccharide with a highly variable MW, ranging from 5 to 1400 kDa. DSS causes erosions in the epithelial monolayer by compromising barrier integrity, resulting in increased colonic epithelial permeability. This allows the dissemination of proinflammatory intestinal content, triggering weight loss, a reduction in colon length, and the presence of blood in the stool (Chassaing *et al.*, 2014).

Ten pairs of 8- to 9-week old littermate female mice were given a 2.7% DSS (MP Biomedical, MW: 36000-50000) solution in 100 µl drinking water *ad libitum* for 7 days. DSS water was changed after 3 days, due to the instability of DSS in solution. During the treatment, clinical signs of colitis were monitored, including bodyweight loss and PLA formation by flow cytometry.

At the end of the treatment, blood was collected by cardiac puncture, as described in **Section 4.1**, to isolate platelet RNA. Then, mice were sacrificed and different clinical parameters analyzed, such as colon length, spleen weight, presence of gross blood in the stool, presence of bacteria in spleen and immune cell infiltration in colon.

To determine the presence of bacteria in spleen, spleens from DSS-treated mice (20 mg) were cut into small pieces and homogenized. Then, two passages were made through a 25G needle and another one through a 70 µm filter (Falcon). Homogenized spleens were plated on non-selective LB-agar plates and grown for 48 h at 37 °C.

To assess immune cell infiltration, we analyzed the presence of NEs, lymphocytes and monocytes in the DSS-treated colon. As it is important to compare the same region of the colon,

the rectal region was minced and homogenized with a mixture of 3 mg collagenase I and 4 mg dispase II (Sigma) for 60 min at 37 °C and 500 rpm stirring. Then, homogenates were sequentially passaged twice through a 25G needle and once through a 40 µm filter (Falcon). Finally, homogenized colons were labeled with anti-CD45-PE/Cy5 + anti-CD115-APC; anti-CD45-PE + anti-Ly6G; or anti-CD45-PE + anti CD11b-PE antibodies (**Table M-6**).

# 20. RNA analysis

## 20.1. RNA purification

### 20.1.1. RNA purification from platelets

Platelets were isolated as described in **Section 4.1**, and RNA purified with the RNeasy Mini Kit (Qiagen 74104), following the manufacturer's instructions. Briefly, platelets were resuspended in RLT Buffer supplemented with 10 µl β-mercaptoethanol, and lysed by two passages through a 26G needle. Then, supernatant was added to the column and three washes with RW1 buffer and one with RPE buffer were performed. Finally, columns were dried by centrifugation at 9000 x *g* for 2 min and 30 µl of RNase-free water was added to elute the RNA.

### 20.1.2. RNA purification from tissue

Colons from DSS-treated mice (40 mg) were cut into small pieces and homogenized with a mixture of 3 mg collagenase I and 4 mg dispase II (Sigma) for 60 min at 37 °C and 500 rpm stirring. Then, two passages were made through a 25G needle and another through a 40 µm filter (Falcon).

RNA was isolated with NZYol (NZYTech), according to the manufacturer´s protocol. Briefly, cell homogenates were incubated with 0.2 ml chloroform for 2 min and centrifuged at 12000 x *g* for 15 min at 4 °C. After centrifugation, the mixture separates into three phases: (i) a lower red, phenol-chloroform phase, (ii) an interphase, and (iii) a colorless upper aqueous phase. We carefully took the aqueous phase (which contains the RNA) and precipitated the RNA with 0.5 ml isopropyl alcohol. After a final wash with 75% ethanol, pellets were air dried for 20 min and then resuspended in 30 µl of RNase-free water.

RNA capillary electrophoresis columns (Agilent Technologies, RNA 6000 Nanochips) were used to determine the concentration and quality of the extracted RNA. RNA samples were kept at -80 °C until use. Only samples with RIN (RNA integrity number) values higher than 7.5 were used for the following procedures.

## 20.2. cDNA synthesis

cDNA synthesis was conducted by a reverse transcription reaction using the First-Strand cDNA Synthesis Kit (NZYTech), following the manufacturer's specifications. Essentially, 0.2 to 1 ng platelet RNA or 1 µg tissue RNA was combined with 10 µl NZYRT 2X Master Mix (which contains oligo(dT)18 primers, random hexamers, $MgCl_2$ and dNTPs), 2 µl NZYRT Enzyme Mix (which contains NZY Reverse Transcriptase and NZY Ribonuclease Inhibitor) and DEPC-treated water (Ambion). The mixture was incubated for 10 min at 25 °C, followed by 30 min at 50 °C.

Finally, 1 µl NZY RNase H was added to samples to eliminate the RNA after incubation for 20 min at 70 °C. The cDNA was stored at -20 °C.

## 20.3. Quantitative PCR

Quantitative PCR (qPCR) allows to measure the amount of the product synthesized during each PCR cycle, which is proportional to the fluorescence signal and can be correlated with the amount of starting product (Woo *et al.*, 1998).

qPCR was used to determine gene expression in platelets and colon from DSS-treated mice. Reaction was performed by mixing 1 µl cDNA with 2X NZYSpeedy qPCR Green Master Mix (NZYTech), 10 µM forward primer, 10 µM reverse primer and RNase-free water. Primers used were designed with the PrimerQuest Tool (Integrated DNA Technologies, IA, USA) (**Table M-13**).

Each experiment was done in triplicate. Gene expression levels were normalized against the housekeeping gene β-actin (*Actb)*.

**Table M-13. Sequence of primers used in qPCR. The canonical names of the genes studied are indicated.**

| Gene | Forward primer (5'-3') | Reverse primer (5'-3') |
|---|---|---|
| *Actb* | TAGACTTCGAGCAGGAGATGG | CAAGAAGGAAGGCTGGAAAG |
| *Ccl2* | CTGCTGCTACTCATTCACCA | CCATTCCTTCTTGGGGTCAG |
| *Cx3cl1* | CCGCGTTCTTCCATTTGTGT | AAGCCACTGGGATTCGTGAG |
| *Cx3cr1* | TCTGCGTGAGACTGGGTGAG | CAGTTCAGGGAAGGAGGTGG |
| *Cxcl4* | CCACCCTGAAGAATGGGAGG | GGCAGCTGATACCTAACTCTCC |
| *Cxcl9* | CGAGGCACGATCCACTACAA | AGGCAGGTTTGATCTCCGTT |
| *Cxcl10* | TGAGAGACATCCCGAGCCAA | GAGGCAGAAAATGACGGCAG |
| *Il1b* | ATCTCGCAGCAGCACATCAA | ACGGGAAAGACACAGGTAGC |
| *Il6* | TGCCTTCTTGGGACTGATGC | TGAAGTCTCCTCTCCGGACT |
| *Itgba2-1* | AGCCCGTGATCTTTCCTAAAC | GCAGCCACAGAGTAACCTAAA |
| *Itgba2-2* | CAGTGAGAGCCAAGAAACAAAC | TGTTGGTGGATCGGGTTAAG |
| *Itga2b-1* | CTCAACCGAGACGGCTATAATG | CTTCACTCTGACCCAGGAATATC |
| *Itga2b-2* | GGCTTCTCAGTGGACTTTCATA | TCTCCTCTTGACTTGCGTTTAG |
| *Itga6-1* | GGTTGTGGAACAGCACATTTC | GCGTGAGGGAGCTTGATATT |
| *Itga6-2* | ACTCAGGGAAGGGTATTGTTTC | GTGCGGACTTCATGTCTCTT |
| *ItgaV-1* | AGAAGACGTTGGGCCTATTG | TGTAAGGCCACTGGAGATTTAG |
| *ItgaV-2* | TTGGCTGCTGTGGAGATAAG | GTCTTCTTCAGTCTCAGGGTTT |
| *ItgaL-1* | GCCTATCCTGAGACCTTCAATC | AGGTTTGCCTCACACTTCTT |
| *ItgaL-2* | CCACAGACTGCAGAACAGAA | GTTGATGGCACGAAAGGTATTG |
| *Itgb1-1* | GACAGTGTGTGTGTAGGAAGAG | GCCTCCACAAATTAAGCCATTAG |
| *Itgb1-2* | CAGGTGTCGTGTTTGTGAATG | GATCTGACCATTTGACGCTAGA |
| *Itgb2-1* | GTGGTAGGTGTCGTACTGATTG | GGGACTTGAGTTTCTCCTTCTC |
| *Itgb2-2* | GCAGTAATGGAGCATCGAGTAT | TCGGAAGCCATGACCTTTAC |
| *Itgb3-1* | GAAGGAGTGTGTGGAGTGTAAG | CTCTTTCACCTGCTCGATGT |

| Gene | Forward primer (5'-3') | Reverse primer (5'-3') |
|---|---|---|
| *Itgb3-2* | GCTCATCTGGAAGCTACTCATC | GTGGAGGTGGCCTCTTTATAC |
| *Nox4* | CCTCAACTGCAGCCTCATCC | CAACAATCTTCTTCTTGTTCTCC |
| *Pdgfb* | ACTTGAACATGACCCGAGCA | ATCTGGAACACCTCTGTGCG |
| *Unc13b* | GTGGATCTGTCTACCTGCTTTG | CTCCACGAACTTGACAGTGAT |
| *Selp* | CTCCTGGCTCTGCTAAGAAAG | GCGTTAGTGAAGACTCCGTATG |
| *Snap23* | CAGCCAGTGGTGGATACATT | CCAGAGCCATGTTCTTTAGGT |
| *Stx11* | AACCAGCTGCTTCTGATAGAC | AGTTGGTGTCGCGCTTAAT |
| *Stxbp2* | CACGCTCACAGCTACTCATAAT | GTCCTGTTCGATGTCCAGAAG |
| *Tgfb* | ATGAACCGGCCCTTCCTGCT | TTGGTATCCAGGGCTCTCCGGT |
| *Tnfa* | ACGTCGTAGCAAACCACCAA | ATCGGCTGGCACCACTAGTT |
| *Vamp-3* | AAGCTCTCGGAGCTAGATGA | TCTTGCAGTTCTTCCACCAATA |
| *Vamp-7* | GCTTGGTGTGGAGGAAACT | TCCTGTCTTGGCAGATGTATT |
| *Vamp-8* | CAGAATGTGGAGCGGATCTT | CTGGGACGTTGTCTTGAAGT |

mRNA expression data were analyzed using the $2^{-\Delta\Delta CT}$ method (Livak & Schmittgen, 2001). The threshold cycle ($C_T$) is defined as the cycle at which fluorescence signal of the amplification curves crosses the threshold line. $C_T$ values of the gene of interest and the housekeeping gene were provided by the real-time PCR equipment software QuantStudio3 and QuantsStudio5 (Thermo Scientific). According to this method, efficiency of primer pairs was analyzed by serial dilutions of the cDNA. Only primers with an efficiency between 80% and 120% were used.

## 21. Statistical analysis

Data have been represented as the mean ± SEM (Standard Error of the Mean) or the mean ± SD (Standard Deviation), as indicated in each figure. At least 2 independent experiments from each genotype (mice and cell lines) were performed. In fluorescence measurements (MFI), the data in each experiment was normalized against the control values, due to the high variability between independent experiments.

The Kolmogorov-Smirnov test was performed to determine if data fit into a normal distribution. To compare between two experimental groups, unpaired Student's t-test was computed when the data were normally distributed. The Mann Whitney's U-test was computed as a non-parametric procedure when the data were not normally distributed. Differences were considered statistically significant when p value was less than or equal to 0.05. Both statistical methods were performed using GraphPad Prism v8 and Sigma Plot v11.0 software.

# RESULTS

# 1. Effect of C3G deletion in platelet hemostatic function

## 1.1. C3G ablation alters platelet function

Previous results from our group, using mouse models with transgenic expression of C3G in platelets, demonstrated that C3G regulates the hemostatic function of platelets through its involvement in the PKC-Rap1 pathway (Gutierrez-Herrero *et al.*, 2012). Based on that, we aimed to confirm this role of C3G using a mouse model with permanent ablation of C3G in MK and platelets (C3G-KO model). The absence of C3G in platelets resulted in increased bleeding diathesis due to lower thrombus formation (Gutierrez-Herrero *et al.*, 2020). This suggests impaired platelet function due to the lack of C3G. Therefore, we analyzed platelet activation and aggregation in C3G-KO platelets.

### 1.1.1. C3G deletion impairs integrin αIIbβ3 activation

To study the effect of C3G ablation on platelet function, we monitored the activation of the major platelet integrin, αIIbβ3, by flow cytometry in platelets stimulated with thrombin, ADP or CRP. We used two different markers: i) an antibody that specifically binds to the active conformation of the integrin (JON/A clone), when platelets were stimulated with thrombin or CRP; ii) AF488-labeled fibrinogen, when platelets were activated with ADP.

Platelets were stimulated with 0.5 and 1 U/ml thrombin, 1, 2, 5 and 10 µg/ml CRP and 10 mM ADP. C3G-KO platelets showed lower activation in response to all agonists used, especially at high concentrations (**Figure R-1**). This result is in agreement with the increased integrin αIIbβ3 activation observed in tgC3G platelets stimulated with thrombin or ADP (Gutierrez-Herrero *et al.*, 2012) and reinforces the idea of a role of C3G in the second wave of Rap1 activation induced by thrombin (Franke *et al.*, 2000). Furthermore, defective integrin activation in C3G-KO platelets after CRP stimulation (**Figure R-1C**) suggests that C3G is also involved in the GPVI or integrin α2β2 pathways.

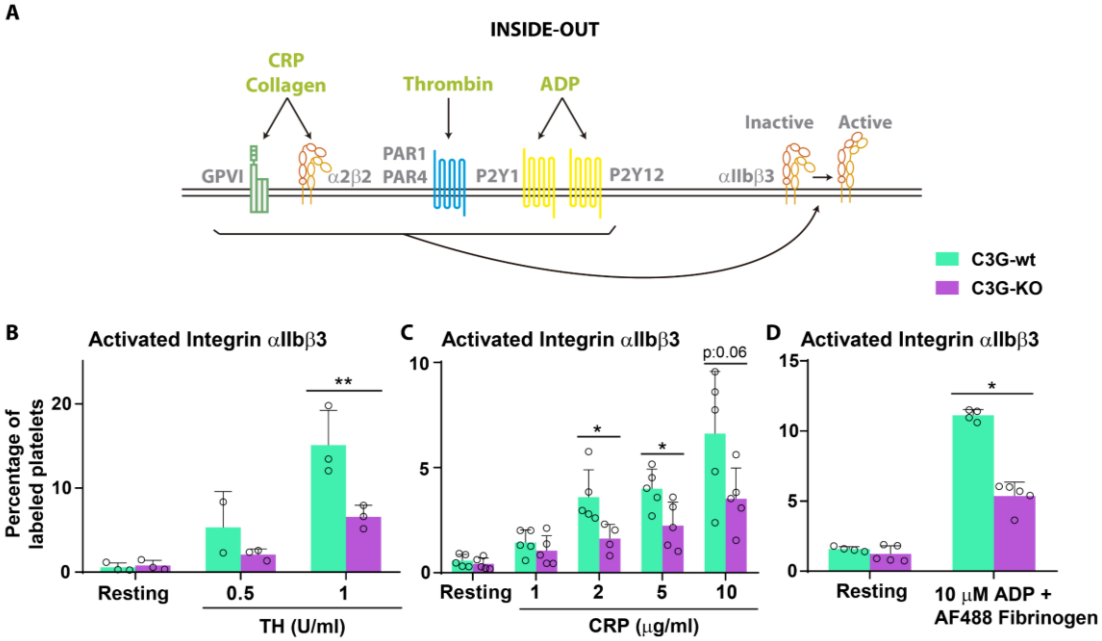

**Figure R-1. C3G-KO platelets display defective integrin αIIbβ3 activation after stimulation with thrombin, CRP or ADP. (A)** Schematic representation of the main inside-out pathways involved in the activation of integrin αIIbβ3. **(B, C)** Washed blood from C3G-wt and C3G-KO mice was stimulated with **(B)** 0.5 or 1 U/ml thrombin (TH), or **(C)** 1, 2, 5 or 10 µg/ml CRP and incubated with JON/A-PE antibody to monitor the percentage of platelets in which the integrin αIIbβ3 was activated. **(D)** Washed blood from C3G-wt and C3G-KO mice was treated with 10 µM ADP in combination with AF488-fibrinogen, and labeled platelets were detected by flow cytometry. The histograms represent the mean ± SD of the percentage of labeled platelets. *p<0.05, **p<0.01. CRP: Collagen related peptide; AF: Alexa Fluor.

These results indicate that C3G is an essential regulator of integrin αIIbβ3 activation upon stimulation of different signaling pathways.

As mentioned, C3G participates in the second wave of thrombin-induced Rap1 activation involving PKC (Gutierrez-Herrero *et al.*, 2012). In addition, we have previously shown that, indeed, PKC regulates C3G in platelets (Gutierrez-Herrero *et al.*, 2020). Thus, we attempted to elucidate which specific PKC isoform is involved in C3G actions in platelets. To this end, we analyzed integrin αIIbβ3 activation in response to thrombin in tgC3G, C3G-KO platelets and their controls, pretreated with inhibitors of the different PKC isoforms. Specifically, we used an inhibitor of cPKCs (Go6976), and two inhibitors of nPKCs (PKCθ inhibitor and Vtx27). As control, we used BIS, a pan-PKC inhibitor.

All PKC inhibitors used completely abrogated integrin αIIbβ3 activation in wtC3G platelets, supporting previous findings on the involvement of different PKCs in platelet activation (Cifuni *et al.*, 2008). However, treatment with Go6976 (PKCα and β inhibitor) did not alter the activation of tgC3G platelets, suggesting that cPKCs did not participate in C3G actions (**Figure R-2A**). In contrast, Vtx27 (PKCδ and θ inhibitor) completely abolished the activation of the integrin in tgC3G platelets. In addition, PKCθ inhibitor had a partial inhibitory effect (alone or in combination with Go6976). This indicates that nPKCs, in particular PKCδ, could be the PKC isoforms involved in the thrombin-C3G-Rap1 pathway in platelets.

In concordance with the above results, PKCθ inhibitor and Vtx27 further decreased integrin αIIbβ3 activation in C3G-KO platelets (**Figure R-2B**). These data reinforce the idea that nPKCs, (probably PKCδ) and C3G participate in a common pathway than regulates platelet integrin activation.

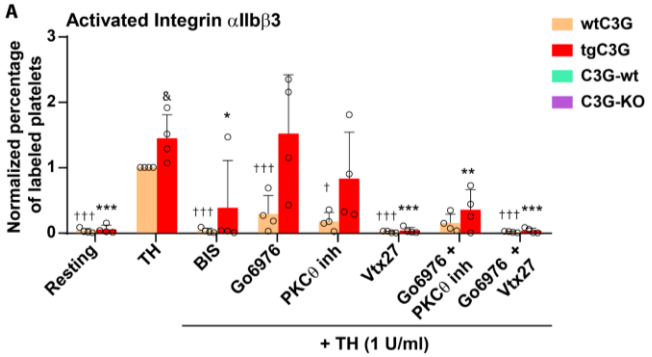

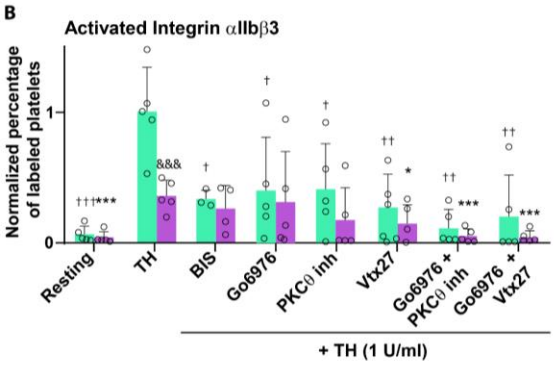


**Figure R-2. C3G regulates integrin αIIbβ3 activation through nPKC isoforms after thrombin stimulation.** Washed blood from **(A)** wtC3G and tgC3G or from **(B)** C3G-wt and C3G-KO mice was pre-treated with either **(A)** 1 μM Go6976, 20 μM PKCθ inhibitor or 100 μM Vtx27 or **(B)** 2 μM Go6976, 40 μM PKCθ inhibitor or 200 μM Vtx27 for 30 min or 5 μM BIS for 5 min prior to stimulation with 1 U/ml thrombin (TH). Then blood was incubated with JON/A-PE antibody to monitor the percentage of platelets in which the integrin αIIbβ3 was activated. The histograms represent the mean ± SEM of the percentage of labeled platelets, normalized against wild-type TH value. &<0.05, &&&<0.001 versus the corresponding wt. †p<0.05, ††p<0.01, †††p<0.001 versus thrombin-stimulated wild-type; *p<0.05, **p<0.01, ***p<0.001 versus thrombin-stimulated tgC3G (upper panel) or C3G-KO (lower panel), respectively.

### 1.1.2. C3G absence affects P-selectin exposure

To gain insight into the role of C3G in platelet activation, we studied the effect of C3G ablation on P-selectin exposure on the platelet surface. P-selectin is a marker of both, platelet activation and α-granule secretion, easy to detect by flow cytometry due to its location as a transmembrane protein.

Consistent with the enhanced P-selectin exposure on the platelet surface observed in tgC3G platelets upon stimulation with different agonists (Gutierrez-Herrero *et al.*, 2012), ablation of C3G in platelets greatly decreased P-selectin exposure after stimulation with thrombin, CRP and PMA (**Figure R-3**). Specifically, C3G-KO platelets exhibited a significant decrease in P-selectin exposure after stimulation with high-dose thrombin or CRP (**Figures R-3A-C**), similarly to the observed with integrin αIIbβ3 activation (**Figure R1**). Moreover, C3G obliteration in platelets almost completely abrogated P-selectin exposure induced by PMA stimulation at both, low and high doses of PMA (**Figures R-3D, E**). This finding supports our previous results in tgC3G platelets, showing increased P-selectin exposure on the platelet surface upon stimulation with thrombin or PMA, which is affected by pre-treatment with BIS (Gutierrez-Herrero *et al.*, 2012).

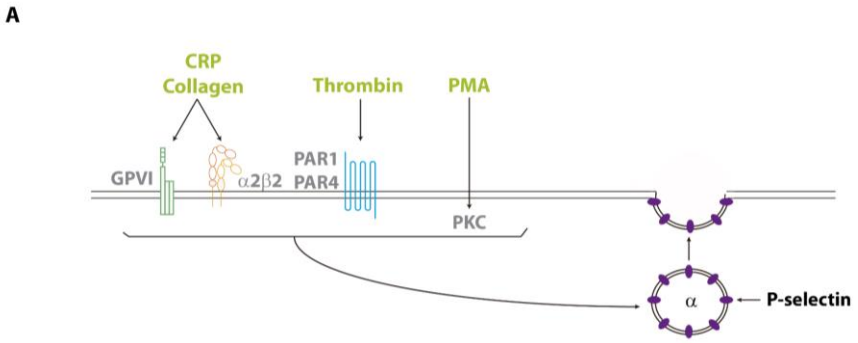

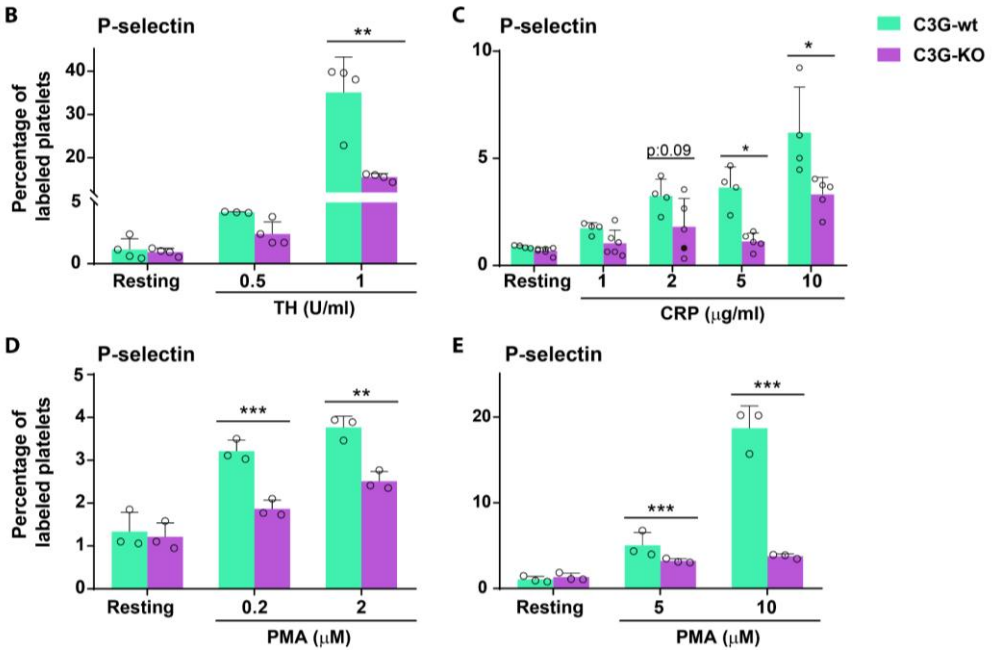


**Figure R-3. C3G-KO platelets show a defective P-selectin exposure on the platelet surface after stimulation with thrombin, CRP or PMA. (A)** Schematic representation of the main pathways involved in α-granule secretion, which results in P-selectin exposure on platelet surface. Washed blood from C3G-wt and C3G-KO mice was stimulated with **(B)** 0.5 or 1 U/ml thrombin (TH), **(C)** 1, 2, 5 or 10 µg/ml CRP, **(D)** 0.2 or 2 µM PMA or **(E)** 5 or 10 µM PMA, and incubated with anti-P-selectin-FITC and anti-CD41-PE to analyze the percentage of platelets with P-selectin exposure on their surface. Histograms represent the mean ± SD of the percentage of labeled platelets. *p<0.05, **p<0.01, ***p<0.001. CRP: Collagen related peptide.

### 1.1.3. C3G regulates P-selectin exposure through novel PKC isoforms

As detailed in the **Introduction**, one of the main functions of PKCs is their participation in platelet secretion, although the specific role of each isoform remains unknown.

To determine whether any PKC isoform also plays a role in C3G function in degranulation, we analyzed P-selectin exposure on the surface of thrombin- or PMA-stimulated tgC3G, C3G-KO platelets and their controls, in the presence of the PKC inhibitors used above. As shown in **Figure R-4A**, and in agreement with results in **Figure R-2**, Vtx27 completely abrogated the increase in P-selectin exposure induced by thrombin, in both tgC3G and wtC3G platelets, whereas Go6976 showed a slight effect on thrombin-stimulated wtC3G platelets but not on tgC3G platelets. PKCθ inhibitor had also a minor effect on P-selectin exposure in tgC3G platelets; therefore, we postulate that PKCδ might be the main PKC isoform acting through C3G in platelet degranulation. Similar results were observed in PMA-stimulated platelets (**Figure R-4B**), in agreement with the existence of a PKC-dependent thrombin-triggered pathway (Cifuni *et al.*, 2008; Gutierrez-Herrero *et al.*, 2012).

Likewise to the integrin activation results, P-selectin exposure on C3G-KO platelets was further affected by BIS, Vtx27 and the combination of Go6976 with PKCθ inhibitor or Vtx27, confirming the participation of C3G and PKCδ in a common pathway during platelet degranulation (**Figures R-4C, D**).

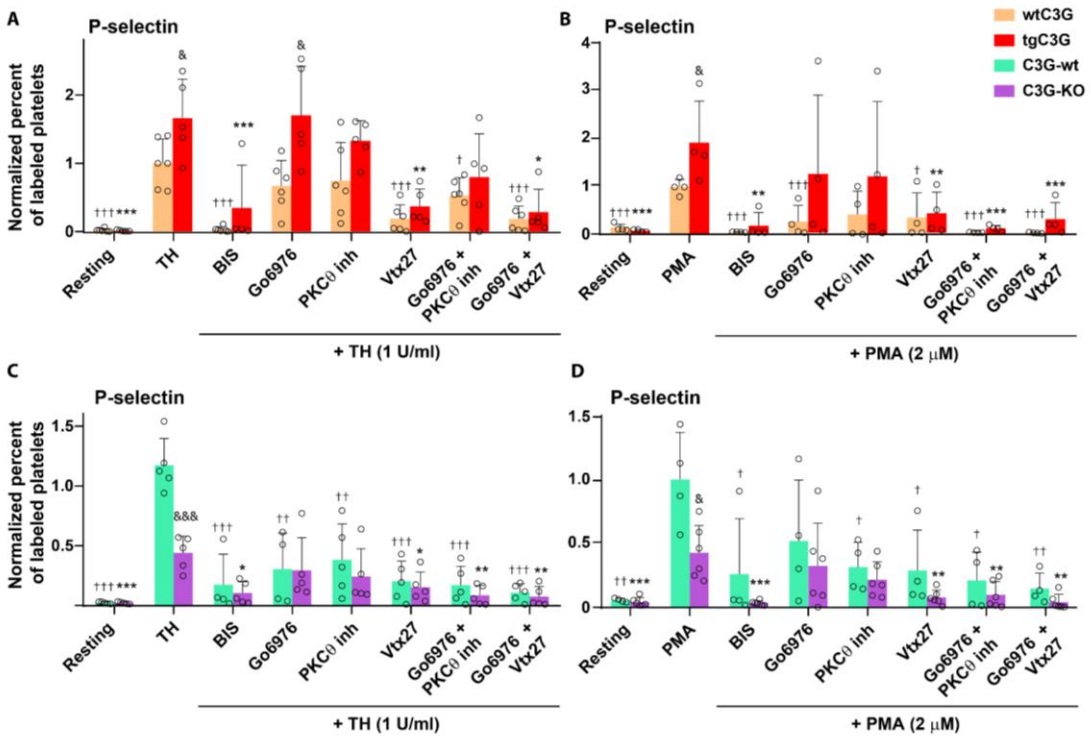


**Figure R-4. C3G function in P-selectin exposure on platelet surface is dependent on PKCδ.** Washed blood from **(A, B)** wtC3G and tgC3G or **(C, D)** C3G-wt and C3G-KO mice was pre-treated with either **(A,B)** 1 μM Go6976, 20 μM PKCθ inhibitor or 100 μM Vtx27 or **(C, D)** 2 μM Go6976, 40 μM PKCθ inhibitor or 200 μM Vtx27 for 30 min or 5 μM BIS for 5 min prior to stimulation with **(A, C)** 1 U/ml thrombin (TH) or **(B, D)** 2 μM PMA. Then blood was incubated with anti-P-selectin-FITC and anti-CD41-PE antibodies to analyze the percentage of platelets in which P-selectin was exposed on their surface. The histograms represent the mean ± SEM of the percentage of labeled platelets normalized against TH-stimulated control platelets. &<0.05, &&<0.01, &&&<0.001 versus their corresponding wild-type. †p<0.05, ††p<0.01, †††p<0.001 versus TH-stimulated wild-type; *p<0.05, **p<0.01, ***p<0.001 versus TH- or PMA-stimulated **(A, B)** tgC3G or **(C, D)** C3G-KO.

Taken together, these data suggest that platelet C3G regulates both, integrin αIIbβ3 activation and α-granule secretion, through novel PKC isoforms, mainly PKCδ.

### 1.1.4. Obliteration of C3G affects platelet aggregation

To complement the platelet activation data, we analyzed the effect of C3G deletion in platelet aggregation. Platelets were incubated with 1 U/ml thrombin, 5 and 10 μg/ml CRP, 10 μM PMA or 10 μM ADP under shaking, and aggregates were monitored by flow cytometry.

Similarly to the activation results, C3G-KO platelets formed significant fewer aggregates in response to all stimuli, mainly thrombin and CRP (Figures R-5A-D).

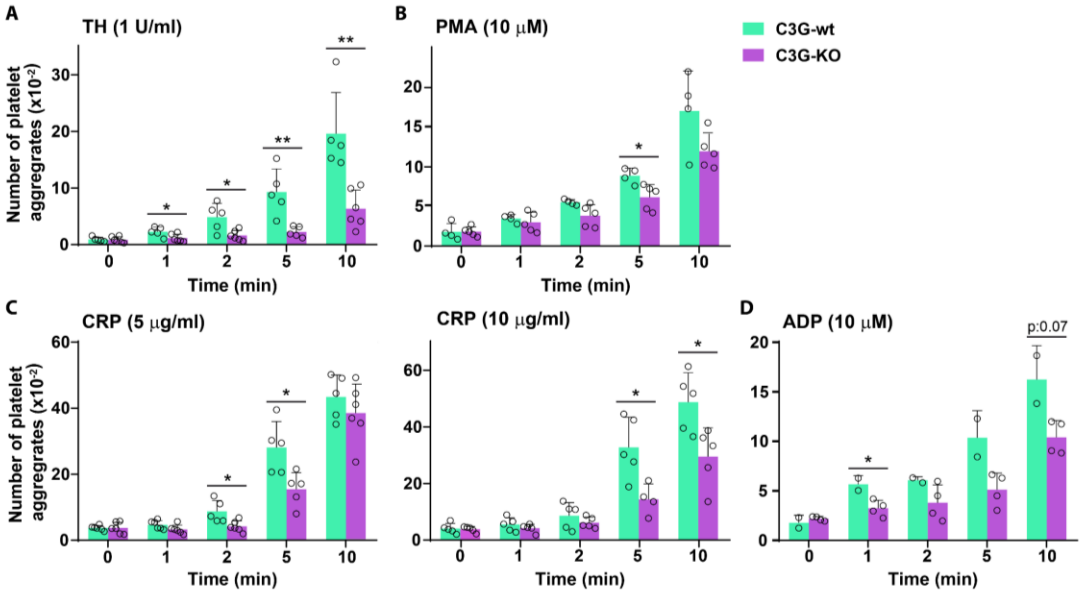


**Figure R-5. C3G regulates platelet aggregation in response to thrombin, PMA, CRP and ADP.** Histograms represent the mean ± SD of the number of platelet aggregates formed upon stimulation with **(A)** 1 U/ml thrombin (TH), **(B)** 10 µm PMA, **(C)** 5 and 10 µg/ml CRP, **(D)** 10 µM ADP, for the indicated time periods from C3G-wt and C3G-KO platelets. *p<0.05, **p<0.01. CRP: Collagen related peptide.

The lower number of aggregates formed in C3G-KO platelets, together with the opposite phenotype observed previously in tgC3G platelets (Gutierrez-Herrero *et al.*, 2012), reinforce the notion of an important role of C3G in platelet aggregation.

## 1.2. C3G ablation leads to decreased Rap1 activation

As mentioned before, Rap1 is the GTPase that controls platelet activation and aggregation (Stefanini & Bergmeier, 2016) and C3G is one of its main activators (Radha *et al.*, 2011). In concordance, we previously observed increased Rap1 activation in tgC3G platelets (Gutierrez-Herrero *et al.*, 2012). Therefore, we wanted to corroborate this functional relationship in our C3G-KO platelets.

C3G-KO and C3G-wt platelets were stimulated with thrombin, CRP and PMA (**Figure R-6A**). We used different concentrations and times of thrombin stimulation to distinguish between the two waves of Rap1 activation described (Franke *et al.*, 2000). C3G-KO platelets presented lower levels of active Rap1 in response to long thrombin exposure (5 min) (**Figure R-6B**) or high-dose thrombin (2 U/ml) (**Figures R-6C**). In contrast, C3G-KO platelets showed no defect in response to lower-dose thrombin (0.2 U/ml) or short exposure (1 min). Similar results were observed with CRP (**Figure R-6D**), confirming the participation of C3G in the second wave of Rap1 activation induced by thrombin, which is dependent on PKC (Franke *et al.*, 2000). In fact, the lack of activation of Rap1 in C3G-KO platelets in response to low-dose PMA confirms this (**Figure R-6E**), and suggests that C3G is the main Rap1 activator under these conditions. The increased levels of Rap1-GTP in C3G-KO platelets upon stimulation with a high concentration of PMA reflect a delay in Rap1 activation and, hence, its slower downregulation, as described (Franke *et al.*, 2000).

Furthermore, these results are in agreement with previous results in tgC3G platelets demonstrating that C3G phosphorylation and activation is regulated by PKC (Gutierrez-Herrero *et al.*, 2020).

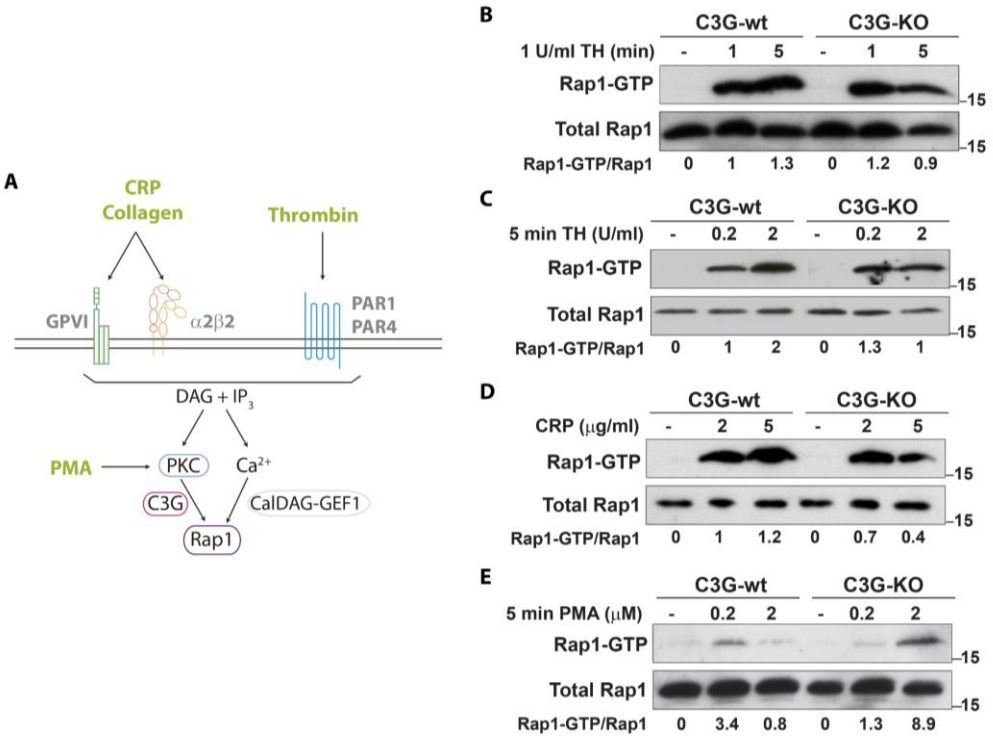


**Figure R-6. C3G regulates Rap1 activation upon platelet stimulation. (A)** Schematic representation of the pathways involved in the activation of Rap1 in platelets after stimulation with the agonists used. Platelets from C3G-wt and C3G-KO mice were stimulated with (**B**) 1 U/ml thrombin (TH) for 1 and 5 min, **(C)** 0.2 and 2 U/ml thrombin (TH) for 5 min, (**D**) 2 and 5 μg/ml CRP for 5 min and **(E)** 0.2 and 2 μM PMA for 5 min. The levels of Rap1-GTP were determined by pull-down assay and immunoblotting using an anti-Rap1 antibody. Values are relative to unstimulated C3G-wt platelets and were normalized to total Rap1 levels. CRP: Collagen related peptide; DAG: diacylglycerol; $IP_3$: inositol trisphosphate.

Our data in C3G-KO platelets are similar to those obtained with tgC3GΔCat platelets and opposite to the data on tgC3G platelets (Gutierrez-Herrero *et al.*, 2012), which validate our findings. Collectively, all these results are in agreement with the phenotype of CalDAG-GEFI-knockout platelets, which showed no significant alterations in aggregation or Rap1 activation in response to PMA, thrombin and collagen at a high dose or under long-term stimulation (Crittenden *et al.*, 2004). Therefore, we confirm that C3G is an important regulator of primary hemostasis, through Rap1.

## 1.3. C3G does not participate in platelet maturation

As mentioned in the **Introduction**, two different types of platelets are found in blood circulation: reticulated or immature platelets and old or mature platelets. Reticulated platelets are newly released from the BM. They are prothrombotic and more reactive due to their larger size, greater degranulation and greater expression of platelet surface receptors and adhesion proteins (Bongiovanni *et al.*, 2022). Reticulated platelets can be identified by their higher amount of RNA compared to old platelets. Based on that, we determined the content of RNA in platelets from the different genotypes by staining them with pyronin Y.

We did not observe differences in RNA content between the different genotypes (Figure R-7), suggesting that C3G is not essential for platelet maturation.

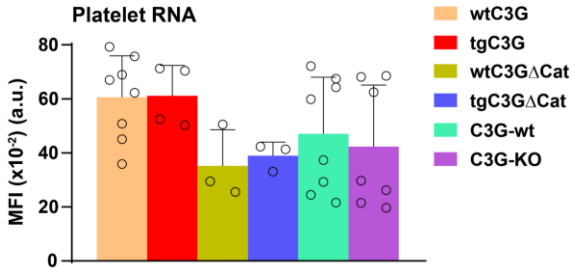


**Figure R-7. C3G does not alter maturity of platelets.** Washed platelets from the indicated genotypes were incubated with Hoechst 33342 (for DNA staining), prior incubation with Pyronin Y, and immediately analyzed by flow cytometry. Histograms represent the mean ± SD of the MFI values. MFI: mean fluorescence intensity; a. u.: arbitrary units.

## 1.4. C3G deficiency in platelets impairs secondary hemostasis

As detailed in the Introduction, during primary hemostasis platelet activation is followed by the secretion of a wide range of factors, which trigger platelet aggregation and stimulate thrombus formation (Golebiewska & Poole, 2015). However, the plug formed is not yet stable. This stabilization occurs during secondary hemostasis.

Since our results demonstrated that C3G participates in primary hemostasis, we wanted to investigate whether C3G could also regulate secondary hemostasis.

### 1.4.1. C3G controls phosphatidylserine exposure on platelet surface

Platelets facilitate the formation of thrombin by providing procoagulant phospholipids, such as PS and phosphatidylcholine (Komiyama *et al.*, 1990).

As a first approach, we measured the percentage of platelets that exposed PS on the surface after stimulation with a combination of thrombin and CRP. Overexpression of C3G in platelets had not effect in PS exposure upon thrombin-CRP mixture stimulation (Figure R-8A). However, C3G-KO platelets showed differential exposure of PS on the surface, compared to C3G-wt platelets: lower PS exposure at 5 µg/ml CRP and higher exposure after stimulation with 10 µg/ml CRP (Figure R-8B). Since a small, but significant, decrease in PS translocation was observed in C3G-KO platelets at low CRP concentration, the high increase observed at 10 µg/ml CRP suggests a compensatory mechanism to counteract the delay of C3G-KO platelets on PS exposure.

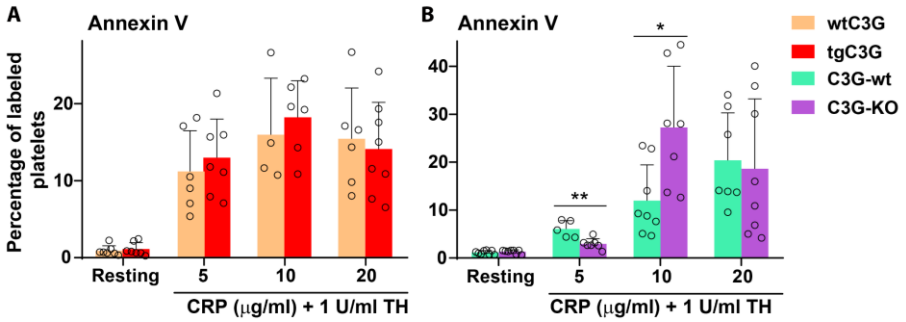


**Figure R-8. C3G deletion, but not C3G overexpression, alters PS exposure on the platelet surface after stimulation.** Washed platelets from **(A)** wtC3G and tgC3G mice or **(B)** C3G-wt and C3G-KO mice were stimulated with 1 U/ml thrombin (TH) in combination with 5, 10 or 20 µg/ml CRP, and labeled with an anti-CD41-FITC antibody and Annexin V-APC for 15 min. Samples were diluted and analyzed by flow cytometry. Histograms represent the mean ± SD of the percentage of labeled platelets. *p<0.05, **p<0.01. CRP: Collagen related peptide; PS: phosphatidylserine.

### 1.4.2. C3G regulates the secretion of coagulation factors

Since C3G-KO platelets showed altered PS exposure and C3G overexpression modulates platelet secretion (Martin-Granado *et al.*, 2017), we wanted to know if C3G could also regulate secondary hemostasis through modulation of the secretion of factors of the coagulation cascade.

Using the Proteome Profiler Mouse Angiogenesis Array Kit (R&D systems), we examined the secretome of tgC3G, C3G-KO platelets and their corresponding wild-type controls, for levels of tissue factor (TF, also known as Coagulation Factor III), the main inhibitor of tissue plasminogen activator (tPA), Serpin E1, the vasoconstrictor endothelin 1, and the coagulation promoter factor PF4. As shown in **Figure R-9**, upon thrombin stimulation, C3G ablation triggered a marked increase in the secretion of these coagulation factors, whereas C3G overexpression caused their retention.

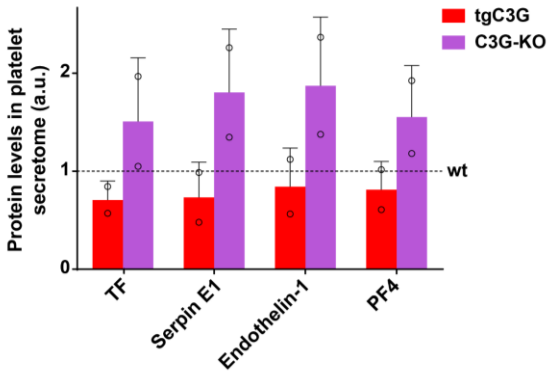


**Figure R-9. C3G regulates the secretion of coagulation factors after thrombin stimulation.** Secretome from thrombin-stimulated tgC3G, C3G-KO platelets and their corresponding wild-types were analyzed using the commercial Mouse Angiogenesis Array Kit. Histograms represent the quantification of TF, Serpin E1, Endothelin-1 and PF4 levels. Data were relativized against the control (wild-type) values, which were given a value of 1 in each independent experiment. Histograms represent the mean ± SD of the protein levels. PF4: platelet factor 4; TF: tissue factor; a.u.: arbitrary units.

These results are in line with a negative role for C3G in the coagulation cascade.

### 1.4.3. C3G obliteration results in impaired thrombin generation

Based on the defects in PS exposure in C3G-KO platelets, we wanted to investigate whether this altered PS exposure could affect thrombin generation. For that, we examined the generation of thrombin after stimulation with TF, phospholipids or a combination of both, using CAT technique.

C3G-KO mice displayed lower thrombin generation in response to 1 pM TF but not in response to phospholipids or the combination of both (Figures R-10A-C). Specifically, C3G-KO mice showed a nearly significant decrease in ETP (Figure R-10D), but not in lag time, thrombin generation peak (Peak) or time to peak (ttPeak) (Figures R-10E, F, G). These results suggest that C3G-KO defects in thrombin generation could be due to a defect in PS exposure, while its secretome could have a procoagulant effect.

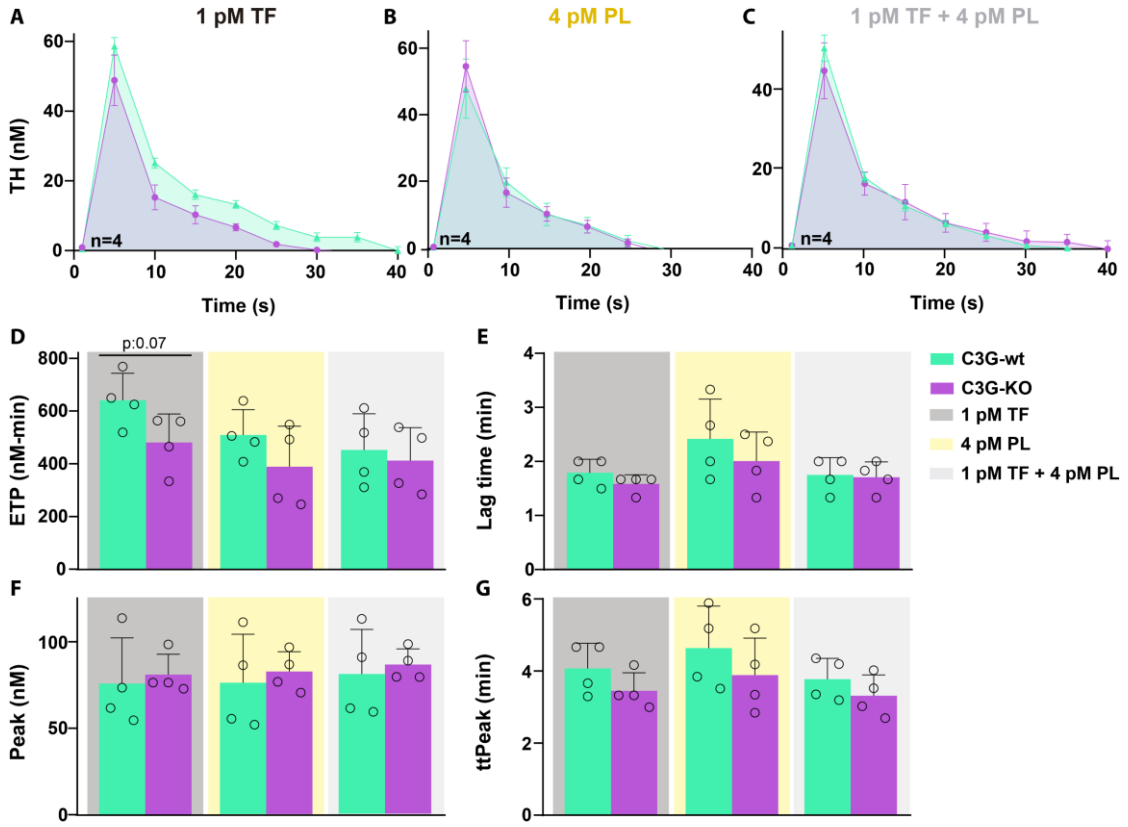


**Figure R-10. C3G deletion results in decreased thrombin generation in response to tissue factor.** Thrombin (TH) generation detected by Calibrated Automated Thrombinography (CAT) of PRP from C3G-wt and C3G-KO mice in response to **(A)** 1 pM TF, **(B)** 4 pM PL and **(C)** the combination of both. Histograms represent the mean ± SD of the **(D)** endogenous thrombin potential or ETP, **(E)** lag time, **(F)** peak thrombin generation or Peak and **(G)** time to peak or ttPeak. TF: tissue factor; PL: phospholipids.

To validate these results we performed a similar analysis in our tgC3G mouse model. In concordance with results in Figure R-8, there were not differences between wtC3G and tgC3G mice in thrombin generation (Figures R-11A-C), although a subtle increase in thrombin generation peak was observed in response to TF (Figure R-11F).

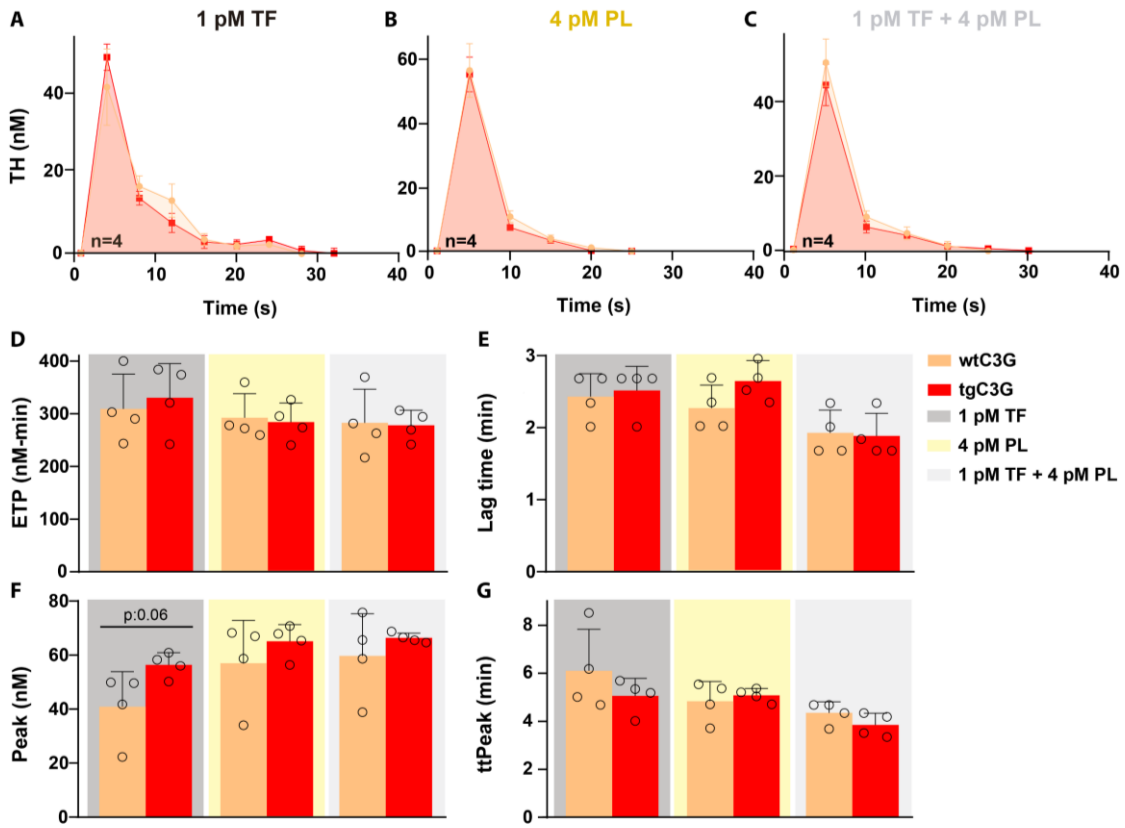


**Figure R-11. C3G overexpression does not affect thrombin generation.** Thrombin (TH) generation detected by Calibrated Automated Thrombinography (CAT) of PRP from wtC3G and tgC3G mice in response to **(A)** 1 pM TF, **(B)** 4 pM PL and **(C)** the combination of both. Histograms represent the mean ± SD of the **(D)** endogenous thrombin potential or ETP, **(E)** lag time **(F)** peak thrombin generation or Peak and **(G)** time to peak thrombin generation or ttPeak. TF: tissue factor; PL: phospholipids.

Results in Figure R-9 suggest that C3G could regulate the secretion of coagulation factors. Based on that, we examined thrombin generation in response to platelet secretomes from tgC3G, C3G-KO platelets and their wild-type controls.

Results in Figures R-12A-D showed that secretome from thrombin-stimulated C3G-KO platelets induced higher, but not significant, thrombin generation (ETP parameter) whereas thrombin-induced tgC3G platelet secretomes showed the opposite tendency. However, there were not differences in lag time, thrombin generation peak (Peak) or time to peak thrombin generation (ttPeak) (Figures R-12E-G).

All these data suggest a positive role of C3G in the regulation of secondary hemostasis, although deletion of C3G would induce a pro-coagulant secretome.

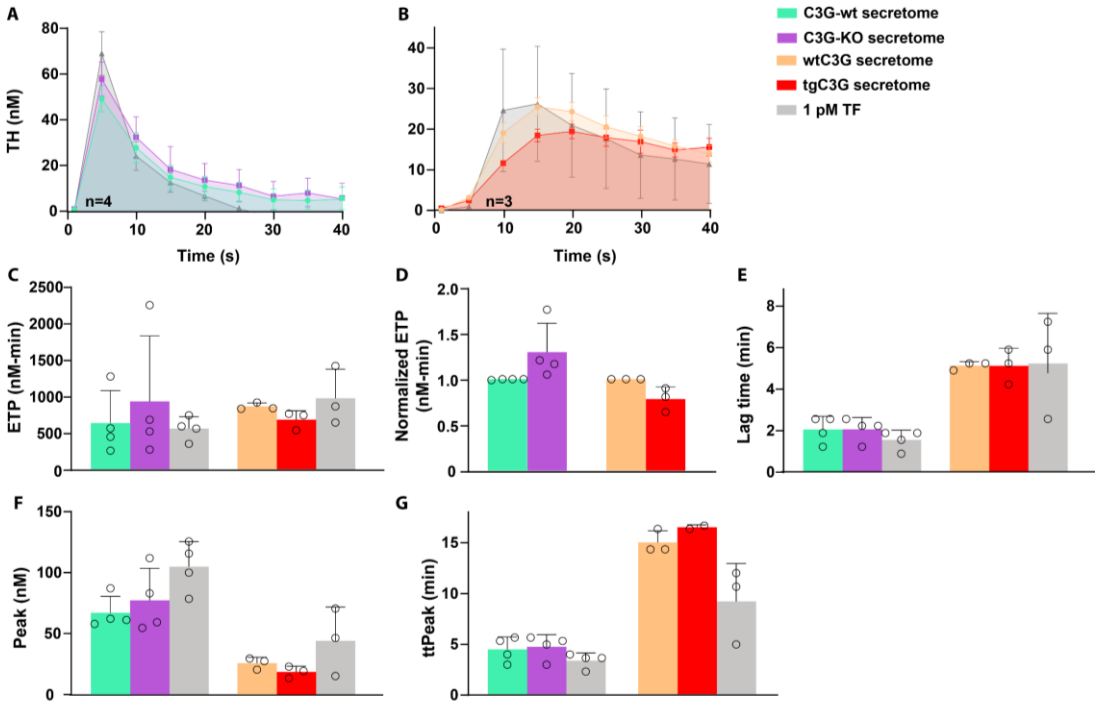


**Figure R-12. C3G obliteration induces a slightly procoagulant secretome, while C3G overexpression would result in an anti-coagulant secretome.** Thrombin (TH) generation detected by Calibrated Automated Thrombinography (CAT) of PRP from C3G-wt and wtC3G mice in response to **(A)** C3G-wt and C3G-KO thrombin-induced secretomes, **(B)** wtC3G and tgC3G thrombin-induced secretomes, respectively. We used 1 pM TF as positive control. Histograms represent the mean ± SD of the **(C)** lag time, **(D)** endogenous thrombin potential or ETP, **(E)** normalized ETP against the ETP values of C3G-wt thrombin-induced secretome, **(F)** peak thrombin generation or Peak and **(G)** time to peak thrombin generation or ttPeak. TF: tissue factor.

Overall, the data in this section confirm our previous results in tgC3G platelets (Gutierrez-Herrero *et al.*, 2012) which, taken together demonstrate an essential role for C3G in platelet hemostasis.

# 2. Role of C3G in platelet spreading and cytoskeleton remodelling

## 2.1. C3G regulates platelet spreading

Our group had previously demonstrated that tgC3G platelets spread more on poly-L-lysine than wtC3G platelets, in response to thrombin. We also observed a larger area of spreading in tgC3GΔCat platelets, compared to their controls. This suggests that C3G has a role in platelet spreading independently of Rap1 activity (Martin-Granado *et al.*, 2017). Thus, we wanted to deep into this process by measuring the spreading capacity of C3G-KO platelets. We also analyzed whether the role of C3G in platelet spreading is dependent on substrates.

### 2.1.1. C3G deletion impairs platelet spreading

First, we performed a spreading assay on IbiTreat plates in real time. Platelets were seeded on the plates and platelet area was measured at different time points (0, 30, 60, 120, 300 and 480 s). C3G-KO platelets presented a significant defect in spreading compared to C3G-wt

platelets after 5 min of spreading. Specifically, C3G-KO platelets failed to form lamellipodia, although they were able to form filopodia (Figures R-13A, B) (Video 1). However, C3G-KO platelets were able to spread at longer times, albeit with significantly less area (Figures R-13C, D), suggesting that they might have a delay in lamellipodia formation.

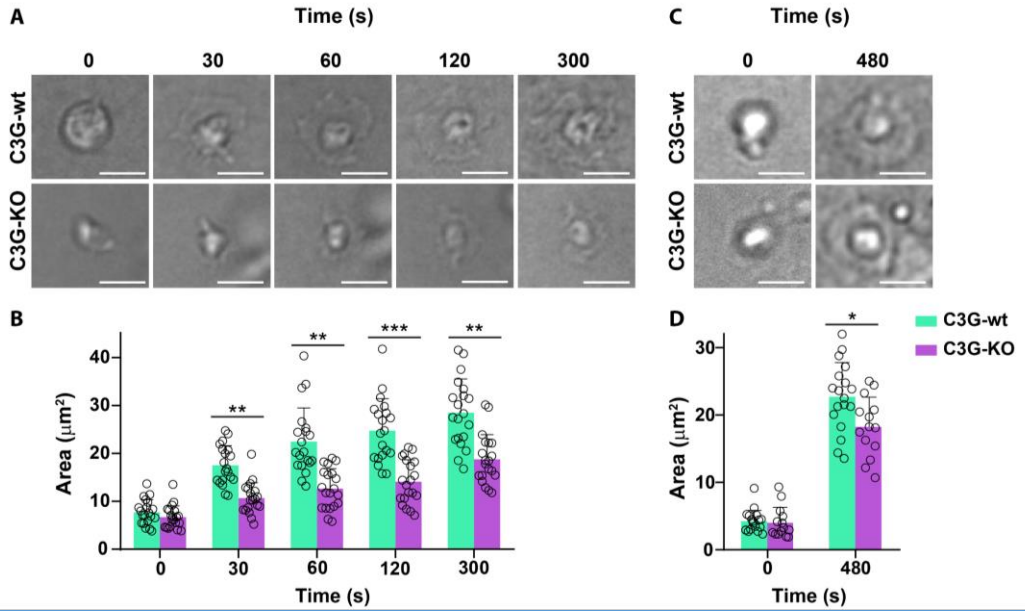


**Figure R-13. C3G ablation delays platelet spreading. (A)** Representative images of C3G-wt and C3G-KO platelets spread on IbiTreat plates at different times (0, 30, 60, 120, 300 s). **(B)** Histogram represents the mean ± SD of platelet area, measured with ImageJ software. **(C)** Representative images of C3G-wt and C3G-KO platelets spread on IbiTreat plates at 0 and 480 s. **(D)** Histogram represents the mean ± SD of platelet area measured with ImageJ software. *p<0.05, **p<0.01, ***p<0.001. Scale bar: 5 µm.

### 2.1.2. Role of C3G in platelet spreading is dependent on substrate

To further evaluate the role of C3G in platelet spreading, we analyzed the effect of C3G deletion, or C3G and C3GΔCat overexpression, in platelet spreading on different substrates (poly-L-lysine, type I collagen, fibrinogen, fibronectin, laminin, osteopontin and vitronectin), after 0.2 U/ml thrombin stimulation.

In line with the results of the IbiTreat assay, C3G-KO platelets exhibited defective spreading, but only on poly-L-lysine, collagen, fibronectin and vitronectin (Figure R-14). C3G deletion affected the spread area (Figures R-14A, B) but not the spread perimeter (Figure R-14C) or platelet shape (Figure R-14D).

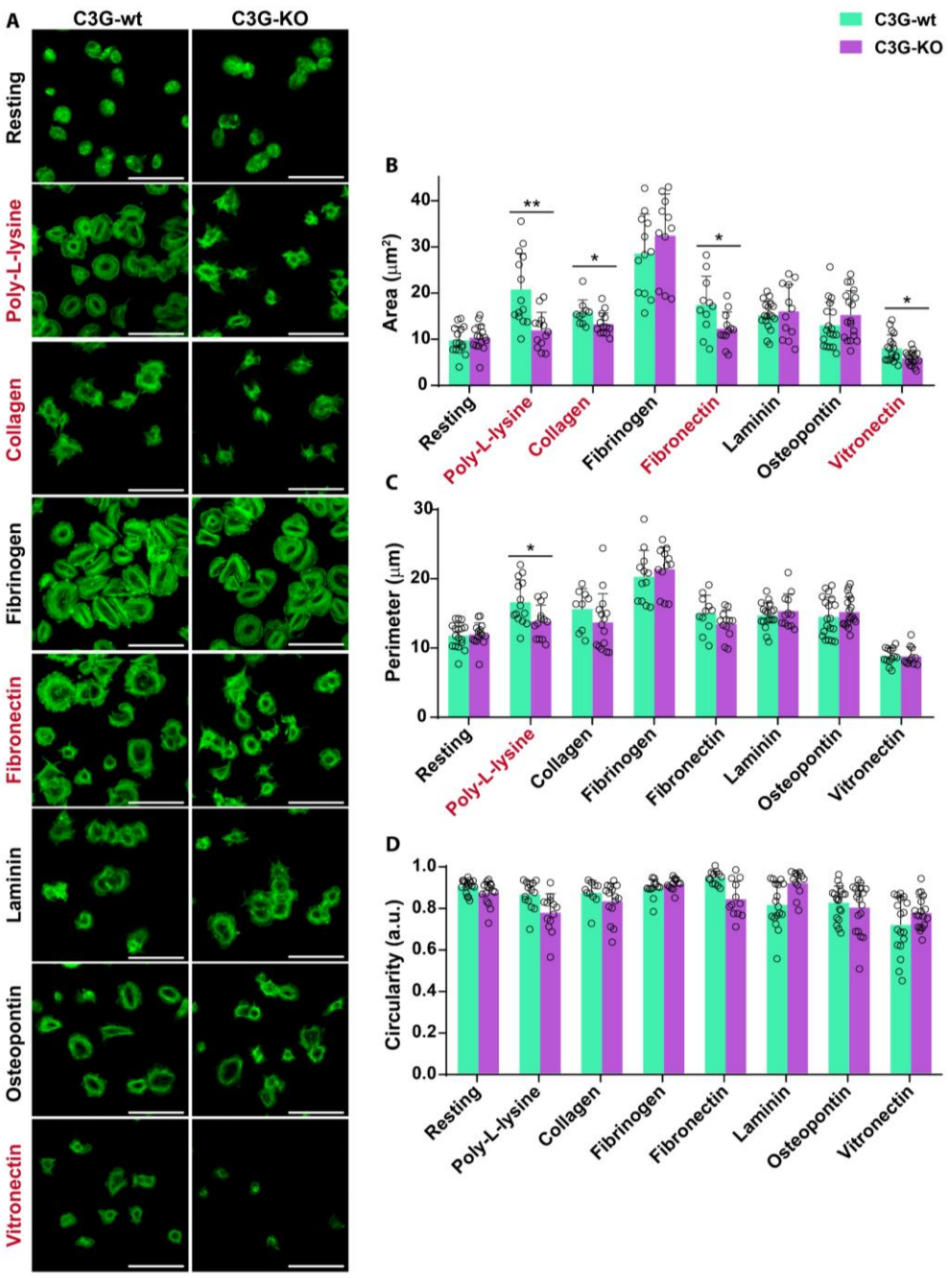


**Figure R-14. After low-dose thrombin stimulation, C3G-KO platelets show a defective spreading on poly-L-lysine, collagen, fibronectin and vitronectin. (A)** Representative images of C3G-wt and C3G-KO platelets spread on poly-L-lysine, type I collagen, fibrinogen, fibronectin, laminin, osteopontin and vitronectin for 30 min after 0.2 U/ml thrombin stimulation. Platelets were stained with Phalloidin to visualize actin cytoskeleton. Scale bar: 5 µm. Histograms represent the mean ± SD of **(B)** platelet area (µm$^2$), **(C)** platelet perimeter (µm) and **(D)** circularity. *p<0.05, **p<0.01. a.u.: arbitrary units. Substrates in which there are differences between genotypes are highlighted in red.

To validate these results, we evaluated the effect of C3G overexpression on spreading. Consistent with our previous results, showing increased spreading of tgC3G platelets on poly-L-lysine (Martin-Granado *et al.*, 2017), and with the results in C3G-KO platelets, tgC3G platelets showed an increased area after 30 min of spreading on collagen, fibronectin and vitronectin (Figures R-15A, B). In contrast, tgC3G platelets failed to spread on osteopontin (Figures R-15A,

B). As with C3G-KO platelets, perimeter and circularity were not affected by C3G overexpression (Figures R-15C, D).

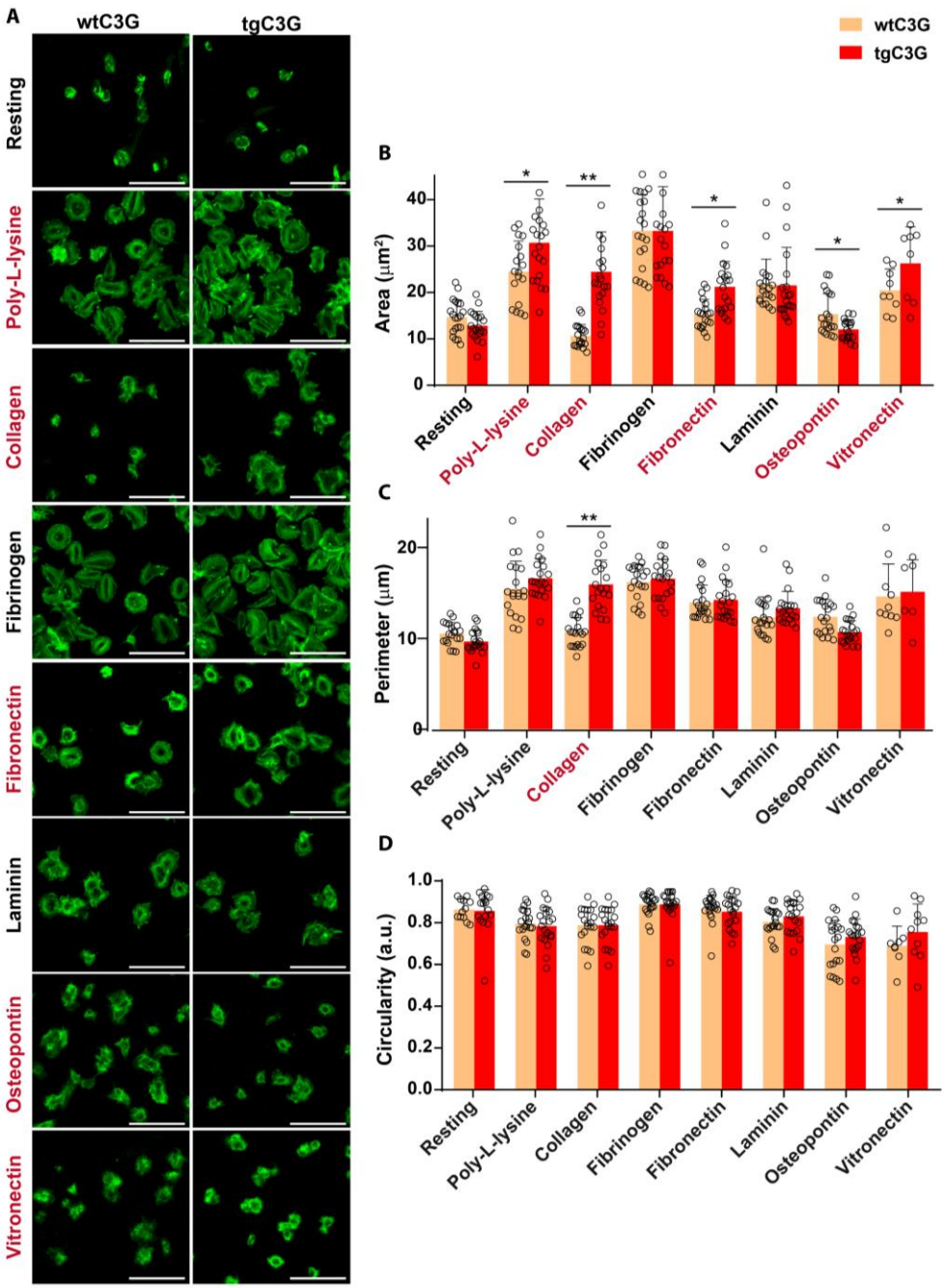


**Figure R-15. tgC3G platelets present greater spreading on poly-L-lysine, collagen, fibronectin and vitronectin, but lower spreading on osteopontin, after low-dose thrombin stimulation. (A)** Representative images of wtC3G and tgC3G platelets spread on poly-L-lysine, type I collagen, fibrinogen, fibronectin, laminin, osteopontin and vitronectin for 30 min after 0.2 U/ml thrombin stimulation for 1 min. Platelets were stained with Phalloidin to visualize actin cytoskeleton. Scale bar: 5 µm. Histograms represent the mean ± SD of **(B)** platelet area (µm$^2$), **(C)** platelet perimeter (µm) and **(D)** circularity. *p<0.05, **p<0.01. a.u.: arbitrary units. Substrates in which there are differences between genotypes are highlighted in red.

These results confirmed the role of C3G in the regulation of platelet spreading in a substrate-dependent manner. Next, we analyzed whether this role of C3G was related to its catalytic (GEF)

activity, by analyzing the spreading ability of tgC3GΔCat platelets. As shown in Figure R-16, tgC3GΔCat platelets exhibited a phenotype similar to that of tgC3G platelets, showing increased spreading on poly-L-lysine, collagen, fibronectin and decreased spreading on osteopontin and vitronectin. These results are in agreement with our previous results on poly-L-lysine (Martin-Granado *et al.*, 2017), and suggest that the role of C3G in platelet spreading is mainly independent of Rap1. However, the different behavior of tgC3G and tgC3GΔCat platelets when spread on vitronectin and the negligible effect of tgC3GΔCat on spreading on fibronectin suggests a putative involvement of Rap1 in some contexts.

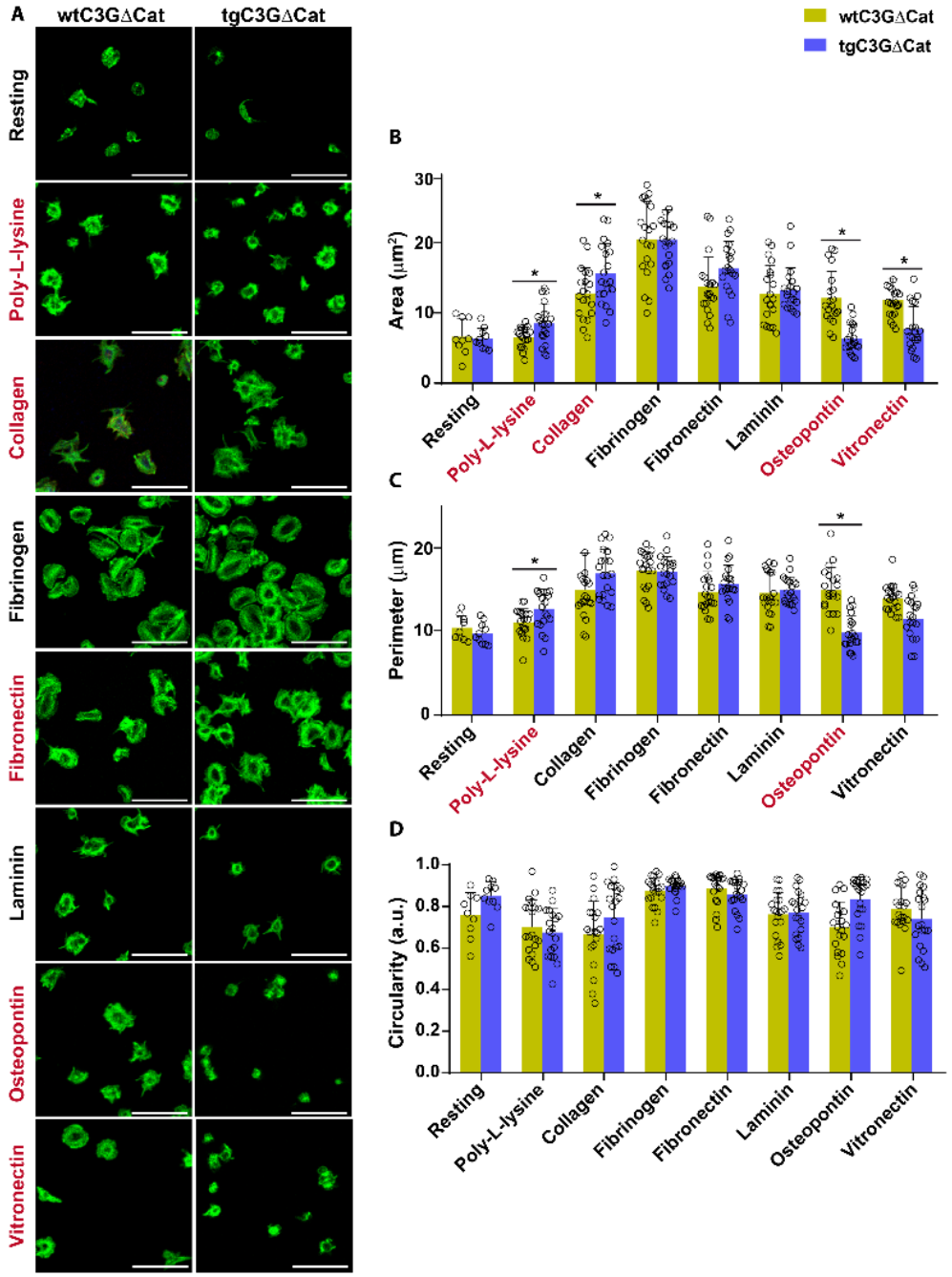


**Figure R-16. tgC3GΔCat platelets display increased spreading on poly-L-lysine, collagen and fibronectin, but fail to spread on osteopontin and vitronectin after low-dose thrombin stimulation.** **(A)** Representative images of wtC3GΔCat and tgC3GΔCat platelets spread on poly-L-lysine, type I

collagen, fibrinogen, fibronectin, laminin, osteopontin and vitronectin for 30 min after 0.2 U/ml thrombin stimulation for 1 min. Platelets were stained with Phalloidin to visualize actin cytoskeleton. Scale bar: 5 µm. Histograms represent the mean ± SD of **(B)** platelet area (µm$^2$), **(C)** platelet perimeter (µm) and **(D)** circularity. *p<0.05. a.u.: arbitrary units. Substrates in which there are differences between genotypes were highlighted in red.

The above results were performed using a low-dose thrombin. Since thrombin triggers different pathways and platelet activation responses depending on the dose and time of exposure (Franke *et al.*, 2000), and the effect of C3G is mainly observed at high-dose thrombin (Gutierrez-Herrero *et al.*, 2012), we performed the spreading analysis using 1 U/ml thrombin. We obtained similar results, i.e. C3G overexpression resulted in a greater spreading area on poly-L-lysine, collagen, and fibronectin, whereas C3G deletion had the opposite effect, with no differences on fibrinogen and laminin with respect to control platelets (Figures R-17A-C). In this case, we also observed differences in platelet perimeter, in correlation with the platelet area.

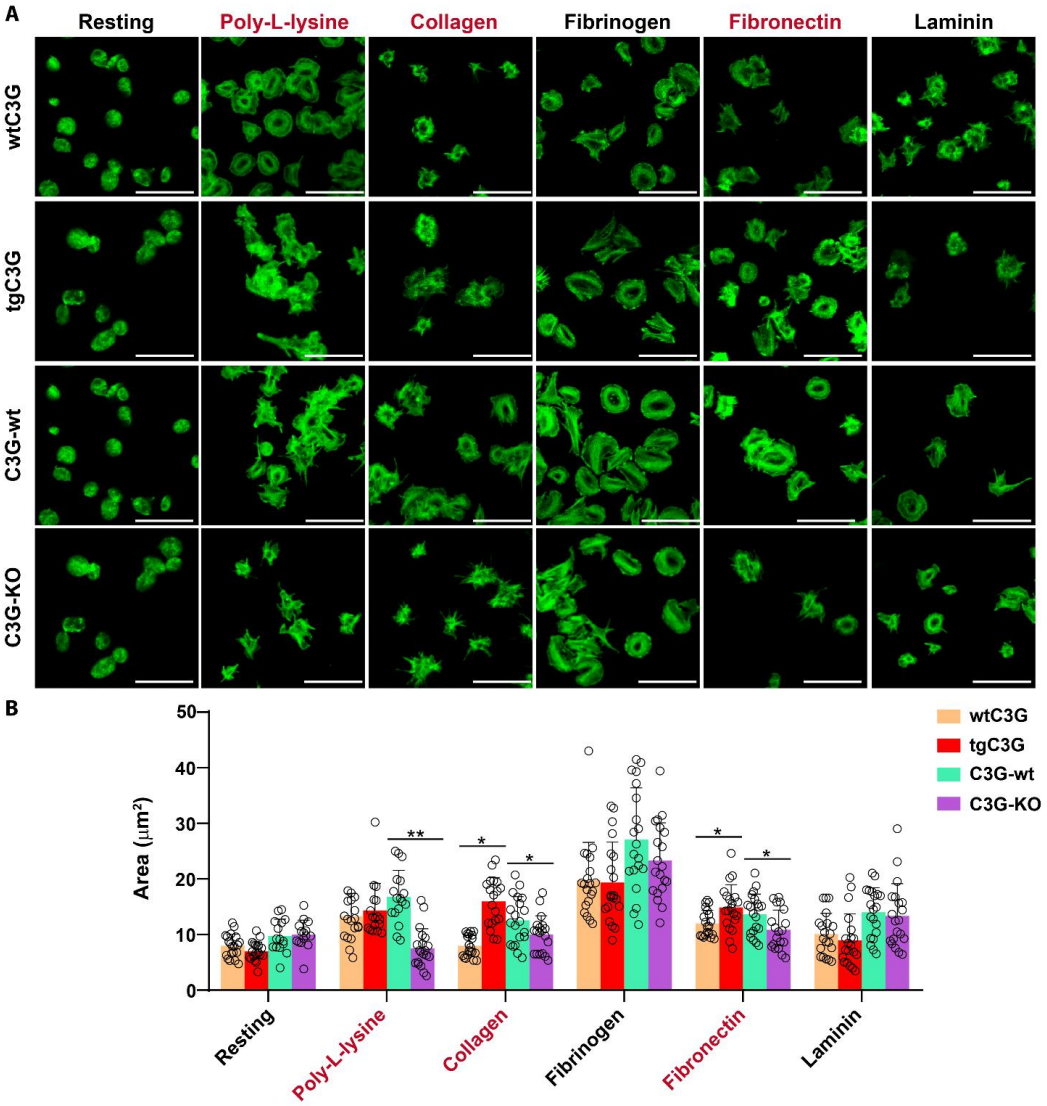

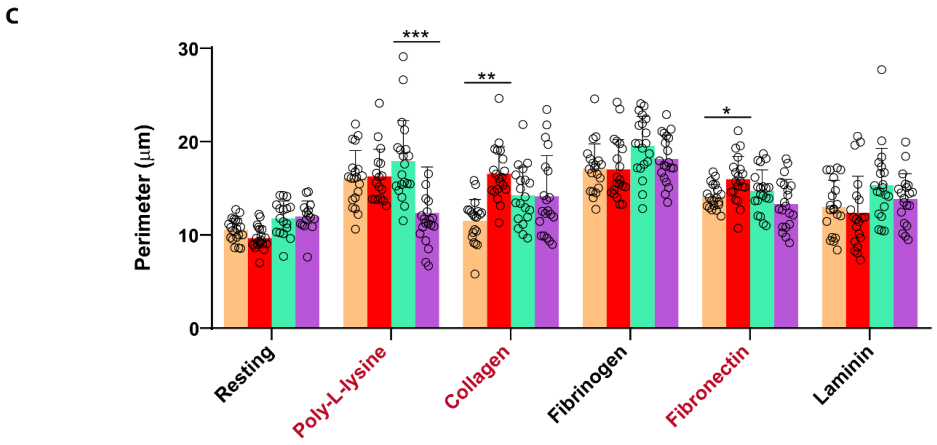


**Figure R-17. C3G regulates platelet spreading on poly-L-lysine, collagen and fibronectin under high-dose thrombin stimulation. (A)** Representative images of tgC3G, C3G-KO platelets and their controls spread on poly-L-lysine, type I collagen, fibrinogen, fibronectin and laminin for 30 min after 1 U/ml thrombin stimulation for 1 min. Platelets were stained with Phalloidin to visualize actin cytoskeleton. Scale bar: 5 µm. Histograms represent the mean ± SD of **(B)** platelet area (µm$^2$) and **(C)** platelet perimeter (µm). *p<0.05, **p<0.01, ***p<0.001. a.u.: arbitrary units. Substrates in which there are differences between genotypes are highlighted in red.

Overall, these data demonstrate a role for C3G in platelet spreading, which is substrate dependent and largely independent of its catalytic activity.

### 2.1.3. C3G acts in the last steps of spreading

Next, we examined in which step of platelet spreading C3G participates. We performed a time-lapse assay, monitoring platelet area and platelet perimeter after 5, 15 and 30 min of spreading.

We did not observe any effect of C3G overexpression or deletion after 5 min of spreading (Figure R-18A). In contrast, after 15 min of spreading we obtained results similar to those of previous experiments, i.e. (i) greater spreading of tgC3G platelets *versus* wtC3G platelets on collagen, fibronectin, and vitronectin and decreased spreading on osteopontin; (ii) decreased spreading of C3G-KO platelets *versus* C3G-wt platelets on collagen, fibronectin and vitronectin (Figure R-18B). These differences were more evident at 30 min (Figure R-18C).

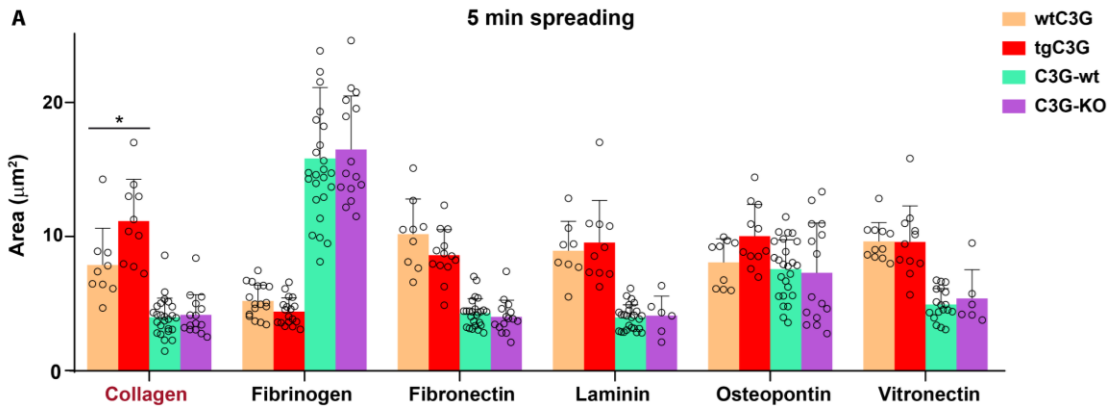

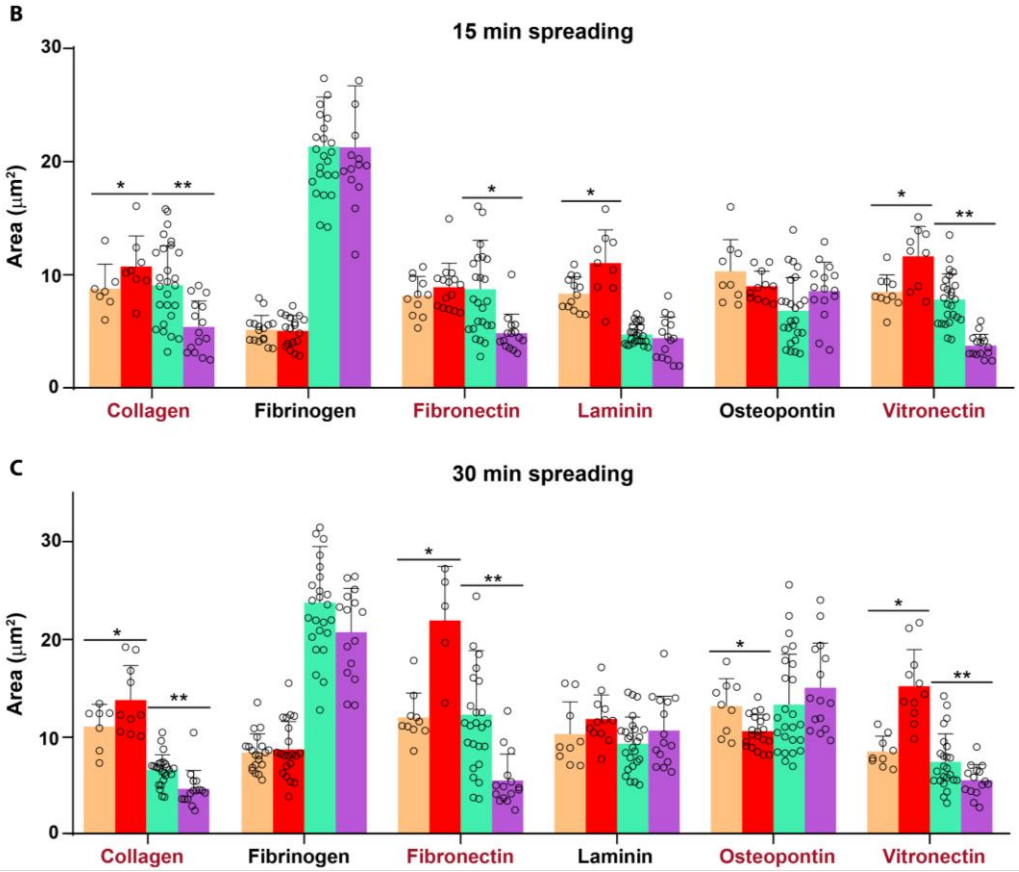


**Figure R-18. C3G overexpression and obliteration affect last steps of spreading on collagen, fibronectin and vitronectin.** TgC3G, C3G-KO platelets and their corresponding wild-types were stimulated with 0.2 U/ml thrombin prior to spreading on type I collagen, fibrinogen, fibronectin, laminin, osteopontin and vitronectin. Histograms represent the mean ± SD of platelet area (µm²) after **(A)** 5 min, **(B)** 15 min and **(C)** 30 min spreading. *p<0.05, **p<0.01. Substrates in which there are differences between genotypes are highlighted in red.

These results suggest that C3G is not required to initiate platelet spreading, but rather is involved in the last steps of spreading.

### 2.1.4. C3G affects platelet receptor expression

The above results suggest that C3G could regulate either the expression or the surface exposure of integrins involved in the interaction of platelets with type I collagen, fibronectin, osteopontin or vitronectin. Therefore, we studied in C3G-KO and control platelets the expression of the major platelet integrin subunits, namely the integrins α2 (ITGA2), α2b (ITGA2B), α6 (ITGA6), αV (ITGAV), αL (ITGAL), β1 (ITGB1), β2 (ITGB2) and β3 (ITGB3) by RT-qPCR using two different primers for each integrin. Results in **Figure R-19A** show a significant decrease in integrin α6, αV and β1 mRNA expression. Integrin α6 participates in adhesion to laminin, whereas αV is involved in adhesion to fibrinogen, fibronectin, osteopontin and vitronectin. Integrin β1 interacts with all the substrates studied except fibrinogen. Therefore, the decreased expression of integrins αV and β1, but not α6, could partially explain the observed spreading phenotype of C3G-KO platelets.

To further analyze the possible involvement of some of the most important platelet receptors in C3G function in platelet spreading, we studied, by flow cytometry, the presence of GPVI (collagen receptor), integrins αIIb (ITGA2B or CD41) and β3 (ITGB3 or CD61), which bind fibrinogen, fibronectin, vitronectin, among others; and glycoprotein Ib alpha (GP1BA or CD42b), which binds vWF and collagen, on the platelet surface of tgC3G, tgC3GΔCat and C3G-KO platelets and their controls. There were not differences in the surface expression of these receptors between the genotypes studied (Figure R-19B).

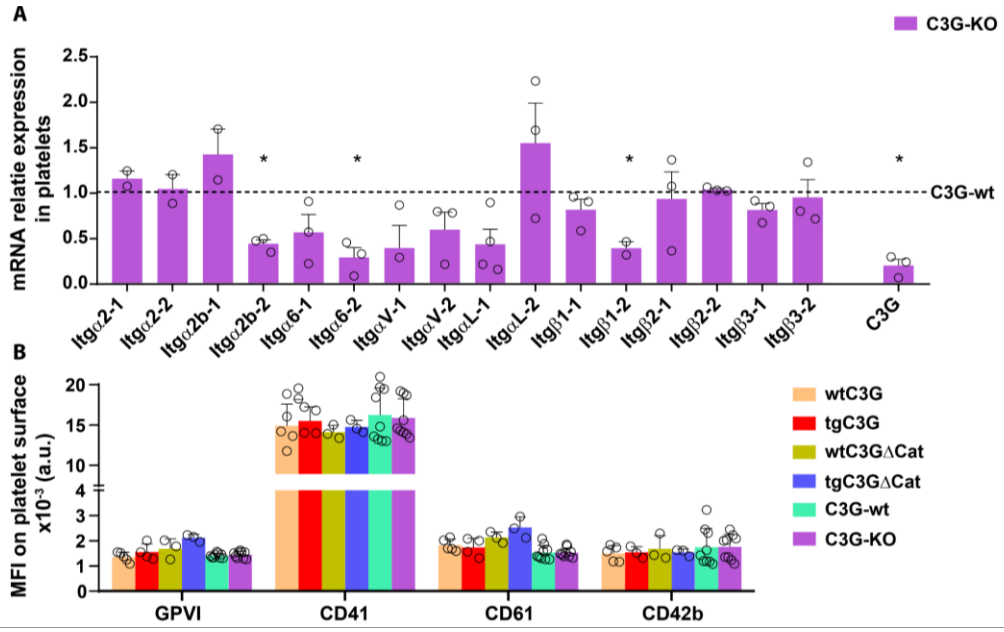


**Figure R-19. C3G regulates α6, αV and β1 mRNA levels but does not regulate membrane exposure of major platelet receptors. (A)** RT-qPCR analysis of the indicated integrin subunits in platelets from C3G-KO and C3G-wt mice using β-actin as housekeeping gen. The expression of *RapGEFI* (C3G) was used as control. *p<0.05. **(B)** Washed blood from C3G-KO and C3G-wt mice was incubated with anti-GPVI-FITC and anti-CD61-PE, or anti-CD42b-PE and anti-CD41-APC antibodies for 15 min. Histograms represent the mean ± SD of the MFI of GPVI, CD41, CD61 and CD42b levels on platelet surface. MFI: mean fluorescence intensity; a.u.: arbitrary units.

Taken together these results, the role of C3G in platelet spreading can only be partially explained by the expression levels of some integrins, such as αV and β1, and differences in the activation of αIIbβ3 integrin. Therefore, the substrate dependence and differences in spreading between tgC3G, tgC3GΔCat and C3G-KO platelets deserve further study.

### 2.1.5. C3G does not regulate microtubule formation

Microtubules play an essential role in platelet spreading (Cuenca-Zamora *et al.*, 2019), thus, we determined whether the role of C3G in spreading is related to microtubule formation.

We first studied the distribution of β-tubulin during platelet spreading on poly-L-lysine, type I collagen, fibrinogen and fibronectin. As shown in Figure R-20, there were not differences in the amount and distribution of β-tubulin between tgC3G and C3G-KO platelets and their controls, suggesting that C3G is not involved in microtubule formation during platelet spreading.

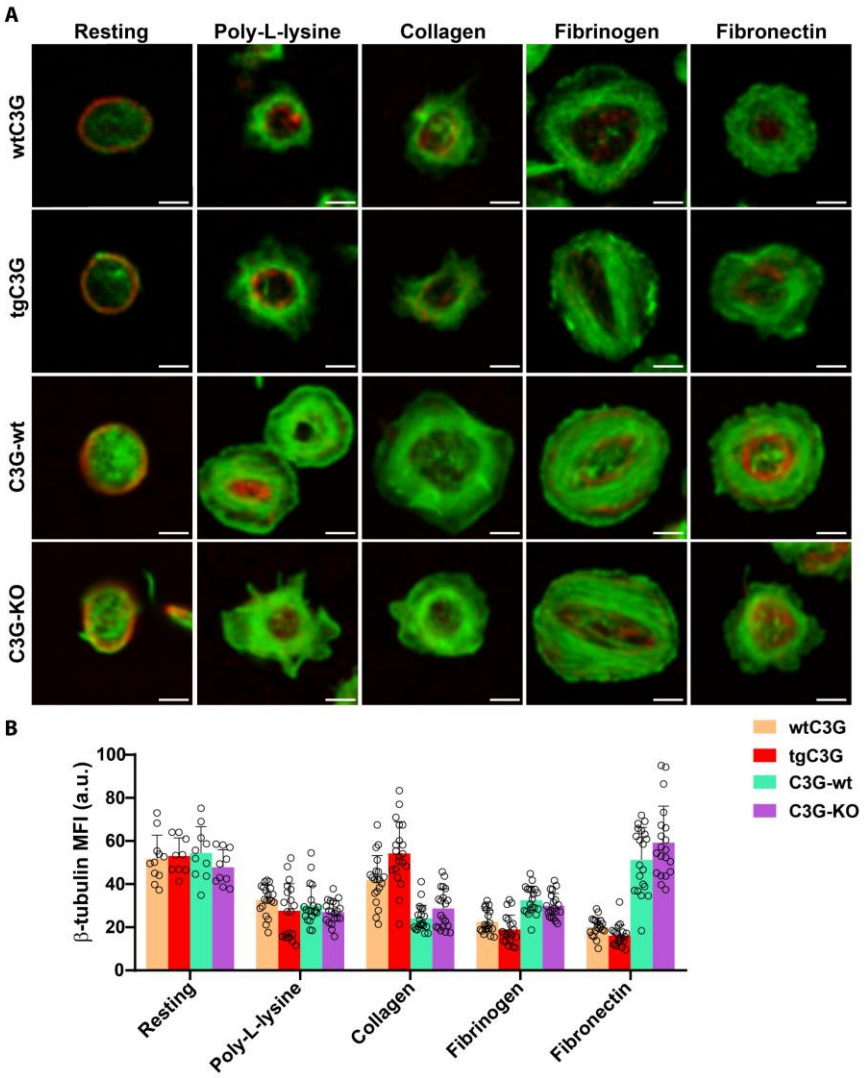


**Figure R-20. C3G does not regulate microtubule formation during platelet spreading. (A)** Representative images of tgC3G and C3G-KO platelets and their respective controls spread on poly-L-lysine, type I collagen, fibrinogen and fibronectin for 30 min after 0.2 U/ml thrombin stimulation for 1 min. Platelets were stained with anti-β-tubulin + AF647 antibody (red) and Phalloidin (green) to visualize microtubules and actin cytoskeleton, respectively. Scale bar: 2 µm. **(B)** Histogram represents the mean ± SD of the MFI of β-tubulin. MFI: mean fluorescence intensity; a.u.: arbitrary units.

### 2.1.6. Role of C3G in actin remodelling during platelet spreading

Since C3G does not modulate microtubule formation, we sought to investigate whether C3G regulates the formation of actin structures.

#### 2.1.6.1. C3G participates in lamellipodia formation

Platelet spreading occurs in four phases: I) adhesion of resting platelets (rounded shape); II) formation of filopodia; III) intermediate stage with a combination of filopodia and lamellipodia; IV) platelets that only have lamellipodia (Bearer *et al.*, 2002).

Based on that, we wanted to investigate, in our C3G modified platelets, whether the observed defects in platelet spreading were due to modifications in the formation of these actin structures.

To address this, we performed a time-lapse spreading assay, analyzing filopodia and lamellipodia formation after 5, 15 or 30 min of spreading in platelets stimulated with thrombin.

Consistent with the alterations in the last steps in spreading, C3G-KO platelets were able to form filopodia on all substrates, but showed a defect in lamellipodia formation on collagen, fibronectin and vitronectin (Figure R-21A), the same substrates in which a defect in spreading was observed. In addition, these results were consistent with those from the spreading assay on IbiTreat plates, in which C3G-KO platelets displayed a delay in lamellipodia formation.

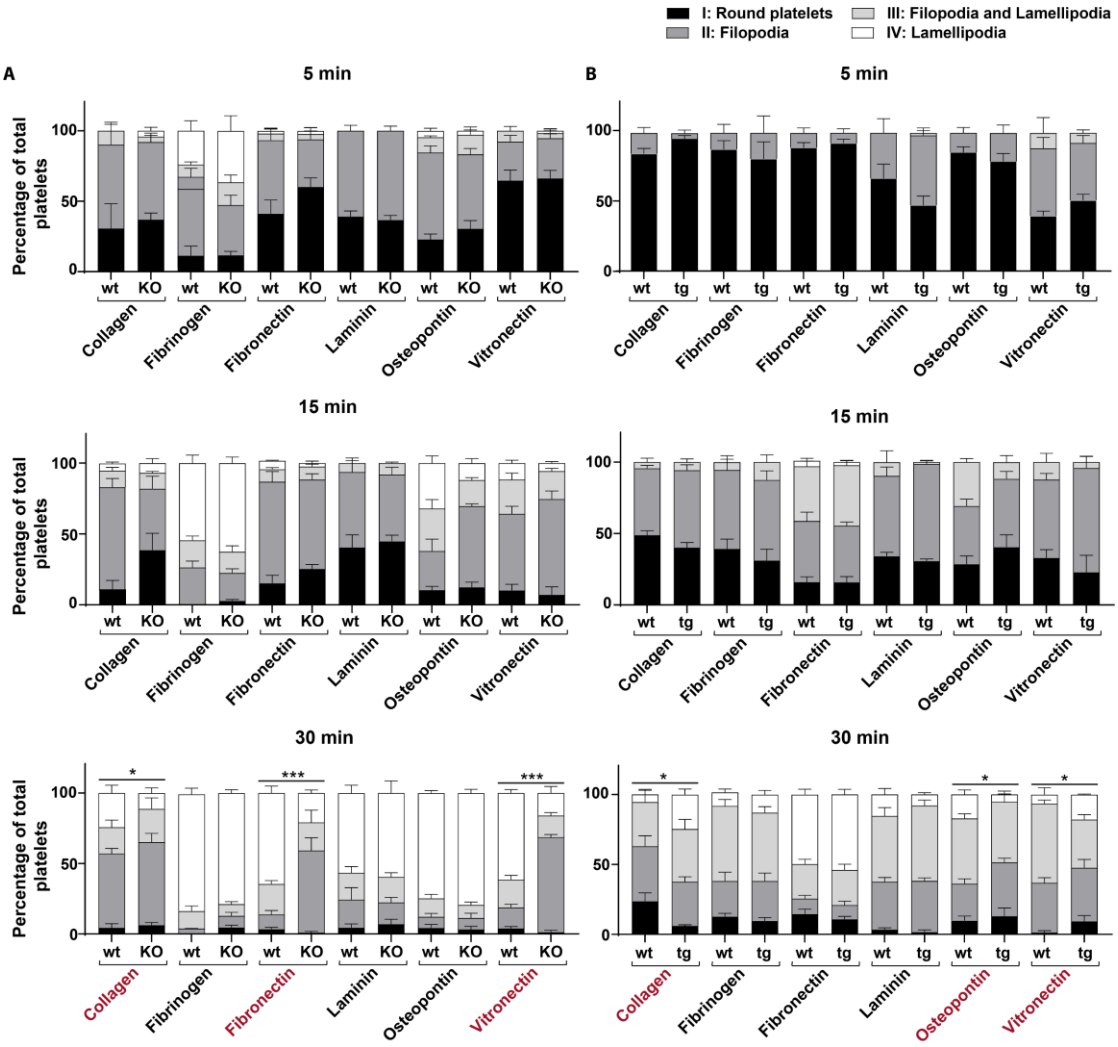


**Figure R-21. C3G regulates lamellipodia formation on collagen, fibronectin and vitronectin during platelet spreading.** Quantification of the different spreading phases in fixed platelets from **(A)** C3G-wt and C3G-KO or **(B)** wtC3G and tgC3G mice, after 5, 15, and 30 min spreading on collagen, fibrinogen, fibronectin, laminin, osteopontin or vitronectin coated coverslips, induced by 0.2 U/ml thrombin for 1 min. Histograms represent the mean ± SEM of the percentage of platelets in the different spreading phases: I: round platelets; II: platelets with filopodia; III: intermediate state with both filopodia and lamellipodia; IV: spread platelets. wt: wild-type; tg: transgenic; KO: knockout. Asterisks refer to quantification of platelets in phase IV. *p<0.05, ***p<0.001. Substrates in which there are differences between genotypes are highlighted in red.

Consistently, C3G overexpression triggered faster lamellipodia formation, although differences with wild-type C3G were subtle. As shown in Figure R-21B, tgC3G platelets showed

a slight increase in lamellipodia formation on collagen and vitronectin, but a decrease on osteopontin.

Notably, we observed differences in platelet spreading between control platelets from the two platelet lineages studied. Thus, wtC3G platelets showed a delay in the formation of spreading structures, compared to C3G-wt platelets, suggesting that the genetic background could influence platelet function.

### 2.1.6.2. C3G is not involved in filopodia formation in platelets

It has been reported that C3G is essential for filopodia formation during spreading on fibronectin in HeLa cells (Radha *et al.*, 2007). Based on that, we explored whether C3G also modulates filopodia formation in platelets.

We analyzed the number of filopodia per platelet after 5 min and 15 min of spreading on collagen, fibrinogen, fibronectin, laminin, osteopontin and vitronectin. There were not significant differences between C3G-KO and C3G-wt platelets on most substrates (Figure R-22), consistent with the results in Figure R-18. This indicates that the role of C3G in platelet spreading is related to lamellipodia formation but not to filopodia formation.

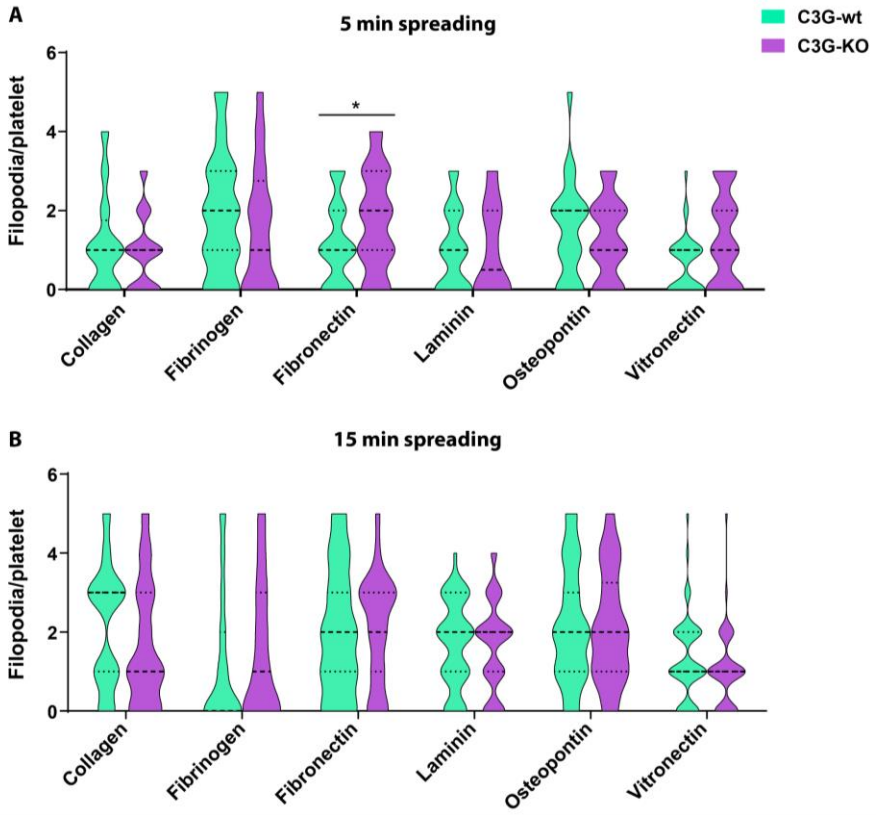


**Figure R-22. C3G deletion does not affect filopodia formation.** Quantification of the number of filopodia in fixed C3G-wt and C3G-KO platelets after **(A)** 5 min and **(B)** 15 min of spreading on collagen, fibrinogen, fibronectin, laminin, osteopontin and vitronectin coated coverslips, induced by 0.2 U/ml thrombin for 1 min. Violin plots represent the median and whiskers are the 25th and 75th percentiles of the number of filopodia per platelet, analyzed with ImageJ. *p<0.05.

### 2.1.7. PKC mediates C3G function in spreading

As mentioned, PKC is crucial for platelet spreading (Harper & Poole, 2010). Therefore, we attempted to elucidate if PKC would also mediate the role of C3G in this process.

To do this, we stimulated tgC3G, C3G-KO platelets and their controls with PMA, in the presence or absence of the pan-PKC inhibitor BIS, to monitor spreading due specifically to the PKC pathway, using poly-L-lysine as substrate. As with thrombin stimulation, C3G overexpression caused a significant greater area of spreading after PMA stimulation, whereas C3G ablation produced a decrease in spreading ability (**Figure R-23**). On the other hand, BIS treatment completely abolished the differences exhibited by tgC3G and C3G-KO platelets relative to their wild-types (**Figure R-23**), demonstrating a functional interaction between C3G and PKC in the regulation of platelet spreading. As with thrombin, we did not observe any difference between genotypes in platelet perimeter after PMA-induced spreading.

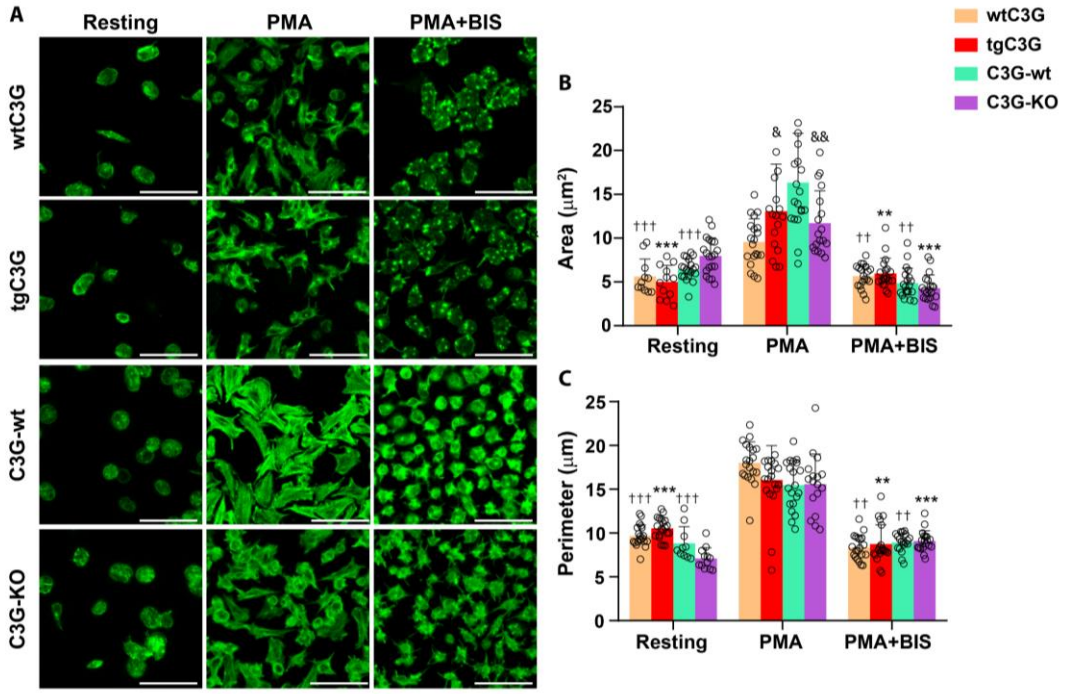


**Figure R-23. C3G promotes platelet spreading on poly-L-lysine through PKC. (A)** Representative images of wtC3G, tgC3G, C3G-wt and C3G-KO platelets spread on poly-L-lysine for 30 min after pre-treatment or not with 5 µM BIS for 5 min, followed by 5 min stimulation with 2 µM PMA. Platelets were stained with Phalloidin to visualize actin cytoskeleton. Scale bar: 5 µm. Histograms represent the mean ± SD of **(B)** platelet area (µm$^2$), **(C)** platelet perimeter (µm). &<0.05, &&<0.01, versus corresponding PMA-stimulated wild-type platelets. ††p<0.01, †††p<0.001 versus PMA-stimulated wild-type platelets; **p<0.01, ***p<0.001 versus PMA-stimulated tgC3G or C3G-KO platelets.

### 2.1.8. C3G regulates Src-dependent spreading and actin cytoskeleton remodelling

To further characterize the C3G pathway in spreading, and since Src kinases regulates C3G phosphorylation (Gutierrez-Herrero *et al.*, 2020) and platelet spreading (Suzuki-Inoue *et al.*, 2003), we analyzed platelet spreading in the presence of the Src inhibitor PP2. PP2 (10 µM for 2 min) completely abolished the increase in platelet area in tgC3G platelets, suggesting the

involvement of Src in this C3G function (Figure R-24). However PP2 did not inhibit spreading in control platelets at the concentration and time used, suggesting the participation of compensatory pathways.

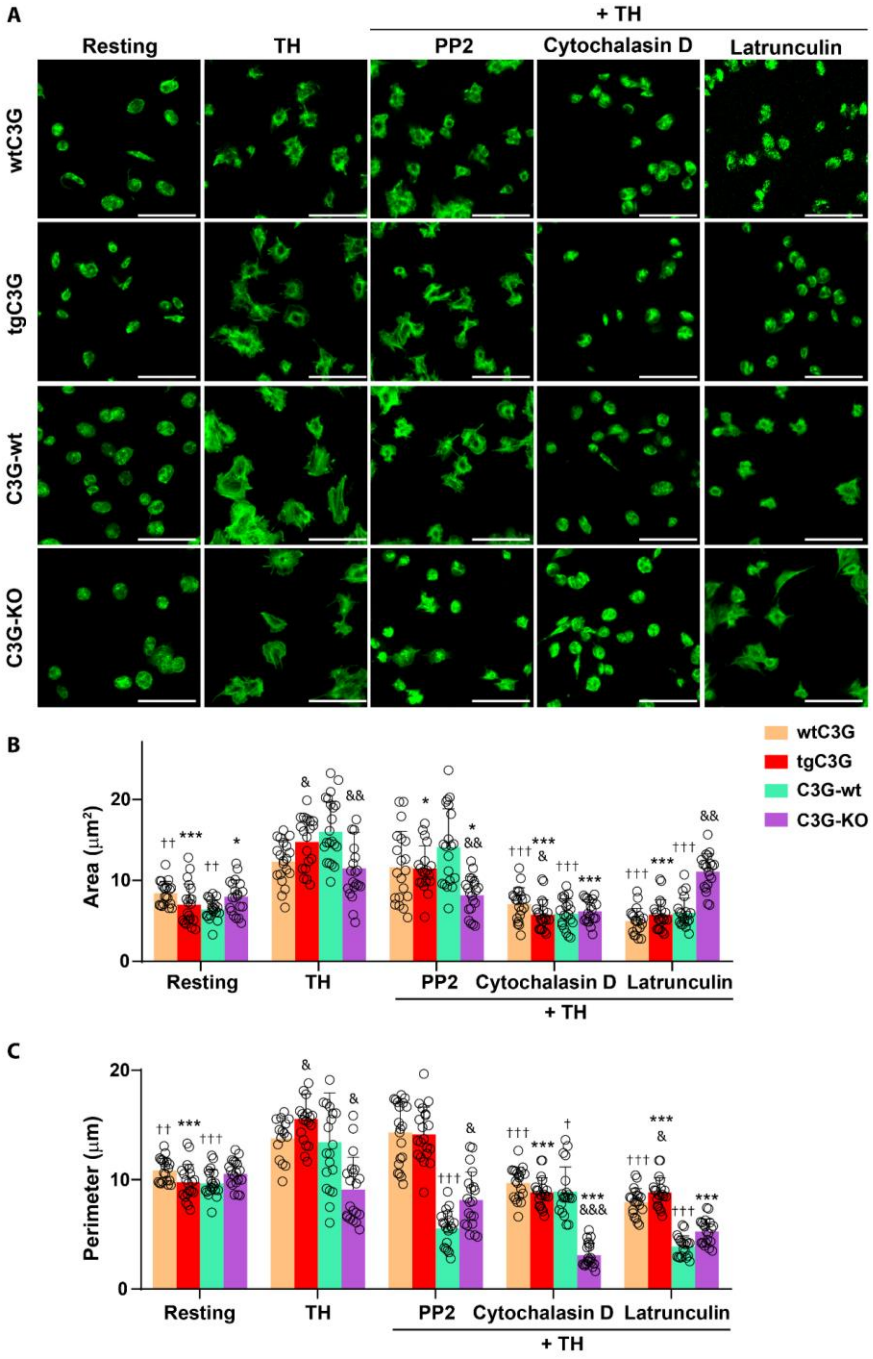


**Figure R-24. C3G participates in Src pathway and actin remodelling during spreading. (A)** Representative images of wtC3G, tgC3G, C3G-wt and C3G-KO platelets spread for 30 min on poly-L-lysine coated coverslips after pre-treatment with 10 µM PP2 for 2 min, 10 µM cytochalasin or 10 µM latrunculin for 45 min, followed by stimulation with 0.2 U/ml thrombin (TH) for 1 min. Platelets were stained with Phalloidin to visualize actin cytoskeleton. Scale bar: 5 µm. Histograms represent the mean ± SD of **(B)** platelet area (µm$^2$), **(C)** platelet perimeter (µm). &<0.05, &&<0.01, versus the corresponding wild-type. †p<0.05, ††p<0.01, †††p<0.001 versus TH-induced wild-type spread platelets; *p<0.05, ***p<0.001 versus TH-stimulated tgC3G or C3G-KO spread platelets.

In addition, we analyzed the alterations in platelet spreading, induced by C3G overexpression or suppression, in the presence or reagents that interfere with actin polymerization, such as cytochalasin D or latrunculin. As shown in **Figure R-24**, and as expected, cytochalasin D- and latrunculin-treated tgC3G and wild-type platelets were unable to spread. In contrast, C3G-KO platelets were only affected by cytochalasin D, but not latrunculin, treatment. This suggests that the absence of C3G could reverse the mechanism inhibited by latrunculin. Both inhibitors prevent actin polymerization; however, while cytochalasin D binds F-actin polymers (Shoji *et al.*, 2012), latrunculin binds actin monomers and enhances the depolymerization from both ends (Fujiwara *et al.*, 2018). These differences could explain the different response of C3G-KO platelets to both treatments.

Since the role of C3G in platelet spreading is dependent on substrate, we studied the effect of PP2, cytochalasin D and latrunculin in C3G-KO and C3G-wt platelets spread on CRP or fibrinogen (negative control). As in the previous assay PP2 did not completely abolished spreading, we increased the treatment time to 5 min.

Treatment with cytochalasin D for 45 min or 5 min exposure to PP2 completely abolished platelet spreading, both in C3G-KO and C3G-wt platelets (**Figure R-25**). In contrast to the results with poly-L-lysine, latrunculin inhibited C3G-KO platelet spreading on CRP or fibrinogen (**Figure R-25**).

All these results support a regulatory role for C3G in actin fiber formation during spreading on different substrates.

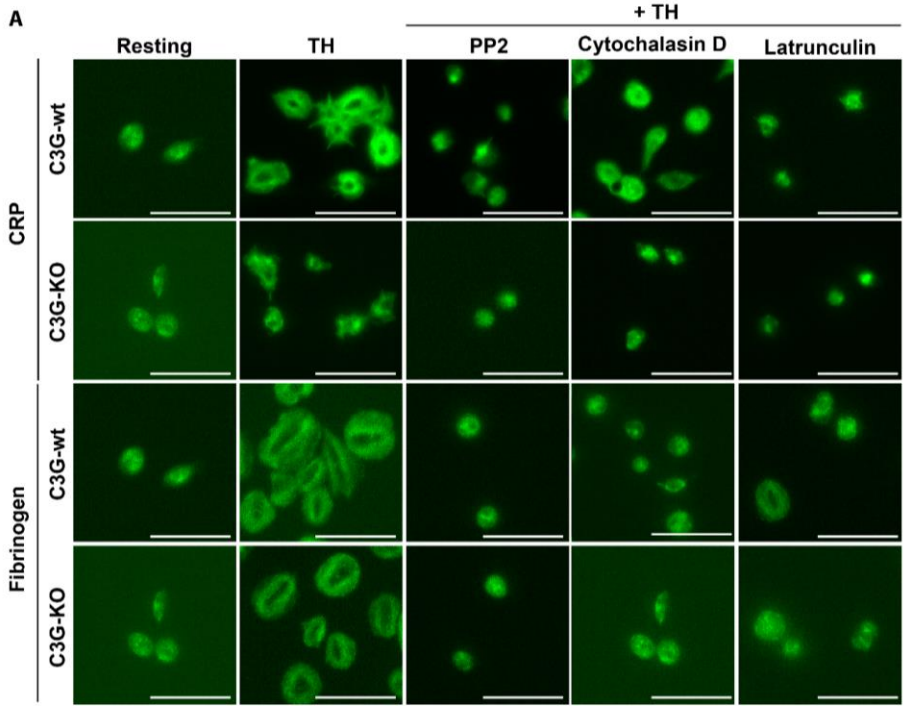

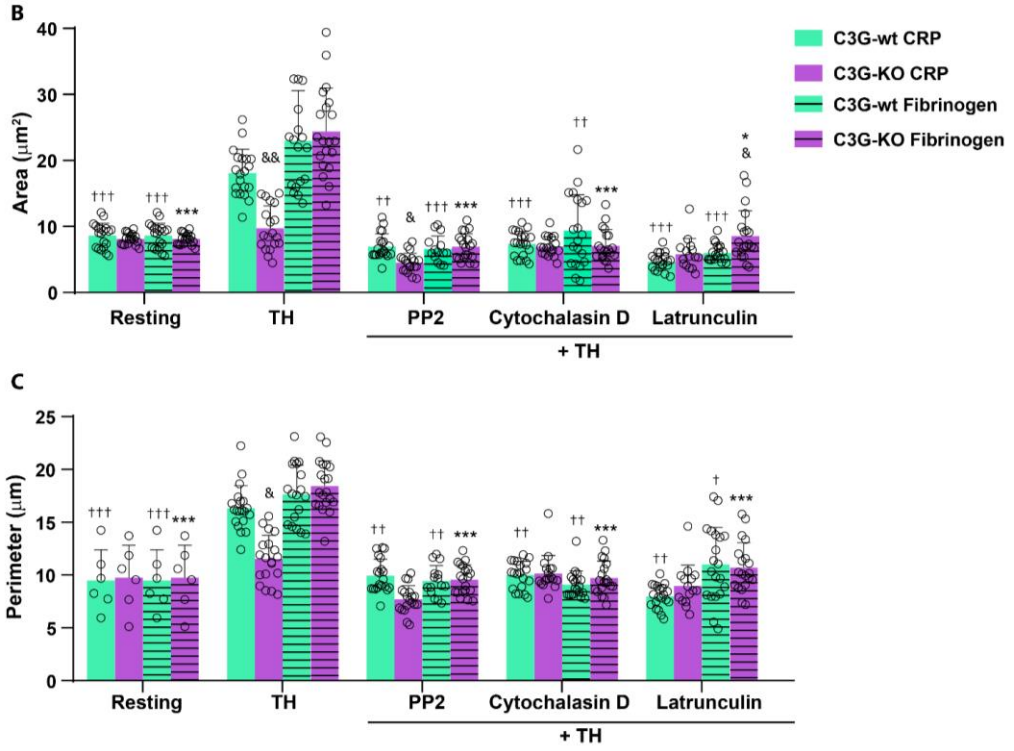


**Figure R-25. C3G regulates actin fiber formation during spreading. (A)** Representative images of C3G-wt and C3G-KO platelets spread on CRP or fibrinogen for 30 min, after pre-treatment with 10 µM PP2 for 5 min, 10 µM cytochalasin and 10 µM latrunculin for 45 min, prior stimulation with 0.2 U/ml thrombin (TH) for 1 min. Platelets were stained with Phalloidin to visualize actin cytoskeleton. Scale bar: 5 µm. Histograms represent the mean ± SD of **(B)** platelet area (µm²) or **(C)** platelet perimeter (µm). &<0.05, &&<0.01 versus wild-type. †p<0.05, ††p<0.01, †††p<0.001 versus TH-induced wild-type spread platelets; *p<0.05, ***p<0.001 versus TH-stimulated tgC3G or C3G-KO spread platelets. CRP: Collagen related peptide.

## 2.1.9. C3G participates in actin turnover during platelet spreading

To gain insight into a possible involvement of platelet C3G in actin cytoskeleton remodelling, we assessed actin turnover in platelets in suspension, stimulated with thrombin, by measuring F-actin fiber formation. As a first approach, we studied the levels of F-actin by flow cytometry. TgC3G platelets showed higher levels of F-actin, in response to thrombin, than wtC3G platelets, whereas C3G-KO platelets presented lower F-actin levels than their corresponding controls (**Figures R-26A, B**).

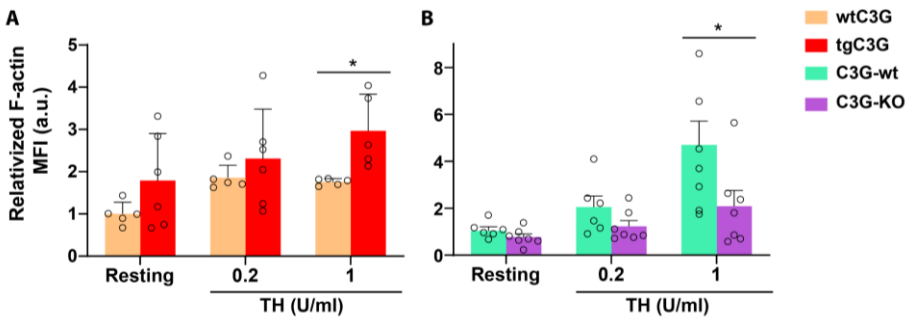


**Figure R-26. C3G regulates F-actin formation upon high-dose thrombin stimulation.** Washed platelets in suspension from **(A)** wtC3G and tgC3G, **(B)** C3G-wt and C3G-KO mice were stimulated with 0.2 or 1 U/ml thrombin (TH) for 1 min before fixing with 2% PFA. After permeabilization with 0.2% Triton X-100,

platelets were stained with Phalloidin and analyzed by flow cytometry. Histograms represent the mean ± SD of Phalloidin MFI normalized against resting control platelets. *p<0.05. MFI: mean fluorescence intensity; a.u.: arbitrary units.

Next, we monitored the formation of actin fibers (F-actin). Based on the regulatory role of C3G in platelet spreading, we examined the F-actin/G-actin ratio in spreading conditions. To do so, platelets were allowed to spread on CRP and fibrinogen for 30 min and the F-actin/G-actin ratio was analyzed by western blot and immunofluorescence.

As shown in **Figure R-27A**, C3G overexpression induced a slight increase in actin polymerization after spreading on CRP but not on fibrinogen. Consistently, and most evidently, C3G-KO platelets showed a decrease in F-actin levels after spreading on CRP but no on fibrinogen (**Figure R-27B**). All these results support a regulatory role for C3G in platelet cytoskeleton remodelling during spreading on collagen.

In addition, we studied the levels of F-actin by immunofluorescence after platelet spreading on fibronectin and laminin. As shown in **Figures R-27C, D**, C3G-KO platelets failed to form F-actin fibers after 30 min of spreading on fibronectin but spread normally on laminin, consistent with the results in **Figures R-14** and **R-17**.

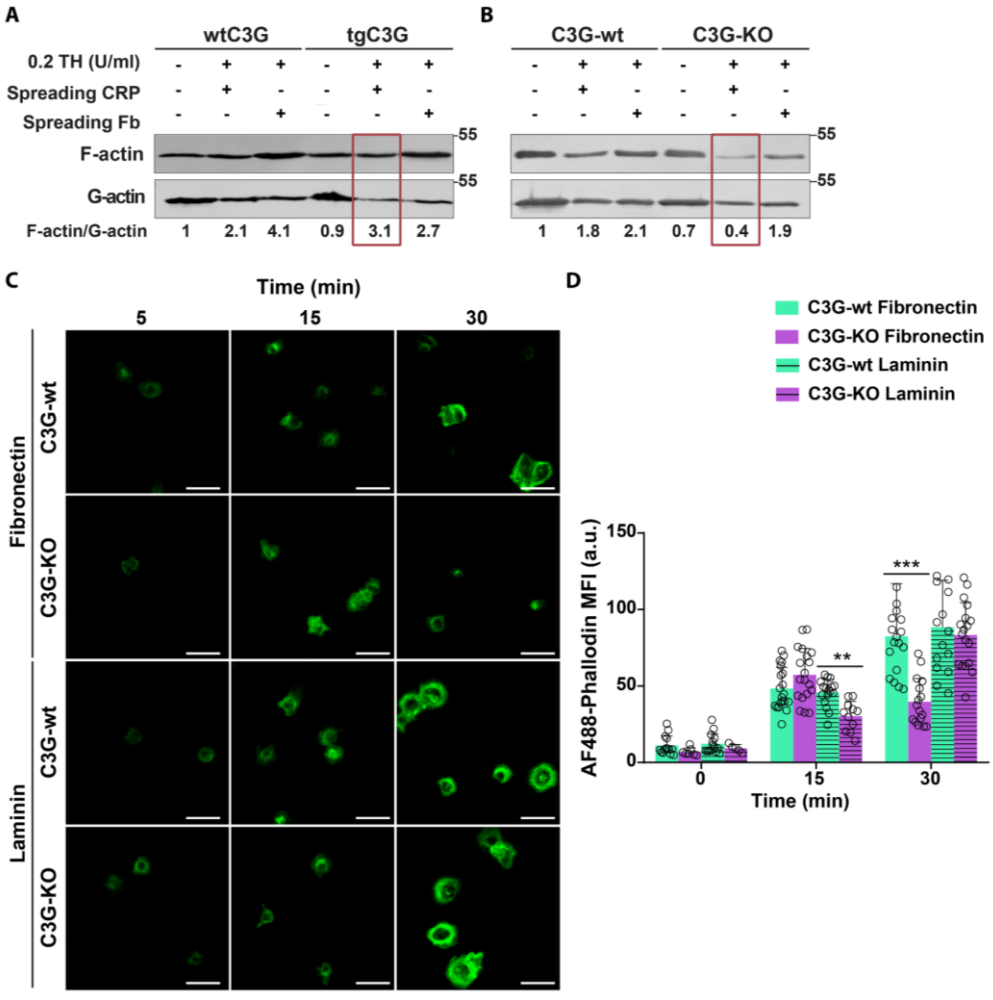

**Figure R-27. C3G regulates actin turnover during spreading on CRP and fibronectin. (A, B)** Platelets from **(A)** wtC3G and tgC3G or **(C)** C3G-wt and C3G-KO mice were stimulated with 0.2 U/ml thrombin (TH) for 1 min and allowed to spread on CRP or fibrinogen for 30 min prior to the lysis. The supernatant containing the soluble G-actin and the urea-solubilized triton X-100-insoluble pellet containing F-actin were subjected to SDS-PAGE and the levels of F-actin and G-actin were detected with an anti-β-Actin antibody. The numbers indicate the ratio F/G actin relativized to wild-type, non-treated platelets. Sp: spreading; CRP: Collagen related peptide; Fb: Fibrinogen. **(C)** Representative images of C3G-wt and C3G-KO platelets spread on fibronectin and laminin for 0, 15 and 30 min after stimulation with 0.2 U/ml thrombin for 1 min. Platelets were stained with Phalloidin to visualize actin cytoskeleton. Scale bar: 5 µm. **(D)** Histogram represents the mean ± SD of AF488-phalloidin MFI. **p<0.01, ***p<0.001. MFI: mean fluorescence intensity; a.u.: arbitrary units.

Based on the lack of effect of latrunculin on C3G-KO platelet spread on poly-L-lysine, we sought to investigate F/G ratio under these conditions. Suspension platelets were pre-treated with 10 µM latrunculin for 45 min and then stimulated with 0.2 U/ml thrombin. As expected, latrunculin inhibited F-actin formation. Moreover, the decreased F-actin formation in C3G-KO platelets was reverted by treatment with latrunculin (Figure R-28), further suggesting that the absence of C3G could prevent the effect of latrunculin.

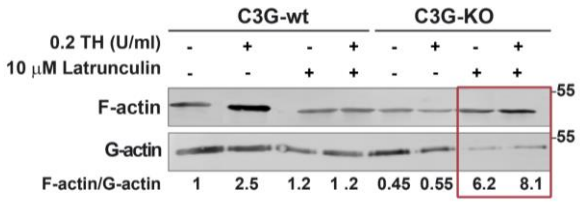


**Figure R-28. Absence of C3G in platelets interferes with latrunculin inhibitory effect.** Washed platelets in suspension from C3G-wt and C3G-KO mice were pre-treated with 10 µM latrunculin for 45 min and stimulated with 0.2 U/ml thrombin (TH) for 1 min prior the lysis. The supernatant containing the soluble G-actin and urea-solubilized triton X-100-insoluble pellet containing F-actin were subjected to SDS-PAGE and the levels of F-actin and G-actin were detected with anti-β-actin antibody. The numbers indicate the ratio F/G actin relativized to non-treated wild-type platelets.

### 2.1.10.C3G regulates Rac1 activation in a Rap1-independent manner

As indicated in the Introduction, Rac1, RhoA and Cdc42 are the main GTPases that regulate actin cytoskeleton dynamics. Rac1 is essential for lamellipodia formation, whereas RhoA is related to platelet shape change and stress fibers formation. In addition, Cdc42 is associated with filopodia formation, although its role in platelets is currently unclear (Elvers, 2016). Since C3G seems to be involved in actin polymerization and lamellipodia formation during spreading, we investigated the participation of C3G in the activation of these GTPases.

Overexpression of C3G increased by two-fold Rac1-GTP levels in 1 U/ml thrombin-stimulated platelets, indicating a role for C3G in this pathway. In concordance, C3G-KO platelets showed a defective Rac1 activation after 1 U/ml thrombin stimulation (Figure R-29A). We did not observe differences in Rac1 activation between tgC3G or C3G-KO and their controls at low thrombin concentration (0.2 U/ml), similar to what was observed in the Rap1 assays (Figure R-6). Surprisingly, tgC3GΔCat platelets showed significantly greater Rac1 activation than their controls under 1 U/ml thrombin (Figure R-29A). This result is in concordance with the greater spreading

of tgC3GΔCat platelets observed in previous results (Figure R-16) and suggests that C3G regulates Rac1 activation in a catalytic (GEF) independent manner.

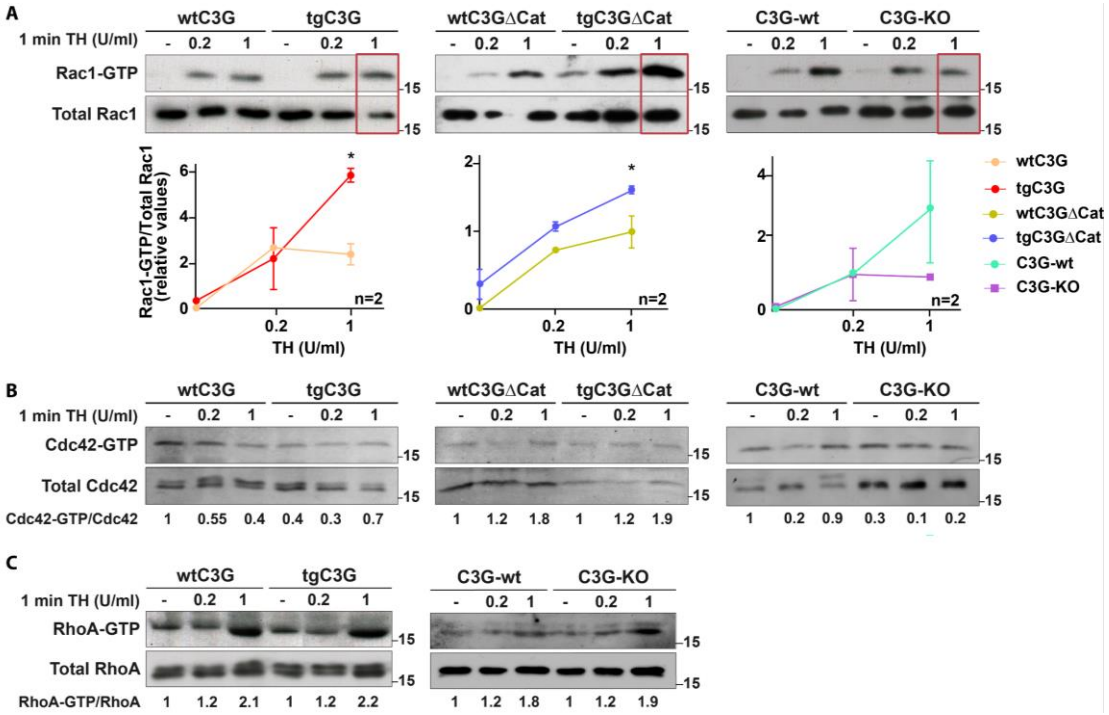


**Figure R-29. C3G regulates Rac1 activation upon platelet stimulation.** Representative pull-down assays to detect **(A)** Rac1-GTP and **(B)** Cdc42-GTP after stimulation with 0.2 or 1 U/ml thrombin (TH) for 1 min in platelets from tgC3G, tgC3GΔCat and C3G-KO mice and their respective wild-types. The levels of Rac1-GTP and Cdc42-GTP were determined using anti-Rac1 or Cdc42 antibodies, respectively. Values are relative to unstimulated wild-type platelets and were normalized to total levels. The line/scatter plots show the mean ± SD of Rac1-GTP levels (n=2). *p<0.05. **(C)** Representative pull-down assays to detect RhoA-GTP after stimulation with 0.2 or 1 U/ml thrombin (TH) for 1 min in platelets from wtC3G and tgC3G or C3G-wt and C3G-KO mice. RhoA-GTP and total RhoA levels were detected using an anti-RhoA antibody. Values are relative to unstimulated wild-type platelets and were normalized to total RhoA levels.

On the other hand, we did not find a direct relationship between thrombin stimulation and Cdc42 activation in control platelets (Figure R-29B), nor did we find a clear effect of C3G on Cdc42-GTP levels. This, together with the fact that no differences in filopodia formation were observed between the different genotypes, suggests that Cdc42 is probably not involved in the C3G function in spreading.

Finally, we examined by pull-down assay if C3G is involved in RhoA activation after thrombin stimulation. In contrast to Cdc42, RhoA was activated by thrombin, mainly at high concentration. However, we did not observe differences between tgC3G and C3G-KO and their respective wild-types (Figure R-29C).

These results are in agreement with the results from platelet spreading experiments and reveal a regulatory role for C3G in lamellipodia formation through Rac1 activation by a GEF-independent mechanism.

### 2.1.11.C3G interacts with proteins involved in cytoskeletal remodelling

To better understand the role of C3G in the regulation of actin cytoskeletal structures in platelets, we studied the possible interaction between C3G and proteins involved in cytoskeletal remodelling.

Actin fiber formation is regulated by different proteins such as Arp2/3 complex, which participates in actin branching, VASP, which regulates filament elongation or cofilin, which modulates filament debranching. Moreover, Arp2/3 complex is activated by NPFs such as WAVE1, WAVE2 or N-WASP (Krause & Gautreau, 2014). Based on this and the results described above, suggesting a role for C3G in cytoskeleton remodelling, we investigated whether C3G interacts with these proteins. Of note, Benz and co-workers demonstrated that VASP forms a ternary complex with CrkL and C3G in platelets, which controls, in parallel with CalDAG-GEFI, Rap1b-dependent platelet activation (Benz *et al.*, 2016).

As a first approach, we analyzed the interaction between C3G and these proteins in HEK-293T cells after co-transfection of HA-C3G with mEmerald-ARP3, tdTomato-VASP, RFP-Abi1, pcDNA-CFP-C4-WAVE2 or mEmerald-WASP1 plasmids. Immunoprecipitation assays showed that C3G interacts with Arp3, WAVE2, VASP and Abi1 but not with WASP1 (**Figure R-30A**).

To further support these results, we did a similar assay in tgC3G platelets, at rest and upon stimulation with 0.5 U/ml thrombin. In consonance with the results in HEK-293T cells, C3G showed interaction with Arp2, Arp3 and VASP in both resting and thrombin-stimulated platelets (**Figure R-30B**). C3G also interacted with β-actin, in agreement with our previous results showing interaction of C3G with β-actin in NIH3T3 cells (Martin-Encabo *et al.*, 2007).

Furthermore, as in the co-transfection assays, C3G also interacted with WAVE2 and Abi1 but not with N-WASP on platelets, reinforcing the notion of its participation in the Rac1 pathway, but not in the Cdc42 pathway, probably through the activation of the Arp2/3 complex. (**Figure R-30B**). On the other hand, C3G does not interact with cofilin, indicating that C3G is not involved in actin debranching. Moreover, results in **Figure R-30C** showed that the interaction between C3G and Arp2 and β-actin also occurs in tgC3GΔCat platelets, which is consistent with previous results (Martin-Encabo *et al.*, 2007), and suggests that the role of C3G in actin cytoskeleton remodelling is independent of its GEF activity. It should be noted that although some of the detected interactions are weak, the observed bands have an intensity similar to or greater than that of CrkL, whose direct interaction with C3G is well established (Rodriguez-Blazquez *et al.*, 2023).

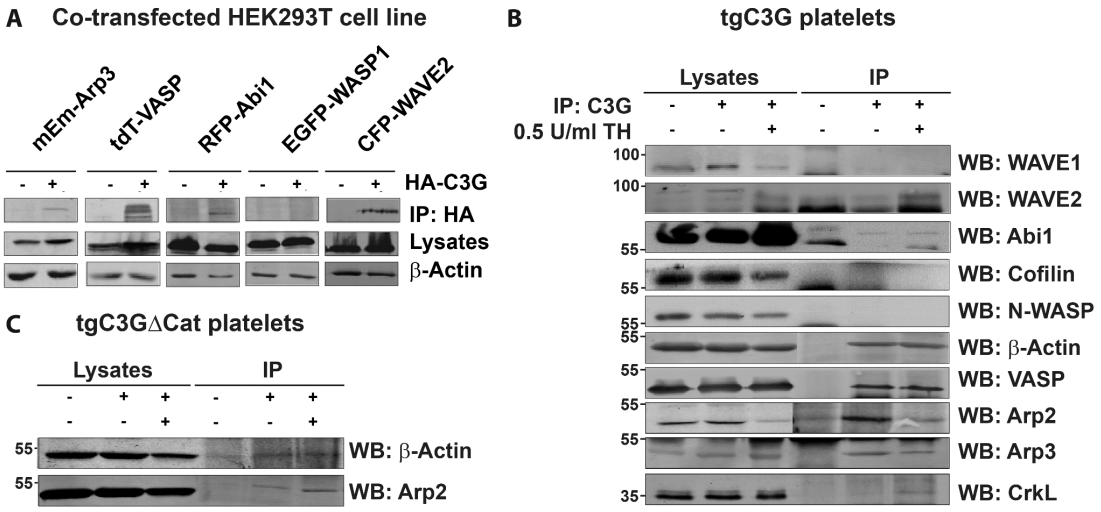


**Figure R-30. C3G interacts with WAVE2, VASP, β-Actin, Abi1, Arp2 and Arp3. (A)** Lysates from co-transfected HEK-293T cells were immunoprecipitated with anti-HA antibody and the levels of Arp3, VASP, Abi1, WASP1 and WAVE2 were detected by western blot. **(B, C)** Lysates from **(B)** tgC3G and **(C)** tgC3GΔCat platelets, resting or stimulated with thrombin (TH) (0.5 U/ml for 1 min) were immunoprecipitated with anti-C3G antibodies (anti-C3G G-4 in the case of WAVE1, Cofilin, Arp3, and anti-C3G C-19 in the case of Abi1, β-Actin, WAVE2, Arp2 and CrkL) and the levels of WAVE1, WAVE2, Abi1, Cofilin, N-WASP, β-Actin, VASP, Arp2, Arp3 and CrkL were detected by western blot. CrkL was used as a positive control and mouse IgG was used as a negative control. IP: immunoprecipitation; IgG: immunoglobulin; WB: western blot; mEm: mEmerald; tdT: tdTomato.

## 2.1.12.C3G regulates Arp2-WAVE2 interaction after thrombin stimulation

So far we have demonstrated that: (i) C3G regulates lamellipodia formation in platelets, (ii) C3G interacts with WAVE1 and Arp2/3 and regulates Rac1 activity, all involved in lamellipodia formation. To deepen the role of C3G in the formation of lamellipodia, we analyzed whether C3G participates in the interaction between WAVE2 and the Arp2/3 complex.

We addressed it by means of immunoprecipitation in platelets stimulated with low (0.2 U/ml) and high (1 U/ml) dose thrombin. Overexpression of C3G induced a subtle increase in the interaction between Arp2 and WAVE2 at 0.2 U/ml thrombin stimulation, indicating that C3G overexpression could facilitate the interaction (Figure R-31A). In consonance, C3G ablation induced a slight decrease, especially at high thrombin stimulation, reinforcing the notion of a putative role of C3G in actin branching (Figure R-31B).

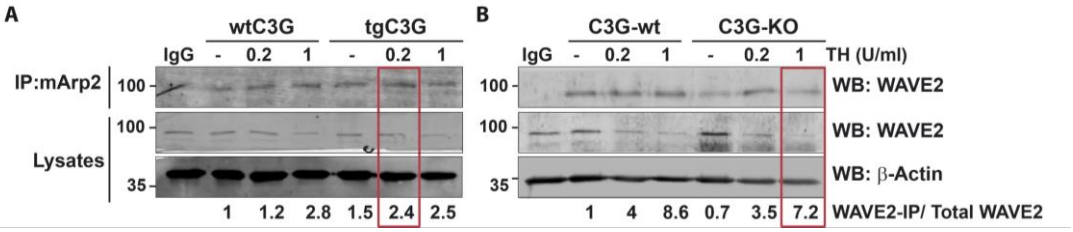


**Figure R-31. C3G regulates WAVE2 and Arp2 interaction in platelets. (A)** Lysates from wtC3G and tgC3G platelets or **(B)** C3G-wt and C3G-KO platelets in both resting and upon stimulation with thrombin (TH) (0.2 and 1 U/ml for 1 min) were immunoprecipitated with anti-Arp2 antibody and the levels of WAVE2 were detected by western blot. β-Actin was used as loading control. Values for WAVE2 immunoprecipitation levels are relative to those of unstimulated wild-type platelets and were

normalized to total WAVE2 levels. Mouse IgG was used as a negative control. IgG: immunoglobulin; IP: immunoprecipitation; WB: western blot.

Taken together, our results indicate that C3G regulates lamellipodia formation through modulation of the Rac1-WAVE2-Arp2/3 pathway. To validate these results, we monitored platelet spreading on CRP and fibrinogen, in tgC3G, C3G-KO platelets and their controls treated with 1A-166 or CK-666, inhibitors of Rac1 and Arp2/3 complex, respectively.

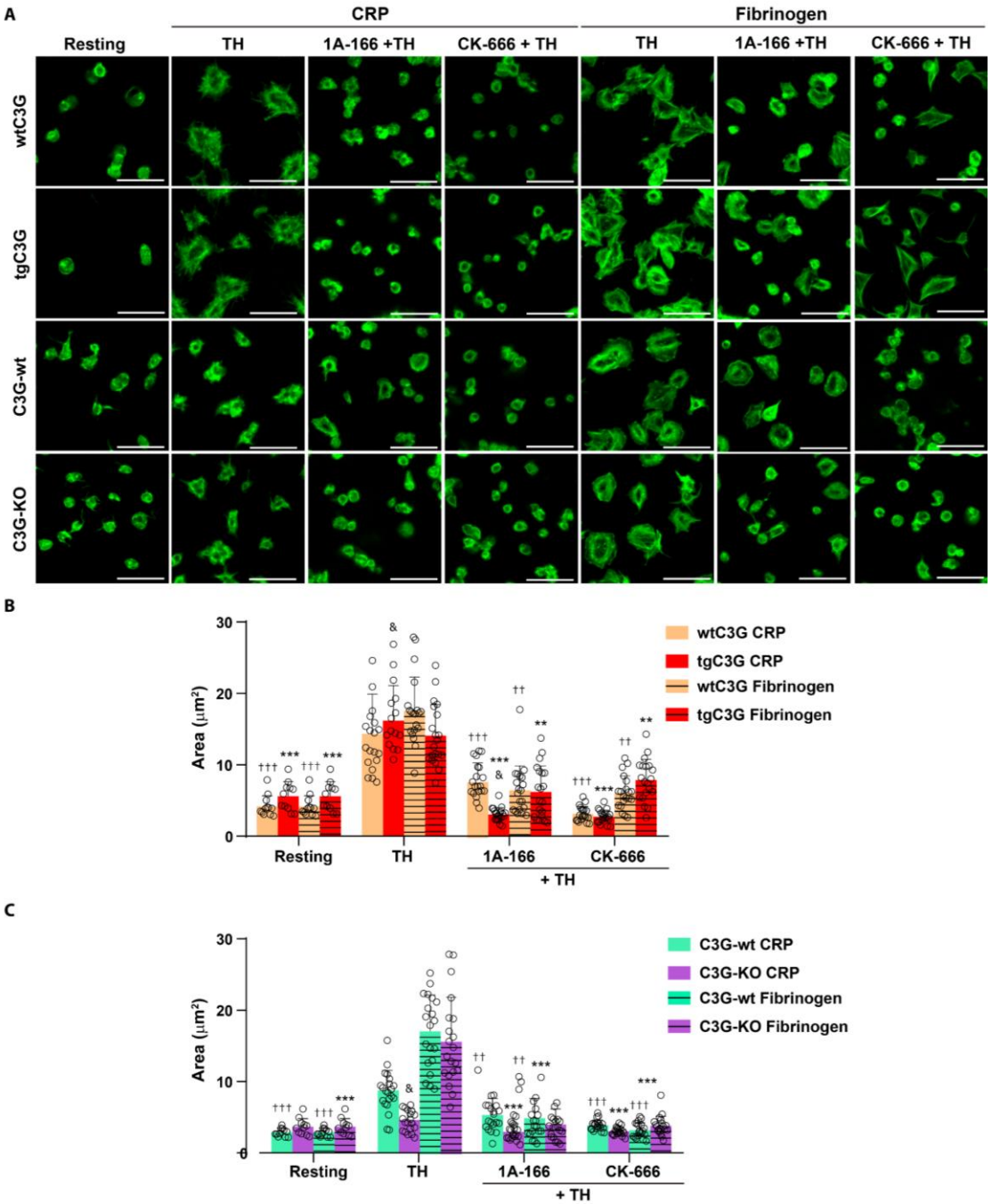


**Figure R-32. The role of C3G in platelet spreading is dependent on Rac1. (A)** Representative images of wtC3G, tgC3G, C3G-wt and C3G-KO platelets spread on CRP and fibrinogen for 30 min after pre-treatment with 50 µM 1A-166 or 50 µM CK-166 for 30 min, prior stimulation with 0.2 U/ml thrombin (TH) for 1 min. Platelet were stained with Phalloidin to visualize actin cytoskeleton. Scale bar: 5 µm. Histograms represent the mean ± SD of platelet area (µm$^2$) of **(B)** wtC3G and tgC3G or **(C)** C3G-wt and C3G-KO platelets**.** &<0.05 versus its wild-type. ††p<0.01, †††p<0.001 versus TH- stimulated wild-type

spread platelets; **p<0.01, ***p<0.001 versus TH-stimulated tgC3G or C3G-KO spread platelets. CRP: Collagen related peptide.

As expected, both inhibitors significantly reduced thrombin-induced spreading in both substrates in all genotypes. However, tgC3G platelets spread on CRP were more sensitive to Rac1 and Arp2/3 inhibition than wtC3G platelets (**Figure R-32**). This result further suggests that the role of C3G in spreading is dependent on Rac1 and Arp2/3.

### 2.1.13.C3G ablation does not affect VASP phosphorylation

Based on our results showing that C3G interacts with VASP in platelets, together with the description of a ternary complex in platelets involving C3G, VASP and CrkL (Benz *et al.*, 2016), we examined whether C3G modulates VASP phosphorylation and, hence, actin elongation.

In platelets, VASP can be phosphorylated at different serine residues, with residues 157 and 239 being the most important for platelet function. Both PKA and PKC phosphorylate VASP at residue Ser157, whereas PKG modulates phosphorylation at Ser239 (Wentworth *et al.*, 2006; Benz *et al.*, 2016). Since phosphorylation at Ser157 modulates the interaction of VASP with CrkL and C3G, we sought to investigate whether C3G could regulate VASP phosphorylation at this residue.

We did not observe significant differences in VASP phosphorylation between C3G-KO and C3G-wt platelets after stimulation with 0.2 U/ml thrombin (**Figure R-33**). As expected, inhibition of PKA and PKC with H89 and BIS, respectively, inhibited thrombin stimulated VASP phosphorylation.

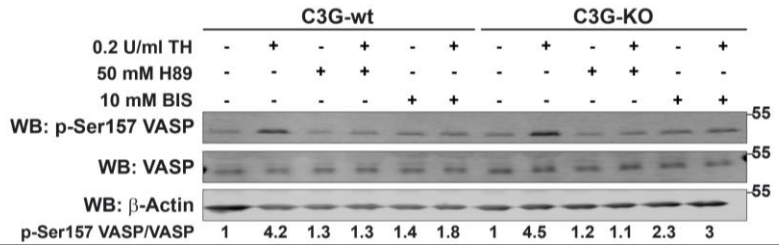


**Figure R-33. C3G absence does not affect VASP phosphorylation at serine 157.** Western blot analysis of VASP phosphorylation in C3G-wt and C3G-KO platelets after treatment with 10 µM BIS for 5 min or 50 µM H89 for 30 min prior to stimulation with 0.2 U/ml thrombin (TH) for 1 min. The levels of p-Ser 157 VASP, VASP and β-Actin, were detected with antibodies anti-phospho-VASP (Ser157), anti-VASP and anti-β-Actin. The numbers indicate phosphorylation of VASP on Ser157, normalized against total VASP. All values are relative to wild-type, non-treated platelets. p: phospho.

Therefore, despite its interaction with VASP, C3G does not regulate VASP phosphorylation in platelets.

## 2.2. C3G controls platelet adhesion

The aforementioned results indicate that C3G participates in platelet spreading and that this function is substrate dependent. Hence, to take a deeper look at this process, we examined platelet adhesion, the first step during spreading.

First, we studied platelet adhesion on IbiTreat plates in real time. Platelets were seeded on the plates and the time it took for platelets to adhere was quantified. Although not significant, C3G-KO platelets presented a small delay in adhesion to IbiTreat plates (**Figure R-34**).

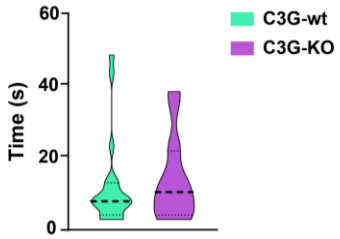


**Figure R-34. C3G absence delays platelet adhesion.** Violin plot represents the median and whiskers are the 25th and 75th percentiles of the adhesion time of C3G-wt and C3G-KO platelets to IbiTreat plates.

### 2.2.1. C3G modulates platelet adhesion on different substrates

Next, we analyzed the effect of both C3G overexpression and absence on platelet adhesion on CRP, fibrinogen, fibronectin and laminin 30 min after seeding.

C3G-KO platelets showed impaired adhesion on fibronectin and laminin in the resting state, while C3G overexpression increased adhesion on fibrinogen and fibronectin (**Figures R-35A, B**). Since C3G does not regulate spreading on fibrinogen, this result suggests a role for C3G in platelet adhesion, which would be independent of its role in spreading.

It should be highlighted that in the absence of stimulation platelets were unable to spread on any substrate except CRP. Therefore, we performed a similar study in the same conditions used in the spreading assays, i.e. under 0.2 U/ml thrombin stimulation. No differences were found in platelet adhesion on CRP, fibrinogen and fibronectin between tgC3G platelets and their wild-types, although an unexpected decrease in adhesion to laminin was observed (**Figures R-35A, C**). However, we found a significant decrease in adhesion on fibronectin in C3G-KO platelets.

These results support a regulatory role for C3G in platelet adhesion. Although the effect of C3G overexpression and deletion on platelet adhesion on different substrates does not exactly match the effect on spreading, we believe that C3G might regulate early steps during spreading by modulating adhesion to certain substrates, consistent with its role in actin polymerization.

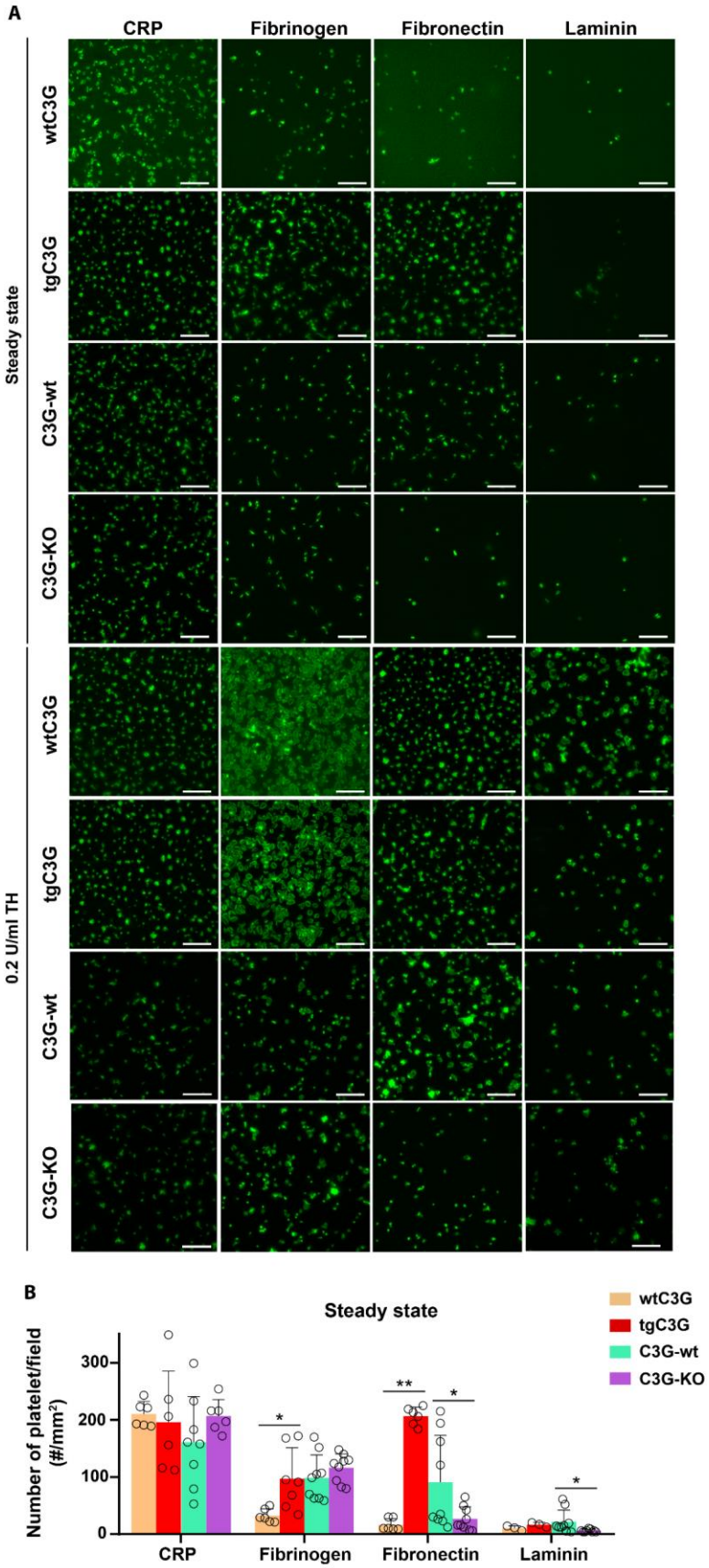
A
CRP
Fibrinogen
Fibronectin
Laminin
Steady state
0.2 U/ml TH
wtC3G
tgC3G
C3G-wt
C3G-KO
B
Steady state
wtC3G
tgC3G
C3G-wt
C3G-KO
Number of platelet/field (#/mm²)
300
200
100
0
CRP
Fibrinogen
Fibronectin
Laminin
*
**
*
*

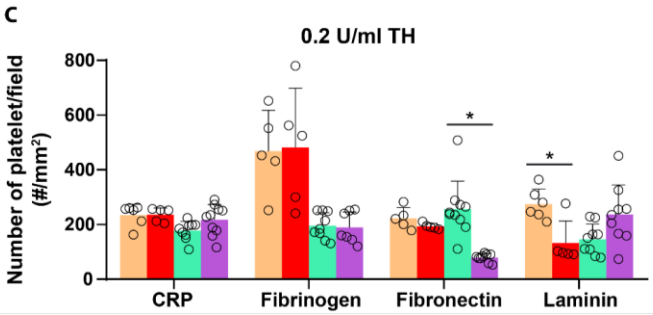


**Figure R-35. C3G regulates platelet adhesion to fibrinogen, fibronectin and laminin. (A)** Representative images of wtC3G, tgC3G, C3G-wt and C3G-KO platelets adhered on CRP, fibrinogen, fibronectin and laminin for 30 min in resting conditions or after 1 min stimulation with 0.2 U/ml thrombin (TH). Equal number of platelets were seeded and after 30 min they were fixed and stained with Phalloidin to visualize actin cytoskeleton. Scale bar: 25 µm. Histograms represent the mean ± SD of the number of platelets per field **(B)** in steady state or **(C)** after thrombin stimulation. *p<0.05, **p<0.01. CRP: Collagen related peptide.

Overall, these results indicate that C3G regulates platelet adhesion, which is probably related to its role in platelet spreading, although both phenotypes are consistent only in the case of fibronectin.

### 2.2.2. C3G regulates the activation of FA proteins

FA are multi-protein complexes that connect actin fibers to the extracellular matrix. Previous results from our group demonstrated that C3G regulates the expression and activation of FA proteins, such as paxillin and FAK, in the K562 cell line (Maia *et al.*, 2013). Based on that, and to clarify whether the alterations in platelet spreading found in C3G deleted platelets are due to alterations in FA formation, we wanted to analyze the putative participation of C3G in FA formation in platelets. To address it, we analyzed vinculin, expression in tgC3G and C3G-KO platelets and their controls after 30 min spreading on CRP, fibrinogen and fibronectin.

Strikingly, both C3G overexpression and ablation triggered a higher number of FAs on CRP (vinculin-positive spots). In addition, tgC3G platelets also presented a significant increase in the number of FAs on fibronectin (**Figures R-36A, B**). Moreover, similar results were found after measuring vinculin MFI (**Figure R-36C**).

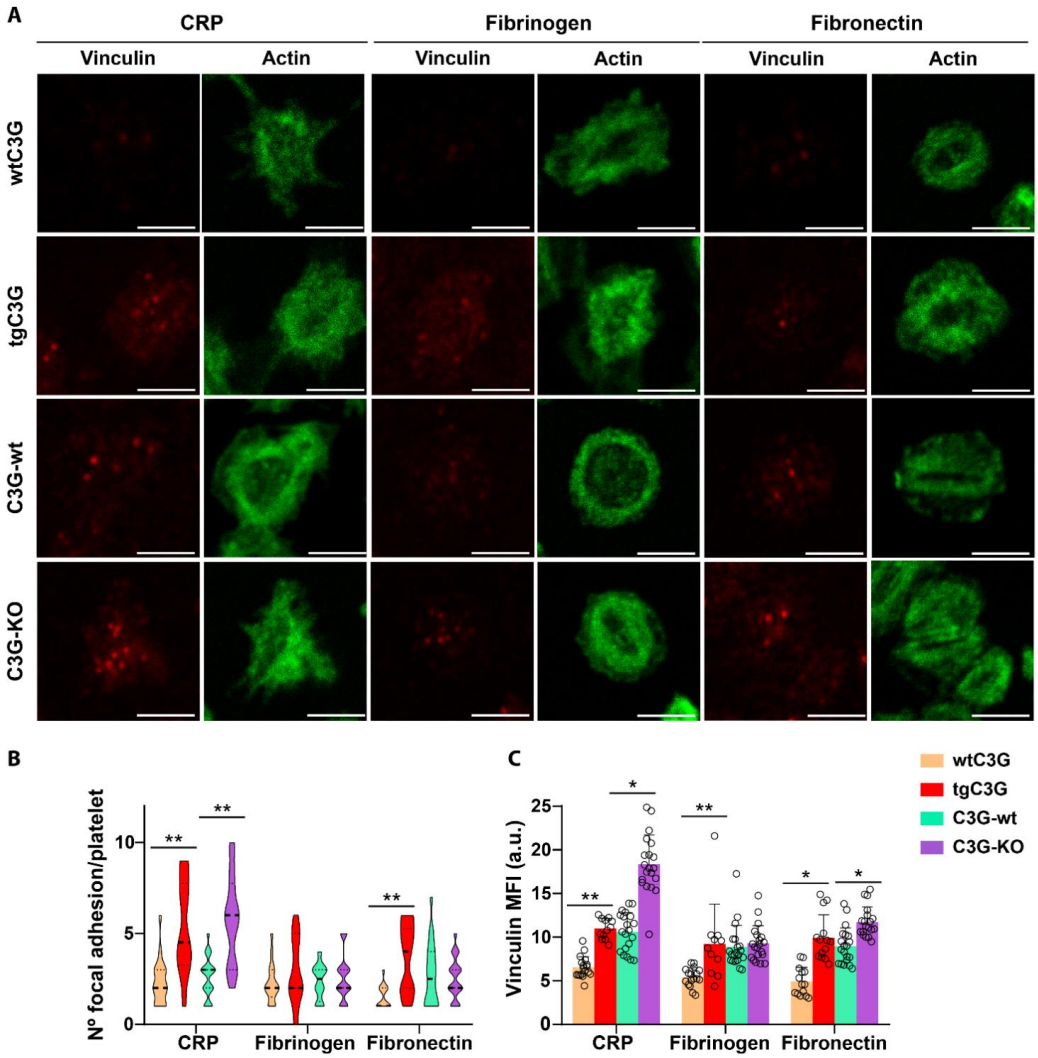


**Figure R-36. C3G regulates the number of FAs after spreading on CRP and fibronectin. (A)** Representative images of wtC3G, tgC3G, C3G-wt and C3G-KO platelets spread on CRP, fibrinogen and fibronectin for 30 min after 1 min stimulation with 0.2 U/ml thrombin. Platelets were stained with an antibody anti-Vinculin + AF568 (red), to visualize FAs, and Phalloidin (green) to visualize actin cytoskeleton. Scale bar: 3 µm. **(B)** The violin plots represent the median and whiskers are the 25th and 75th percentiles of the number of FAs per platelet and **(C)** the histograms represent the mean ± SD of MFI of vinculin. *p<0.05, **p<0.01. CRP: Collagen related peptide; MFI: mean fluorescence intensity; a.u.: arbitrary units.

These data suggest that C3G regulates FA formation, so we next examined by immunofluorescence the phosphorylation of some FA proteins, such as c-Cbl, paxillin or p130Cas, after platelet spreading.

A significant decrease in c-Cbl and paxillin phosphorylation was observed in C3G-KO platelets after spreading on CRP, compared to C3G-wt platelets, whereas the opposite was observed on fibronectin (Figures R-37A). In contrast, p130Cas phosphorylation was increased in C3G-KO platelets, versus C3G-wt platelets, spread on CRP (Figures R-37B).

On the other hand, tgC3G platelets showed decreased levels of phospho-paxillin and phospho-p130Cas when spread on CRP, and lower levels of phospho-c-Cbl and increased levels of paxillin phosphorylation after spreading on fibronectin (Figures R-37C).

Taken together these results suggest that C3G might play a negative role in thrombin-mediated c-Cbl phosphorylation in fibronectin spreading platelets and in p130Cas phosphorylation in CRP spreading platelets, but a positive role in c-Cbl-phosphorylation in CRP spreading platelets, being the results of phospho-paxillin more difficult to interpret.

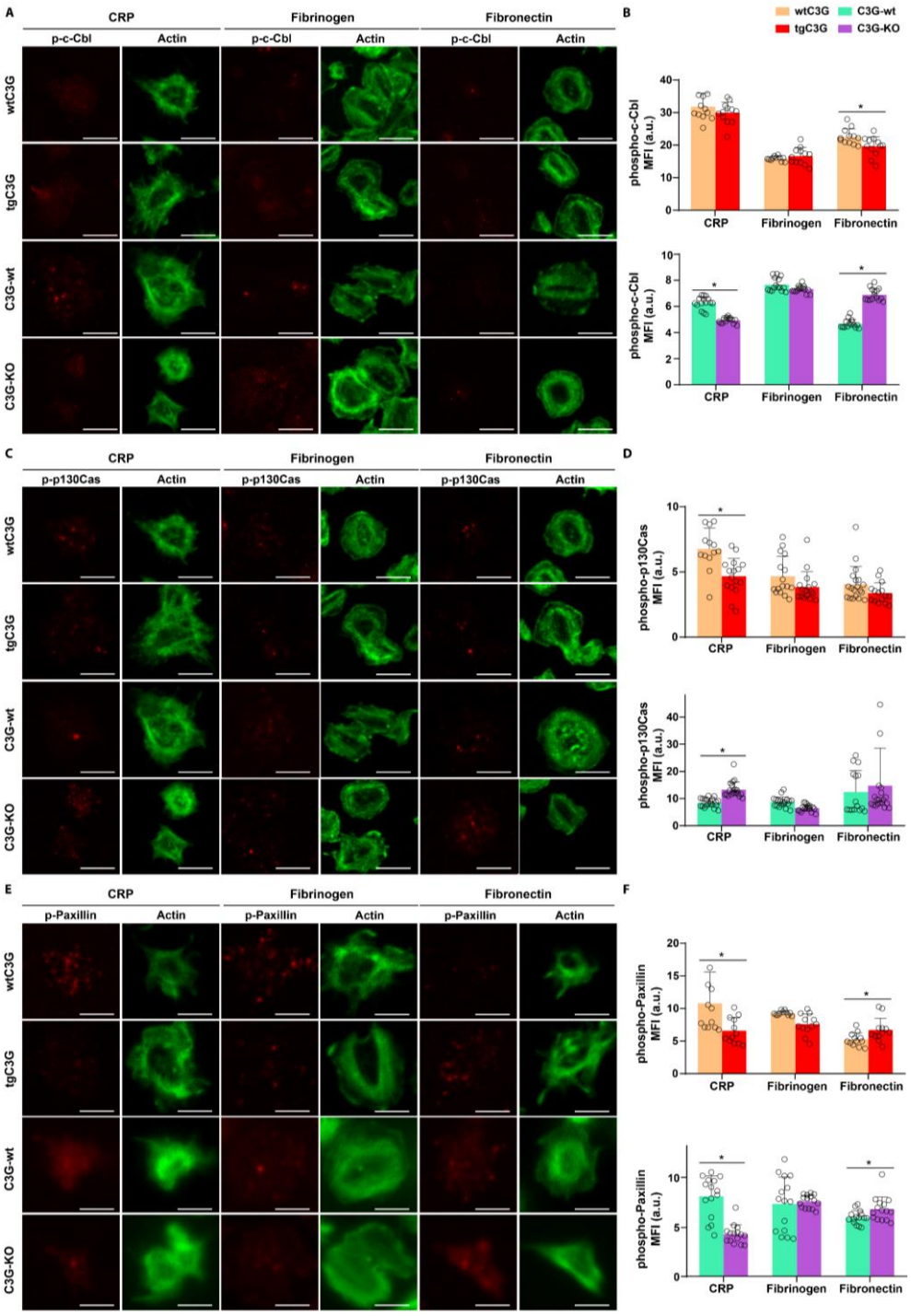


**Figure R-37. C3G modulates the phosphorylation of c-Cbl, paxillin and p130Cas after platelet spreading on CRP and fibronectin**. **(A, C, D)** Representative images of wtC3G, tgC3G, C3G-wt and C3G-KO platelets spread on CRP, fibrinogen and fibronectin for 30 min after 1 min stimulation with 0.2 U/ml thrombin. Platelet were stained with **(A)** anti-phospho-c-Cbl + AF568 (red), **(C)** anti-phospho-p130Cas + AF568 (red) or **(E)** anti-phospho-paxillin + AF568 (red) to visualize FAs, and Phalloidin (green) to visualize actin cytoskeleton. Histograms represent the mean ± SD of **(B)** phospho-c-Cbl, **(D)** phospho-

p130Cas and **(F)** phospho-paxillin levels in wtC3G and tgC3G platelets (upper panels) or C3G-wt and C3G-KO platelets (bottom panels) after spreading on CRP, fibrinogen and fibronectin for 30 min. *p<0.05. CRP: Collagen related peptide; MFI: mean fluorescence intensity; a.u.: arbitrary units; p: phospho.

Finally, we analyzed by immunoprecipitation assays whether C3G interacts with FA proteins. Results in **Figure R-38** show that C3G interacts with talin, p130Cas, c-Cbl, vinculin and FAK in platelets and that this interaction is regulated by thrombin stimulation. Of note, C3G interaction with c-Cbl disappeared in response to thrombin, in concordance with the lower phospho-c-Cbl levels observed in thrombin-stimulated tgC3G platelets on fibronectin.

It should be highlighted the difficulty to detect these interactions. For example, interaction between C3G and vinculin is detected in some experiments in resting conditions whereas in others is only detected after thrombin stimulation. Furthermore, we did not detect interaction between C3G and paxillin or β-catenin, despite the fact that it has been shown in other studies (Dayma *et al.*, 2012; Maia *et al.*, 2013). This is probably due to the dynamism of all these interactions. The interaction between C3G and p130Cas has been previously described in the literature (Maia *et al.*, 2009).

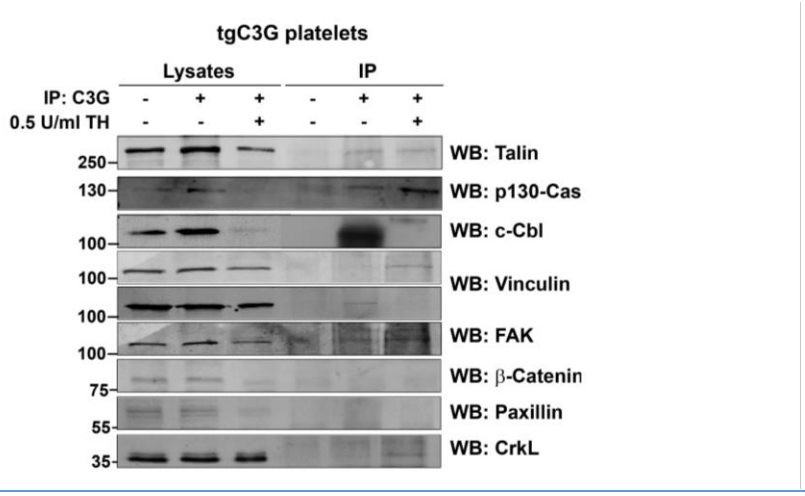


**Figure R-38. C3G forms complexes with Talin, p130-Cas, c-Cbl, vinculin and FAK in platelets, in resting conditions and upon thrombin stimulation.** Lysates from resting and thrombin (0.5 U/ml for 1 min)-stimulated tgC3G platelets were immunoprecipitated with an anti-C3G antibody (anti-C3G-G4 in the case of talin, p130-Cas, FAK and paxillin and anti-C3G-C19 in the case of c-Cbl, Vinculin and β-Catenin) and the levels of talin, c-Cbl, paxillin, vinculin, FAK, β-catenin and CrkL were detected by western blot. CrkL was used as positive control and mouse IgG was used as a negative control. IP: immunoprecipitation; WB: western blot; TH: thrombin.

Taken together, these results strongly suggest a role for C3G in FA dynamics, which support its role in platelet adhesion.

## 2.3. Absence of C3G in platelets impairs clot retraction

Since retraction of fibrin clots requires platelet integrins to be connected to the actin cytoskeleton (Haling *et al.*, 2011), and given the role of C3G in integrin activation (**Figure R-2**) and in actin cytoskeleton remodelling, we examined whether C3G participates in this process.

Indeed, C3G-KO platelets were defective in thrombin-induced clot retraction (**Figure R-39B**), with a larger clot weight and higher extruded volume noted, compared to C3G-wt platelets

(Figures R-39C, D). In contrast, overexpression of C3G had no effect in this process (Figures R-39A, C, D). This suggests that a minimal level of C3G is required for platelet clot retraction.

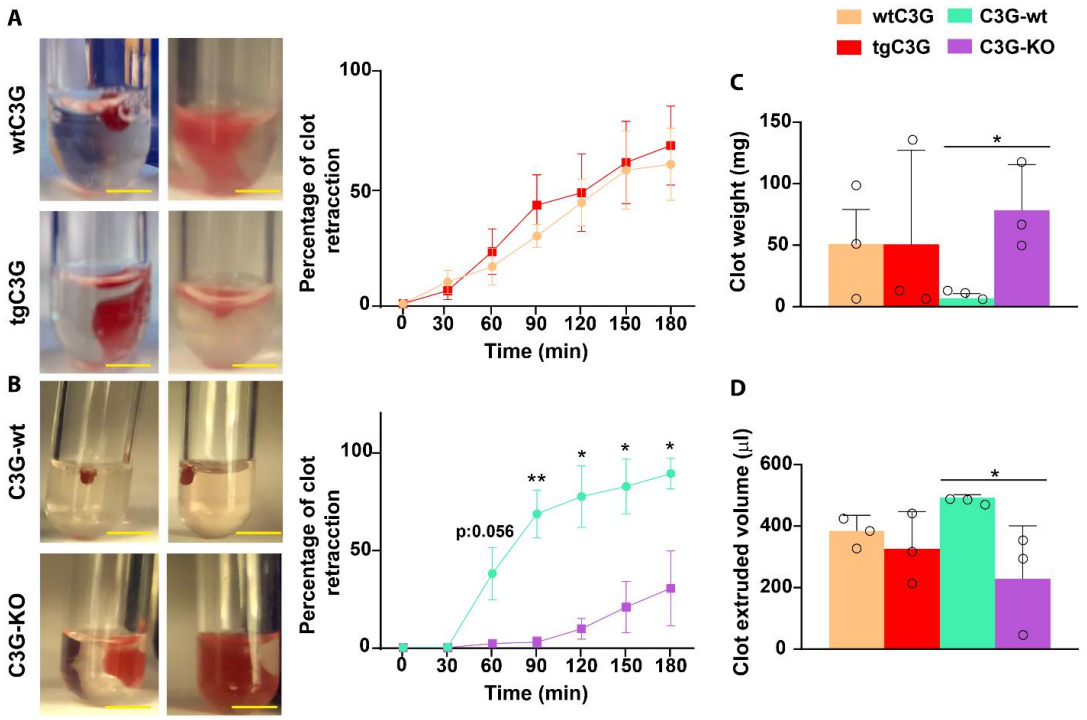


**Figure R-39. C3G absence, but not C3G overexpression, affects clot retraction. (A)** Representative images and quantification of the ability of clot retraction of PRP from wtC3G and tgC3G mice or **(B)** C3G-wt and C3G-KO mice. Clot formation was initiated by adding 1 U/ml thrombin and photographed each 30 min for 3 h. **(C)** Clot weight and **(D)** clot extruded volume were monitored at the end point of the experiment. Histograms and line/scatter plots represent the mean ± SEM. *p<0.05, **p<0.01. Scale bar: 5 mm.

Taken together, our results indicate that C3G regulates outside-in signaling through regulation of actin cytoskeleton dynamics.

# 3. C3G participation in platelet vesicular trafficking

## 3.1. Deletion of C3G promoted protein release in response to thrombin

Previous results of our group, using transgenic mouse models, demonstrated that C3G modulates platelet α-granule secretion. Specifically, C3G overexpression induces the retention of angiogenic factors, such as TSP-1 and VEGF upon thrombin stimulation, leading to a proangiogenic secretome both *in vivo* and *in vitro* (Martin-Granado *et al.*, 2017). Hence, we sought to examine whether the absence of C3G also alters platelet secretion. As shown in Figure R-40, C3G-KO platelets released a higher amount of protein compared to C3G-wt platelets, following 0.2 U/ml thrombin stimulation for 5 min.

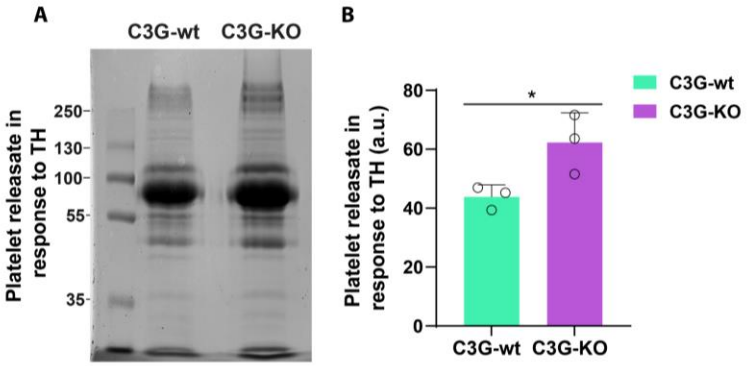


**Figure R-40. C3G-KO platelets secrete more protein upon thrombin stimulation. (A)** SDS-PAGE of 20 µl secretome from C3G-wt and C3G-KO platelets stimulated with 0.2 U/ml thrombin (TH) for 5 min at 1100 rpm at 37 °C. Proteins were visualized with Colloidal Blue Staining. **(B)** Histogram represents the mean ± SD of the quantification of proteins in the releasate in response to thrombin. *p<0.05.

## 3.2. C3G ablation did not result in changes in platelet structure

Since C3G deletion in platelets produces a greater secretion of proteins after thrombin stimulation, we decided to examine whether this was due to increased granule content. As mentioned in the **Introduction**, platelets present three different types of granules: α-granules, δ-granules and lysosomes, so we studied the number and structure of the different types of granules by transmission electronic microscopy in C3G-wt and C3G-KO platelets.

C3G obliteration did not affect either platelet morphology or platelet size under resting conditions, as C3G-KO platelets displayed the same area, perimeter and circularity as C3G-wt platelets. Furthermore, there were not differences in the number of α-granules or δ-granules between genotypes, suggesting that C3G is not essential for granule biogenesis (**Figure R-41**).

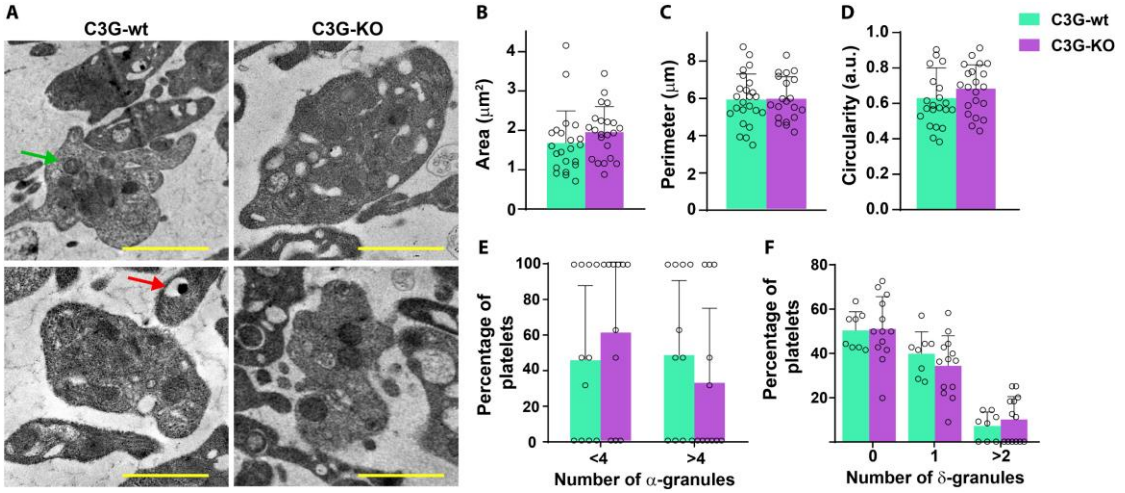


**Figure R-41. C3G absence does not affect platelet structure. (A)** Representative images of transmission electronic microscopy of C3G-wt and C3G-KO platelets in steady-state conditions. Scale bar: 0.5 µm. Histograms represent the quantification of the **(B)** platelet area, **(C)** platelet perimeter, **(D)** platelet circularity. **(E)** and **(F)** represent the percentage of platelets with more or less than 4 α-granules **(E)** or with 0, 1 or more than 2 δ-granules (**F**) (media ± SD). The red arrow points to a δ-granule, whereas the green arrow indicates an α-granule.

The fact that the increased platelet secretion observed in C3G-KO platelets is not caused by an increase in granule number points to defective secretory machinery. This suggests that C3G might be a regulator of platelet secretion, consistent with previous data from tgC3G platelets (Martin-Granado *et al.*, 2017).

## 3.3. C3G regulates the secretion of α-granules but no δ-granules or lysosomes

Given the observed differences in thrombin-induced secretomes and defects in P-selectin (an α-granule protein) exposure on the platelet surface between the different C3G platelet genotypes, we wondered whether C3G could modulate the secretion of all platelet granules or whether it is specific for α-granules.

To analyze δ-granule secretion we studied, by flow cytometry, the exposure of CD63 (a δ-granule transmembrane protein) on the platelet surface after stimulation with calcium, thrombin or a mixture of both. The results in **Figure R-42A** did not show differences between the three genotypes studied and their controls, indicating that C3G is not essential for δ-granule release. To complement these data, we studied the amount of ATP released, after stimulation with increasing concentrations of thrombin, by bioluminescence using the CellTiter Glo 2.0 kit. Consistent with the above results, neither C3G overexpression nor C3G absence altered ATP secretion (**Figure R-42B**). This data confirmed that C3G is not involved in δ-granule secretion.

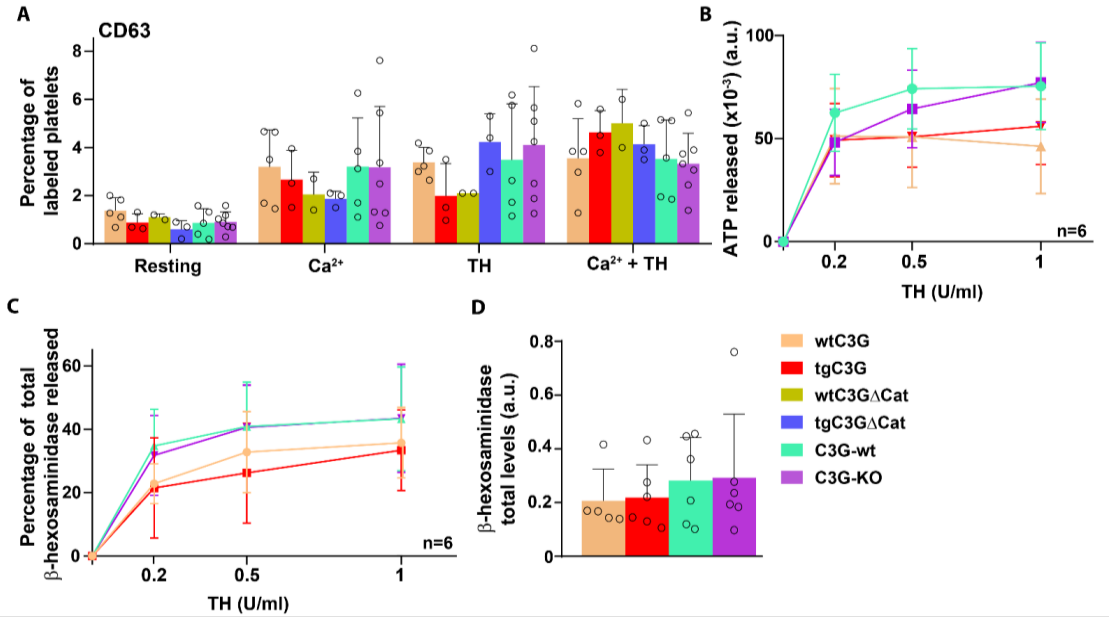


**Figure R-42. C3G does not regulate δ-granule and lysosome secretion in platelets. (A)** Washed blood from tgC3G, tgC3GΔCat, C3G-KO and their wild-type mice was stimulated with 2 mM calcium and/or 0.5 U/ml thrombin (TH) and incubated with anti-CD63 antibody to monitor, by flow cytometry, the percentage of CD63 exposed on the platelet surface. **(B)** PRP from wtC3G, tgC3G, C3G-wt and C3G-KO mice was stimulated with thrombin (TH) (0.2, 0.5 or 1 U/ml) for 10 min at 37 °C, under stirring conditions. ADP levels in platelet secretomes were detected by bioluminescence using the CellTiter Glo 2.0 kit. **(C)** Platelets from wtC3G, tgC3G, C3G-wt and C3G-KO mice were stimulated with different concentrations of thrombin (TH) (0.2, 0.5 and 1 U/ml) for 20 min at 37 °C. Platelet secretomes were mixed with the same volume of 5 mM 4-NAG (4-Nitrophenyl N-acetyl-β-D-glucosaminidase) in Citrate Phosphate Buffer. β-hexosaminidase levels were measured by absorbance at 405 nm. The graph

represents the percentage of hexosaminidase released with respect to the total levels represented in D. **(D)** Quantification of total levels of β-hexosaminidase in resting tgC3G and C3G-KO platelets and their respective wild-types. Histograms and line/scatter plots represent the mean ± SD. a.u.: arbitrary units.

Finally, we determined the involvement of C3G in lysosome secretion by studying the release of β-hexosaminidase after thrombin stimulation. No differences in the amount of β-hexosaminidase released in response to thrombin were observed between the different genotypes (Figure R-42C). In addition, total levels of β-hexosaminidase in C3G-KO and tgC3G platelets were equivalent to their wild-types (Figure R-42D).

Overall, these data demonstrate that the role of C3G in platelet secretion is restricted to α-granule secretion, with no effect on δ-granule or lysosomal secretion.

## 3.4. C3G obliteration leads to changes in α-granule distribution

As C3G-KO platelets exhibited a marked increase in protein secretion from α-granules but displayed defective P-selectin exposure on the platelet surface, we sought to investigate the distribution of α-granules after thrombin stimulation. As a first approach, we examined, by western blot, the distribution of P-selectin in cytosolic and membrane fractions.

As expected, in response to thrombin, P-selectin is recruited from the cytosol to the membrane in C3G-wt platelets. C3G-KO platelets displayed a higher accumulation of P-selectin in the membrane fraction in resting conditions (Figure R-43). However, after thrombin stimulation, C3G-KO platelets showed lower levels of P-selectin in the membrane, which rather accumulated in the cytosolic fraction.

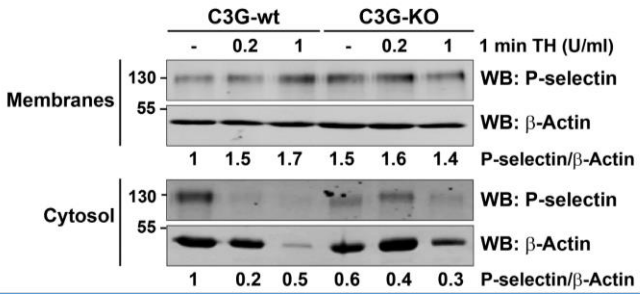


**Figure R-43. C3G absence alters P-selectin distribution in platelets.** Western blot analysis of P-selectin levels in the membrane (upper) or cytosolic (lower) fractions from resting, and 0.2 or 1 U/ml thrombin (TH)-stimulated C3G-wt or C3G-KO platelets. β-actin was used as loading control. The values of the P-selectin/β-actin ratio were relativized to those of resting C3G-wt platelets.

To reinforce these data, we performed immunofluorescence staining with an anti-P-selectin antibody. The results in Figure R-44A revealed lower global levels of P-selectin in C3G-KO platelets, compared to C3G-wt platelets under resting conditions. However, upon thrombin stimulation P-selectin levels in C3G-KO platelets equaled those in C3G-wt platelets, although a higher signal could be detected in the membrane of C3G-wt platelets, according to the results in Figure R-43. The greater increment found in C3G-KO platelets could be due to increased protein synthesis or granule fusion.

Some authors describe different subpopulations of α-granules depending on the expression of VAMP-3, VAMP-7 and VAMP-8 (Peters *et al.*, 2012; Battinelli *et al.*, 2019). Since previous results from our group demonstrated that C3G interacts with VAMP-7 in both, platelets and K562 cells (Martin-Granado *et al.*, 2017), we investigated whether C3G could specifically affect the distribution of VAMP-7 granules. For comparison, we also investigated the distribution of VAMP-8 granules. As shown in **Figures R-44B, C**, the levels of VAMP-7 and VAMP-8 were lower in C3G-KO platelets than in C3G-wt platelets, under resting conditions. However, as with P-selectin, upon thrombin stimulation VAMP-7 and VAMP-8 fluorescence levels were significantly increased in C3G-KO, but not in wild-type platelets (**Figures R-44B, C**).

Eckly and co-workers described that there are two different modes of vesicle exocytosis in platelets: i) single mode, in which individual granules fuse to the PM or to OCS; ii) compound mode in which, prior to fusion to the PM, there is granule-to-granule fusion, resulting in the formation of large multigranular compartments, thereby increasing the fluorescence signal (Eckly *et al.*, 2016). Based on that, the increased fluorescence levels of P-selectin, VAMP-7 and VAMP-8 found in C3G-KO platelets after thrombin stimulation suggest that C3G ablation might promote compound exocytosis.

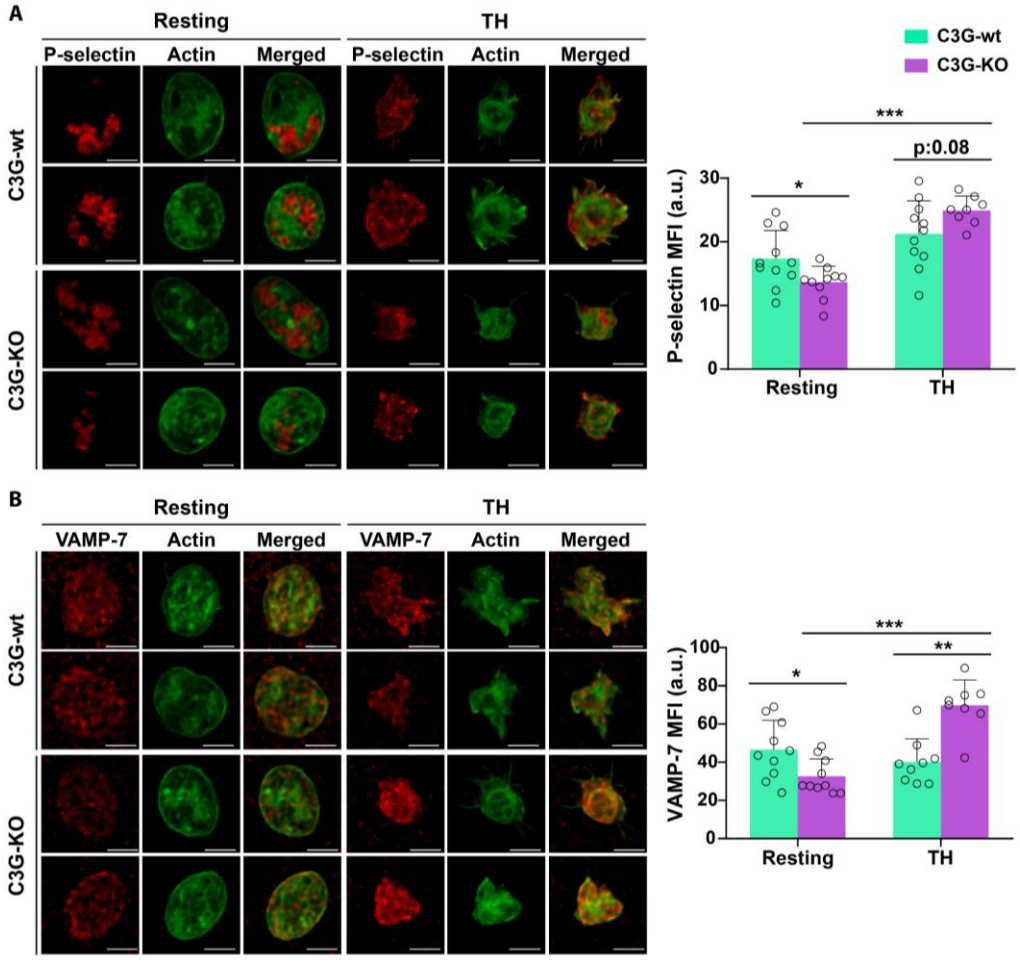

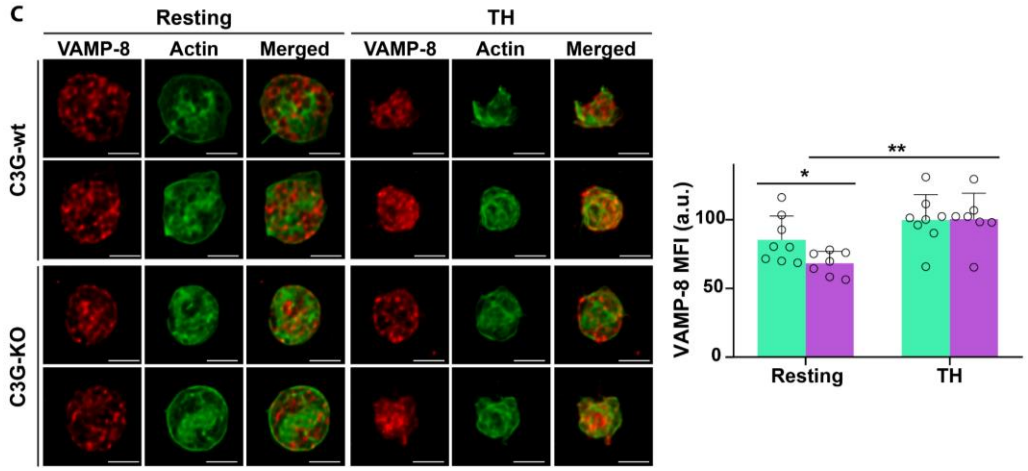


**Figure R-44. C3G deletion in platelets alters VAMP-7 and VAMP-8 α-granule distribution.** Representative immunofluorescence confocal microscopy images (left panel) of C3G-wt and C3G-KO platelets stimulated with 0.5 U/ml thrombin (TH) for 1 min and labeled with antibodies **(A)** anti-P-selectin + Cy3, **(B)** anti-VAMP-8 + AF568, or **(C)** anti-VAMP-7 + AF568 (red), and with phalloidin (green). Scale bar: 2 µm. Histograms (right panels) represent the mean ± SD of the MFI of P-selectin (upper), VAMP-7 (middle) or VAMP-8 (lower) in resting platelets and in response to thrombin. *p<0.05, **p<0.01, ***p<0.001. MFI: mean fluorescence intensity; a.u.: arbitrary units.

In the resting state, α-granules are distributed throughout the platelet; however, upon platelet stimulation they are recruited to the PM or translocated to the central granulomere prior to release into the OCS (Eckly *et al.*, 2016).

In Figure R-44B two different distribution patterns of VAMP-7 α-granules in C3G-KO platelets under resting conditions can be observed: i) central pattern distribution (C3G-KO-1), where VAMP-7 α-granules are found throughout the platelet, mainly in the center, as in C3G-wt platelets; ii) periphery/membrane pattern distribution (C3G-KO-2), in which VAMP-7 α-granules are concentrated near the PM. To analyze it in detail, we quantified the distribution of the different types of granules along platelet diameter (Figure R-45). Notably, the frequency of both VAMP-7 α-granule distribution patterns was similar (55% central pattern, 45% periphery pattern) (Figure R-45B). There were no differences in the distribution of P-selectin or VAMP-8 α-granules between C3G-wt and C3G-KO platelets (Figures R45A, C).

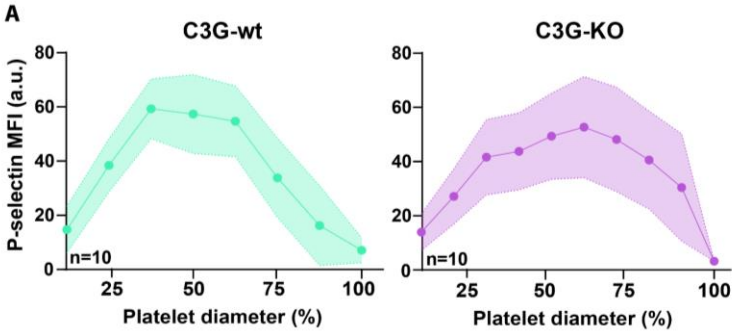

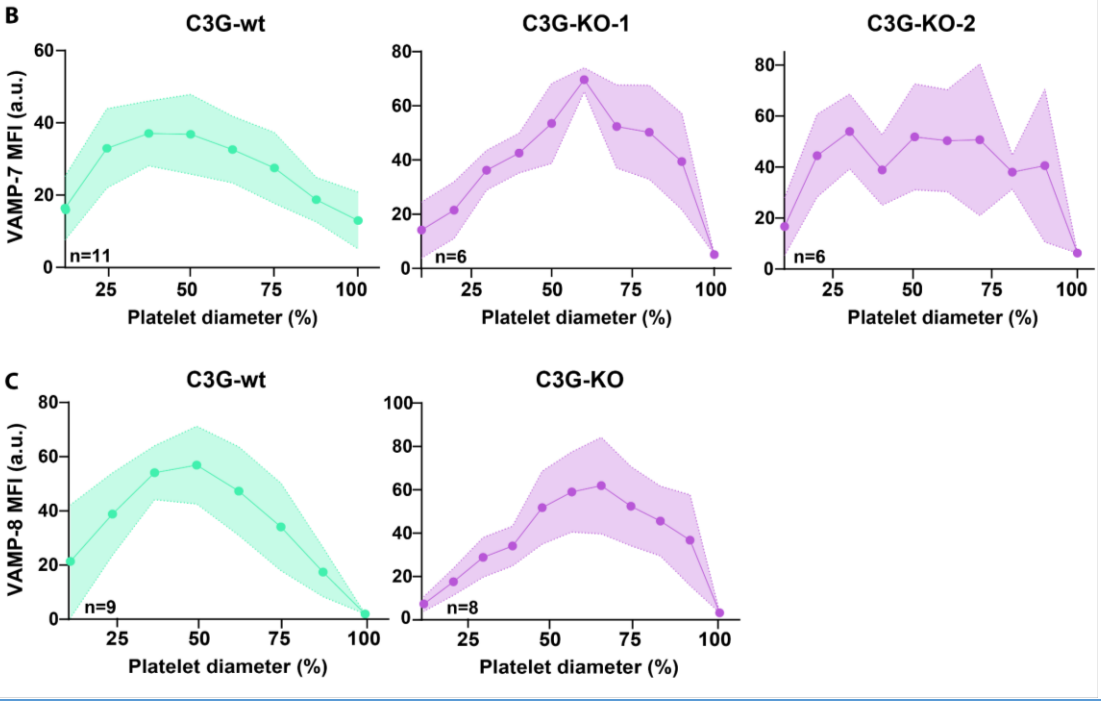


**Figure R-45. C3G absence alters VAMP-7 α-granule distribution in resting platelets.** Analysis of the distribution along the platelet diameter of **(A)** P-selectin α-granules, **(B)** VAMP-7 α-granules and **(C)** VAMP-8 α-granules in C3G-wt (left) and C3G-KO (right) platelets. Two different patterns of VAMP-7 α-granule distribution are shown in C3G-KO platelets. Line/scatter plots represent the mean ± SD of the P-selectin, VAMP-7 and VAMP-8 MFI. MFI: mean fluorescence intensity; a.u.: arbitrary units.

Based on the decreased MFI levels of P-selectin, VAMP-7 and VAMP-8 found in resting C3G-KO platelets, we investigated whether C3G could regulate the levels of these proteins and of other proteins also involved in platelet secretion, such as SNAP23, Stx11, Sec3 and Munc18-b. Indeed, C3G obliteration resulted in decreased levels of P-selectin and VAMP-7, according to the previous results; however C3G did not regulate VAMP-8, SNAP23, Stx11, Sec3 or Munc18-b levels (Figure R-46A). Consistent with the western blot analysis, C3G-KO platelets also showed reduced levels of P-selectin and VAMP-7 mRNA (Figure R-46B). In addition, C3G-KO platelets also showed a significant decrease in Munc18-b mRNA expression and a significant increase in VAMP-3 and Stx11 expression, which was not reflected in changes in protein expression.

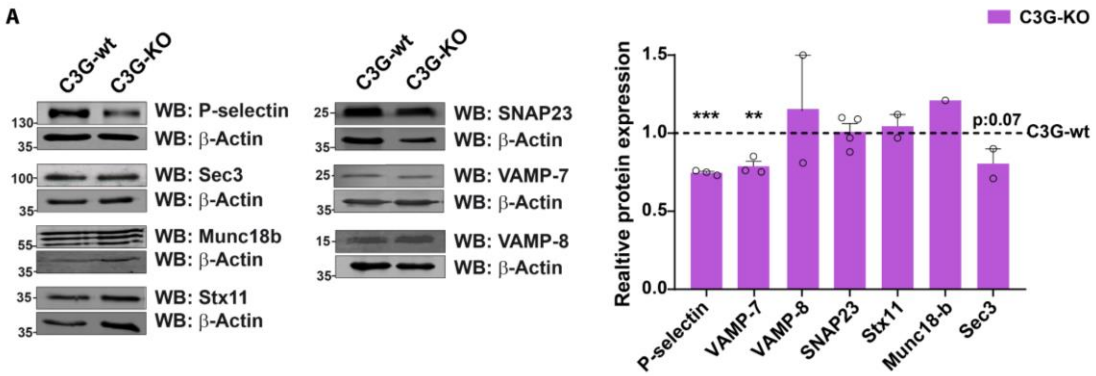

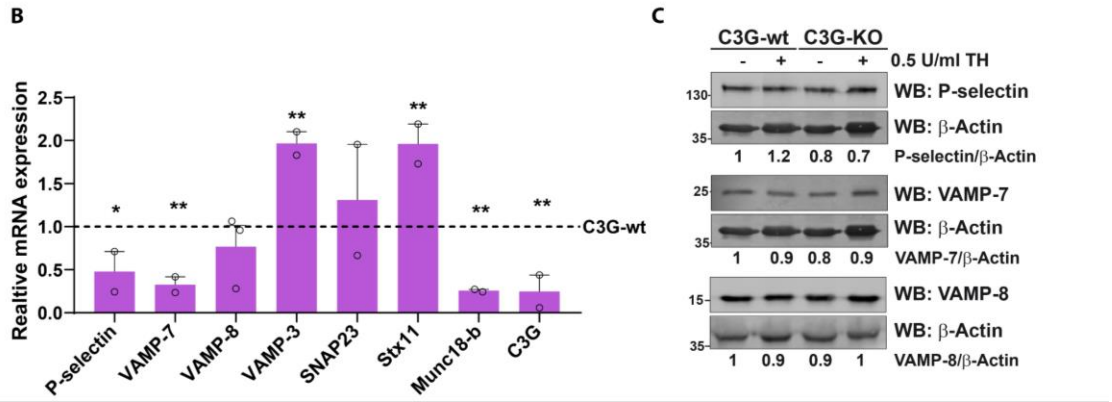


**Figure R-46. C3G absence triggers a decrease in the expression of P-selectin and VAMP-7. (A)** Western blot analysis of P-selectin, Sec3, Munc18-b, Syntaxin 11 (Stx11), SNAP23, VAMP-7 and VAMP-8 protein levels in lysates from C3G-wt and C3G-KO resting platelets (left panels). Histogram represents the densitometric analysis of the protein levels of these platelet secretion regulators. Data are relative to unstimulated wild-type platelets and were normalized to β-actin total levels. **(B)** RT-qPCR analysis of the expression of the indicated genes in mRNA from C3G-KO and C3G-wt platelets using β-*actin* as housekeeping gene. C3G (*Rapgef1*) was used as control. **(C)** Western blot analysis of P-selectin, VAMP-7 and VAMP-8 levels in resting and 0.5 U/ml thrombin-stimulated C3G-wt and C3G-KO platelets. β-actin was used as loading control. Values were normalized against to those of resting C3G-wt platelets. *p<0.05, **p<0.01, ***p<0.001. TH: thrombin.

Finally, to clarify whether the increased MFI levels of P-selectin, VAMP-7 and VAMP-8 in C3G-KO platelets after thrombin stimulation were due to protein synthesis or compound exocytosis, we examined protein levels by western blot in resting and thrombin-stimulated C3G-wt and C3G-KO platelets. Figure R-46C showed that thrombin did not induce an increase in the levels of these proteins in C3G-KO platelets. This result confirmed that the increase in MFI in Figure R-44 was not due to increased protein synthesis but rather to granule fusion, indicating that C3G absence could favor a compound exocytosis.

## 3.5. C3G does not participate in platelet endocytosis

Since C3G participates in platelet secretion, we wanted to analyze its putative participation in platelet endocytosis.

To address this, we incubated platelets with AF488 Fibrinogen for different times (5, 15 and 30 min) and the amount of endocytosed fibrinogen was measured by immunofluorescence. As shown in Figure R-47, there were no differences in fibrinogen levels between the different genotypes and their controls. This suggests that C3G would only be involved in platelet secretion but not in endocytosis.

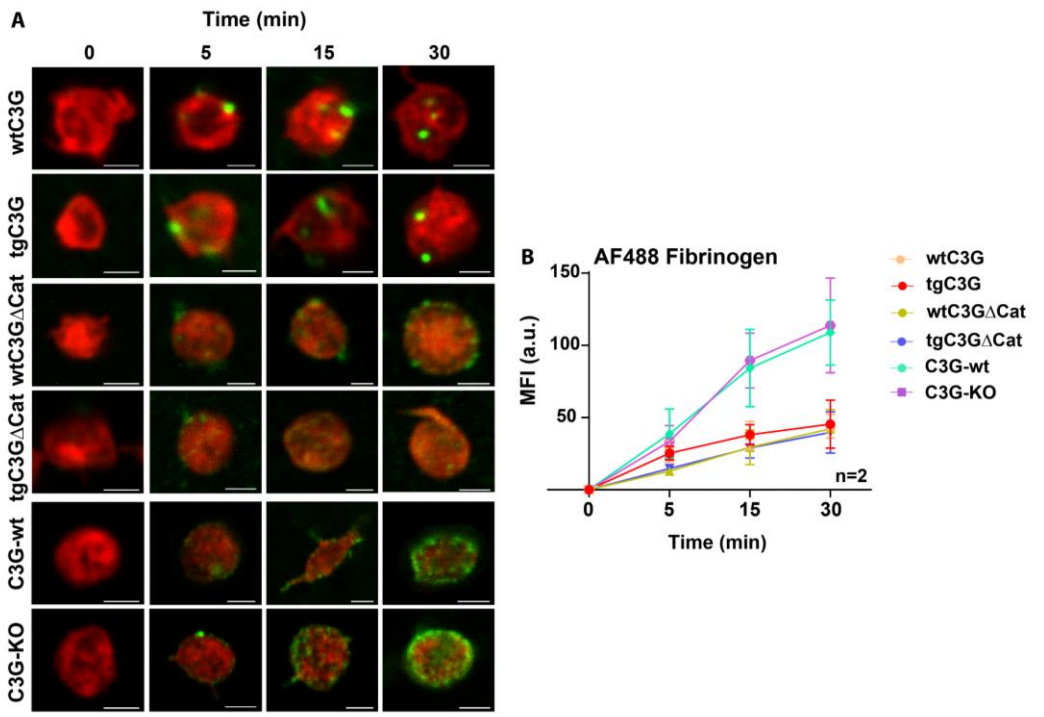


**Figure R-47. C3G does not modify platelet endocytosis of fibrinogen. (A)** Representative images of tgC3G, tgC3GΔCat and C3G-KO platelets and their wild-types incubated with 5 µM AF488-labeled fibrinogen (green) for different times (0, 5, 15 and 30 min) at 37 °C. Platelets were fixed and stained with Phalloidin-AF647 (red). Scale bar: 0.5 µm. **(B)** Line/scatter plot represents the quantification of the MFI (Mean ± SD) of AF488 fibrinogen endocytosed by platelets at the different times. AF: Alexa Fluor; MFI: mean fluorescence intensity; a.u.: arbitrary units.

## 3.6. C3G is involved in RalA activation but not in Rab27b activation

There are many GTPases involved in the regulation of vesicular trafficking, such as Ral, Rab and Arf GTPases. Ral GTPases participate in the tethering of vesicles to the PM, through the regulation of the exocyst complex, whereas Rab proteins regulate vesicle transport from the Golgi to the PM (Walsh *et al.*, 2019).

Notably, double RalA and RalB KO platelets present a phenotype similar to that of C3G-KO platelets; i.e., decreased exposure of P-selectin in the membrane but with normal cargo release after stimulation (Wersall *et al.*, 2018). Additionally, Ral is an effector of Rap1 in many systems (Bos *et al.*, 2001). Therefore, we investigated whether C3G could regulate Ral activation in platelets and whether this was via Rap1.

We analyzed RalA activation in response to thrombin in tgC3G, tgC3GΔCat and C3G-KO platelets and their controls. As shown in **Figure R-48A**, tgC3G platelets exhibited a two-fold increase in RalA-GTP levels after stimulation with 1 U/ml thrombin, compared to wtC3G platelets. Furthermore, in both C3G-KO platelets and tgC3GΔCat platelets we observed a decrease in RalA activation after 1 U/ml thrombin stimulation (**Figure R-48A**). This result suggests that the Rap1-RalA pathway could mediate the role of C3G in platelet secretion.

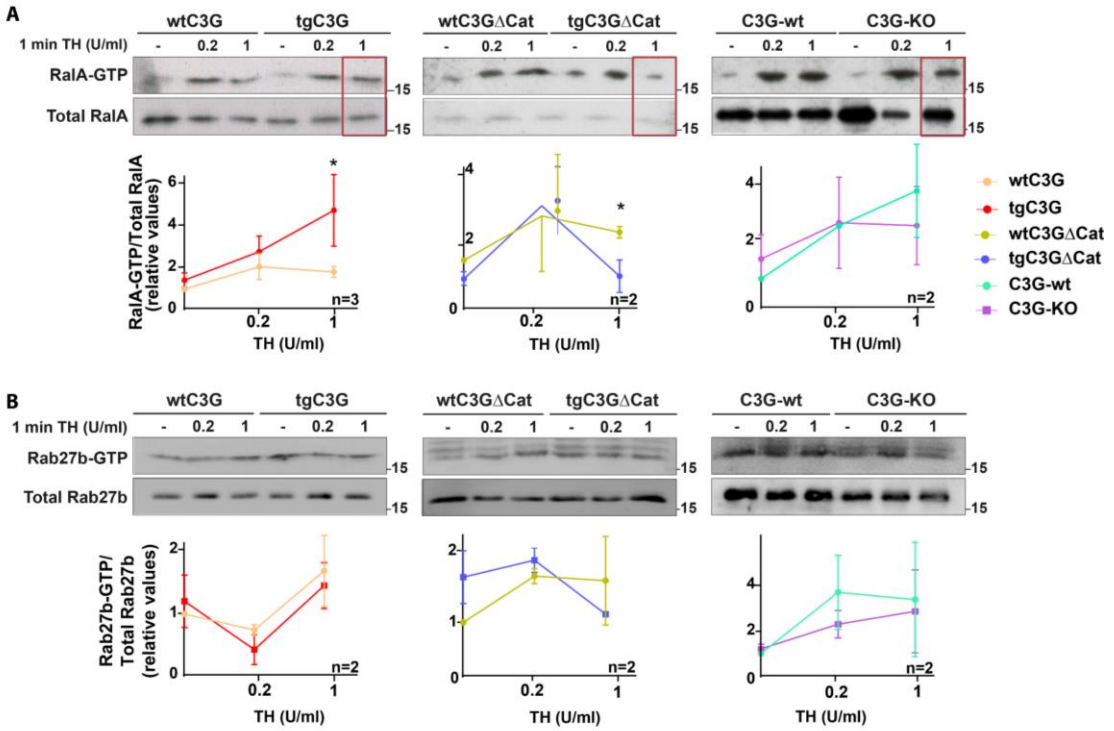


**Figure R-48. C3G regulates RalA activation but not Rab27b activation in thrombin-stimulated platelets.** Pull-down assays to detect **(A)** RalA-GTP and **(B)** Rab27b-GTP after stimulation of tgC3G, tgC3GΔCat, C3G-KO and their respective wild-types platelets with 0.2 and 1 U/ml thrombin (TH) for 1 min. The levels of RalA-GTP and Rab27b-GTP were detected by immunoblotting using anti-RalA and anti-Rab27b antibodies, respectively. A representative blot from 2-3 experiments is depicted for each assay. Values in graphs are relative to unstimulated wild-type platelets and normalized to total levels. *p<0.05.

As mentioned above, Rab27b participates in vesicle trafficking to the PM. Based on the differential distribution of VAMP-7 positive α-granules observed in resting C3G-KO platelets, we studied whether this could be related to alterations in Rab27b activation. Thus, we performed a Rab27b activation assay in tgC3G, C3GΔCat and C3G-KO platelets and their controls upon thrombin stimulation, but we found no differences in Rab27b-GTP levels between the different genotypes (Figure R-48B).

This result, together with results in Figures R-44 and R-45, indicates that the abnormal distribution of VAMP-7-α-granules observed in C3G-KO platelets is not due to defects in vesicular targeting but probably to defects in the actin cytoskeleton, supporting a role for C3G in actin remodelling.

## 3.7. C3G regulates trans-SNARE complex formation

RalA is necessary for the anchorage of vesicles to the PM, prior to the formation of the trans-SNARE complex (Nishida-Fukuda, 2019). Since C3G is involved in RalA activation, we studied whether C3G could participate in the granule-membrane association. For that, we first studied the possible interaction between C3G and proteins involved in vesicle secretion.

Previous results from the group demonstrated that C3G interacts with the v-SNARE protein VAMP-7 in resting and thrombin-stimulated platelets (Martin-Granado *et al.*, 2017). Consistently,

immunoprecipitation assays in co-transfected HEK-293T cells showed that C3G interacted with VAMP-7, VAMP-8, VAMP-3, VARP and slightly with Sec3. No interaction with Exo70 was detected (Figure R-49A).

To confirm these interactions in platelets, we performed immunoprecipitation assays in tgC3G platelets at rest and after stimulation with 0.5 U/ml thrombin. We found that C3G interacted with VAMP-8 and VARP in platelets, but not with Sec3 or Exo70 (Figure R-49B).

We also investigated the interaction of C3G with t-SNARE proteins, such as SNAP23 and Stx11, and with other proteins of the exocyst complex, such as Sec5 and Sec10. Results in Figure R-49B showed that C3G interacted with SNAP23 and Stx11, but not with the exocyst complex proteins. Remarkably, the interaction of C3G with Stx11 only occurred in resting platelets.

Based on the effect of C3G on P-selectin distribution, we studied a putative interaction between C3G and P-selectin. However, as shown in Figure R-49B, no interaction between the two proteins was detected. Finally, we found that C3G interacted with Munc18-b, a regulator of vesicle docking (Figure R-49B). Moreover, this interaction (together with the interaction with VARP) was mediated by the catalytic domain of C3G, since it was not dectected in tgC3GΔCat platelets (Figure R-49C), which is consistent with its role in RalA activation via Rap1.

The interaction of C3G with SNARE proteins indicates that C3G would participate in the last step of exocytosis, the formation of the trans-SNARE complex, probably through RalA-Rap1 pathway.

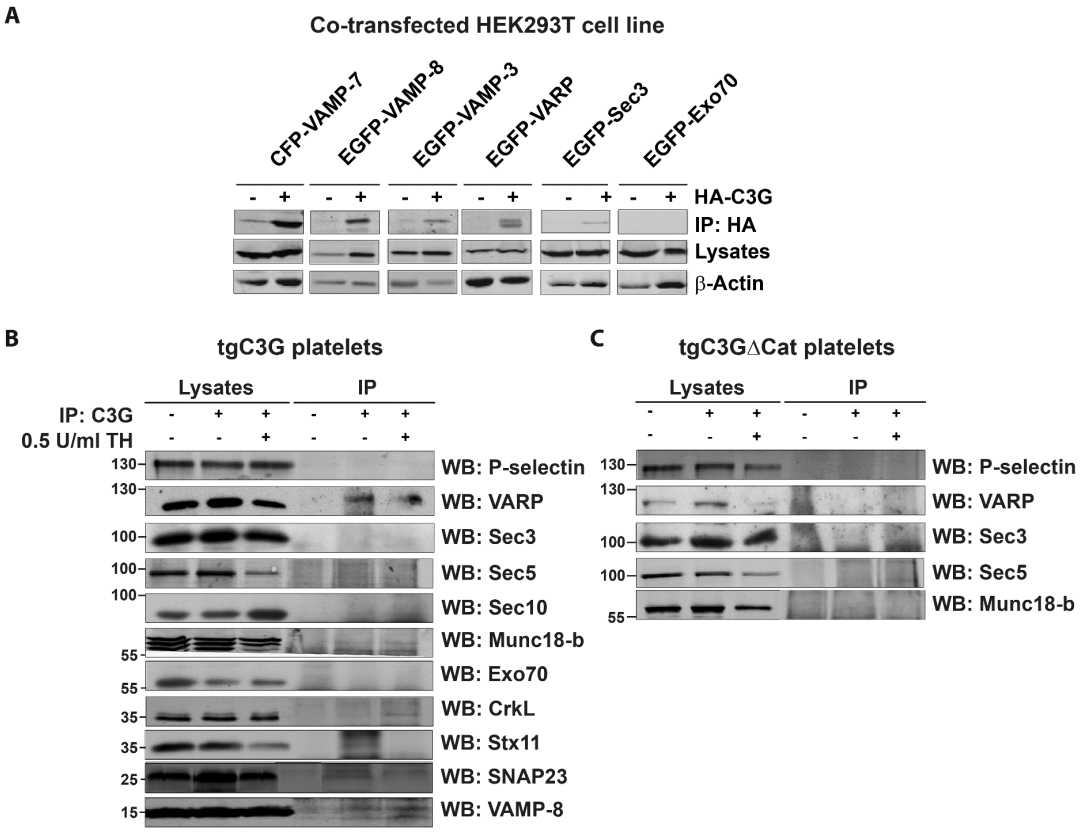

**Figure R-49. C3G interacts with VARP, Munc18-b, Stx11, SNAP23, VAMP-3 and VAMP-8. (A)** Lysates from HEK-293T cells co-transfected with HA-C3G plus the indicated proteins, were immunoprecipitated with an anti-HA antibody and the levels of VAMP-7, VAMP-8, VAMP-3, VARP, Sec3 and Exo70 were detected by western blot. Lysates from **(B)** tgC3G or **(C)** tgC3GΔCat platelets both at rest and after thrombin (TH) stimulation (0.5 U/ml for 1 min) were immunoprecipitated with anti-C3G G-4 antibody and the levels of P-selectin, VARP, Sec3, Sec5, Sec10, Munc18-b, Exo70, CrkL, Stx11, SNAP23 and VAMP-8 were detected by western blot. CrkL was used as a positive control and mouse IgG was used as a negative control. IP: immunoprecipitation; WB: western blot; Stx11: Syntaxin 11.

Koseoglu and co-workers described a complex formed by Arp2, VAMP-7 and VARP in resting platelets that regulates α-granule secretion. Specifically, VARP sequesters VAMP-7 and Arp2/3, avoiding VAMP-7 fusion with t-SNAREs and Arp2/3 actions on actin cytoskeleton remodelling, thus, preventing α-granule secretion. Following platelet stimulation, VARP releases both proteins, which results in granule secretion and actin polymerization (Koseoglu *et al.*, 2015). Thus, VARP links exocytosis with actin cytoskeleton reorganization during platelet activation.

Since C3G interacts with Arp2, VARP and VAMP-7, we studied, by immunoprecipitation assays in lysates of tgC3G and C3G-KO platelets and their controls, whether C3G participates in the Arp2/VARP/VAMP-7 complex. C3G overexpression increased the interaction between Arp2 and VARP, in a thrombin-dependent manner (Figure R-50A). Consistently, C3G ablation resulted in less interaction of Arp2 with VARP, VAMP-7 and VAMP-8 (Figure R-50B). This suggests a positive role for C3G in the formation of this complex.

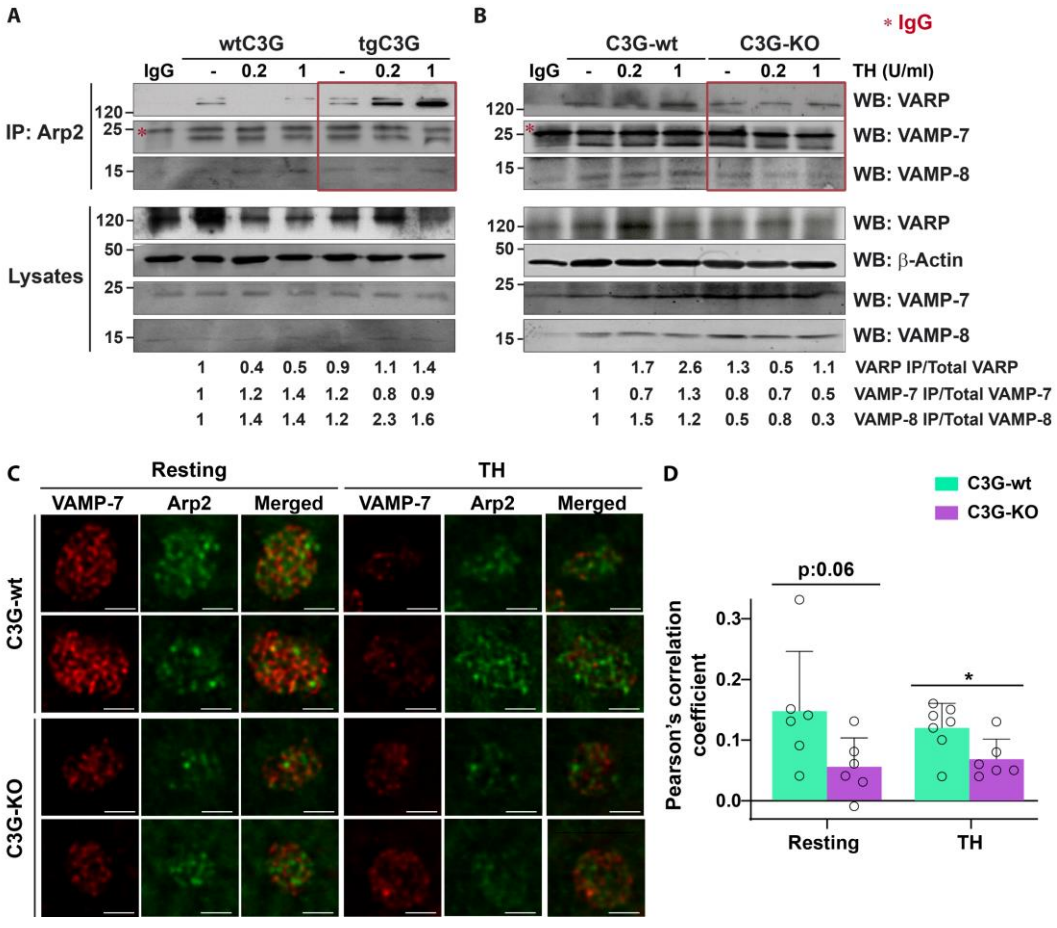

**Figure R-50. C3G regulates the Arp2/VARP/VAMP-7 complex.** Lysates from **(A)** wtC3G and tgC3G or **(B)** C3G-wt and C3G-KO platelets, both at rest and after thrombin (TH) stimulation (0.2 or 1 U/ml for 1 min) were immunoprecipitated with an anti-Arp2 antibody and the levels of VARP, VAMP-7, β-Actin and VAMP-8 were detected by western blot. IP: immunoprecipitation; WB: western blot. Values are relative to unstimulated wild-type platelets and normalized to total levels. * Indicates unspecific band (IgG). **(C)** Representative immunofluorescence confocal microscopy images of C3G-wt and C3G-KO platelets stimulated with 1 U/ml TH for 1 min and labeled with anti-VAMP-7 + AF568 (red) and anti-Arp2 + AF647 (green). Scale bar: 2 µm. **(D)** Histogram shows the Pearson's Correlation Coefficients (mean ± SD) of the intensity values of VAMP-7 and Arp2 under the indicated experimental conditions. *p<0.05.

To validate these results, we monitored the interaction between Arp2 and VAMP-7, in C3G-KO platelets and their controls, measuring their colocalization by immunofluorescence. C3G deletion decreased the interaction between Arp2 and VAMP-7, both in resting and thrombin-stimulated platelets (Figures R-50C-D). These findings support the notion that C3G is required for the formation of the Arp2-VARP-VAMP-7 complex in platelets.

The above result suggests a negative role of C3G in the formation of the trans-SNARE complex. Therefore, based on the interaction of C3G with the SNARE proteins, SNAP23, Stx11 and Munc18-b, we next examined the possible involvement of C3G in the formation of this complex, by monitoring the interaction between SNAP23 and VAMP-7.

As shown in Figure R-51A, overexpression of C3G resulted in less interaction between SNAP23 and VAMP-7, especially after 1 U/ml thrombin stimulation, consistent with the greater C3G interaction with the Arp2/VARP/VAMP-7 complex. In agreement, C3G-KO platelets presented higher levels of VAMP-7 in SNAP23 precipitates, indicating a higher rate of trans-SNARE complex formation (Figure R-51B). No relevant differences were found in VAMP-8 levels in the immunoprecipitates.

These data suggest that C3G would regulate the formation of the trans-SNARE complex, probably by sequestering VARP and VAMP-7, so VAMP-7 would not be available to interact with SNAP23. To validate these results, we studied the interaction of VAMP-7 with SNAP23 and Stx11 by immunofluorescence. Although not significant, the results in Figures R-51C-E showed a greater interaction between VAMP-7 and SNAP23 in C3G-KO platelets under low thrombin stimulation. We did not see differences in the interaction between VAMP-7 and Stx11. This result reinforces the idea that C3G obliteration favors the formation of the trans-SNARE complex.

In conclusion, C3G might act as a brake of platelet secretion through the regulation of the Arp2/VARP/VAMP-7 complex. This could explain the increased secretion observed in C3G-KO platelets upon thrombin stimulation.

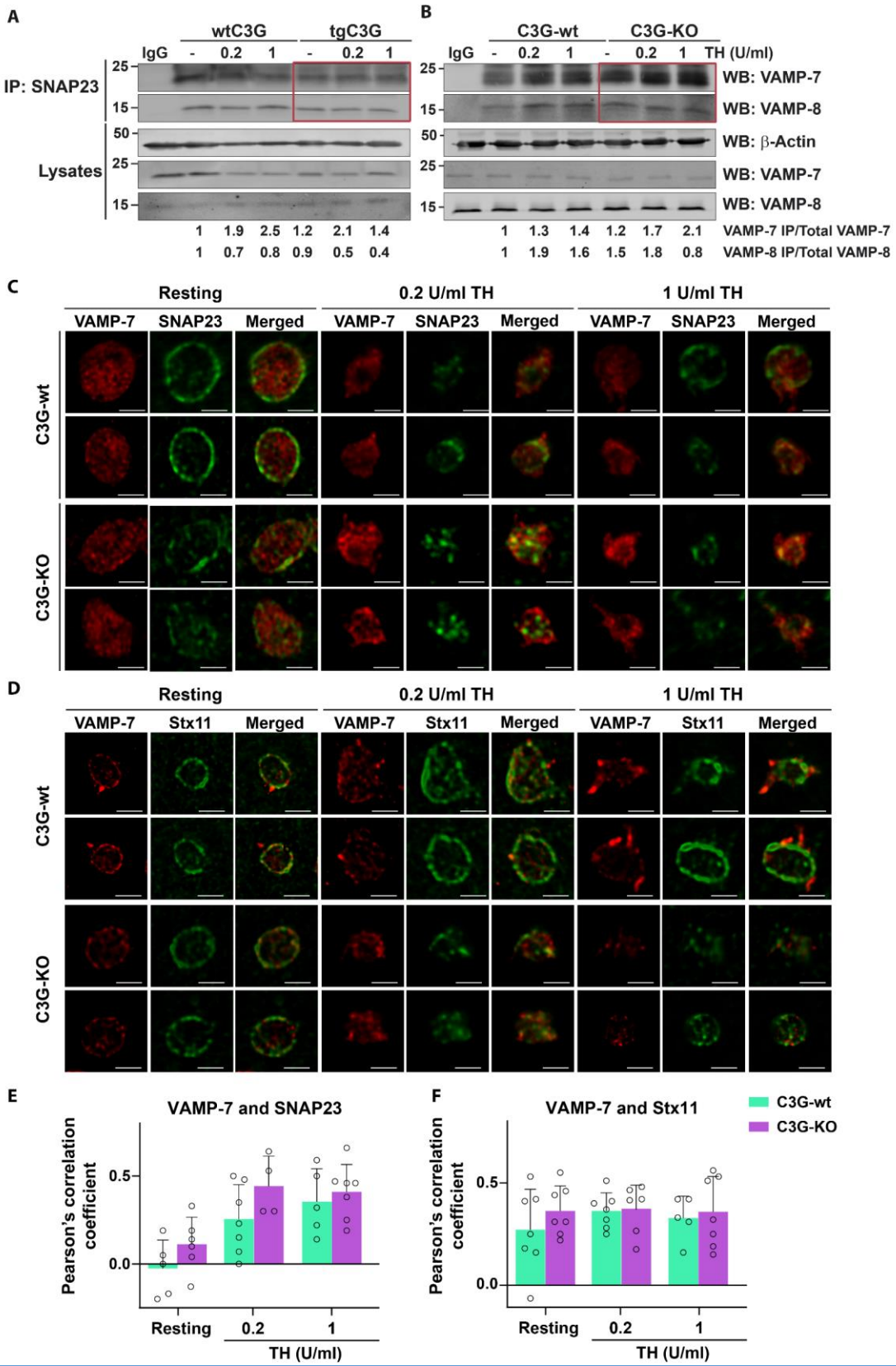


**Figure R-51. C3G regulates the trans-SNARE complex formation.** Lysates from **(A)** wtC3G and tgC3G platelets or **(B)** C3G-wt and C3G-KO platelets, both at rest and after thrombin (TH) stimulation (0.2 or 1 U/ml for 1 min) were immunoprecipitated with an anti-SNAP23 antibody and the levels of VAMP-7 and VAMP-8 were detected by western blot. β-actin was used as loading control. IP: immunoprecipitation; WB: western blot. Values are relative to unstimulated wild-type platelets and

were normalized to total levels. **(C, D)** Representative immunofluorescence confocal microscopy images of C3G-wt and C3G-KO platelets stimulated with 0.2 and 1 U/ml thrombin (TH) for 1 min and labeled with anti-VAMP-7 + AF647 (red) and **(C)** anti-SNAP23 + AF568 (green) or **(D)** anti-Stx11 + AF568 (green). Scale bar: 2 µm. **(E, F)** Histograms show the Pearson's Correlation Coefficients (mean ± SD) of the intensity values of **(E)** VAMP-7 and SNAP23 or **(F)** VAMP-7 and Stx11. Stx11: Syntaxin 11.

## 3.8. C3G ablation in platelets promotes a kiss-and-run exocytosis

The above findings, showing a decrease in P-selectin exposure but a marked increase in platelet secretion upon stimulation, suggest that C3G-KO platelets might display a kiss-and-run phenotype. To demonstrate this, we monitored platelet exocytosis by staining platelet granules with FM1-43, a widely used dye for imaging vesicle exocytosis and endocytosis. After granule exocytosis there is a decrease in FM1-43 signal, due to the dye being released or smearing across the PM.

C3G-KO and C3G-wt platelets, stained with FM1-43, were spread on IbiTreat plates and imaged for 1 min. While C3G-wt platelets showed decreased fluorescence over time, indicating a normal, fuse and collapse, exocytosis, two different exocytosis patterns were found in C3G-KO platelets: i) fuse and collapse exocytosis (C3G-KO-1), with kinetics similar to that of C3G-wt platelets, ii) kiss-and-run exocytosis (C3G-KO-2), in which FM1-43 signal is not lost, indicating that there is no fusion of the granules with the PM (**Figure R-52**). It should be highlighted that we found a higher percentage of granules undergoing normal exocytosis than kiss-and-run exocytosis in the C3G-KO platelets (67.5% vs 32.5%). In addition, we observed a higher number of fused granules in C3G-KO platelets, indicative of compound exocytosis, compared to C3G-wt platelets.

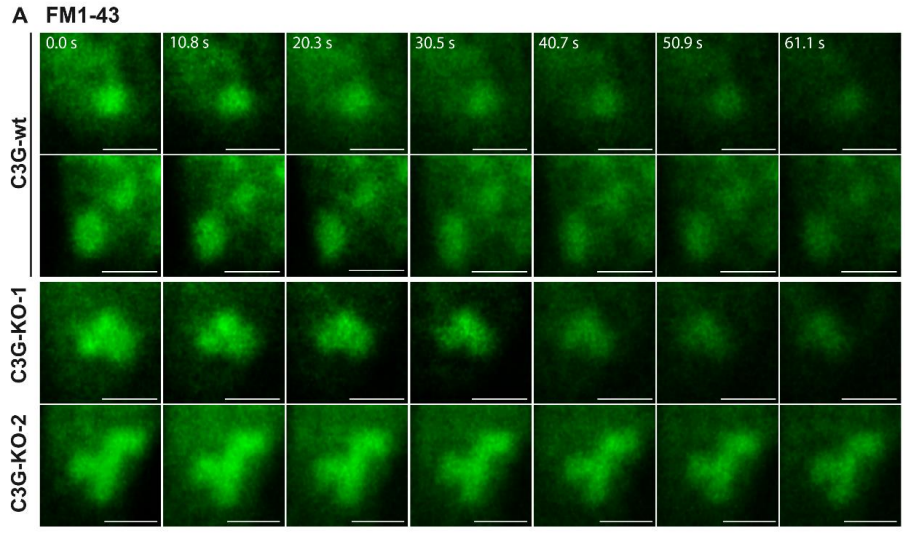

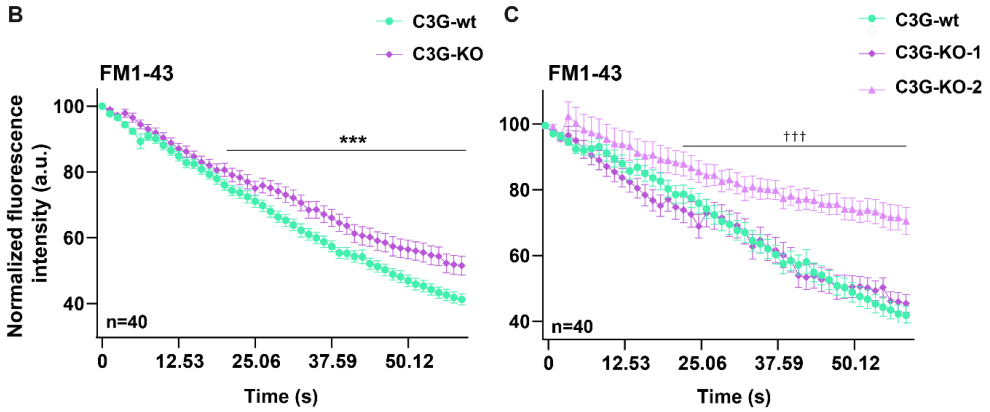


**Figure R-52. C3G-KO platelets showed a kiss-and-run phenotype during platelet spreading. (A)** Representative images of granules from C3G-wt and C3G-KO platelet spread on a µ-Slide 8-well plate (Ibidi) after staining with 10 µm FM1-43. Images were taken every 10 s for 1 min. **(B)** Scatter plot representing the quantification of MFI (Mean ± SEM) of individual FM1-43-stained granules from all C3G-wt and C3G-KO platelets analyzed. **(C)** Same analysis as in B but C3G-KO platelets were separated in two categories depending on their phenotype: fuse and collapse (lower graph) or kiss-and-run (upper graph) exocytosis. ***p<0.001. †††p<0.001 C3G-KO-2 versus C3G-wt.

Results from **Figures R-44 and R-46** suggested that C3G ablation could favor a compound exocytosis. To confirm this, we quantified the number of single or compound granules in C3G-KO and C3G-wt platelets stained with FM1-43 and spread on IbiTreat plates for 1 min. As shown in **Figure R-53**, C3G-KO spread platelets presented a lower percentage of single granules and a higher percentage of compound granules, compared to C3G-wt platelets. This result confirms that the absence of C3G favors granule-to-granule fusion during exocytosis.

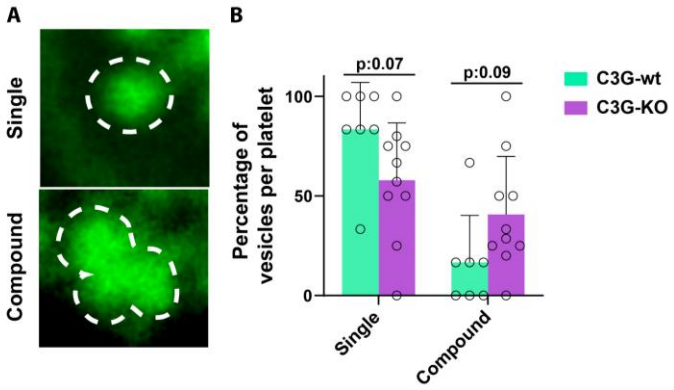


**Figure R-53. C3G absence favors compound exocytosis. (A)** Representative images showing single and compound granules. **(B)** Histogram represents the mean ± SD of the percentage of single or compound vesicles in platelets of each genotype.

## 3.9. C3G regulates trans-SNARE complex formation during platelet spreading

As mentioned in **Introduction**, granule secretion is linked to platelet spreading (Peters *et al.*, 2012). Since C3G-KO platelets displayed less spreading (**Figures R-13 and R-14**) and less P-selectin exposure upon activation (**Figure R-3**), indicative of lower α-granule membrane incorporation into the PM, we wanted to know if C3G could regulate α-granule distribution during platelet spreading.

For this, we studied the formation of the trans-SNARE complex during platelet spreading, measuring the colocalization between VAMP-7 and SNAP23 or Stx11 during spreading on poly-L-lysine. As shown in Figure R-54, C3G absence induced a greater interaction between VAMP-7 and SNAP23 or Stx11 after 30 min of spreading.

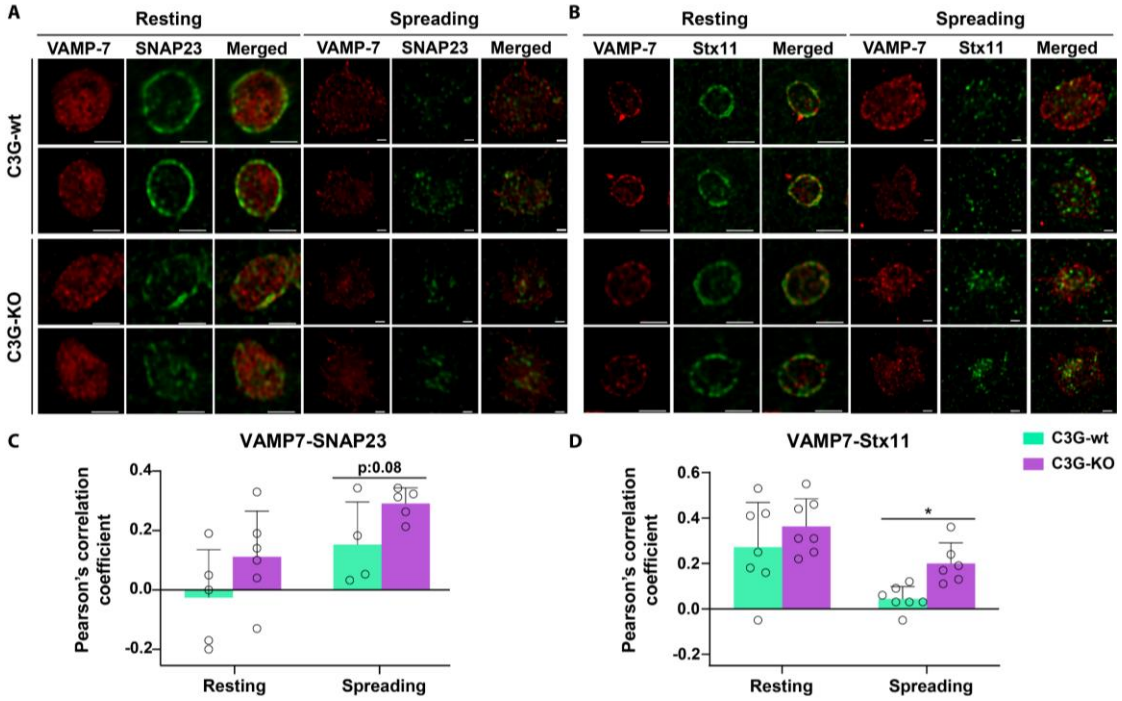


**Figure R-54. C3G regulates the trans-SNARE complex formation during spreading.** Representative immunofluorescence confocal microscopy images of C3G-wt and C3G-KO platelets stimulated with 0.2 U/ml thrombin for 1 min and spread on poly-L-lysine for 30 min. Platelets were fixed and labeled with anti-VAMP-7 + AF647 (red) and **(A)** anti-SNAP23 + AF568 (green) or **(B)** anti-Stx11 + AF568 (green). Scale bar: 2 µm. **(C, D)** Histograms show the Pearson's Correlation Coefficients (mean ± SD) of the intensity values of **(C)** VAMP-7 and SNAP23 or **(D)** VAMP-7 and Stx11. *p<0.05. Stx11: Syntaxin 11.

Finally, we studied the influence of SNAP23 in the interaction of C3G with VARP, VAMP-7 and Stx11, using SNAP23-KO platelets spreading on poly-L-Lysine or fibrinogen. Figure R-55 shows a greater interaction between C3G and VAMP-7 or Stx11 in the absence of SNAP23, mainly on fibrinogen, with no change in the C3G-VARP interaction. This result would confirm the participation of C3G in the trans-SNARE complex formation, where C3G would probably play a negative role by competing with SNAP23 for binding to VAMP-7 and Stx11.

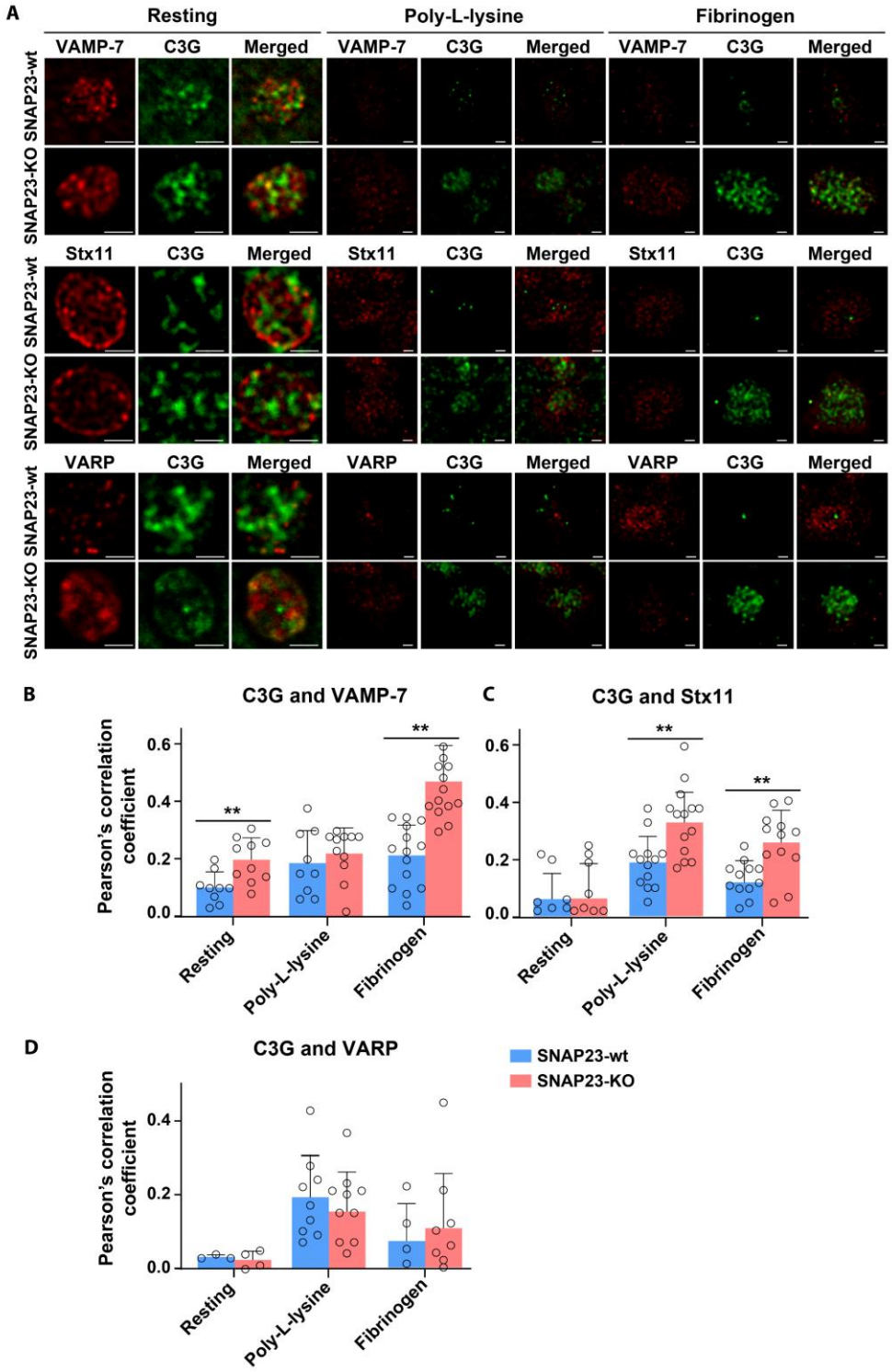


**Figure R-55. SNAP23 regulates the interaction of C3G with VAMP-7 and Stx11 during platelet spreading. (A)** Representative immunofluorescence confocal microscopy images of SNAP23-wt and SNAP23-KO platelets stimulated with 0.2 U/ml thrombin for 1 min and spread on poly-L-lysine or fibrinogen for 30 min. Platelets were fixed and labeled with anti-C3G + AF405 (green) and anti-VAMP-7 + AF568 (green), or anti-Stx11 + AF568 (green), or anti-VARP + AF568 (green). Scale bar: 2 µm. **(B, C, D)** Histograms show the Pearson's Correlation Coefficients (mean ± SD) of the intensity values of **(B)** C3G and VAMP-7, **(C)** C3G and Stx11 and **(D)** C3G and VARP. **p<0.01. Stx11: Syntaxin 11.

All these data demonstrate that C3G deletion in platelets promotes a kiss-and-run exocytosis. This is supported by the defective incorporation of vesicle membrane into the PM and the increased secretion of α-granule content, due to increased trans-SNARE complex formation. This kiss-and-run phenotype, together with the decreased ability to form lamellipodia, would explain the impaired spreading observed in these platelets.

## 3.10. Analysis of the implication of C3G in vesicular secretion using the PC12 cell line

PC12 cells (rat pheochromocytoma cell line) are one of the most widely used cell models to study secretion. Therefore, we aimed to investigate whether C3G role in platelet secretion also applies to this model. For this purpose, we generated stable cell lines with modified C3G expression. On the one hand, we used lentiviral particles to overexpress a wild-type C3G (C3G-wt) and a hyperactive C3G mutant (C3G-Y554H) (both GFP fusion proteins, (Carabias *et al.*, 2020)). On the other hand, we used a shRNA construct (pLVTHM-C3Gi) to silence it ((Ortiz-Rivero *et al.*, 2018)). The expression of C3G in the transfected PC12 clones was confirmed by western blot (**Figure R-56**). In the C3G-wt and C3G-Y554H mutant clones two different C3G proteins were detected, the endogenous (lower band) and the GFP-fusion protein (upper band). The pLVTHM-C3Gi mutant showed a 2-fold decrease in C3G expression, compared to the control (pLVTHM-empty).

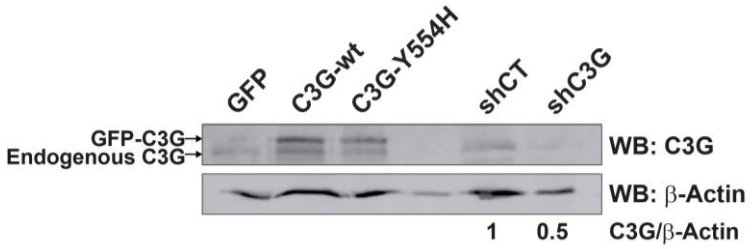


**Figure R-56. Analysis of the expression of C3G in PC12 transgenic cell lines.** Representative western blot showing C3G expression detected with anti-C3G F-4 antibody. β-Actin was used as loading control. The C3G/β-Actin ratio was shown. GFP, C3G-wt and C3G-Y554H were cell lines generated with lentiviral plasmid pLenti-C-mEGFP-IRES-BSD (Carabias *et al.*, 2020), whereas shCT and shC3G were generated with plasmid pLVTHM (Ortiz-Rivero *et al.*, 2018).

### 3.10.1. C3G controls NPY-secretion after KCl stimulation

First, we investigated in the C3G PC12 mutants, expressing tdOrange-NPY, whether C3G modulates the kinetics of dense-core vesicle exocytosis. For that, we analyzed by TIRFM the dynamics of single vesicle-PM fusion events, by monitoring the kinetics of the increase and decrease of the tdOrange signal, indicative of granule exocytosis.

Overexpression of wild type C3G resulted in a slightly lower AUC of tdOrange fluorescence, indicating faster secretion kinetics (**Figures R-57A-C**) (Video 2). In contrast, overexpression of C3G-Y554H mutant significantly slowed the kinetics of tdOrange-NPY release, manifested by increased AUC. On the other hand, C3G-silencing significantly increased the release rate of tdOrange-NPY (**Figures R-57D-F**) (Video 2).

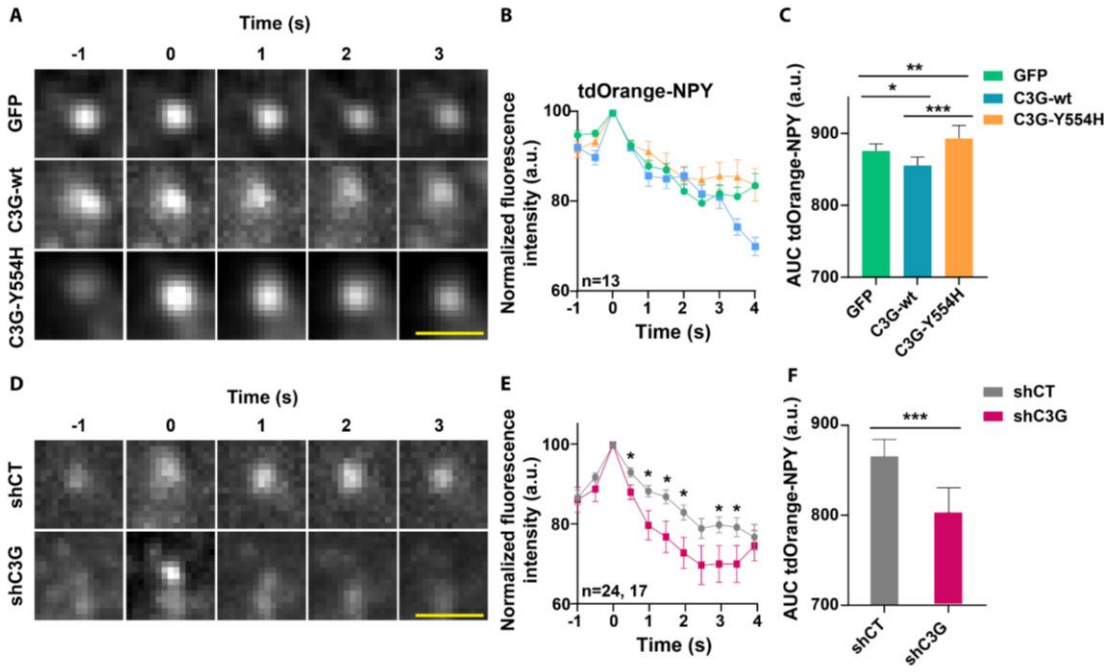


**Figure R-57. Effect of C3G hyperactivation or silencing on the kinetics of tdOrange-NPY release in PC12 cells. (A)** Representative sequential images of a single tdOrange-NPY vesicle observed after 70 mM KCl stimulation of control cells (GFP) cells expressing C3G-wt and cells expressing the active mutant C3G-Y554H, acquired at 300-ms intervals, through a TIRF microscope. **(B)** Line/scatter plot represents the mean ± SEM of the time course of the fluorescence intensity changes measured in tdOrange-NPY vesicles. The mean fluorescence intensity at the time of fusion (maximum intensity) was set to 100% (n= 13 vesicles in each experiment). **(C)** Histogram represents the mean ± SD of AUC (area under the curve) of the fluorescence intensity changes measured in the center of tdOrange-NPY vesicles. **(D)** Representative sequential images of a single tdOrange-NPY vesicle observed after 70 mM KCl stimulation of control cells (shCT) and C3G silencing cells (shC3G), acquired at 300-ms intervals, through a TIRF microscope. **(E)** Line/scatter plot represents the mean ± SEM of the time course of the fluorescence intensity changes measured in tdOrange-NPY vesicles. The mean fluorescence intensity at the time of fusion was set to 100% (n= 24 and 17 vesicles respectively). **(F)** Histogram represents the mean ± SD of AUC of the fluorescence intensity changes measured in the center of tdOrange-NPY vesicles. *p<0.05, **p<0.01, ***p<0.001. Scale bar: 1 µm. a.u.: arbitrary units; NPY: Neuropeptide Y.

Next, we analyzed the number of secretion events that occurs in our C3G mutant PC12 cells. As shown in Figure R-58, overexpression of C3G-Y554H mutant resulted in lower number of docked vesicles (Figures R-58A, B), but higher number of exocytic events (Figures R-58A, C), according to vesicles identified in Figure R-57. Overexpression of wild type C3G also induced a lower number of docked vesicles but did not result in changes in the number of exocytic events. Neither C3G-wt nor C3G-Y554H induced changes in granule area (Figure R-58D).

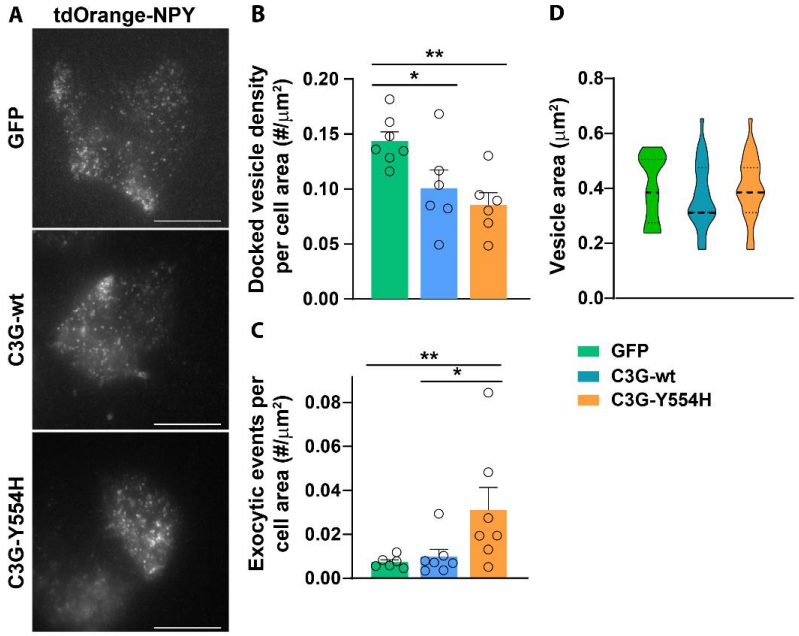


**Figure R-58. Effect of C3G-wt or C3G-Y554H overexpression in PC12 cells on the number and exocytosis of td-Orange-NPY docked granules. (A)** Representative images of tdOrange-NPY-electroporated GFP, C3G-wt and C3G-Y554H PC12 cells, acquired through a TIRF microscope. Scale bar: 20 µm. Histograms represents **(B)** the mean ± SD of the number of docked vesicles per cell, relativized to cell area and **(C)** the number of exocytic events per cell area, after KCl stimulation monitored for 1 min. **(D)** Violin plots represents the median and whiskers are the 25th and 75th percentiles of vesicle area (n=7). *p<0.05, **p<0.01. NPY: Neuropeptide Y.

In addition, shC3G cells displayed a significant higher number of docked vesicles, while presenting a lower number of exocytic events after KCl stimulation (Figures R-59A-C). Furthermore, shC3G cells had smaller granules, compared to shCT cells (Figure R-59D).

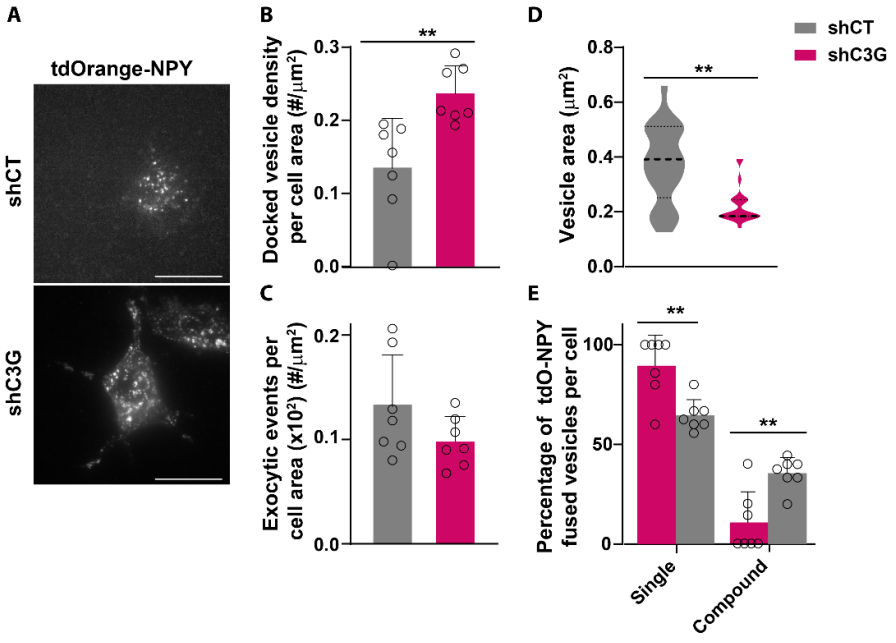


**Figure R-59. Effect of C3G silencing in PC12 cells on the number and exocytosis of td-Orange-NPY docked granules. (A)** Representative images of tdOrange-NPY-electroporated shCT and shC3G PC12

cells acquired through a TIRF microscope. Scale bar: 20 µm. Histogram represents the mean ± SD of **(B)** the number of docked vesicles per area or **(C)** the number of exocytic events per cell area after KCl stimulation, monitored for 1 min. **(D)** Violin plots represent the median and whiskers are the 25th and 75th percentiles of vesicle area (n=7 cells). **(E)** Histogram represents the mean ± SD of the percentage of tdOrange-NPY vesicles that displayed single or compound (granule fusion before fusion to the PM) exocytosis after KCl stimulation (n=7 cells). **p<0.01. tdO: tdOrange; PM: plasma membrane; NPY: Neuropeptide Y.

Based on previous data (Figures R-44 and R-53), showing that C3G absence in platelets would promote compound exocytosis, we studied granule fusion in our C3G mutant PC12 cells. As shown in Figure R-59E, shC3G cells showed a significant increase in the number of fused granules prior to their fusion with the PM (compound exocytosis). No significant granule fusion was observed in C3G-wt and C3G-Y554H PC12 cells (data not shown).

### 3.10.2.C3G controls the amount of protein released in PC12 cells

Based on the previous results, showing that C3G-KO platelets released a higher amount of protein compared to C3G-wt platelets (Figure R40), we sought to quantify secretion in C3G PC12 mutants. As shown in Figure R-60, overexpression of C3G-wt and C3G-Y554H mutant induced a increased protein, compared to the GFP control. Consistently, shC3G cells secreted a lower amount of protein that shCT cells.

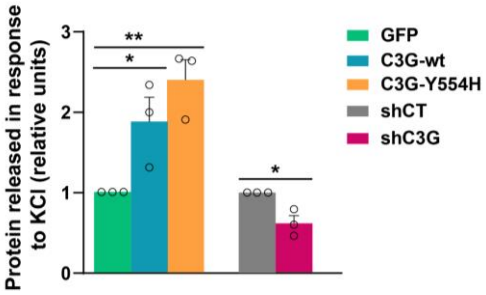


Figure R-60. **C3G modulates protein release after KCl stimulation.** Histogram represents the mean ± SEM of the relativized amount of protein released after stimulation with KCl at 37 ˚C for 1 h. The protein was quantified by the Bradford assay. *p<0.05, **p<0.01.

Overall, these data indicate that C3G regulates granule secretion in PC12 cells after KCl stimulation. C3G hyperactivation induced slower secretion but a greater number of exocytic events and increased protein release, whereas C3G silencing triggered the opposite phenotype, i.e., faster but less frequent secretion. In addition, C3G silencing promotes compound exocytosis. These data are consistent with those observed in platelets and confirm the role of C3G in the regulation of granule secretion.

## 4. Role of C3G in platelet-mediated inflammation

As mentioned in Introduction, platelets are regulators of the immune response, playing a crucial role in immune surveillance and inflammation during infection. On the one hand, platelet receptors can interact with pathogens, facilitating their clearance, or with immune cells, such as monocytes or NEs, triggering their activation. On the other hand, platelets secrete different factors, contained in α-granules, that modulates the immune response (Finsterbusch *et al.*,

2018). Based on the evidence that C3G regulates the secretion of different platelet factors, such as angiogenic factors (Martin-Granado *et al.*, 2017; Hernandez-Cano *et al.*, 2022) or coagulation factors (this work), we sought to examine whether C3G could also regulate the secretion of immune factors from platelets.

## 4.1. C3G regulates the secretion of inflammatory factors in response to thrombin

Platelets secrete a variety of factors, such as CXCL1 or CCL5 chemokines, which are involved in the recruitment of leukocytes. In addition, platelets secrete PF4 (also known as CXCL4), which reinforces NE adhesion to damaged endothelium, or CXCL7, which contributes to the revascularization of damaged endothelium (Durrant *et al.*, 2017).

We used the Proteome Profiler Mouse Angiogenesis Array Kit to detect the presence of inflammatory factors in the secretome of tgC3G, C3G-KO and their wild-type platelets. As shown in **Figure R-61**, C3G ablation triggered a higher secretion of PF4, IL-1α, CX3CL1, GM-CSF, CCL2 and CCL3 among others, whereas C3G overexpression showed the opposite phenotype, i.e., the retention of inflammatory factors.

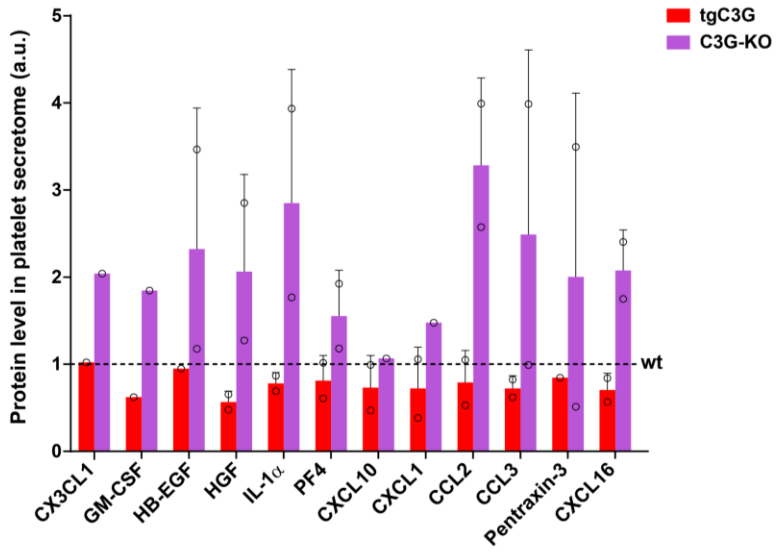


**Figure R-61. C3G regulates the secretion of platelet inflammatory factors after thrombin stimulation.** Histograms represents the quantification (mean ± SD) of CX3CL1, GM-CSF, HB-EGF, HGF, IL-1α, PFA, CXCL10, CXCL1, CCL2, CCL3, Pentraxin-3 and CXCL16 protein levels in thrombin-induced secretomes from tgC3G and C3G-KO platelets and their wild-type controls, using the Proteome Profiler Mouse Angiogenesis Array Kit (R&D systems). Data were normalized against the corresponding control values. a.u.: arbitrary units.

These data suggest that C3G could modulate platelet function in inflammation through its role in platelet secretion.

## 4.2. C3G controls platelet interaction with leukocytes

Platelets interact with leukocytes through different receptors, mainly P-selectin and CD40L. Since C3G regulates P-selectin exposure after thrombin stimulation, we studied, by flow cytometry, whether C3G could also regulate CD40L exposure on the platelet surface.

Consistent with the P-selectin results, C3G overexpression induced increased CD40L exposure in response to 1 U/ml thrombin, whereas C3G obliteration abrogated CD40L exposure after thrombin stimulation (Figure R-62).

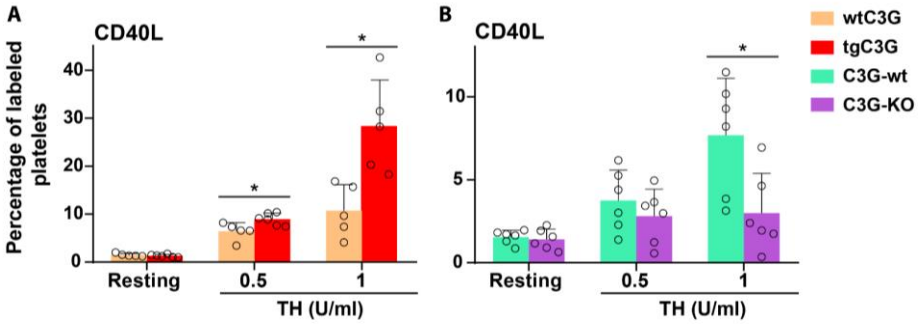


**Figure R-62. C3G regulates CD40L exposure on platelet surface in response to thrombin.** Washed blood from **(A)** wtC3G and tgC3G, **(B)** C3G-wt and C3G-KO mice was stimulated with 0.5 or 1 U/ml thrombin (TH) and incubated with anti-CD40L-PE and anti-CD41-FITC antibodies to analyze the percentage of platelets with CD40L on their surface by flow cytometry. Histograms represent the mean ± SD of the percentage of labeled platelets. *p<0.05.

The role of C3G in regulating CD40L and P-selectin exposure on the platelet surface suggests that C3G might modulate platelet-leukocyte interaction. So, next we analyzed the formation of PLAs using flow cytometry.

Results in Figure R-63A show that tgC3G platelets formed a greater number of PLAs under resting conditions and in response to thrombin (0.5 and 1 U/ml), consistent with the greater P-selectin and CD40L exposure on the platelet surface. In concordance, C3G-KO platelets were unable to form PLAs in response to thrombin (Figure R-63B).

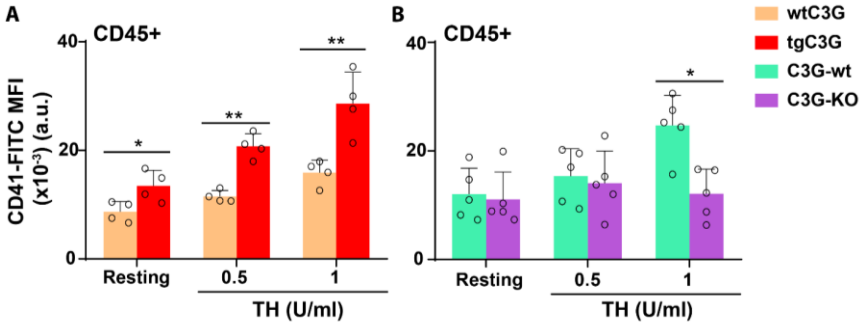


**Figure R-63. C3G regulates PLA formation in response to thrombin.** Lysed blood from **(A)** wtC3G and tgC3G, **(B)** C3G-wt and C3G-KO mice was stimulated with 0.5 or 1 U/ml thrombin (TH) and incubated with anti-CD41-FITC (platelet marker) and anti-CD45-PE/Cy5 (leukocyte marker) antibodies. Histograms represent the mean ± SD of CD41 MFI in the CD45-positive gate. *p<0.05, **p<0.01. a.u.: arbitrary units; MFI: mean fluorescence intensity.

To determine which membrane protein, P-selectin or CD40L, is involved in C3G-mediated PLA formation, we performed a similar assay, previously adding anti-P-selectin or anti-CD40L antibodies to block their corresponding ligands. Anti-P-selectin antibodies completely abolished the increased PLA formation observed in tgC3G platelets after 1 U/ml thrombin stimulation (Figure R-64A). In contrast, anti-CD40L antibodies did not affect PLA formation in our conditions. This result suggests that C3G would participate in PLA formation mainly through the regulation of P-selectin exposure in the platelet membrane.

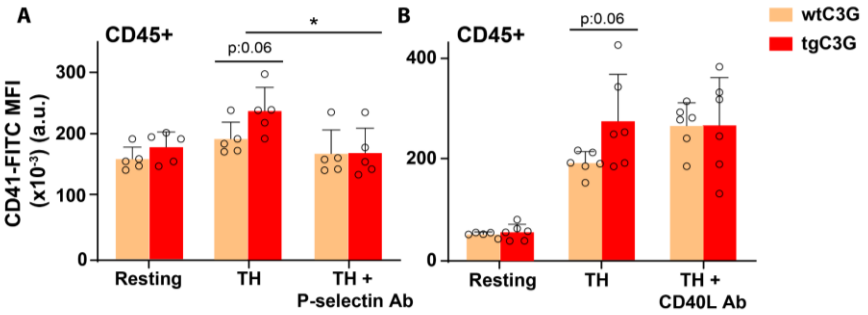


**Figure R-64. P-selectin is involved in C3G-mediated PLA formation.** Lysed blood from wtC3G and tgC3G mice was stimulated with 1 U/ml thrombin (TH) for 15 min, together with **(A)** anti-P-selectin-FITC or **(B)** anti-CD40L-PE antibodies. Then, samples were incubated with anti-CD41-FITC/APC (platelet marker) and anti-CD45-PE/Cy5 (leukocyte marker) antibodies and analyzed by flow cytometry. Histograms represent the mean ± SD of CD41 MFI in the CD45-positive gate. *p<0.05. Ab: antibody. a.u.: arbitrary units; MFI: mean fluorescence intensity.

To deepen this process, we studied what type of leukocytes were involved in the PLAs regulated by C3G. To do this, we performed a similar assay using CD45+Gr1+ as the NE marker, CD45+CD115+ as the monocyte marker and CD45+Cd11b- as the lymphocyte marker.

C3G overexpression in platelets resulted in a nearly significant increase in platelet-NE aggregates and a similar trend with lymphocytes (Figures R-65A, C left panel), while it did not affect PLA formation involving monocytes (Figure R-65B left panel). Consistently, C3G-KO platelets displayed the opposite phenotype; thus, C3G ablation resulted in a significant decrease in NE-platelet interaction in response to 1 U/ml thrombin (Figures R-65A, C right panels), and monocyte- and lymphocyte-platelet interactions showed a similar trend (Figures R-65B, C right panels).

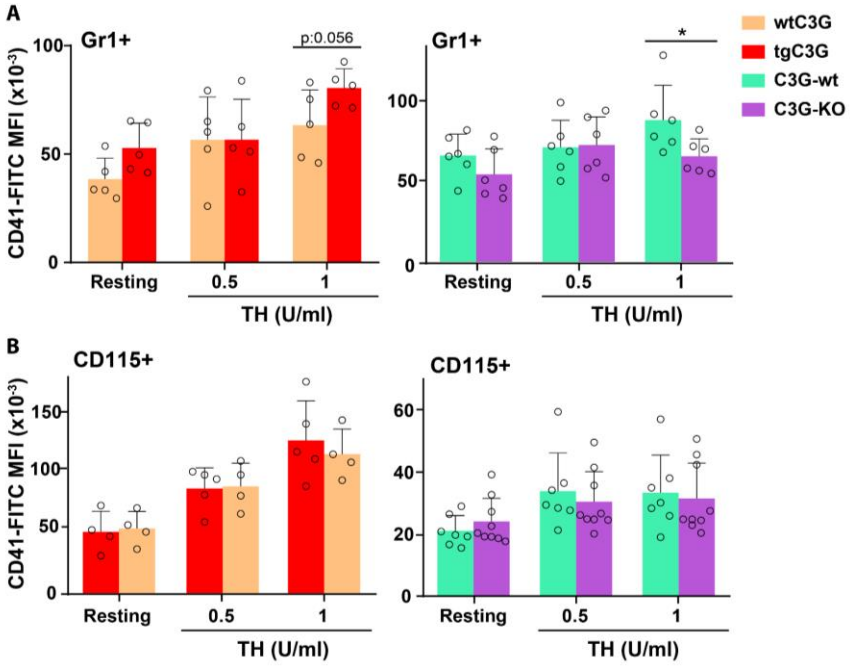

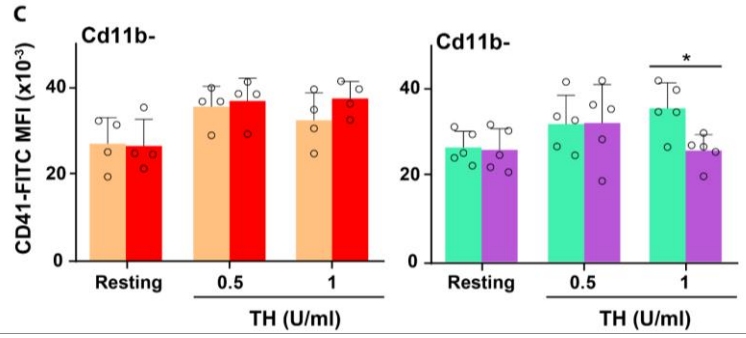


**Figure R-65. C3G regulates platelet interaction with NEs and lymphocytes in response to thrombin.** Lysed blood from wtC3G and tgC3G (left panels) and C3G-wt and C3G-KO (right panels) mice was stimulated with 0.5 or 1 U/ml thrombin (TH) and incubated with antibodies against **(A)** CD45-PE/Cy5 + Gr1-FITC to label NEs; **(B)** CD45-PE/Cy5 + CD115-PE to label monocytes; and **(C)** CD45-PE/Cy5 + Cd11b-AF647 to label lymphocytes, all combined with anti-CD41-FITC or anti-CD41-PE antibodies to label platelets. Histograms represent the mean ± SD of the relativized CD41 MFI values in the different gates, obtained by flow cytometry. *p<0.05, **p<0.01. a.u.: arbitrary units; MFI: mean fluorescence intensity.

To better understand the formation of PLAs involving lymphocytes, we separately studied the interaction between platelets and B and T lymphocytes. C3G ablation resulted in a decrease in B lymphocyte-platelet interaction, whereas it did not trigger any change in the formation of T lymphocyte-platelet aggregates (Figures R-66A, B right panels). Consistently, C3G overexpression induced a higher, although not significant, interaction of platelets with B lymphocytes but not with T lymphocytes (Figures R-66A, B left panels).

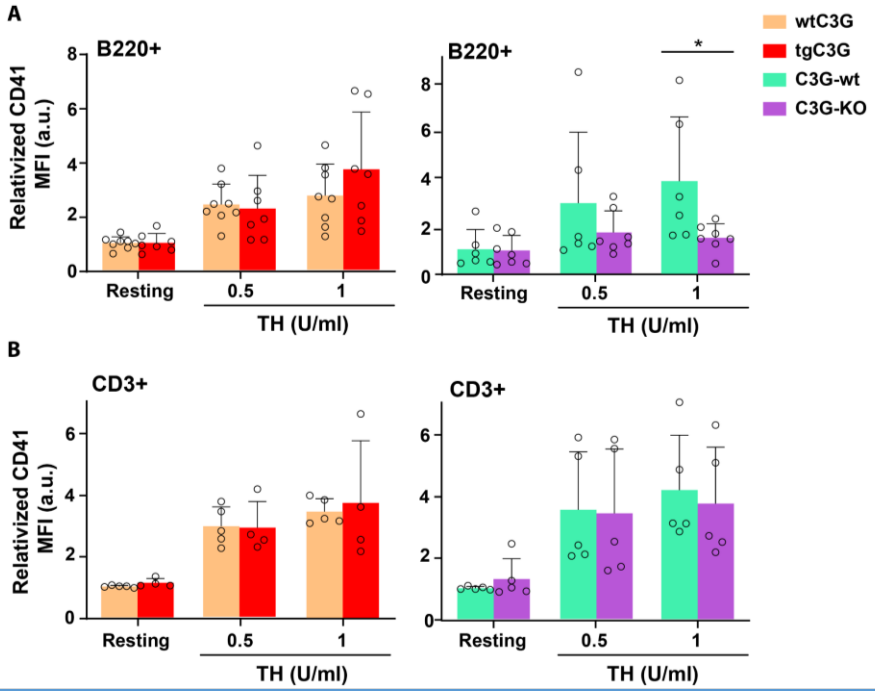


**Figure R-66. C3G regulates platelet interaction with B (but not T) lymphocytes in response to thrombin.** Lysed blood from wtC3G and tgC3G (left panel) and C3G-wt and C3G-KO (right panel) mice was stimulated with 0.5 or 1 U/ml thrombin (TH) and incubated with antibodies against **(A)** CD45-PE/B220-FITC to label B lymphocytes; **(B)** CD45-PE/CD3-APC to label T lymphocytes, all combined with anti-CD41-FITC or anti-CD41-PE antibodies to label platelets. Histograms represent the mean ± SD of the relativized CD41 MFI values in the different gates, obtained by flow cytometry. *p<0.05. a.u.: arbitrary units; MFI: mean fluorescence intensity.

These *in vitro* data suggest that C3G might regulate platelet-mediated inflammation through modulation of platelet secretion and P-selectin/CD40L exposure on the surface, resulting in changes in NE-platelet and B lymphocyte-platelet interactions.

## 4.3. C3G regulates platelet-induced NET formation

Platelets play a crucial role in NE activation, resulting in the formation of NETs. NET release is the last response of activated NEs; NETs consist of DNA decorated with histones and granules and their function is to neutralize pathogens. NET formation is a regulated multi-step process involving chromatin condensation, permeabilization of nuclear envelope and PM, and release of DNA and protein from granules (Filep, 2022). Since C3G modulates platelet-NE interaction, we wanted to study whether platelet C3G could modulate the ability of NEs to form NETs.

First, we analyzed the percentage of NEs undergoing NETosis after platelet activation with thrombin. To address it, we used SYTOX Green, a dye with affinity for extracellular DNA. Flow cytometry assays showed that C3G overexpression in platelets induced increased NET formation, both at rest and under thrombin stimulation, whereas the absence of C3G resulted in decreased NETosis, in response to 1 U/ml thrombin (Figure R-67).

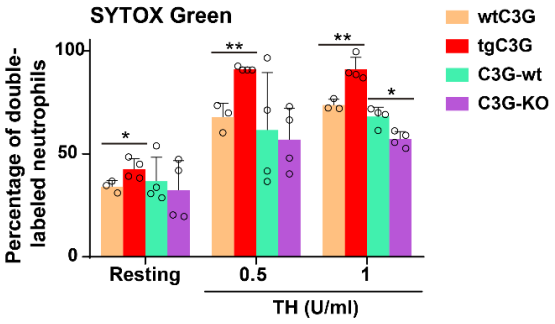


**Figure R-67. Platelet C3G regulates NETosis upon thrombin stimulation.** Washed blood from wtC3G, tgC3G, C3G-wt and C3G-KO mice was stimulated with 0.5 or 1 U/ml thrombin (TH) and incubated with anti-Gr1-FITC antibodies (NE marker) and SYTOX-Green (cell-impermeable DNA marker) to analyze, by flow cytometry, the percentage of SYTOX Green-labeled NEs in the Gr1-positive gate. Histogram represents the mean ± SD of the percentage of double labeled NEs. *p<0.05, **p<0.01. NE: neutrophil.

To gain insight into this process, and since the role of platelets in inflammation is mediated by platelet secretion and receptor exposure, we sought to investigate which of these events were behind the role of platelet C3G in NETosis. Isolated naive NEs were incubated with resting platelets, thrombin-activated platelets or thrombin-induced secretomes and the increase in SYTOX Green fluorescence was recorded over time using a plate reader.

Consistent with the above flow cytometry results, both resting and thrombin activated tgC3G platelets induced a greater increase of fluorescence than wtC3G platelets (Figures R-68A, B left panel). However, thrombin-induced secretomes from tgC3G platelets caused less NET formation than those from wtC3G platelets, suggesting that C3G overexpression induced secretome is not involved in NETosis or may even play a negative role (Figure R-68C left panel). This latter hypothesis is consistent with the lower levels of inflammatory factors detected in tgC3G platelet secretomes (Figure R-61).

As expected, C3G-KO platelets induced the opposite trend, i.e., less NET formation at rest and after thrombin stimulation, while their thrombin-induced secretome produced a subtle increase in NET formation (Figure R-68 right panel), in agreement with the highest levels of inflammatory factors found in C3G-KO secretomes (Figure R-61).

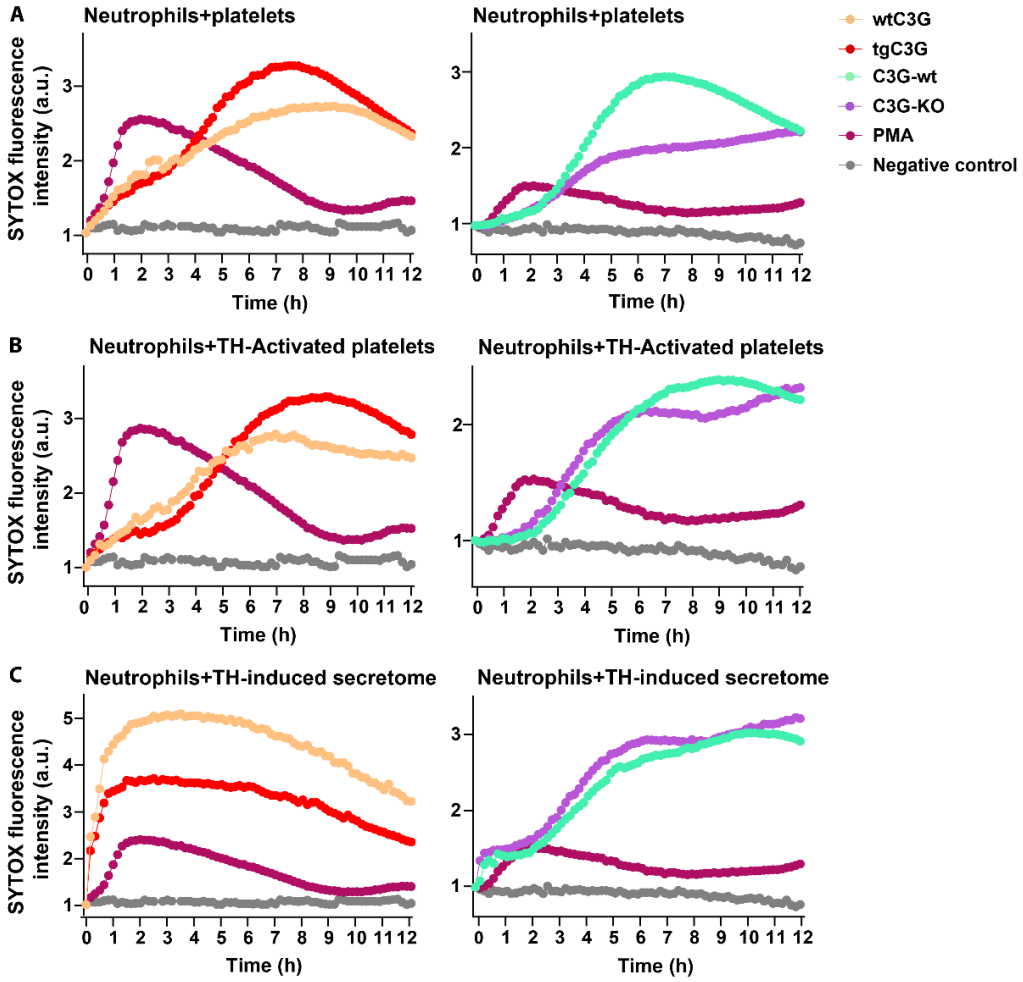


Figure R-68. **Platelet C3G regulates NETosis upon thrombin stimulation**. Wild-type isolated NEs were incubated with either **(A)** resting platelets, **(B)** TH-activated platelets or **(C)** TH-induced secretomes of wtC3G and tgC3G mice (left panels) or C3G-wt and C3G-KO mice (right panels). The mixture was incubated with 5 µM SYTOX Green and the fluorescence intensity was read every 10 min for 12 h at 37 °C in a plate reader. As a positive control, NEs were stimulated with 300 nM PMA, while as a negative control we used naive NEs. TH: Thrombin; NE: neutrophils.

To validate these results, we analyzed NET formation by a different approach; we co-cultured wild-type naive NEs with resting or thrombin-activated tgC3G or wtC3G platelets for 2 h at 37 °C. Then, cells were fixed and stained with Hoechst and anti-NE elastase antibodies. Three different categories of NEs (described in M&M) were monitored by immunofluorescence, according to DNA and elastase distribution (Figure R-69A). TgC3G platelets induced a higher number of NEs undergoing NETosis than wtC3G platelets (Figure R-69B), consistent with the results in Figure R-68.

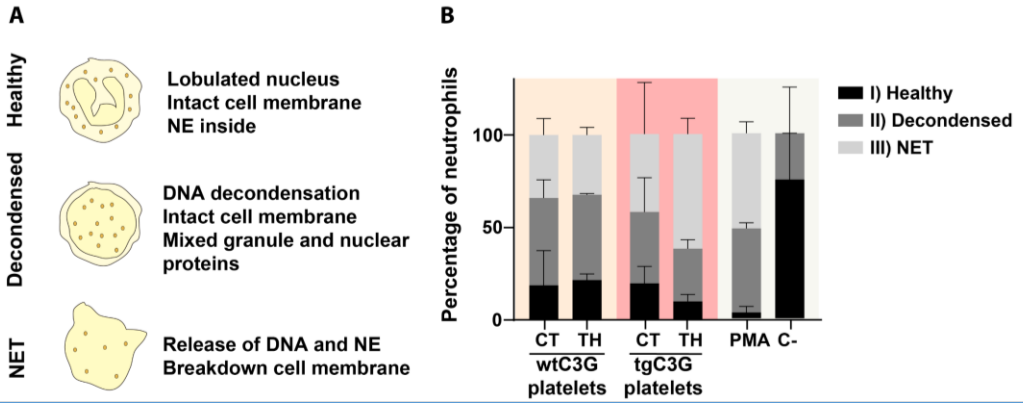


**Figure R-69. Platelet C3G regulates NETosis upon thrombin stimulation. (A)** Schematic representation of the three different categories or NEs established: I) Healthy NEs; II) Decondensed DNA NEs; III) NE starting NETosis. **(B)** Wild-type isolated NEs were incubated with resting platelets (CT) or TH-activated platelets of tgC3G and wtC3G mice for 2 h at 37 °C. Then, they were fixed and stained with Hoechst 33342 and an anti-NE elastase antibody. Histogram represents the mean ± SD of the percentage of NE in each step. NEs were incubated with 100 nM PMA as positive control. C-: naive NEs; TH: thrombin; NE: neutrophil.

Overall, these data revealed a new function of platelet C3G in modulating NET formation *in vitro.* Since NETs are present in thrombi, providing a scaffold for platelet activation and coagulation (Stark, 2019), these results are consistent with the role of C3G in thrombin-induced platelet coagulation (Figure R-5, (Gutierrez-Herrero *et al.*, 2012; Gutierrez-Herrero *et al.*, 2020)).

## 4.4. C3G obliteration leads to progression of DSS-induced colitis

Inflammatory bowel disease (IBD) is a chronic disorder that groups two main subtypes: ulcerative colitis and Crohn's disease. IBD patients report abdominal pain, bloody diarrhea and weight loss. IBD is associated with a hypercoagulable state and increased thrombosis, suggesting that platelets play a crucial role in IBD (Petrey *et al.*, 2019). Additionally, NEs play an essential role in the maintenance of intestinal homeostasis during inflammation, contributing to the recruitment to other immune cells and the release of mediators for the resolution of the inflammatory process (Fournier & Parkos, 2012).

Based on that, and our previous results demonstrating a role for C3G in the secretion of inflammatory factors and in PLA formation, we wanted to know if platelet C3G could regulate IBD *in vivo*. For that, we used the DSS model, which mimics a colitis disease.

Contrary to expectations, we observed that the absence of C3G in platelets triggered an increase in weight loss, indicative of an advance in the onset of DSS–induced ulcerative colitis symptoms. Mice experienced weight gain during the first days of DSS-treatment, as described in the literature (Chassaing *et al.*, 2014), with a maximum at day 4 after induction. However, C3G-KO mice suffered a subtle decrease in weight initially, followed by a slight increase at day 4, although much less than in the wild-type mice (Figure R-70). At the end of experiment (day 7), C3G-KO mice presented a significantly lower weight compared to C3G-wt mice.

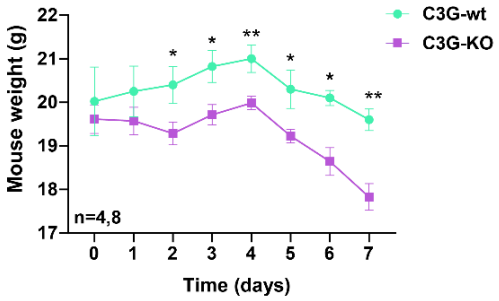


**Figure R-70. C3G ablation in platelets accelerates DSS-induced weight loss in mice.** C3G-wt and C3G-KO mice were treated with DSS for 7 days and mouse weight loss was monitored daily. n= 4 (C3G-wt), n= 8 (C3G-KO). *p<0.05, **p<0.01.

Since DSS treatment induces diarrhea and blood in stools, we examined at the end of the experiment whether the marked weight loss in C3G-KO mice could be due to these symptoms. C3G-KO mice presented bloody stools accompanied by diarrhea, whereas C3G-wt mice only showed loose stools (Table R-1).

**Table R-1. Description of symptoms of mice treated with DSS for 7 days, indicating their identification tag and genotype.**

| Mice | Genotype | Symptoms |
|---|---|---|
| L666 | C3G-wt | Loose stools |
| L669 | C3G-wt | Loose stools |
| L667 | C3G-KO | Blood presence and loose stools |
| L668 | C3G-KO | Blood presence and liquid stools |
| L670 | C3G-KO | Blood presence and liquid stools |
| L671 | C3G-KO | Blood presence and loose stools |

DSS treatment results in splenomegaly and decreased colon length, due to increased colonic epithelial permeability (Chassaing *et al.*, 2014). We examined colon length and spleen weight, and found no differences between genotypes. However, we detected a significant increase in the number of bacterial colonies in spleen extracts from C3G-KO mice compared to C3G-wt mice after DSS treatment (Figure R-71).

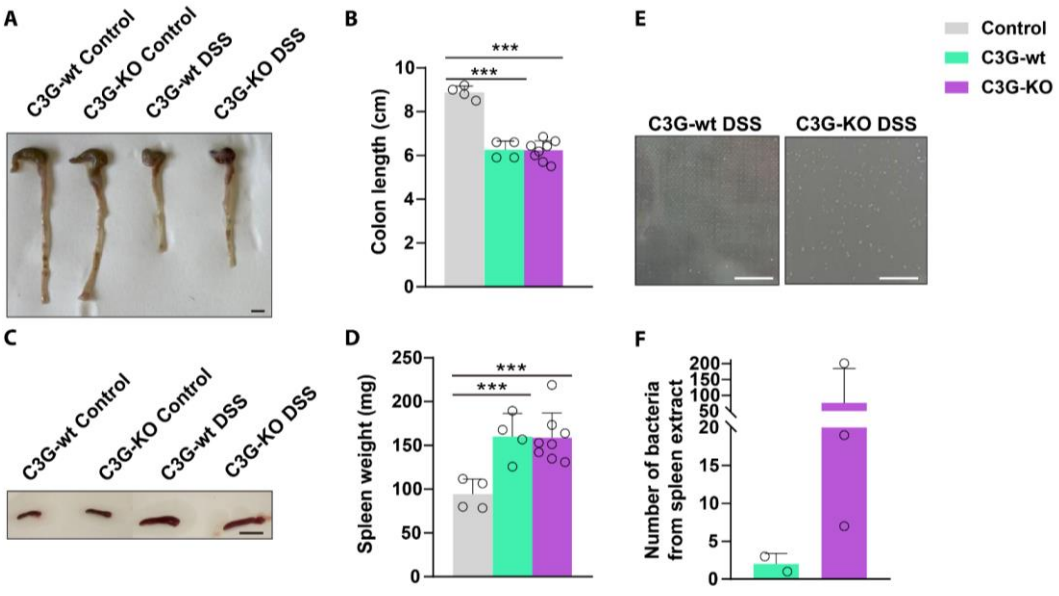

**Figure R-71. C3G-KO mice present increased bacteria dissemination after DSS-induced colitis, but C3G knockout does not affect colon length or spleen size. (A)** Representative images of colon of control mice and DSS-treated C3G-wt and C3G-KO mice for 7 days. Scale bar: 0.5 cm **(B)** Histogram represents the mean ± SD of colon length. **(C)** Representative images of spleens from control and DSS-treated mice. Scale bar: 0.25 cm. **(D)** Histogram represents the mean ± SD of the spleen weights. **(E)** Representative images of bacterial colonies in spleen extracts from DSS-treated C3G-wt and C3G-KO mice. Scale bar: 1 cm. **(F)** Histogram shows the quantification of the number of bacterial colonies in spleen extracts from mice treated with DSS for 7 days, cultured in a non-selective agar plates for 48 h at 37 °C. ***p<0.001.

Since C3G modulates PLA formation *in vitro*, we studied PLA formation at 0, 4 and 7 days of DSS treatment. Flow cytometry assays showed a significant decrease in the formation of circulating platelet-NE aggregates at day 4 in C3G-KO mice compared to C3G-wt mice. However, at day 7, C3G-KO mice presented a higher number of aggregates (Figure R-72A). This result correlates with the weight changes observed in C3G-KO mice at days 4 and 7. In contrast, there were not differences in platelet-monocyte or platelet-lymphocyte aggregates (Figures R-72B-D).

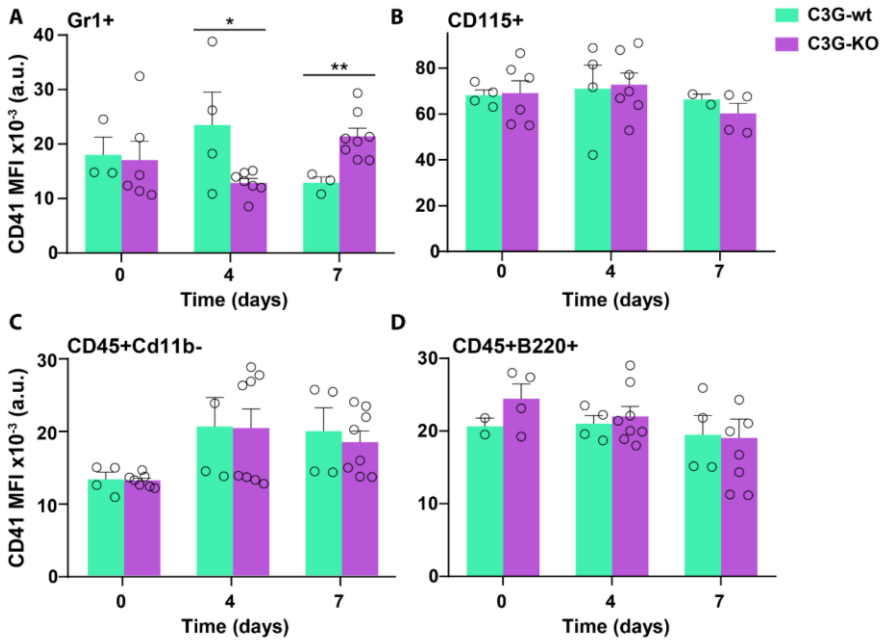


**Figure R-72. Platelet C3G regulates platelet-NE interactions during DSS treatment.** Lysed blood from DSS-treated C3G-KO and C3G-wt mice was stained with antibodies against **(A)** CD45-PE/Cy5 + Gr1-FITC to label NEs, **(B)** CD45-PE/Cy5 + CD115-PE to label monocytes, **(C)** CD45-PE/Cy5 + CD11b-AF 647 to label lymphocytes, **(D)** CD45-PE/Cy5 + B220-FITC to label B lymphocytes; all combined with anti-CD41-FITC o CD41-PE antibodies to label platelets. Histograms represent the mean ± SD of the MFI of CD41 in the different gates, measured by flow cytometry. *p<0.05, **p<0.01. a.u.: arbitrary units; MFI: mean fluorescence intensity.

Additionally, C3G-KO mice treated with DSS showed a marked time-dependent increase in NEs, but not in monocytes, in blood (Figures R-73A-C), reinforcing the above results. However, there were not differences in platelet count between genotypes. In addition, we did not find differences between genotypes in the recruitment of inflammatory cells in the colon, monitored by flow cytometry (Figure R-73D). Further studies are needed to determine if there is more PLA formation or NET formation in this tissue.

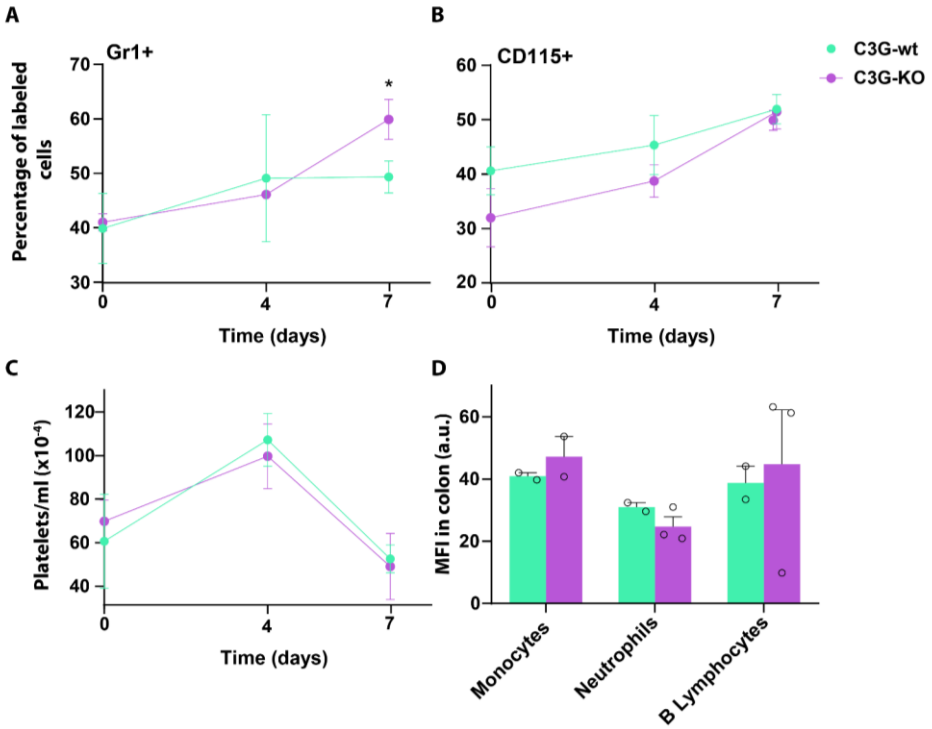


**Figure R-73. DSS-treated C3G-KO mice present an increase in NEs in peripheral blood, but not in colon, without differences in the number of lymphocytes or platelets.** Lysed blood from DSS-treated C3G-KO and C3G-wt mice was stained with antibodies against **(A)** CD45-PE/Cy5 + Gr1-FITC to label NEs, **(B)** CD45-PE/Cy5 + CD115-PE to label monocytes, and the percentage of labeled cells was analyzed by flow cytometry. **(C)** Washed blood, extracted at 0, 4 and 7 days of DSS treatment, was stained with anti-CD41-PE antibodies and the number of platelets/ml was monitored by flow cytometry. **(D)** Immune cell infiltration was monitored by studying Gr1-, CD115- and B220+ MFI in colon extracts by flow cytometry. Histograms represent the mean ± SD of the MFIs. *p<0.05. a.u.: arbitrary units; MFI: mean fluorescence intensity.

Finally, we studied by qPCR the expression of some inflammatory chemokines in the colon of DSS-treated mice (day 7). C3G-KO mice presented increased colonic expression of *Cxcl1,* a NE chemoattractant (Gleissner *et al.*, 2008). Additionally, C3G-KO mice showed a marked increase in the mRNA expression of some pro-inflammatory chemokines, such as *Tgf*β*, il1*β and *il6* (Figure R-74A). However, we observed a marked reduction in the expression of *Pf4 and Tnfα*. Consistently, we observed the opposite tendency in platelets from DSS-treated mice. Thus, C3G-KO platelets presented an increased in *Pf4* and *Tnfα* expression and a decrease in the expression of *il6* (Figure R-74B). One possible explanation is that platelets selectively capture or secrete these factors during the inflammatory response.

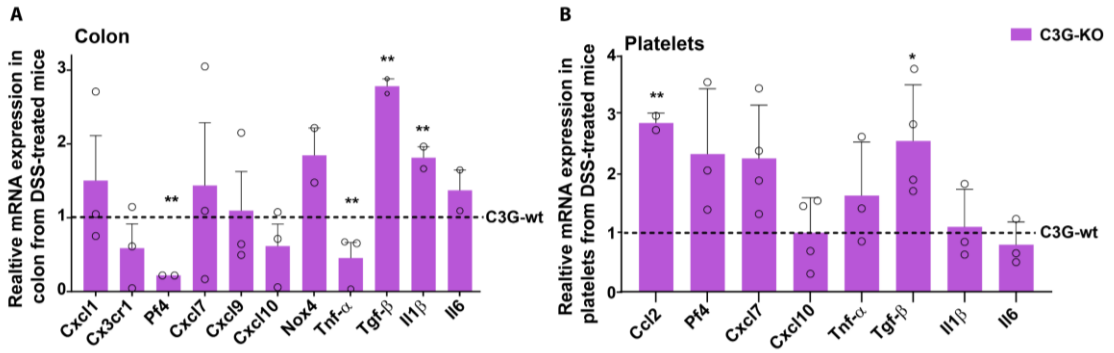


**Figure R-74. Platelet C3G regulates chemokine expression in the colon and in platelets after DSS treatment**. **(A)** RT-qPCR analysis of the indicated inflammatory chemokines in mRNA from colon extracts of C3G-KO and C3G-wt mice treated with DSS for 7 days. **(B)** A similar analysis was performed in mRNA from platelets of the same DSS-treated animals. β-*actin* was used as housekeeping gene. Values were relativized to those in wild-type samples. *p<0.05, **p<0.01.

Although further studies must be performed to fully characterize the precise role of platelet C3G in the progression of DSS-induced colitis, these results are the first evidence implicating platelet C3G as a mediator of PLA formation and NE recruitment during IBD.

# DISCUSSION

In the present work, we have provided new insights into the involvement of C3G in platelet function. These include additional data on its role in platelet hemostatic function, with important contributions to its role in spreading and granule secretion, as well as new data on its implication in platelet-mediated inflammatory response. For this purpose, we have used different approaches: i) three different C3G mouse models, ii) the pheochromocytoma PC12 cell line, where we have generated different C3G mutants to unveil the role of C3G in exocytosis, and iii) an *in vivo* mouse model of DSS-induced colitis, which has revealed a role for platelet C3G in IBD.

## 1. C3G is essential for platelet hemostasis

Rap1 GTPases are the main regulators of platelet function in response to different agonists, such as thrombin, ADP or collagen. Indeed, Rap1 modulates the inside-out response through the control of integrin αIIbβ3 activation, responsible for platelet aggregation, and the exposure of P-selectin (Shattil *et al.*, 1998; Chrzanowska-Wodnicka *et al.*, 2005; Zhang *et al.*, 2011). In platelets, Rap1 activation, induced by thrombin, is regulated by CalDAG-GEFI and PKC in two different phases: i) a first wave mediated by CalDAG-GEFI, which involves $Ca^{2+}$; ii) a second wave modulated by PKC in a $Ca^{2+}$-independent manner (Franke *et al.*, 2000). Crittenden, and co-workers, showed that CalDAG-GEFI knockout platelets display normal platelet activation and aggregation in response to PMA or high/long-term doses of thrombin, thus, confirming the existence of these two sequential pathways (Crittenden *et al.*, 2004).

In this line, previous results from the group demonstrated that C3G overexpression in platelets induces greater platelet activation and aggregation and that this function depends on its GEF activity (Gutierrez-Herrero *et al.*, 2012). Furthermore, C3G regulates platelet function through its involvement in the PKC-Rap1 pathway (Gutierrez-Herrero *et al.*, 2012). In addition, the absence of C3G in platelets causes increased bleeding diathesis and decreased thrombus formation in mice (Gutierrez-Herrero *et al.*, 2020). Furthermore, our group demonstrated that C3G also plays a role in megakaryopoiesis, especially in pathological situations (Ortiz-Rivero *et al.*, 2018; Hernandez-Cano *et al.*, 2022).

The role of C3G in primary hemostasis, regulating inside-out signaling, was confirmed by the studies on C3G-KO platelets. C3G-KO platelets showed defects in integrin αIIbβ3 activation and P-selectin exposure downstream of many agonists, such as thrombin, CRP, PMA and ADP. These defects were accompanied by impaired aggregation and thrombus formation. The participation of C3G in the PKC-dependent second wave of Rap1 activation was further supported by results showing that C3G-KO platelets displayed defective Rap1 activation in response to high-dose thrombin or CRP, or under prolonged stimulation, as well as in response to PMA, a direct PKC activator. In addition, PKC proteins regulate C3G phosphorylation in platelets (Gutierrez-Herrero *et al.*, 2020). Thus, these results confirmed that C3G is the GEF implicated in the activation of Rap1 through the PKC pathway.

PKC proteins play a crucial role in platelet function; however, the role of each isoform is not fully understood. Since the PKC-C3G-Rap1 pathway acts in a calcium-independent manner, we hypothesized that C3G might be regulated by nPKCs. Indeed, inhibition of PKCδ completely abolished the differences exhibited by tgC3G and C3G-KO platelets, relative to their wild-types,

both in integrin αIIbβ3 activation and P-selectin exposure. This strongly suggests that the role of C3G in primary hemostasis is mediated by nPKCs, mainly PKCδ.

Regarding the participation of C3G in platelet maturation, the quantification of the RNA content demonstrated that C3G has no impact on this process. This is consistent with our previous observation that neither overexpression nor absence of C3G affects platelet number under basal conditions (Ortiz-Rivero *et al.*, 2018; Hernandez-Cano *et al.*, 2022).

In addition to its role in primary hemostasis, in this work we present the first evidence for the involvement of C3G in the regulation of secondary hemostasis.

Platelets play a crucial role in secondary hemostasis by providing a surface for the activation of coagulation complexes (regulated by the exposure of procoagulant phospholipids, such as PS), and by serving as a reservoir of coagulation factors (Golebiewska & Poole, 2015). Interestingly, C3G-KO platelets showed a significant decrease in PS translocation at low CRP concentrations. However, they exhibited greater PS translocation than control platelets in response to a medium concentration of CRP, suggesting that alternative mechanisms (e.g., activation of CalDAG-GEFI) could compensate for the C3G-KO platelet defect. Unexpectedly, C3G overexpression did not induce changes in PS exposure, suggesting that low C3G levels are necessary but sufficient to induce PS translocation.

Previous results from the group demonstrated that C3G modulates the platelet secretome (Martin-Granado *et al.*, 2017). Consistently, we observed a greater release of coagulation factors in the absence of C3G, while C3G overexpression caused their retention. In fact, the secretome from thrombin-stimulated C3G-KO platelets contained an increased amount of thrombin, whereas C3G overexpression in platelets led to a secretome with lower levels of thrombin. In contrast, C3G absence resulted in a lower amount of thrombin in the PRP, which is in agreement with the defective PS translocation found in C3G-KO platelets. However, this defective thrombin formation in C3G-KO platelets was observed only after TF stimulation, but not in response to phospholipids or the combination of both, suggesting that the deficiency in PS translocation could be compensated by the procoagulant secretome of these platelets. In this line, it has been described that cPKC activation induces suppression of platelet procoagulant activity (Strehl *et al.*, 2007); however, we did not observe this effect in our tgC3G platelets, supporting the hypothesis that nPKC, and not cPKC, are the regulators of C3G activity.

Overall, our findings, together with previous results, reinforce the notion of an essential role of C3G in platelet function, despite its modest expression in platelets, contributing to the maintenance of adequate hemostasis in parallel to the CalDAG-GEFI pathway. C3G overexpression would lead to an aggregatory phenotype, characterized by more active platelets. In contrast, C3G absence would trigger a secretory phenotype accompanied by defective platelet aggregation and activation.

## 2. C3G plays a role in spreading through the regulation of actin cytoskeleton dynamics

Previous findings of our group demonstrated the participation of C3G in platelet spreading independently of its GEF activity. Specifically, both C3G and C3GΔCat overexpression induce a

greater spread area on poly-L-lysine, compared to their respective controls (Martin-Granado *et al.*, 2017).

Consistently, in this work, we have shown that C3G-KO platelets exhibited impaired spreading on poly-L-lysine, further supporting a role for C3G in platelet spreading. Furthermore, the role of C3G in spreading depends on the substrate; specifically, C3G promoted platelet spreading on poly-L-lysine, collagen/CRP, fibronectin and vitronectin, but not on fibrinogen or laminin, with less clear results in relation to osteopontin. Thus, both tgC3G and tgC3GΔCat platelets presented lower spread area on osteopontin, whereas C3G-KO platelets spread normally. Moreover, the different behavior of tgC3G and tgC3GΔCat platelets when spread on vitronectin, and the negligible effect of tgC3GΔCat on spreading on fibronectin suggests a putative involvement of Rap1 in this C3G function in some contexts. Additionally, the observed differences only apply to the spread area but not to the platelet perimeter or circularity. Contrary to expectations, platelet perimeter does not have to be affected by membrane incorporation during spreading. In fact, a greater perimeter does not imply a greater spread area, since the intermediate state with filopodia could present the same, or greater, perimeter than a fully spread platelet (Mori *et al.*, 2012; Schurr *et al.*, 2019) (**Figure D-1**).

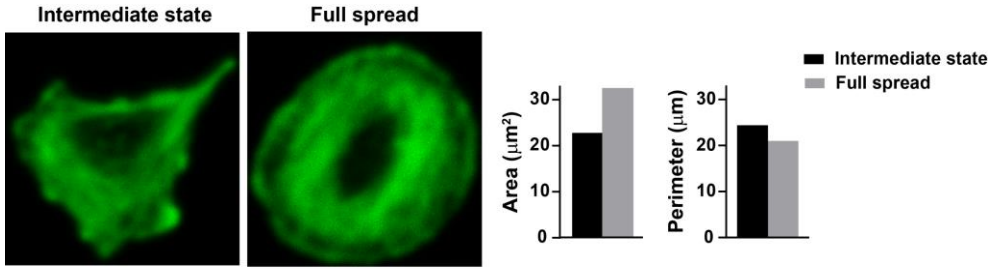


**Figure D-1. Representation and quantification of the area and perimeter of different spreading stages.** On the left is a platelet in a state of intermediate spreading, showing filopodia. A fully spread platelet with lamellipodia is shown on the right. Histograms represent the area (μm$^2$) and perimeter (μm) of both platelets.

The fact that this role of C3G was substrate-dependent suggested that C3G would be involved downstream of only specific receptors. This phenotype has been previously described in the literature. For example, PKCθ only regulates platelet spreading on fibrinogen but not on collagen/CRP (Hall *et al.*, 2008), suggesting that other PKC isoforms are involved in spreading on collagen, and therefore, may be involved in C3G actions. In addition, Tspan18 (a regulator of thromboinflammation) knockout platelets show defective spreading on collagen but not on fibrinogen (Gavin *et al.*, 2020). A plausible explanation was that C3G might regulate the functionality, or expression, of major integrins involved in outside-in signaling. In fact, C3G-KO platelets displayed decreased expression of integrins αV and β1, which could partially explain the observed phenotype. Specifically, this could explain the effect of C3G on spreading on fibronectin, since αVβ1 is one of the fibronectin receptors in platelets (Bennett *et al.*, 2009). However, there were no differences in the levels of the main receptors on the platelet surface. Although more studies should be conducted to clarify this point, one possible explanation is that spreading on certain substrates would depend on the activation of the integrin αIIbβ3.

In this study, we have unveiled that C3G is associated with the formation of lamellipodia, but not filopodia. This is in contrast to results from other cellular models, such as HeLa cells, in which

C3G is essential for filopodia formation (Radha *et al.*, 2007). As discussed above, C3G is downstream of PKC in the modulation of primary hemostasis. In fact, PKC also modulates C3G role in spreading, since PKC inhibition with BIS abolished the differences observed between tgC3G and C3G-KO platelets and their respective wild-types. Of note, the absence of PKCδ induces a phenotype similar to that observed in C3G-KO platelets, an intermediate state with only filopodia and not with lamellipodia (Pula *et al.*, 2006), further supporting the involvement of this novel PKC isoform in C3G actions in platelets.

Src proteins are involved in the response to most platelet agonists (Senis *et al.*, 2014) and are essential to regulate C3G activation in platelets (Gutierrez-Herrero *et al.*, 2020) and other cell types (Radha *et al.*, 2004; Rodriguez-Blazquez *et al.*, 2023). Moreover, during platelet spreading, Src kinases regulate the generation of F-actin fibers and control the recruitment of cytoskeletal regulatory proteins, such as WASP, Arp2/3 complex, Rac1, talin or vinculin (De Kock & Freson, 2020). Additionally, Src plays a crucial role in α2β1-mediated spreading. PP2, an inhibitor of Src, completely abolished the observed differences in platelet spreading between tgC3G and C3G-KO platelets and their respective controls, indicating that Src mediates the role of C3G in platelet spreading. Notably, PP2 did not completely inhibit spreading in control platelets, indicating that tgC3G platelets would exhibit increased sensitive to PP2, as previously described for other inhibitors (Gutierrez-Herrero *et al.*, 2020). In this line, alternative pathways that regulate spreading in the absence of Src have been described (Inoue *et al.*, 2003).

On the other hand, we have observed that C3G modulates the actin cytoskeleton but not the microtubules. In fact, C3G controlled actin polymerization, both in suspension and during spreading, in a GEF-independent manner. Overexpression of C3G and C3GΔCat triggered increased formation of actin filaments, whereas C3G absence induced a defect in actin polymerization. Consistently, the observed defects in actin polymerization were detected in the same substrates in which C3G induced alterations in spreading.

The fact that C3G-KO platelets were not affected by latrunculin treatment and, only by cytochalasin D, suggests that the mechanism by which C3G would regulate actin turnover is related to the mechanism of action of latrunculin. In fact, latrunculin reversed the defective F-actin formation of C3G-KO platelets. Latrunculin sequesters the actin monomers, while cytochalasin D binds to the F-actin ends (Shoji *et al.*, 2012; Fujiwara *et al.*, 2018). Therefore, it is reasonable to speculate that C3G might modulate actin polymerization through its interaction with actin monomers. This is supported by the interaction detected between C3G and β-actin in this work and in previous works (Martin-Encabo *et al.*, 2007; Sasi Kumar *et al.*, 2015).

In agreement with the observed role of C3G in lamellipodia formation, C3G modulated the activation of Rac1, the main GTPase involved in this process (McCarty *et al.*, 2005). Indeed, C3G overexpression led to increased Rac1 activation under high-dose thrombin, whereas C3G-KO platelet exhibited the opposite phenotype. Interestingly, and in concordance with the spreading results, tgC3GΔCat platelets also showed elevated Rac1-GTP levels. All these results support the idea that C3G would modulate actin turnover in a Rap1-independent manner. Rap1 also regulates Rac1 in platelets (Stefanini *et al.*, 2012), hence, this result points to a complex regulatory mechanism of Rac1 activation, highlighting the importance of cytoskeletal dynamics in platelet biology.

Rac1 controls lamellipodia formation via WAVE/Arp2/3 (McCarty *et al.*, 2005). Consistently, C3G facilitated the interaction between Arp2 and WAVE2, probably through its participation in the Arp2/3-WAVE2 complexes. In addition to its interaction with WAVE2, Arp2 and Arp3, C3G also associated with Abi1, in resting and thrombin-stimulated platelets. Abi1 is a positive regulator of fibronectin adhesion (Li *et al.*, 2007), and its interaction with C3G has been previously demonstrated in CML cells (Maia *et al.*, 2013). Moreover, the interaction between Arp2 and β-actin was also detected in tgC3GΔCat platelets, further supporting that the role of C3G in actin cytoskeleton remodeling is independent of its GEF activity. The involvement of Rac1 and Arp2 in the role of C3G in spreading was confirmed by results showing that inhibition of Rac1 or Arp2 abolished the differences between tgC3G and C3G-KO platelets and their controls in platelet spreading. Additionally, VASP protein, which is the main regulator of actin filament elongation, and is commonly associated with filopodia formation, also participates in lamellipodia formation (Rottner *et al.*, 1999; Damiano-Guercio *et al.*, 2020). Thus, the interaction of C3G with VASP further supports a role for C3G in lamellipodia formation.

It is reasonable to speculate that C3G could modulate Rac1 activity through its interaction with proteins harboring SH3 domains, such as c-Cbl, whose role in spreading through the CrkL-C3G-Rap1-Rac1 pathway has been described in fibroblasts (Lee *et al.*, 2008). The interaction between C3G and c-Cbl has been demonstrated in several cell models (Uemura & Griffin, 1999; Maia *et al.*, 2013). Indeed, recent results from the group demonstrated a functional relationship between C3G and c-Cbl in platelets, where C3G plays a positive role in Src-mediated c-Cbl phosphorylation, affecting Mpl ubiquitination, internalization and degradation via proteasome and lysosome systems (Hernandez-Cano *et al.*, 2022). In platelets, c-Cbl also modulates outside-in signaling; indeed, c-Cbl knockout platelets exhibit defective spreading and clot retraction (Buitrago *et al.*, 2011). In addition, some studies described a role for c-Cbl in lamellipodia formation through the regulation of Rac1 by Vav, PI3K and Crk proteins (Scaife & Langdon, 2000; Buitrago *et al.*, 2011).

Vav proteins are the main activators of Rac GTPases (Abe *et al.*, 2000). In platelets, Vav1 participates in platelet aggregation, however, Vav1 knockout platelets spread normally on fibrinogen (Pearce *et al.*, 2002). Double deletion of Vav1 and Vav3 impairs platelet aggregation and spreading triggered by GPVI signaling; however, deletion of Vav3 alone has no effect (Pearce *et al.*, 2004). This suggests that Vav1 plays a role in platelet spreading on collagen but not on fibrinogen. Additionally, previous results described an interaction between C3G and Vav1 and Vav2 by their SH3-binding domain (Maia *et al.*, 2013). Our results, together with the literature, suggest that C3G would regulate lamellipodia formation through c-Cbl/Crk/Vav1/Rac1.

On the other hand, the role of C3G in adhesion has been described in several cell models, being an essential gene for embryonic development due to this function (Ohba *et al.*, 2001; Voss *et al.*, 2003; Voss *et al.*, 2006). Indeed, C3G colocalizes with FA proteins, such as Abl, p38αMAPK, c-Cbl, p130Cas, Abi1, FAK and paxillin in K562 cell line (Maia *et al.*, 2013). Platelet adhesion precedes spreading and involves the assembly of actin filaments to form filopodia (Sorrentino *et al.*, 2015). In this work we observed a positive effect of C3G in platelet adhesion on fibronectin and laminin, but not on CRP or fibrinogen. The regulatory role of C3G in fibronectin adhesion correlates with its effect in platelet spreading on the same substrate. In addition, αVβ1 is one of the fibronectin receptors in platelets, and decreased expression of both subunits was found in

C3G-KO platelets. Based on that, we speculate that C3G might be the main regulator of platelet adhesion and spreading on fibronectin. In contrast, the defects found in adhesion, but not in spreading on laminin in our tgC3G and C3G-KO platelets, could indicate that C3G is not a major regulator of platelet spreading on this substrate. Moreover, platelet adhesion is mediated by FA complexes, while spreading is regulated by actin cytoskeleton dynamics, involving Rho GTPases. Based on that, it is reasonable to speculate that C3G could regulate both processes through different pathways. A different role in platelet adhesion and spreading has also been described for other proteins, such as Arf6, which modulates spreading but not adhesion, among others (Huang *et al.*, 2016; Nguyen *et al.*, 2021).

In addition, our results suggest that C3G would modulate FA complexes in platelets, since it interacted with talin, p130Cas, c-Cbl, vinculin and FAK in a thrombin-dependent manner. Contrarily to the expected, C3G did not interact with paxillin or β-catenin in platelets, despite the fact that these interactions have been demonstrated in other cell types (Dayma *et al.*, 2012; Maia *et al.*, 2013). In fact, C3G regulated the number of FAs formed during spreading on CRP and fibronectin; however, both overexpression and deletion of C3G induced increased formation of FAs. This suggests a dual role for C3G in the regulation of FA complexes in platelets, probably by promoting or inhibiting the interaction between the different components or their function. A dual role of C3G has also been observed in the regulation of apoptosis (Maia *et al.*, 2009) or in its role in different tumors (Manzano *et al.*, 2021a). Furthermore, C3G modulated the phosphorylation of c-Cbl and p130Cas in a substrate-dependent manner. These results further support a role for C3G in the modulation of FA complexes. It must be taken into account that FA formation is a very dynamic process, which makes its study difficult, and can explain why some results are hard to interpret. This is reinforced by the contradictory results obtained in different experiments when studying the interaction between vinculin and C3G. On the other hand, the role of C3G in FA formation could be associated with Src and Pyk2 kinases, since both participate in the recruitment of c-Cbl to FA complexes and modulate cell attachment (Sanjay *et al.*, 2001). Specifically, Pyk2 modulates outside-in signaling through c-Cbl phosphorylation and regulates Rap1 activation (Cipolla *et al.*, 2013), suggesting that C3G could be downstream of Pyk2. This point will be clarified in future studies.

Our results also revealed a role for C3G in clot retraction. C3G-KO platelets presented a significant delay in clot retraction, further supporting a role for C3G in outside-in signaling, by linking integrin activation with cytoskeletal mechanical forces (Huang *et al.*, 2019).

All these results support the notion that C3G contributes to outside-in signaling by regulating actin dynamics through the regulation of Rac1, and that this role of C3G is, at least in part, independent of it GEF activity.

## 3. C3G controls the secretion of platelet α-granules

We have previously described that C3G modulates the secretion of angiogenic factors from platelets. Specifically, C3G overexpression causes the retention of VEGF, bFGF, SDF-1 and TSP-1 after thrombin stimulation (Martin-Granado *et al.*, 2017; Hernandez-Cano *et al.*, 2022), while C3G ablation induces the release of VEGF and SDF-1 and the retention of TSP-1 (Hernandez-Cano *et al.*, 2022). Additionally, in this work we have shown that C3G modulates the release of coagulant factors; tgC3G platelets retained them, while C3G absence induced greater release, in

response to thrombin. Furthermore, we observed that C3G-KO platelets release a higher overall amount of protein compared to C3G-wt platelets. All these suggest that C3G could play a role in platelet granule secretion. These defects in granule secretion observed in our C3G mutant platelets were not due to changes in granule number, and were only associated with α-granules and not δ-granules or lysosomes. Curiously, while C3G ablation triggered a marked increase in protein secretion from α-granules, it led to defective P-selectin exposure on the platelet surface, suggesting a kiss-and-run phenotype.

Interestingly, the levels of P-selectin-, VAMP-7- and VAMP-8-positive α-granules (monitored by fluorescence) were lower in C3G-KO platelets under resting conditions, whereas upon thrombin stimulation these levels increased (higher fluorescence signal), suggesting that the absence of C3G could promote a compound exocytosis. Indeed, VAMP-7 α-granules exhibited two different distribution patterns in C3G-KO platelets; granules distributed throughout the platelet and granules with a peripheral distribution (closer to the PM). A plausible explanation is that under resting conditions, the α-granules are separated from each other by cytoplasmic actin filaments, which would act as a brake on granule secretion (Gremmel *et al.*, 2016). Since C3G absence induced defects in actin filament formation, these defects could cause the peripheral distribution observed in VAMP-7 α-granules.

Consistent with the levels detected by fluorescence in resting conditions, we found reduced RNA and protein levels of P-selectin, VAMP-7 and Sec3 in C3G-KO platelets, even though C3G absence did not affect the number of α-granules. This could explain the lower levels of P-selectin on the surface found in C3G-KO platelets after thrombin stimulation (see **Figure R-3**). However, we detected higher amount of P-selectin in the membrane fraction in C3G-KO platelets at rest, while upon thrombin stimulation P-selectin was retained in the cytoplasmic fraction. Therefore, the lower levels of P-selectin on the surface found in activated C3G-KO platelets could be due to the failure of the vesicles to fuse with the PM. This idea is reinforced by the fact that only a decrease in v-SNAREs and P-selectin levels was observed in C3G-KO platelets, but not an alteration in the expression of t-SNARE proteins. Therefore, we hypothesize that while in wild-type platelets the granules are fused to the membrane, in C3G-KO platelets the vesicles are not fused to the PM, but rather they are recycled, inducing a kiss-and-run phenotype.

C3G modulates RalA activation in response to high doses of thrombin. In agreement with previous results from the group, which demonstrated that the role of C3G in secretion partially depends on its GEF activity (Martin-Granado *et al.*, 2017), tgC3G platelets exhibited greater RalA activation, while C3G-KO and tgC3GΔCat platelets showed lower levels of RalA-GTP. Indeed, RalGEFs (Ral activators) are effectors of Rap1, whose role in α-granule secretion upon platelet stimulation has been documented (Stefanini *et al.*, 2018). Interestingly, double RalA and RalB knockout platelets also exhibit a kiss-and-run phenotype, similar to that observed in C3G-KO platelets (Wersall *et al.*, 2018), further supporting a functional relationship between these proteins. In addition, Ral A/B knockout platelets also present less P-selectin exposure on the platelet surface, although they release cargo normally from α-granules (Wersall *et al.*, 2018).

On the other hand, the fact that C3G does not regulate Rab27 activation is in agreement with our results showing that C3G does not modulate δ-granule secretion. It is reasonable to speculate that, in addition to cytoskeletal defects, the observed peripheral distribution of VAMP-

7 α-granules could also be due to abnormal activation of Rab GTPases, specifically Rab4, due its association with α-granules (Shirakawa *et al.*, 2000). This point will be addressed in future works.

Consistent with a possible role of C3G in the regulation of the secretory machinery, previous results from the group demonstrated that C3G interacts with VAMP-7, in both resting and thrombin-stimulated platelets (Martin-Granado *et al.*, 2017). Here, we show that C3G also interacts with other v-SNAREs, such as VAMP-8, with t-SNAREs, such as SNAP23 and Stx11, as well as with regulators, such as Munc18-b, but not with components of exocyst complex. This indicates that C3G could modulate the formation of the trans-SNARE complex. These interactions were not detected in tgC3GΔCat platelets, further supporting the involvement of Rap1b in the role of C3G in secretion. Moreover, C3G overexpression induced decreased trans-SNARE complex formation, whereas C3G absence induced the opposite phenotype, suggesting a negative role for C3G in the formation of this complex. This is consistent with the increased release of α-granule content observed in C3G-KO platelets in response to thrombin.

As mentioned above, the kiss-and-run phenotype observed in C3G-KO platelets differs from that in Ral A/B knockout platelets in the greater cargo release in the former. A defective tethering/docking, leading to impaired membrane incorporation, could explain kiss-and-run secretion, whereas the increased cargo release observed in C3G-KO platelets could be explained by increased trans-SNARE complex formation (**Figure D-2**). This indicates that C3G might also play roles independent of Ral in platelet secretion.

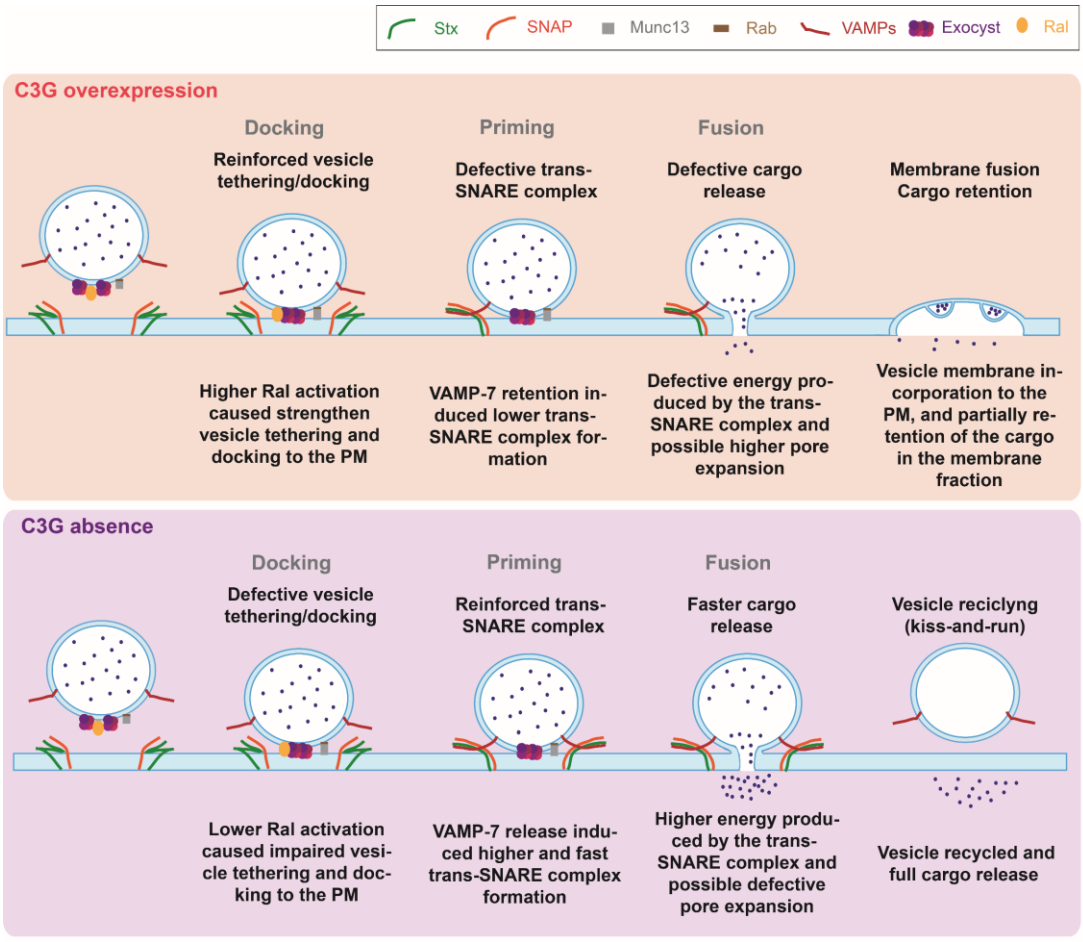

**Figure D-2. Schematic representation of the participation of C3G in α-granule secretion.** Granule exocytosis is regulated by SNARE proteins through several steps. In docking, the vesicles approach the PM through the exocyst complex and the action of Rab-Munc13. Then, v-SNAREs (VAMPs) and t-SNAREs (SNAPs and Stxs) associate forming the trans-SNARE complex, which provides the energy needed for membrane fusion. After fusion the cargo is released. C3G overexpression would result in a increased Ral activation, which would enhance vesicle tethering/docking, while impairing trans-SNARE complex formation, resulting in vesicle membrane incorporation but partial cargo release. Conversely, C3G absence would induce the opposite phenotype, resulting in a kiss-and-run secretion, where the cargo is fully released but the vesicle membrane is not incorporated into the PM. Stx: Syntaxin.

The complex formed by VARP, VAMP-7 and Arp2/3 proteins plays an important role in the regulation of the trans-SNARE complex in platelets. In resting conditions, this complex prevents uncontrolled granule secretion or cytoskeleton remodelling (Koseoglu *et al.*, 2015). Overexpression of C3G increased the formation of this complex in a thrombin dependent manner, whereas C3G deletion induced the opposite phenotype, supporting the participation of C3G in this complex. This data indicate that C3G would help VARP in controlling granule secretion. Furthermore, this C3G role in the prevention of granule exocytosis would explain the retention of granule content observed in tgC3G platelets and the higher release observed in the C3G-KO platelets.

All these results support the participation of C3G in α-granule secretion at two different levels. On the one hand, it would favour tethering/docking by promoting Ral GTPase activation; on the other hand, it would modulate the VARP-Arp2/3-VAMP-7 complex, probably by sequestering VARP and VAMP-7. Hence, VAMP-7 would not be available to interact with SNAP23, thus restricting fusion (**Figure D-3**).

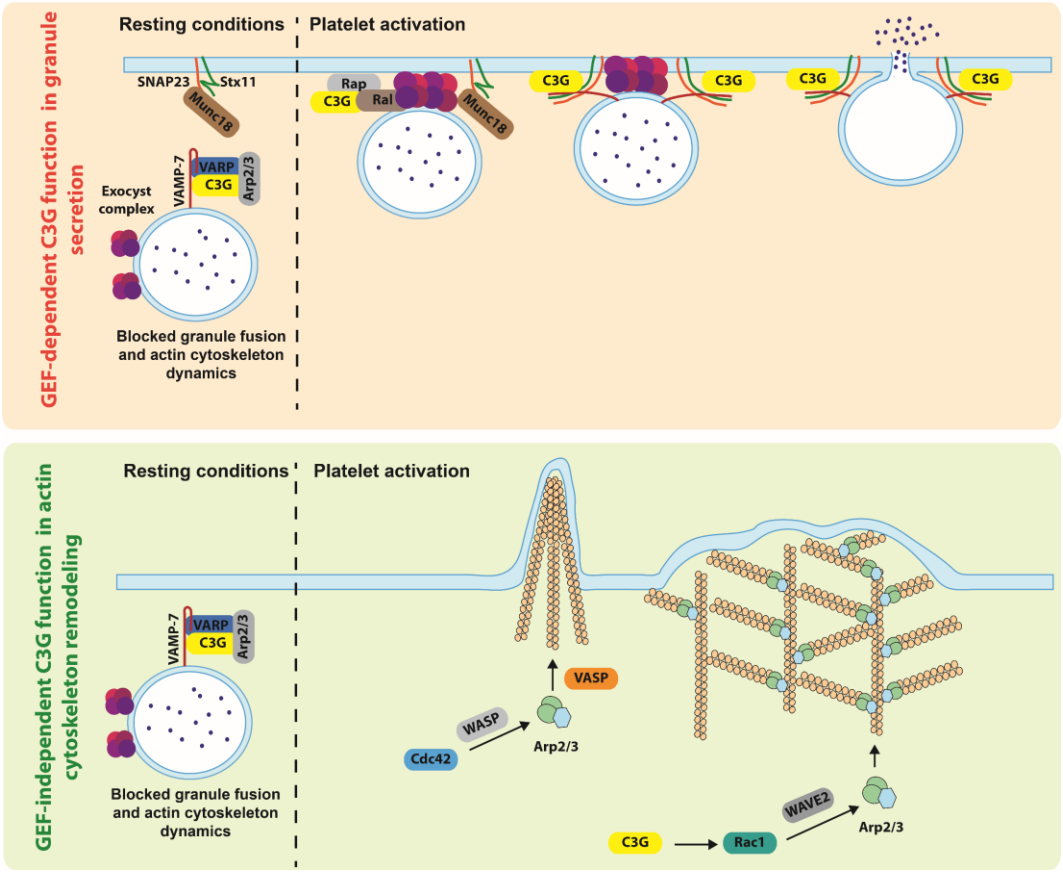

**Figure D-3. Schematic representation of the participation of C3G in α-granule secretion and platelet spreading.** In resting conditions, C3G would form a complex with VARP, VAMP-7 and Arp2/3 preventing uncontrolled granule secretion or actin dynamics. Upper panel: Upon stimulation, C3G would participate in vesicle tethering/docking and in the trans-SNARE complex formation, which provides the energy needed for membrane fusion. Lower panel: After platelet stimulation, C3G would participate in actin branching through the regulation of Rac1/WAVE2/Arp2/3 pathway, thus regulating lamellipodia formation.

Previous results from the group demonstrated that C3G interacts with VAMP-7 through its SNARE domain, which is involved in the interaction with the t-SNAREs SNAP23 and Stx11 (Martin-Granado *et al.*, 2017). This could explain why C3G overexpression decreased SNARE complex formation; C3G would compete with SNAP23 and Stx11 for binding to VAMP-7. In agreement, in the absence of SNAP23, a greater interaction of C3G with VAMP-7 and Stx11 was observed.

After granule secretion, the granule membrane is incorporated into the PM to facilitate the formation of filopodia and lamellipodia during platelet spreading (Flaumenhaft *et al.*, 2005). VAMP-7 is essential for spreading, as only α-granules expressing VAMP-7 translocate to lamellipodia (Koseoglu *et al.*, 2015). C3G-KO platelets displayed increased trans-SNARE complex formation during platelet spreading, but without a reduction in VAMP-7 levels. This suggests that VAMP-7 α-granules are not incorporated into the PM, reinforcing the idea of a kiss-and-run phenotype in these platelets. This impaired membrane incorporation, together with the lower activation of Rac1 are probably the cause of the delayed lamellipodia formation observed in C3G-KO platelets.

Our results revealed a contradictory function of C3G on the Arp2/3 complex. TgC3G platelets showed increased VARP/VAMP-7/Arp2/3 complex formation (implying Arp2/3 retention (Koseoglu *et al.*, 2015)), while at the same time C3G overexpression induced increased Arp2-WAVE2 interaction upon thrombin stimulation. A plausible explanation, in addition to the dynamism of these interactions, is that active WAVE2 would have more affinity for Arp2/3 than VARP, replacing it and triggering actin remodeling for lamellipodia formation. In C3G-KO platelets, decreased VARP/VAMP-7/Arp2/3 complex formation would cause less retention of Arp2; however, due to the lower Rac1 activation, Arp2 could not be activated by WAVE2 to form lamellipodia. The increased F-actin/G-actin rate found in tgC3G platelets and the decreased rate found in C3G-KO platelets support these hypotheses.

The kiss-and-run phenotype of the C3G-KO platelets was confirmed by immunofluorescence on platelets stained with FM1-43, a membrane granule dye. While C3G-wt platelets only displayed normal (fuse and collapse) exocytosis, C3G-KO platelets showed a high percentage of granules undergoing kiss-and-run exocytosis.

Kiss-and-run exocytosis is usually associated with slower and partial cargo release (Wang *et al.*, 2003); however, most kiss-and-run events have been reported to be able to release cargo as quickly and completely as fuse and collapse fusion, the only difference being that, in this case, pore formation is transient (Wu *et al.*, 2014). There are several proteins that regulate pore formation that could be related to C3G, such as the exocyst complex, PKC or dynamin. The exocyst complex facilitates the proper formation and spatial organization of SNARE complexes and is required for coupling tethering and fuse and collapse exocytosis. In fact, Exo70 subunit

can act as a molecular switch between the two exocytic modes (An *et al.*, 2021). Although we did not detect an interaction between C3G and Exo70 in platelets, C3G could modulate exocyst function through the regulation of Ral activation. Indeed, the similarities between C3G-KO platelets and double RalA/B knockout platelets, both exhibiting defective vesicle tethering leading to a kiss-and-run phenotype (Wersall *et al.*, 2018), support the participation of C3G and Ral in a common pathway that regulates tethering.

Dynamin proteins are crucial to regulate fusion pore expansion; in fact, dynamin stimulation reduces the number of kiss-and-run events, but not full fusion events (Jackson *et al.*, 2015). In T-cells, C3G activation is dependent on dynamin 2 through modulation of the FAK/Pyk2 pathway, which triggers C3G phosphorylation by SFKs, leading to Rap1 activation and, hence, cell adhesion (Eppler *et al.*, 2017). Additionally, PKC proteins remove Gi-mediated inhibition of fusion pore opening, thus promoting secretion (Chen *et al.*, 2005). Given the functional relationship between PKC and C3G in platelets (Gutierrez-Herrero *et al.*, 2012), this role of PKC in fusion pore opening could be related to the kiss-and-phenotype of C3G-KO platelets. That is, a possible explanation for the defective vesicle tethering/docking of C3G-KO platelets, despite having increased trans-SNARE complex formation, could be a defect in pore formation, resulting in a kiss-and-run phenotype. Further studies will clarify whether the role of C3G in kiss-and-run secretion depends on dynamins or PKC.

Moreover, the abnormally increased trans-SNARE complex formation found in C3G-KO platelets could also explain the kiss-and-run phenotype found in these platelets. Initially, three or more trans-SNARE complexes are needed for a correct fusion pore formation; however, fusion pore expansion requires the dynamic release of the complex, since restricted mobility of the SNARE complexes prevent pore expansion (Sharma & Lindau, 2018). C3G absence induced a higher trans-SNARE complex formation, however, its release might not be dynamic enough, which would prevent fusion pore expansion, thus promoting kiss-and-run events. In contrast, C3G overexpression would induce a stable vesicle tethering and enhanced pore expansion which, however, cannot compensate for defective trans-SNARE complex formation, leading to lower secretion, despite a greater membrane incorporation (spreading). According to that, correct formation of the trans-SNARE complex is probably required for full secretion of the cargo. Supporting this, previous studies have detected the retention of cargo molecules in the plasma membrane of tgC3G platelets (Martin-Granado *et al.*, 2017).

The involvement of C3G in granule secretion was confirmed in the PC12 cell line. Overexpression of an active C3G mutant induced slower NPY secretion, while C3G absence triggered the opposite phenotype. However, C3G upregulated the number of vesicles docked to the PM and the number of exocytic events in PC12 cells. Therefore, C3G appears to play opposite roles in PC12 cells and platelets with respect to granule secretion, i.e., C3G overexpression caused increased cargo release, while C3G silencing promoted lower secretion. This contradictory phenotype could be explained by the different functionality of the VARP-VAMP-7 complex in platelets and in neurons. In neurons, VARP positively regulates VAMP-7, inducing the formation of the trans-SNARE complex (Burgo *et al.*, 2009); however, as mentioned, in platelets the VAMP-7-VARP interaction promotes the opposite effect (Koseoglu *et al.*, 2015).

On the other hand, C3G absence induced compound secretion in both systems, platelets and in PC12 cells. One possible explanation is that C3G could negatively regulate granule-granule

fusion through its interaction with VAMP-8, the main regulator of this exocytic mode (Behrendorff *et al.*, 2011).

In summary, in this work we present evidence on a role of C3G in the regulation of the secretory machinery, probably through the activation of Rap1b, as well as in the regulation of the actin cytoskeleton dynamics through mechanisms, at least partially, independent on its GEF-activity (**Figure D-3**).

## 4. Platelet C3G modulates the inflammatory response

In the last part of the work, we have studied the implication of platelet C3G in the inflammatory response *in vitro* and *in vivo*.

Platelets secrete a large number of inflammatory mediators, such as chemokines and interleukins (Manne *et al.*, 2017). As expected, C3G also modulated the release of inflammatory factors upon thrombin stimulation; C3G overexpression in platelets triggered an anti-inflammatory secretome, while C3G-KO platelets released a pro-inflammatory secretome. Among others, C3G modulated the secretion of factors that regulate neutrophil activation (PF4 and CXCL1), and monocyte/Mϕ activation and recruitment (CCL2 or CCL3). Moreover, we detected CXCL10 in platelet secretome, despite the fact that there is no evidence in the literature about its presence in platelets.

C3G promoted increased exposure of P-selectin and CD40L on the platelet surface, while the opposite was found in C3G-KO platelets. However, only the increased exposure of P-selectin explains the higher PLA formation observed in tgC3G platelets in response to thrombin stimulation, since blocking of P-selectin, but not CD40L, completely suppressed the differences between tgC3G and wtC3G platelets. Moreover, C3G regulated PLA formation with NEs and B lymphocytes, but not with monocytes or T lymphocytes.

P-selectin is essential for NETosis through its interaction with PSGL-1 (Etulain *et al.*, 2015). Thus, consistent with their increased platelet-NE formation and P-selectin exposure, tgC3G platelets induced higher NETosis, both at rest and after thrombin stimulation. In concordance, C3G-KO platelets elicited defects in NETosis, but only under high-dose thrombin. However, the secretome of thrombin-stimulated tgC3G platelets induced a lower NETosis than that of wtC3G platelets, in agreement with its anti-inflammatory composition. However, it appears that the increased exposure of P-selectin on the platelet surface of tgC3G platelets can compensate for their anti-inflammatory secretome. In contrast, the secretome of thrombin-activated C3G-KO platelets produced levels of NETosis only slightly higher than those induced by C3G-wt releasate, indicating a low effect of the secretome in NETosis. In agreement, this pro-inflammatory secretome of C3G-KO platelets could not compensate for their defects in P-selectin and CD40L exposure.

Overall, our results support a role for C3G in platelet-mediated inflammatory response *in vitro,* through NE activation.

Unexpectedly, despite the lower PLA and NETosis observed *in* vitro in C3G-KO platelets, C3G absence significantly accelerated the symptoms of DSS-induced colitis. C3G-KO mice suffered

significant weight loss accompanied by diarrhea and bloody stools. Additionally, the absence of C3G triggered greater bacteria dissemination. C3G also modulated PLA formation with NE *in vivo*, but not with monocytes or lymphocytes, consistent with the *in vitro* data, supporting a role for C3G in platelet-NE interaction. In agreement, NE-platelet aggregates are elevated in patients with ulcerative colitis, playing an essential role in its progression; in fact, suppression of these aggregates suppresses colon inflammation (Yamamoto-Furusho & Mendieta-Escalante, 2020). These aggregates are an important source of inflammatory mediators, which can maintain or amplify inflammatory responses. Both NEs and platelets accumulate in the colonic microvasculature during colitis, leading to microvascular dysfunction and tissue damage (Vowinkel *et al.*, 2007).

DSS-treated C3G-KO mice presented higher NE counts in blood after 7 days, with not differences in monocyte or platelet numbers. DSS-treatment induced increased platelet production on day 4, however, platelet number decreased on day 7 to values below normal, possibly related to the presence of diarrhea and blood in the stools. The absence of differences in platelet number between C3G-KO mice and their controls contradicts the role of C3G in thrombopoiesis in pathological situations, observed with 5-fluorouracil (5-FU) treatment or tumor cell implantation (Ortiz-Rivero *et al.*, 2018; Hernandez-Cano *et al.*, 2022). This suggests that C3G would promote megakaryopoiesis only in certain pathological scenarios, probably those involving platelet depletion, such as those produced by 5-FU or by tumor-induced platelet aggregation. Further studies must be conducted to clarify this point. Additionally, there were no differences in the recruitment of inflammatory cells to the colon.

Finally, C3G-absence in platelets triggered a higher expression of inflammatory factors, such as TGF-β and IL-1β in the colon after DSS treatment, both cytokines inducing leukocyte activation and differentiation. In contrast, C3G ablation induced a lower expression of PF4 and TNF-α, which are involved in monocyte chemotaxis and differentiation to Mϕ, ROS generation and NE activation (Thomas & Storey, 2015). On the other hand, after DSS treatment, C3G-KO platelets showed increased expression of CCL2 (involved in monocyte recruitment), PF4 and TGF-β. The opposite expression levels of these cytokines in colon and platelets of C3G-KO mice after DSS treatment, suggests that platelets could either endocytose them or express and secrete them, during the inflammatory response. Further studies studying the expression of these factors in non-treated mice will be necessary to determine whether these differences in expression are due to DSS-treatment or to the absence of C3G in platelets. In addition, studies in tgC3G should be conducted to clarify whether C3G could act as a protector against ulcerative colitis, as indicated by our current data.

In conclusion, in this work we present evidence of a role for C3G in the modulation of platelet spreading through the regulation of lamellipodia formation via its participation in the Rac1/WAVE2/Arp2/3 pathway, which is independent of its GEF function. In addition, C3G would regulate the secretion of α-granules by modulating the formation of the trans-SNARE and the VARP/VAMP-7/Arp2/3 complexes, as well as the activation of Ral, in a Rap1-dependent manner. Finally, we present preliminary results, both *in vitro* and *in vivo*, on a novel role of the C3G protein in the platelet-mediated inflammatory response, through the regulation of PLA formation, with NE and B lymphocytes, and the release of inflammatory factors.

# CONCLUSIONS/ CONCLUSIONES

# CONCLUSIONS

1. Deletion of C3G in platelets causes defective inside-out signaling, downstream of most agonists, through alterations in the PKCδ-Rap1 pathway, affecting integrin αIIbβ3 activation, P-selectin exposure, and platelet aggregation.

2. C3G modulates secondary hemostasis by controlling phosphatidylserine translocation and secretion of coagulation factors.

3. C3G plays a positive role in platelet spreading in a substrate-dependent manner. Specifically, C3G regulates spreading on poly-L-lysine, collagen/CRP, fibronectin, and vitronectin. This function is mediated by PKC and Src proteins.

4. C3G contributes to lamellipodia formation by modulating actin fiber formation through its participation in the Rac1/WAVE2/Arp2/3 pathway. This function is, at least partially, independent on its GEF activity.

5. Absence of C3G impairs clot retraction, supporting a role for C3G in outside-in signaling, by linking integrin activation with cytoskeletal mechanical forces.

6. C3G is required for proper α-granule secretion, acting as a negative regulator of this process. C3G deletion induces increased protein release, whereas C3G overexpression promotes cargo retention.

7. C3G regulates α-granule secretion by modulating trans-SNARE and VARP/VAMP-7/Arp2/3 complex formation, as well as Ral activation, in a Rap1-dependent manner.

8. C3G promotes the platelet-mediated inflammatory response in vitro, through the regulation of P-selectin and CD40L exposure. Thus, C3G overexpression results in increased neutrophil activation and PLA formation, whereas C3G deletion triggers the opposite phenotype.

9. Absence of C3G in platelets significantly accelerates the symptoms of DSS-induced colitis through regulation of PLA formation.

# CONCLUSIONES

1. La deleción de C3G en las plaquetas causa una señalización *inside-out* defectuosa, en respuesta de la mayoría de los agonistas, a través de alteraciones en la vía PKCδ-Rap1, afectando a la activación de la integrina αIIbβ3, la exposición de la P-selectina y la agregación plaquetaria.

2. C3G modula la hemostasia secundaria mediante el control de la translocación de fosfatidilserina y la secreción de factores de coagulación.

3. C3G desempeña un papel positivo en la extensión plaquetaria o *spreading* de forma dependiente del sustrato. En concreto, C3G regula la extensión sobre poli-L-lisina, colágeno/CRP, fibronectina y vitronectina. Esta función está mediada por las proteínas PKC y Src.

4. C3G contribuye a la formación de lamelipodios modulando la formación de fibras de actina a través de su participación en la vía Rac1/WAVE2/Arp2/3. Esta función está mediada, al menos parcialmente, por las proteínas PKC y Src. Esta función es, al menos parcialmente, independiente de su actividad GEF.

5. La ausencia de C3G altera retracción del coágulo, lo que apoya el papel de C3G en la señalización *outside-in*, al vincular la activación de la integrina con las fuerzas mecánicas del citoesqueleto.

6. C3G es necesaria para la secreción adecuada de gránulos α, actuando como regulador negativo de este proceso. La deleción de C3G induce un aumento de la liberación de proteínas, mientras que la sobreexpresión de C3G promueve la retención de la carga.

7. C3G regula la secreción de gránulos α modulando la formación de complejos trans-SNARE y VARP/VAMP-7/Arp2/3, así como la activación de Ral, de manera dependiente de Rap1.

8. C3G promueve la respuesta inflamatoria mediada por plaquetas in vitro, a través de la regulación de la exposición a P-selectina y CD40L,. Así, la sobreexpresión de C3G produce un aumento de la activación de neutrófilos y de la formación de PLA, mientras que la deleción de C3G desencadena el fenotipo opuesto.

9. La ausencia de C3G en las plaquetas acelera significativamente los síntomas de la colitis inducida por DSS a través de la regulación de la formación de PLA.

# REFERENCES

Abe, K., Rossman, K.L., Liu, B., Ritola, K.D., Chiang, D., Campbell, S.L., Burridge, K. & Der, C.J. (2000) Vav2 is an activator of Cdc42, Rac1, and RhoA. *J Biol Chem*, **275**, 10141-10149.

Adam, F., Kauskot, A., Kurowska, M., Goudin, N., Munoz, I., Bordet, J.C., Huang, J.D., Bryckaert, M., Fischer, A., Borgel, D., de Saint Basile, G., Christophe, O.D. & Menasche, G. (2018) Kinesin-1 Is a New Actor Involved in Platelet Secretion and Thrombus Stability. *Arterioscler Thromb Vasc Biol*, **38**, 1037-1051.

Aguilar, A., Weber, J., Boscher, J., Freund, M., Ziessel, C., Eckly, A., Magnenat, S., Bourdon, C., Hechler, B., Mangin, P.H., Gachet, C., Lanza, F. & Leon, C. (2019) Combined deficiency of RAB32 and RAB38 in the mouse mimics Hermansky-Pudlak syndrome and critically impairs thrombosis. *Blood Adv*, **3**, 2368-2380.

Akbar, H., Shang, X., Perveen, R., Berryman, M., Funk, K., Johnson, J.F., Tandon, N.N. & Zheng, Y. (2011) Gene targeting implicates Cdc42 GTPase in GPVI and non-GPVI mediated platelet filopodia formation, secretion and aggregation. *PLoS One*, **6**, e22117.

Al Hawas, R., Ren, Q., Ye, S., Karim, Z.A., Filipovich, A.H. & Whiteheart, S.W. (2012) Munc18b/STXBP2 is required for platelet secretion. *Blood*, **120**, 2493-2500.

Amaral, E., Guatimosim, S. & Guatimosim, C. (2011) Using the fluorescent styryl dye FM1-43 to visualize synaptic vesicles exocytosis and endocytosis in motor nerve terminals. *Methods Mol Biol*, **689**, 137-148.

An, S.J., Rivera-Molina, F., Anneken, A., Xi, Z., McNellis, B., Polejaev, V.I. & Toomre, D. (2021) An active tethering mechanism controls the fate of vesicles. *Nat Commun*, **12**, 5434.

Andre, P. (2004) P-selectin in haemostasis. *Br J Haematol*, **126**, 298-306.

Arnout, J., Hoylaerts, M.F. & Lijnen, H.R. (2006) Haemostasis. *Handb Exp Pharmacol*, 1-41.

Aslan, J.E. & McCarty, O.J. (2013) Rho GTPases in platelet function. *J Thromb Haemost*, **11**, 35-46.

Aszodi, A., Pfeifer, A., Ahmad, M., Glauner, M., Zhou, X.H., Ny, L., Andersson, K.E., Kehrel, B., Offermanns, S. & Fassler, R. (1999) The vasodilator-stimulated phosphoprotein (VASP) is involved in cGMP- and cAMP-mediated inhibition of agonist-induced platelet aggregation, but is dispensable for smooth muscle function. *EMBO J*, **18**, 37-48.

Bakogiannis, C., Sachse, M., Stamatelopoulos, K. & Stellos, K. (2019) Platelet-derived chemokines in inflammation and atherosclerosis. *Cytokine*, **122**, 154157.

Battinelli, E.M., Thon, J.N., Okazaki, R., Peters, C.G., Vijey, P., Wilkie, A.R., Noetzli, L.J., Flaumenhaft, R. & Italiano, J.E. (2019) Megakaryocytes package contents into separate alpha-granules that are differentially distributed in platelets. *Blood Adv*, **3**, 3092-3098.

Bearer, E.L., Prakash, J.M. & Li, Z. (2002) Actin dynamics in platelets. *Int Rev Cytol*, **217**, 137-182.

Behrendorff, N., Dolai, S., Hong, W., Gaisano, H.Y. & Thorn, P. (2011) Vesicle-associated membrane protein 8 (VAMP8) is a SNARE (soluble N-ethylmaleimide-sensitive factor attachment protein receptor) selectively required for sequential granule-to-granule fusion. *J Biol Chem*, **286**, 29627-29634.

Bender, M. & Palankar, R. (2021) Platelet Shape Changes during Thrombus Formation: Role of Actin-Based Protrusions. *Hamostaseologie*, **41**, 14-21.

Bennett, J.S., Berger, B.W. & Billings, P.C. (2009) The structure and function of platelet integrins. *J Thromb Haemost*, **7 Suppl 1**, 200-205.

Bentfeld-Barker, M.E. & Bainton, D.F. (1982) Identification of primary lysosomes in human megakaryocytes and platelets. *Blood*, **59**, 472-481.

Benz, P.M., Laban, H., Zink, J., Gunther, L., Walter, U., Gambaryan, S. & Dib, K. (2016) Vasodilator-Stimulated Phosphoprotein (VASP)-dependent and -independent pathways regulate thrombin-induced activation of Rap1b in platelets. *Cell Commun Signal*, **14**, 21.

Berg, S., Kutra, D., Kroeger, T., Straehle, C.N., Kausler, B.X., Haubold, C., Schiegg, M., Ales, J., Beier, T., Rudy, M., Eren, K., Cervantes, J.I., Xu, B., Beuttenmueller, F., Wolny, A., Zhang, C., Koethe, U., Hamprecht, F.A. & Kreshuk, A. (2019) ilastik: interactive machine learning for (bio)image analysis. *Nat Methods*, **16**, 1226-1232.

Berry, S., Dawicki, D.D., Agarwal, K.C. & Steiner, M. (1989) The role of microtubules in platelet secretory release. *Biochim Biophys Acta*, **1012**, 46-56.

Berthold, M.R., Cebron, N., Dill, F., Gabriel, T.R., Kötter, T., Meinl, T., Ohl, P., Thiel, K. & Wiswedel, B. (2009) KNIME-the Konstanz information miner: version 2.0 and beyond. *AcM SIGKDD Exp Newsletter*, **11**, 26–31.

Bongiovanni, D., Han, J., Klug, M., Kirmes, K., Viggiani, G., von Scheidt, M., Schreiner, N., Condorelli, G., Laugwitz, K.L. & Bernlochner, I. (2022) Role of Reticulated Platelets in Cardiovascular Disease. *Arterioscler Thromb Vasc Biol*, **42**, 527-539.

Bos, J.L. (1998) All in the family? New insights and questions regarding interconnectivity of Ras, Rap1 and Ral. *EMBO J*, **17**, 6776-6782.

Bos, J.L., de Rooij, J. & Reedquist, K.A. (2001) Rap1 signalling: adhering to new models. *Nat Rev Mol Cell Biol*, **2**, 369-377.

Bos, J.L., Rehmann, H. & Wittinghofer, A. (2007) GEFs and GAPs: critical elements in the control of small G proteins. *Cell*, **129**, 865-877.

Bradford, M.M. (1976) A rapid and sensitive method for the quantitation of microgram quantities of protein utilizing the principle of protein-dye binding. *Anal Biochem*, **72**, 248-254.

Broos, K., Feys, H.B., De Meyer, S.F., Vanhoorelbeke, K. & Deckmyn, H. (2011) Platelets at work in primary hemostasis. *Blood Rev*, **25**, 155-167.

Buensuceso, C.S., Obergfell, A., Soriani, A., Eto, K., Kiosses, W.B., Arias-Salgado, E.G., Kawakami, T. & Shattil, S.J. (2005) Regulation of outside-in signaling in

platelets by integrin-associated protein kinase C beta. *J Biol Chem*, **280**, 644-653.

Buitrago, L., Langdon, W.Y., Sanjay, A. & Kunapuli, S.P. (2011) Tyrosine phosphorylated c-Cbl regulates platelet functional responses mediated by outside-in signaling. *Blood*, **118**, 5631-5640.

Burgo, A., Sotirakis, E., Simmler, M.C., Verraes, A., Chamot, C., Simpson, J.C., Lanzetti, L., Proux-Gillardeaux, V. & Galli, T. (2009) Role of Varp, a Rab21 exchange factor and TI-VAMP/VAMP7 partner, in neurite growth. *EMBO Rep*, **10**, 1117-1124.

Canault, M. & Alessi, M.C. (2020) RasGRP2 Structure, Function and Genetic Variants in Platelet Pathophysiology. *Int J Mol Sci*, **21**.

Carabias, A., Gomez-Hernandez, M., de Cima, S., Rodriguez-Blazquez, A., Moran-Vaquero, A., Gonzalez-Saenz, P., Guerrero, C. & de Pereda, J.M. (2020) Mechanisms of autoregulation of C3G, activator of the GTPase Rap1, and its catalytic deregulation in lymphomas. *Sci Signal*, **13**.

Cardenas, E.I., Breaux, K., Da, Q., Flores, J.R., Ramos, M.A., Tuvim, M.J., Burns, A.R., Rumbaut, R.E. & Adachi, R. (2018) Platelet Munc13-4 regulates hemostasis, thrombosis and airway inflammation. *Haematologica*, **103**, 1235-1244.

Cardenas, E.I., Gonzalez, R., Breaux, K., Da, Q., Gutierrez, B.A., Ramos, M.A., Cardenas, R.A., Burns, A.R., Rumbaut, R.E. & Adachi, R. (2019) Munc18-2, but not Munc18-1 or Munc18-3, regulates platelet exocytosis, hemostasis, and thrombosis. *J Biol Chem*, **294**, 4784-4792.

Cerecedo, D. (2013) Platelet cytoskeleton and its hemostatic role. *Blood Coagul Fibrinolysis*, **24**, 798-808.

Cesarman-Maus, G. & Hajjar, K.A. (2005) Molecular mechanisms of fibrinolysis. *Br J Haematol*, **129**, 307-321.

Chari, R., Getz, T., Nagy, B., Jr., Bhavaraju, K., Mao, Y., Bynagari, Y.S., Murugappan, S., Nakayama, K. & Kunapuli, S.P. (2009) Protein kinase C[delta] differentially regulates platelet functional responses. *Arterioscler Thromb Vasc Biol*, **29**, 699-705.

Chassaing, B., Aitken, J.D., Malleshappa, M. & Vijay-Kumar, M. (2014) Dextran sulfate sodium (DSS)-induced colitis in mice. *Curr Protoc Immunol*, **104**, 15 25 11-15 25 14.

Chatterjee, M., Huang, Z., Zhang, W., Jiang, L., Hultenby, K., Zhu, L., Hu, H., Nilsson, G.P. & Li, N. (2011) Distinct platelet packaging, release, and surface expression of proangiogenic and antiangiogenic factors on different platelet stimuli. *Blood*, **117**, 3907-3911.

Chen, X.K., Wang, L.C., Zhou, Y., Cai, Q., Prakriya, M., Duan, K.L., Sheng, Z.H., Lingle, C. & Zhou, Z. (2005) Activation of GPCRs modulates quantal size in chromaffin cells through G(betagamma) and PKC. *Nat Neurosci*, **8**, 1160-1168.

Chiang, S.H., Baumann, C.A., Kanzaki, M., Thurmond, D.C., Watson, R.T., Neudauer, C.L., Macara, I.G., Pessin, J.E. & Saltiel, A.R. (2001) Insulin-stimulated GLUT4 translocation requires the CAP-dependent activation of TC10. *Nature*, **410**, 944-948.

Chiang, S.H., Chang, L. & Saltiel, A.R. (2006) TC10 and insulin-stimulated glucose transport. *Methods Enzymol*, **406**, 701-714.

Chicka, M.C., Ren, Q., Richards, D., Hellman, L.M., Zhang, J., Fried, M.G. & Whiteheart, S.W. (2016) Role of Munc13-4 as a Ca2+-dependent tether during platelet secretion. *Biochem J*, **473**, 627-639.

Chrzanowska-Wodnicka, M., Smyth, S.S., Schoenwaelder, S.M., Fischer, T.H. & White, G.C., 2nd (2005) Rap1b is required for normal platelet function and hemostasis in mice. *J Clin Invest*, **115**, 680-687.

Chu, Y., Guo, H., Zhang, Y. & Qiao, R. (2021) Procoagulant platelets: Generation, characteristics, and therapeutic target. *J Clin Lab Anal*, **35**, e23750.

Chung, S.H., Polgar, J. & Reed, G.L. (2000) Protein kinase C phosphorylation of syntaxin 4 in thrombin-activated human platelets. *J Biol Chem*, **275**, 25286-25291.

Cifuni, S.M., Wagner, D.D. & Bergmeier, W. (2008) CalDAG-GEFI and protein kinase C represent alternative pathways leading to activation of integrin alphaIIbbeta3 in platelets. *Blood*, **112**, 1696-1703.

Ciobanasu, C., Faivre, B. & Le Clainche, C. (2013) Integrating actin dynamics, mechanotransduction and integrin activation: the multiple functions of actin binding proteins in focal adhesions. *Eur J Cell Biol*, **92**, 339-348.

Cipolla, L., Consonni, A., Guidetti, G., Canobbio, I., Okigaki, M., Falasca, M., Ciraolo, E., Hirsch, E., Balduini, C. & Torti, M. (2013) The proline-rich tyrosine kinase Pyk2 regulates platelet integrin alphaIIbbeta3 outside-in signaling. *J Thromb Haemost*, **11**, 345-356.

Cognasse, F., Duchez, A.C., Audoux, E., Ebermeyer, T., Arthaud, C.A., Prier, A., Eyraud, M.A., Mismetti, P., Garraud, O., Bertoletti, L. & Hamzeh-Cognasse, H. (2022) Platelets as Key Factors in Inflammation: Focus on CD40L/CD40. *Front Immunol*, **13**, 825892.

Collado, A., Marques, P., Escudero, P., Rius, C., Domingo, E., Martinez-Hervas, S., Real, J.T., Ascaso, J.F., Piqueras, L. & Sanz, M.J. (2018) Functional role of endothelial CXCL16/CXCR6-platelet-leucocyte axis in angiotensin II-associated metabolic disorders. *Cardiovasc Res*, **114**, 1764-1775.

Crittenden, J.R., Bergmeier, W., Zhang, Y., Piffath, C.L., Liang, Y., Wagner, D.D., Housman, D.E. & Graybiel, A.M. (2004) CalDAG-GEFI integrates signaling for platelet aggregation and thrombus formation. *Nat Med*, **10**, 982-986.

Cuenca-Zamora, E.J., Ferrer-Marin, F., Rivera, J. & Teruel-Montoya, R. (2019) Tubulin in Platelets: When the Shape Matters. *Int J Mol Sci*, **20**.

Damiano-Guercio, J., Kurzawa, L., Mueller, J., Dimchev, G., Schaks, M., Nemethova, M., Pokrant, T., Bruhmann, S., Linkner, J., Blanchoin, L., Sixt, M., Rottner, K. & Faix, J. (2020) Loss of Ena/VASP interferes with lamellipodium architecture, motility and integrin-dependent adhesion. *Elife*, **9**.

Dayma, K. & Radha, V. (2011) Cytoskeletal remodeling by C3G to induce neurite-like extensions and inhibit motility in highly invasive breast carcinoma cells. *Biochim Biophys Acta*, **1813**, 456-465.

Dayma, K., Ramadhas, A., Sasikumar, K. & Radha, V. (2012) Reciprocal Negative Regulation between the Guanine Nucleotide Exchange Factor C3G and beta-Catenin. *Genes Cancer*, **3**, 564-577.

De Cuyper, I.M., Meinders, M., van de Vijver, E., de Korte, D., Porcelijn, L., de Haas, M., Eble, J.A., Seeger, K., Rutella, S., Pagliara, D., Kuijpers, T.W., Verhoeven, A.J., van den Berg, T.K. & Gutierrez, L. (2013) A novel flow cytometry-based platelet aggregation assay. *Blood*, **121**, e70-80.

De Falco, V., Castellone, M.D., De Vita, G., Cirafici, A.M., Hershman, J.M., Guerrero, C., Fusco, A., Melillo, R.M. & Santoro, M. (2007) RET/papillary thyroid carcinoma oncogenic signaling through the Rap1 small GTPase. *Cancer Res*, **67**, 381-390.

De Kock, L. & Freson, K. (2020) The (Patho)Biology of SRC Kinase in Platelets and Megakaryocytes. *Medicina (Kaunas)*, **56**.

Deshmane, S.L., Kremlev, S., Amini, S. & Sawaya, B.E. (2009) Monocyte chemoattractant protein-1 (MCP-1): an overview. *J Interferon Cytokine Res*, **29**, 313-326.

Dominguez, R. (2009) Actin filament nucleation and elongation factors--structure-function relationships. *Crit Rev Biochem Mol Biol*, **44**, 351-366.

Duleh, S.N. & Welch, M.D. (2010) WASH and the Arp2/3 complex regulate endosome shape and trafficking. *Cytoskeleton (Hoboken)*, **67**, 193-206.

Dunn, K.W., Kamocka, M.M. & McDonald, J.H. (2011) A practical guide to evaluating colocalization in biological microscopy. *Am J Physiol Cell Physiol*, **300**, C723-742.

Durrant, T.N., van den Bosch, M.T. & Hers, I. (2017) Integrin alphaIIbbeta3 outside-in signaling. *Blood*, **130**, 1607-1619.

Ebermeyer, T., Cognasse, F., Berthelot, P., Mismetti, P., Garraud, O. & Hamzeh-Cognasse, H. (2021) Platelet Innate Immune Receptors and TLRs: A Double-Edged Sword. *Int J Mol Sci*, **22**.

Eckly, A., Rinckel, J.Y., Proamer, F., Ulas, N., Joshi, S., Whiteheart, S.W. & Gachet, C. (2016) Respective contributions of single and compound granule fusion to secretion by activated platelets. *Blood*, **128**, 2538-2549.

Elvers, M. (2016) RhoGAPs and Rho GTPases in platelets. *Hamostaseologie*, **36**, 168-177.

Eppler, F.J., Quast, T. & Kolanus, W. (2017) Dynamin2 controls Rap1 activation and integrin clustering in human T lymphocyte adhesion. *PLoS One*, **12**, e0172443.

Estevez, B. & Du, X. (2017) New Concepts and Mechanisms of Platelet Activation Signaling. *Physiology (Bethesda)*, **32**, 162-177.

Estevez, B., Shen, B. & Du, X. (2015) Targeting integrin and integrin signaling in treating thrombosis. *Arterioscler Thromb Vasc Biol*, **35**, 24-29.

Etulain, J., Martinod, K., Wong, S.L., Cifuni, S.M., Schattner, M. & Wagner, D.D. (2015) P-selectin promotes neutrophil extracellular trap formation in mice. *Blood*, **126**, 242-246.

Falet, H., Hoffmeister, K.M., Neujahr, R. & Hartwig, J.H. (2002) Normal Arp2/3

complex activation in platelets lacking WASp. *Blood*, **100**, 2113-2122.

Filep, J.G. (2022) Targeting Neutrophils for Promoting the Resolution of Inflammation. *Front Immunol*, **13**, 866747.

Finsterbusch, M., Schrottmaier, W.C., Kral-Pointner, J.B., Salzmann, M. & Assinger, A. (2018) Measuring and interpreting platelet-leukocyte aggregates. *Platelets*, **29**, 677-685.

Fish, K.N. (2009) Total internal reflection fluorescence (TIRF) microscopy. *Curr Protoc Cytom*, **Chapter 12**, Unit12 18.

Fitch-Tewfik, J.L. & Flaumenhaft, R. (2013) Platelet granule exocytosis: a comparison with chromaffin cells. *Front Endocrinol (Lausanne)*, **4**, 77.

Flaumenhaft, R., Dilks, J.R., Rozenvayn, N., Monahan-Earley, R.A., Feng, D. & Dvorak, A.M. (2005) The actin cytoskeleton differentially regulates platelet alpha-granule and dense-granule secretion. *Blood*, **105**, 3879-3887.

Flevaris, P., Li, Z., Zhang, G., Zheng, Y., Liu, J. & Du, X. (2009) Two distinct roles of mitogen-activated protein kinases in platelets and a novel Rac1-MAPK-dependent integrin outside-in retractile signaling pathway. *Blood*, **113**, 893-901.

Fournier, B.M. & Parkos, C.A. (2012) The role of neutrophils during intestinal inflammation. *Mucosal Immunol*, **5**, 354-366.

Franco, A.T., Corken, A. & Ware, J. (2015) Platelets at the interface of thrombosis, inflammation, and cancer. *Blood*, **126**, 582-588.

Franke, B., van Triest, M., de Bruijn, K.M., van Willigen, G., Nieuwenhuis, H.K., Negrier, C., Akkerman, J.W. & Bos, J.L. (2000) Sequential regulation of the small GTPase Rap1 in human platelets. *Mol Cell Biol*, **20**, 779-785.

Fu, G., Deng, M., Neal, M.D., Billiar, T.R. & Scott, M.J. (2021) Platelet-Monocyte Aggregates: Understanding Mechanisms and Functions in Sepsis. *Shock*, **55**, 156-166.

Fujiwara, I., Zweifel, M.E., Courtemanche, N. & Pollard, T.D. (2018) Latrunculin A Accelerates Actin Filament Depolymerization in Addition to Sequestering Actin Monomers. *Curr Biol*, **28**, 3183-3192 e3182.

Fukuda, M. (2013) Rab27 effectors, pleiotropic regulators in secretory pathways. *Traffic*, **14**, 949-963.

Gavin, R.L., Koo, C.Z. & Tomlinson, M.G. (2020) Tspan18 is a novel regulator of thrombo-inflammation. *Med Microbiol Immunol*, **209**, 553-564.

Ge, S., White, J.G. & Haynes, C.L. (2012) Cytoskeletal F-actin, not the circumferential coil of microtubules, regulates platelet dense-body granule secretion. *Platelets*, **23**, 259-263.

Gilio, K., Harper, M.T., Cosemans, J.M., Konopatskaya, O., Munnix, I.C., Prinzen, L., Leitges, M., Liu, Q., Molkentin, J.D., Heemskerk, J.W. & Poole, A.W. (2010) Functional divergence of platelet protein kinase C (PKC) isoforms in thrombus formation on collagen. *J Biol Chem*, **285**, 23410-23419.

Gleissner, C.A., von Hundelshausen, P. & Ley, K. (2008) Platelet chemokines in vascular

disease. *Arterioscler Thromb Vasc Biol*, **28**, 1920-1927.

Goggs, R., Williams, C.M., Mellor, H. & Poole, A.W. (2015) Platelet Rho GTPases-a focus on novel players, roles and relationships. *Biochem J*, **466**, 431-442.

Golebiewska, E.M., Harper, M.T., Williams, C.M., Savage, J.S., Goggs, R., Fischer von Mollard, G. & Poole, A.W. (2015) Syntaxin 8 regulates platelet dense granule secretion, aggregation, and thrombus stability. *J Biol Chem*, **290**, 1536-1545.

Golebiewska, E.M. & Poole, A.W. (2015) Platelet secretion: From haemostasis to wound healing and beyond. *Blood Rev*, **29**, 153-162.

Goley, E.D. & Welch, M.D. (2006) The ARP2/3 complex: an actin nucleator comes of age. *Nat Rev Mol Cell Biol*, **7**, 713-726.

Gotoh, T., Hattori, S., Nakamura, S., Kitayama, H., Noda, M., Takai, Y., Kaibuchi, K., Matsui, H., Hatase, O., Takahashi, H. & et al. (1995) Identification of Rap1 as a target for the Crk SH3 domain-binding guanine nucleotide-releasing factor C3G. *Mol Cell Biol*, **15**, 6746-6753.

Gotoh, T., Niino, Y., Tokuda, M., Hatase, O., Nakamura, S., Matsuda, M. & Hattori, S. (1997) Activation of R-Ras by Ras-guanine nucleotide-releasing factor. *J Biol Chem*, **272**, 18602-18607.

Gracheva, E.O., Maryon, E.B., Berthelot-Grosjean, M. & Richmond, J.E. (2010) Differential Regulation of Synaptic Vesicle Tethering and Docking by UNC-18 and TOM-1. *Front Synaptic Neurosci*, **2**, 141.

Graham, G.J., Ren, Q., Dilks, J.R., Blair, P., Whiteheart, S.W. & Flaumenhaft, R. (2009) Endobrevin/VAMP-8-dependent dense granule release mediates thrombus formation in vivo. *Blood*, **114**, 1083-1090.

Green, D. (2006) Coagulation cascade. *Hemodial Int*, **10 Suppl 2**, S2-4.

Gremmel, T., Frelinger, A.L., 3rd & Michelson, A.D. (2016) Platelet Physiology. *Semin Thromb Hemost*, **42**, 191-204.

Guerrero, C., Fernandez-Medarde, A., Rojas, J.M., Font de Mora, J., Esteban, L.M. & Santos, E. (1998) Transformation suppressor activity of C3G is independent of its CDC25-homology domain. *Oncogene*, **16**, 613-624.

Guerrero, C., Martin-Encabo, S., Fernandez-Medarde, A. & Santos, E. (2004) C3G-mediated suppression of oncogene-induced focus formation in fibroblasts involves inhibition of ERK activation, cyclin A expression and alterations of anchorage-independent growth. *Oncogene*, **23**, 4885-4893.

Guidetti, G.F., Torti, M. & Canobbio, I. (2019) Focal Adhesion Kinases in Platelet Function and Thrombosis. *Arterioscler Thromb Vasc Biol*, **39**, 857-868.

Gutierrez-Berzal, J., Castellano, E., Martin-Encabo, S., Gutierrez-Cianca, N., Hernandez, J.M., Santos, E. & Guerrero, C. (2006) Characterization of p87C3G, a novel, truncated C3G isoform that is overexpressed in chronic myeloid leukemia and interacts with Bcr-Abl. *Exp Cell Res*, **312**, 938-948.

Gutierrez-Herrero, S., Fernandez-Infante, C., Hernandez-Cano, L., Ortiz-Rivero, S.,

Guijas, C., Martin-Granado, V., Gonzalez-Porras, J.R., Balsinde, J., Porras, A. & Guerrero, C. (2020) C3G contributes to platelet activation and aggregation by regulating major signaling pathways. *Signal Transduct Target Ther*, **5**, 29.

Gutierrez-Herrero, S., Maia, V., Gutierrez-Berzal, J., Calzada, N., Sanz, M., Gonzalez-Manchon, C., Pericacho, M., Ortiz-Rivero, S., Gonzalez-Porras, J.R., Arechederra, M., Porras, A. & Guerrero, C. (2012) C3G transgenic mouse models with specific expression in platelets reveal a new role for C3G in platelet clotting through its GEF activity. *Biochim Biophys Acta*, **1823**, 1366-1377.

Gutierrez-Uzquiza, A., Arechederra, M., Molina, I., Banos, R., Maia, V., Benito, M., Guerrero, C. & Porras, A. (2010) C3G down-regulates p38 MAPK activity in response to stress by Rap-1 independent mechanisms: involvement in cell death. *Cell Signal*, **22**, 533-542.

Haling, J.R., Monkley, S.J., Critchley, D.R. & Petrich, B.G. (2011) Talin-dependent integrin activation is required for fibrin clot retraction by platelets. *Blood*, **117**, 1719-1722.

Hall, K.J., Harper, M.T., Gilio, K., Cosemans, J.M., Heemskerk, J.W. & Poole, A.W. (2008) Genetic analysis of the role of protein kinase Ctheta in platelet function and thrombus formation. *PLoS One*, **3**, e3277.

Hall, K.J., Jones, M.L. & Poole, A.W. (2007) Coincident regulation of PKCdelta in human platelets by phosphorylation of Tyr311 and Tyr565 and phospholipase C signalling. *Biochem J*, **406**, 501-509.

Hamad, M.A., Krauel, K., Schanze, N., Gauchel, N., Stachon, P., Nuehrenberg, T., Zurek, M. & Duerschmied, D. (2022) Platelet Subtypes in Inflammatory Settings. *Front Cardiovasc Med*, **9**, 823549.

Harper, M.T. & Poole, A.W. (2010) Diverse functions of protein kinase C isoforms in platelet activation and thrombus formation. *J Thromb Haemost*, **8**, 454-462.

Hauser, W., Knobeloch, K.P., Eigenthaler, M., Gambaryan, S., Krenn, V., Geiger, J., Glazova, M., Rohde, E., Horak, I., Walter, U. & Zimmer, M. (1999) Megakaryocyte hyperplasia and enhanced agonist-induced platelet activation in vasodilator-stimulated phosphoprotein knockout mice. *Proc Natl Acad Sci U S A*, **96**, 8120-8125.

Heijnen, H. & van der Sluijs, P. (2015) Platelet secretory behaviour: as diverse as the granules ... or not? *J Thromb Haemost*, **13**, 2141-2151.

Henkel, A.W., Mouihate, A. & Welzel, O. (2019) Differential Release of Exocytosis Marker Dyes Indicates Stimulation-Dependent Regulation of Synaptic Activity. *Front Neurosci*, **13**, 1047.

Hernandez-Cano, L., Fernandez-Infante, C., Herranz, O., Berrocal, P., Lozano, F.S., Sanchez-Martin, M.A., Porras, A. & Guerrero, C. (2022) New functions of C3G in platelet biology: Contribution to ischemia-induced angiogenesis, tumor metastasis and TPO clearance. *Front Cell Dev Biol*, **10**, 1026287.

Hirata, T., Nagai, H., Koizumi, K., Okino, K., Harada, A., Onda, M., Nagahata, T., Mikami, I., Hirai, K., Haraguchi, S., Jin, E., Kawanami, O., Shimizu, K. & Emi, M. (2004) Amplification, up-regulation and over-expression of C3G (CRK SH3 domain-binding guanine nucleotide-

releasing factor) in non-small cell lung cancers. *J Hum Genet*, **49**, 290-295.

Hoffmann, J.J. (2014) Reticulated platelets: analytical aspects and clinical utility. *Clin Chem Lab Med*, **52**, 1107-1117.

Hogan, C., Serpente, N., Cogram, P., Hosking, C.R., Bialucha, C.U., Feller, S.M., Braga, V.M., Birchmeier, W. & Fujita, Y. (2004) Rap1 regulates the formation of E-cadherin-based cell-cell contacts. *Mol Cell Biol*, **24**, 6690-6700.

Hong, W. & Lev, S. (2014) Tethering the assembly of SNARE complexes. *Trends Cell Biol*, **24**, 35-43.

Huang, J., Li, X., Shi, X., Zhu, M., Wang, J., Huang, S., Huang, X., Wang, H., Li, L., Deng, H., Zhou, Y., Mao, J., Long, Z., Ma, Z., Ye, W., Pan, J., Xi, X. & Jin, J. (2019) Platelet integrin alphaIIbbeta3: signal transduction, regulation, and its therapeutic targeting. *J Hematol Oncol*, **12**, 26.

Huang, Y., Joshi, S., Xiang, B., Kanaho, Y., Li, Z., Bouchard, B.A., Moncman, C.L. & Whiteheart, S.W. (2016) Arf6 controls platelet spreading and clot retraction via integrin alphaIIbbeta3 trafficking. *Blood*, **127**, 1459-1467.

Imai, K., Nonoyama, S. & Ochs, H.D. (2003) WASP (Wiskott-Aldrich syndrome protein) gene mutations and phenotype. *Curr Opin Allergy Clin Immunol*, **3**, 427-436.

Inoue, K., Kodama, T. & Daida, H. (2012) Pentraxin 3: a novel biomarker for inflammatory cardiovascular disease. *Int J Vasc Med*, **2012**, 657025.

Inoue, O., Suzuki-Inoue, K., Dean, W.L., Frampton, J. & Watson, S.P. (2003) Integrin alpha2beta1 mediates outside-in regulation of platelet spreading on collagen through activation of Src kinases and PLCgamma2. *J Cell Biol*, **160**, 769-780.

Italiano, J.E., Jr. & Battinelli, E.M. (2009) Selective sorting of alpha-granule proteins. *J Thromb Haemost*, **7 Suppl 1**, 173-176.

Italiano, J.E., Jr., Richardson, J.L., Patel-Hett, S., Battinelli, E., Zaslavsky, A., Short, S., Ryeom, S., Folkman, J. & Klement, G.L. (2008) Angiogenesis is regulated by a novel mechanism: pro- and antiangiogenic proteins are organized into separate platelet alpha granules and differentially released. *Blood*, **111**, 1227-1233.

Ivaska, J. (2012) Unanchoring integrins in focal adhesions. *Nat Cell Biol*, **14**, 981-983.

Jackson, J., Papadopulos, A., Meunier, F.A., McCluskey, A., Robinson, P.J. & Keating, D.J. (2015) Small molecules demonstrate the role of dynamin as a bi-directional regulator of the exocytosis fusion pore and vesicle release. *Mol Psychiatry*, **20**, 810-819.

Jansen, E.E. & Hartmann, M. (2021) Clot Retraction: Cellular Mechanisms and Inhibitors, Measuring Methods, and Clinical Implications. *Biomedicines*, **9**.

Jonnalagadda, D., Izu, L.T. & Whiteheart, S.W. (2012) Platelet secretion is kinetically heterogeneous in an agonist-responsive manner. *Blood*, **120**, 5209-5216.

Joshi, S. & Whiteheart, S.W. (2017) The nuts and bolts of the platelet release reaction. *Platelets*, **28**, 129-137.

Jurk, K. & Kehrel, B.E. (2005) Platelets: physiology and biochemistry. *Semin Thromb Hemost*, **31**, 381-392.

Kamykowski, J., Carlton, P., Sehgal, S. & Storrie, B. (2011) Quantitative immunofluorescence mapping reveals little functional coclustering of proteins within platelet alpha-granules. *Blood*, **118**, 1370-1373.

Kanji, R., Gue, Y.X., Memtsas, V. & Gorog, D.A. (2021) Fibrinolysis in Platelet Thrombi. *Int J Mol Sci*, **22**.

Kaplan, M.J. & Radic, M. (2012) Neutrophil extracellular traps: double-edged swords of innate immunity. *J Immunol*, **189**, 2689-2695.

Kavalali, E.T. & Jorgensen, E.M. (2014) Visualizing presynaptic function. *Nat Neurosci*, **17**, 10-16.

Kholmukhamedov, A. & Jobe, S. (2019) Procoagulant Platelets Get Squeezed to Define the Boundaries of the Hemostatic Plug. *Arterioscler Thromb Vasc Biol*, **39**, 5-6.

Kirsch, K.H., Georgescu, M.M. & Hanafusa, H. (1998) Direct binding of p130(Cas) to the guanine nucleotide exchange factor C3G. *J Biol Chem*, **273**, 25673-25679.

Knudsen, B.S., Feller, S.M. & Hanafusa, H. (1994) Four proline-rich sequences of the guanine-nucleotide exchange factor C3G bind with unique specificity to the first Src homology 3 domain of Crk. *J Biol Chem*, **269**, 32781-32787.

Komiyama, Y., Pedersen, A.H. & Kisiel, W. (1990) Proteolytic activation of human factors IX and X by recombinant human factor VIIa: effects of calcium, phospholipids, and tissue factor. *Biochemistry*, **29**, 9418-9425.

Konopatskaya, O., Gilio, K., Harper, M.T., Zhao, Y., Cosemans, J.M., Karim, Z.A., Whiteheart, S.W., Molkentin, J.D., Verkade, P., Watson, S.P., Heemskerk, J.W. & Poole, A.W. (2009) PKCalpha regulates platelet granule secretion and thrombus formation in mice. *J Clin Invest*, **119**, 399-407.

Koseoglu, S., Peters, C.G., Fitch-Tewfik, J.L., Aisiku, O., Danglot, L., Galli, T. & Flaumenhaft, R. (2015) VAMP-7 links granule exocytosis to actin reorganization during platelet activation. *Blood*, **126**, 651-660.

Koupenova, M., Clancy, L., Corkrey, H.A. & Freedman, J.E. (2018) Circulating Platelets as Mediators of Immunity, Inflammation, and Thrombosis. *Circ Res*, **122**, 337-351.

Krause, M. & Gautreau, A. (2014) Steering cell migration: lamellipodium dynamics and the regulation of directional persistence. *Nat Rev Mol Cell Biol*, **15**, 577-590.

Laviolette, M.J., Nunes, P., Peyre, J.B., Aigaki, T. & Stewart, B.A. (2005) A genetic screen for suppressors of Drosophila NSF2 neuromuscular junction overgrowth. *Genetics*, **170**, 779-792.

Lee, H., Gaughan, J.P. & Tsygankov, A.Y. (2008) c-Cbl facilitates cytoskeletal effects in v-Abl transformed fibroblast through Rac1- and Rap1-mediated

signaling. *Int J Biochem Cell Biol*, **40**, 1930-1943.

Lelliott, P.M., Momota, M., Lee, M.S.J., Kuroda, E., Iijima, N., Ishii, K.J. & Coban, C. (2019) Rapid Quantification of NETs In Vitro and in Whole Blood Samples by Imaging Flow Cytometry. *Cytometry A*, **95**, 565-578.

Li, F., Tiwari, N., Rothman, J.E. & Pincet, F. (2016) Kinetic barriers to SNAREpin assembly in the regulation of membrane docking/priming and fusion. *Proc Natl Acad Sci U S A*, **113**, 10536-10541.

Li, N. (2008) Platelet-lymphocyte cross-talk. *J Leukoc Biol*, **83**, 1069-1078.

Li, Y., Clough, N., Sun, X., Yu, W., Abbott, B.L., Hogan, C.J. & Dai, Z. (2007) Bcr-Abl induces abnormal cytoskeleton remodeling, beta1 integrin clustering and increased cell adhesion to fibronectin through the Abl interactor 1 pathway. *J Cell Sci*, **120**, 1436-1446.

Li, Z., Delaney, M.K., O'Brien, K.A. & Du, X. (2010) Signaling during platelet adhesion and activation. *Arterioscler Thromb Vasc Biol*, **30**, 2341-2349.

Livak, K.J. & Schmittgen, T.D. (2001) Analysis of relative gene expression data using real-time quantitative PCR and the 2(-Delta Delta C(T)) Method. *Methods*, **25**, 402-408.

Lo, S.H. (2006) Focal adhesions: what's new inside. *Dev Biol*, **294**, 280-291.

Lowenstein, C.J. (2017) VAMP-3 mediates platelet endocytosis. *Blood*, **130**, 2816-2818.

Ma, C., Li, W., Xu, Y. & Rizo, J. (2011) Munc13 mediates the transition from the closed syntaxin-Munc18 complex to the SNARE complex. *Nat Struct Mol Biol*, **18**, 542-549.

Ma, Y.Q., Qin, J. & Plow, E.F. (2007) Platelet integrin alpha(IIb)beta(3): activation mechanisms. *J Thromb Haemost*, **5**, 1345-1352.

Maia, V., Ortiz-Rivero, S., Sanz, M., Gutierrez-Berzal, J., Alvarez-Fernandez, I., Gutierrez-Herrero, S., de Pereda, J.M., Porras, A. & Guerrero, C. (2013) C3G forms complexes with Bcr-Abl and p38alpha MAPK at the focal adhesions in chronic myeloid leukemia cells: implication in the regulation of leukemic cell adhesion. *Cell Commun Signal*, **11**, 9.

Maia, V., Sanz, M., Gutierrez-Berzal, J., de Luis, A., Gutierrez-Uzquiza, A., Porras, A. & Guerrero, C. (2009) C3G silencing enhances STI-571-induced apoptosis in CML cells through p38 MAPK activation, but it antagonizes STI-571 inhibitory effect on survival. *Cell Signal*, **21**, 1229-1235.

Manne, B.K., Xiang, S.C. & Rondina, M.T. (2017) Platelet secretion in inflammatory and infectious diseases. *Platelets*, **28**, 155-164.

Mansour, A., Roussel, M., Gaussem, P., Nedelec-Gac, F., Pontis, A., Flecher, E., Bachelot-Loza, C. & Gouin-Thibault, I. (2020) Platelet Functions During Extracorporeal Membrane Oxygenation. Platelet-Leukocyte Aggregates Analyzed by Flow Cytometry as a Promising Tool to Monitor Platelet Activation. *J Clin Med*, **9**.

Manzano, S., Gutierrez-Uzquiza, A., Bragado, P., Cuesta, A.M., Guerrero, C. &

Porras, A. (2021a) C3G Protein, a New Player in Glioblastoma. *Int J Mol Sci*, **22**.

Manzano, S., Gutierrez-Uzquiza, A., Bragado, P., Sequera, C., Herranz, O., Rodrigo-Faus, M., Jauregui, P., Morgner, S., Rubio, I., Guerrero, C. & Porras, A. (2021b) C3G downregulation induces the acquisition of a mesenchymal phenotype that enhances aggressiveness of glioblastoma cells. *Cell Death Dis*, **12**, 348.

Margetic, S. (2012) Inflammation and haemostasis. *Biochem Med (Zagreb)*, **22**, 49-62.

Mark, B.L., Jilkina, O. & Bhullar, R.P. (1996) Association of Ral GTP-binding protein with human platelet dense granules. *Biochem Biophys Res Commun*, **225**, 40-46.

Martegani, E., Vanoni, M., Zippel, R., Coccetti, P., Brambilla, R., Ferrari, C., Sturani, E. & Alberghina, L. (1992) Cloning by functional complementation of a mouse cDNA encoding a homologue of CDC25, a Saccharomyces cerevisiae RAS activator. *EMBO J*, **11**, 2151-2157.

Martin-Encabo, S., Santos, E. & Guerrero, C. (2007) C3G mediated suppression of malignant transformation involves activation of PP2A phosphatases at the subcortical actin cytoskeleton. *Exp Cell Res*, **313**, 3881-3891.

Martin-Fernandez, M.L., Tynan, C.J. & Webb, S.E. (2013) A 'pocket guide' to total internal reflection fluorescence. *J Microsc*, **252**, 16-22.

Martin-Granado, V., Ortiz-Rivero, S., Carmona, R., Gutierrez-Herrero, S., Barrera, M., San-Segundo, L., Sequera, C., Perdiguero, P., Lozano, F., Martin-Herrero, F., Gonzalez-Porras, J.R., Munoz-Chapuli, R., Porras, A. & Guerrero, C. (2017) C3G promotes a selective release of angiogenic factors from activated mouse platelets to regulate angiogenesis and tumor metastasis. *Oncotarget*, **8**, 110994-111011.

Matsuda, M., Tanaka, S., Nagata, S., Kojima, A., Kurata, T. & Shibuya, M. (1992) Two species of human CRK cDNA encode proteins with distinct biological activities. *Mol Cell Biol*, **12**, 3482-3489.

Maurer, M. & von Stebut, E. (2004) Macrophage inflammatory protein-1. *Int J Biochem Cell Biol*, **36**, 1882-1886.

May, A.E., Langer, H., Seizer, P., Bigalke, B., Lindemann, S. & Gawaz, M. (2007) Platelet-leukocyte interactions in inflammation and atherothrombosis. *Semin Thromb Hemost*, **33**, 123-127.

Maynard, D.M., Heijnen, H.F., Horne, M.K., White, J.G. & Gahl, W.A. (2007) Proteomic analysis of platelet alpha-granules using mass spectrometry. *J Thromb Haemost*, **5**, 1945-1955.

McCarty, O.J., Larson, M.K., Auger, J.M., Kalia, N., Atkinson, B.T., Pearce, A.C., Ruf, S., Henderson, R.B., Tybulewicz, V.L., Machesky, L.M. & Watson, S.P. (2005) Rac1 is essential for platelet lamellipodia formation and aggregate stability under flow. *J Biol Chem*, **280**, 39474-39484.

Miki, H., Sasaki, T., Takai, Y. & Takenawa, T. (1998) Induction of filopodium formation by a WASP-related actin-depolymerizing protein N-WASP. *Nature*, **391**, 93-96.

Miller, S.A., Dykes, D.D. & Polesky, H.F. (1988) A simple salting out procedure for

extracting DNA from human nucleated cells. *Nucleic Acids Res*, **16**, 1215.

Mion, D., Bunel, L., Heo, P. & Pincet, F. (2022) The beginning and the end of SNARE-induced membrane fusion. *FEBS Open Bio*, **12**, 1958-1979.

Mitra, S.K., Hanson, D.A. & Schlaepfer, D.D. (2005) Focal adhesion kinase: in command and control of cell motility. *Nat Rev Mol Cell Biol*, **6**, 56-68.

Mitsios, J.V., Prevost, N., Kasirer-Friede, A., Gutierrez, E., Groisman, A., Abrams, C.S., Wang, Y., Litvinov, R.I., Zemljic-Harpf, A., Ross, R.S. & Shattil, S.J. (2010) What is vinculin needed for in platelets? *J Thromb Haemost*, **8**, 2294-2304.

Molinie, N. & Gautreau, A. (2018) The Arp2/3 Regulatory System and Its Deregulation in Cancer. *Physiol Rev*, **98**, 215-238.

Montague, S.J., Lim, Y.J., Lee, W.M. & Gardiner, E.E. (2020) Imaging Platelet Processes and Function-Current and Emerging Approaches for Imaging in vitro and in vivo. *Front Immunol*, **11**, 78.

Mori, J., Wang, Y.J., Ellison, S., Heising, S., Neel, B.G., Tremblay, M.L., Watson, S.P. & Senis, Y.A. (2012) Dominant role of the protein-tyrosine phosphatase CD148 in regulating platelet activation relative to protein-tyrosine phosphatase-1B. *Arterioscler Thromb Vasc Biol*, **32**, 2956-2965.

Morrell, C.N., Aggrey, A.A., Chapman, L.M. & Modjeski, K.L. (2014) Emerging roles for platelets as immune and inflammatory cells. *Blood*, **123**, 2759-2767.

Murugappan, S., Shankar, H., Bhamidipati, S., Dorsam, R.T., Jin, J. & Kunapuli, S.P. (2005) Molecular mechanism and functional implications of thrombin-mediated tyrosine phosphorylation of PKCdelta in platelets. *Blood*, **106**, 550-557.

Nagy, B., Jr., Bhavaraju, K., Getz, T., Bynagari, Y.S., Kim, S. & Kunapuli, S.P. (2009) Impaired activation of platelets lacking protein kinase C-theta isoform. *Blood*, **113**, 2557-2567.

Nakamura, L., Bertling, A., Brodde, M.F., Zur Stadt, U., Schulz, A.S., Ammann, S., Sandrock-Lang, K., Beutel, K., Zieger, B. & Kehrel, B.E. (2015) First characterization of platelet secretion defect in patients with familial hemophagocytic lymphohistiocytosis type 3 (FHL-3). *Blood*, **125**, 412-414.

Nechipurenko, D.Y., Receveur, N., Yakimenko, A.O., Shepelyuk, T.O., Yakusheva, A.A., Kerimov, R.R., Obydennyy, S.I., Eckly, A., Leon, C., Gachet, C., Grishchuk, E.L., Ataullakhanov, F.I., Mangin, P.H. & Panteleev, M.A. (2019) Clot Contraction Drives the Translocation of Procoagulant Platelets to Thrombus Surface. *Arterioscler Thromb Vasc Biol*, **39**, 37-47.

Nguyen, H.T.T., Xu, Z., Shi, X., Liu, S., Schulte, M.L., White, G.C. & Ma, Y.Q. (2021) Paxillin binding to the PH domain of kindlin-3 in platelets is required to support integrin alphaIIbbeta3 outside-in signaling. *J Thromb Haemost*, **19**, 3126-3138.

Nishibori, M., Cham, B., McNicol, A., Shalev, A., Jain, N. & Gerrard, J.M. (1993) The protein CD63 is in platelet dense granules, is deficient in a patient with Hermansky-Pudlak syndrome, and appears identical to granulophysin. *J Clin Invest*, **91**, 1775-1782.

Nishida-Fukuda, H. (2019) The Exocyst: Dynamic Machine or Static Tethering Complex? *Bioessays*, **41**, e1900056.

Nishizuka, Y. (1986) Perspectives on the role of protein kinase C in stimulus-response coupling. *J Natl Cancer Inst*, **76**, 363-370.

Nishizuka, Y. (1988) The molecular heterogeneity of protein kinase C and its implications for cellular regulation. *Nature*, **334**, 661-665.

Noguchi, H., Ikegami, T., Nagadoi, A., Kamatari, Y.O., Park, S.Y., Tame, J.R. & Unzai, S. (2015) The structure and conformational switching of Rap1B. *Biochem Biophys Res Commun*, **462**, 46-51.

Nurden, A.T. (2022) Molecular basis of clot retraction and its role in wound healing. *Thromb Res*.

Oda, A., Miki, H., Wada, I., Yamaguchi, H., Yamazaki, D., Suetsugu, S., Nakajima, M., Nakayama, A., Okawa, K., Miyazaki, H., Matsuno, K., Ochs, H.D., Machesky, L.M., Fujita, H. & Takenawa, T. (2005) WAVE/Scars in platelets. *Blood*, **105**, 3141-3148.

Offermanns, S. (2000) The role of heterotrimeric G proteins in platelet activation. *Biol Chem*, **381**, 389-396.

Offermanns, S., Toombs, C.F., Hu, Y.H. & Simon, M.I. (1997) Defective platelet activation in G alpha(q)-deficient mice. *Nature*, **389**, 183-186.

Ohba, Y., Ikuta, K., Ogura, A., Matsuda, J., Mochizuki, N., Nagashima, K., Kurokawa, K., Mayer, B.J., Maki, K., Miyazaki, J. & Matsuda, M. (2001) Requirement for C3G-dependent Rap1 activation for cell adhesion and embryogenesis. *EMBO J*, **20**, 3333-3341.

Ohba, Y., Mochizuki, N., Yamashita, S., Chan, A.M., Schrader, J.W., Hattori, S., Nagashima, K. & Matsuda, M. (2000) Regulatory proteins of R-Ras, TC21/R-Ras2, and M-Ras/R-Ras3. *J Biol Chem*, **275**, 20020-20026.

Okino, K., Nagai, H., Nakayama, H., Doi, D., Yoneyama, K., Konishi, H. & Takeshita, T. (2006) Inactivation of Crk SH3 domain-binding guanine nucleotide-releasing factor (C3G) in cervical squamous cell carcinoma. *Int J Gynecol Cancer*, **16**, 763-771.

Ortiz-Rivero, S., Baquero, C., Hernandez-Cano, L., Roldan-Etcheverry, J.J., Gutierrez-Herrero, S., Fernandez-Infante, C., Martin-Granado, V., Anguita, E., de Pereda, J.M., Porras, A. & Guerrero, C. (2018) C3G, through its GEF activity, induces megakaryocytic differentiation and proplatelet formation. *Cell Commun Signal*, **16**, 101.

Paul, D.S., Casari, C., Wu, C., Piatt, R., Pasala, S., Campbell, R.A., Poe, K.O., Ghalloussi, D., Lee, R.H., Rotty, J.D., Cooley, B.C., Machlus, K.R., Italiano, J.E., Jr., Weyrich, A.S., Bear, J.E. & Bergmeier, W. (2017) Deletion of the Arp2/3 complex in megakaryocytes leads to microthrombocytopenia in mice. *Blood Adv*, **1**, 1398-1408.

Pearce, A.C., Senis, Y.A., Billadeau, D.D., Turner, M., Watson, S.P. & Vigorito, E. (2004) Vav1 and vav3 have critical but redundant roles in mediating platelet activation by collagen. *J Biol Chem*, **279**, 53955-53962.

Pearce, A.C., Wilde, J.I., Doody, G.M., Best, D., Inoue, O., Vigorito, E., Tybulewicz, V.L., Turner, M. & Watson, S.P. (2002) Vav1, but not Vav2, contributes to platelet aggregation by CRP and thrombin, but neither is required for regulation of phospholipase C. *Blood*, **100**, 3561-3569.

Pears, C.J., Thornber, K., Auger, J.M., Hughes, C.E., Grygielska, B., Protty, M.B., Pearce, A.C. & Watson, S.P. (2008) Differential roles of the PKC novel isoforms, PKCdelta and PKCepsilon, in mouse and human platelets. *PLoS One*, **3**, e3793.

Peters, C.G., Michelson, A.D. & Flaumenhaft, R. (2012) Granule exocytosis is required for platelet spreading: differential sorting of alpha-granules expressing VAMP-7. *Blood*, **120**, 199-206.

Petrey, A.C., Obery, D.R., Kessler, S.P., Zawerton, A., Flamion, B. & de la Motte, C.A. (2019) Platelet hyaluronidase-2 regulates the early stages of inflammatory disease in colitis. *Blood*, **134**, 765-775.

Pike, J.A., Simms, V.A., Smith, C.W., Morgan, N.V., Khan, A.O., Poulter, N.S., Styles, I.B. & Thomas, S.G. (2021) An adaptable analysis workflow for characterization of platelet spreading and morphology. *Platelets*, **32**, 54-58.

Pleines, I., Eckly, A., Elvers, M., Hagedorn, I., Eliautou, S., Bender, M., Wu, X., Lanza, F., Gachet, C., Brakebusch, C. & Nieswandt, B. (2010) Multiple alterations of platelet functions dominated by increased secretion in mice lacking Cdc42 in platelets. *Blood*, **115**, 3364-3373.

Pleines, I., Elvers, M., Strehl, A., Pozgajova, M., Varga-Szabo, D., May, F., Chrostek-Grashoff, A., Brakebusch, C. & Nieswandt, B. (2009) Rac1 is essential for phospholipase C-gamma2 activation in platelets. *Pflugers Arch*, **457**, 1173-1185.

Pleines, I., Hagedorn, I., Gupta, S., May, F., Chakarova, L., van Hengel, J., Offermanns, S., Krohne, G., Kleinschnitz, C., Brakebusch, C. & Nieswandt, B. (2012) Megakaryocyte-specific RhoA deficiency causes macrothrombocytopenia and defective platelet activation in hemostasis and thrombosis. *Blood*, **119**, 1054-1063.

Pollard, T.D. (2016) Actin and Actin-Binding Proteins. *Cold Spring Harb Perspect Biol*, **8**.

Popovic, M., Rensen-de Leeuw, M. & Rehmann, H. (2013) Selectivity of CDC25 homology domain-containing guanine nucleotide exchange factors. *J Mol Biol*, **425**, 2782-2794.

Pradhan, S., Khatlani, T., Nairn, A.C. & Vijayan, K.V. (2017) The heterotrimeric G protein Gbeta(1) interacts with the catalytic subunit of protein phosphatase 1 and modulates G protein-coupled receptor signaling in platelets. *J Biol Chem*, **292**, 13133-13142.

Priego, N., Arechederra, M., Sequera, C., Bragado, P., Vazquez-Carballo, A., Gutierrez-Uzquiza, A., Martin-Granado, V., Ventura, J.J., Kazanietz, M.G., Guerrero, C. & Porras, A. (2016) C3G knock-down enhances migration and invasion by increasing Rap1-mediated p38alpha activation, while it impairs tumor growth through p38alpha-independent mechanisms. *Oncotarget*, **7**, 45060-45078.

Pryzdial, E.L.G., Lee, F.M.H., Lin, B.H., Carter, R.L.R., Tegegn, T.Z. & Belletrutti, M.J.

(2018) Blood coagulation dissected. *Transfus Apher Sci*, **57**, 449-457.

Pula, G., Schuh, K., Nakayama, K., Nakayama, K.I., Walter, U. & Poole, A.W. (2006) PKCdelta regulates collagen-induced platelet aggregation through inhibition of VASP-mediated filopodia formation. *Blood*, **108**, 4035-4044.

Radha, V., Mitra, A., Dayma, K. & Sasikumar, K. (2011) Signalling to actin: role of C3G, a multitasking guanine-nucleotide-exchange factor. *Biosci Rep*, **31**, 231-244.

Radha, V., Rajanna, A., Gupta, R.K., Dayma, K. & Raman, T. (2008) The guanine nucleotide exchange factor, C3G regulates differentiation and survival of human neuroblastoma cells. *J Neurochem*, **107**, 1424-1435.

Radha, V., Rajanna, A., Mitra, A., Rangaraj, N. & Swarup, G. (2007) C3G is required for c-Abl-induced filopodia and its overexpression promotes filopodia formation. *Exp Cell Res*, **313**, 2476-2492.

Radha, V., Rajanna, A. & Swarup, G. (2004) Phosphorylated guanine nucleotide exchange factor C3G, induced by pervanadate and Src family kinases localizes to the Golgi and subcortical actin cytoskeleton. *BMC Cell Biol*, **5**, 31.

Reed, G.L. (2004) Platelet secretory mechanisms. *Semin Thromb Hemost*, **30**, 441-450.

Rendu, F. & Brohard-Bohn, B. (2001) The platelet release reaction: granules' constituents, secretion and functions. *Platelets*, **12**, 261-273.

Repsold, L. & Joubert, A.M. (2021) Platelet Function, Role in Thrombosis, Inflammation, and Consequences in Chronic Myeloproliferative Disorders. *Cells*, **10**.

Rodrigues, M., Kosaric, N., Bonham, C.A. & Gurtner, G.C. (2019) Wound Healing: A Cellular Perspective. *Physiol Rev*, **99**, 665-706.

Rodriguez-Blazquez, A., Carabias, A., Moran-Vaquero, A., de Cima, S., Luque-Ortega, J.R., Alfonso, C., Schuck, P., Manso, J.A., Macedo-Ribeiro, S., Guerrero, C. & de Pereda, J.M. (2023) Crk proteins activate the Rap1 guanine nucleotide exchange factor C3G by segregated adaptor-dependent and -independent mechanisms. *Cell Commun Signal*, **21**, 30.

Romer, L.H., Birukov, K.G. & Garcia, J.G. (2006) Focal adhesions: paradigm for a signaling nexus. *Circ Res*, **98**, 606-616.

Rossi, G., Lepore, D., Kenner, L., Czuchra, A.B., Plooster, M., Frost, A., Munson, M. & Brennwald, P. (2020) Exocyst structural changes associated with activation of tethering downstream of Rho/Cdc42 GTPases. *J Cell Biol*, **219**.

Rottner, K., Behrendt, B., Small, J.V. & Wehland, J. (1999) VASP dynamics during lamellipodia protrusion. *Nat Cell Biol*, **1**, 321-322.

Rotty, J.D., Wu, C. & Bear, J.E. (2013) New insights into the regulation and cellular functions of the ARP2/3 complex. *Nat Rev Mol Cell Biol*, **14**, 7-12.

Rowley, J.W., Oler, A.J., Tolley, N.D., Hunter, B.N., Low, E.N., Nix, D.A., Yost, C.C., Zimmerman, G.A. & Weyrich, A.S. (2011) Genome-wide RNA-seq analysis of

human and mouse platelet transcriptomes. *Blood*, **118**, e101-111.

Samson, A.L., Alwis, I., Maclean, J.A.A., Priyananda, P., Hawkett, B., Schoenwaelder, S.M. & Jackson, S.P. (2017) Endogenous fibrinolysis facilitates clot retraction in vivo. *Blood*, **130**, 2453-2462.

Samuelsson, J., Alonso, S., Ruiz-Larroya, T., Cheung, T.H., Wong, Y.F. & Perucho, M. (2011) Frequent somatic demethylation of RAPGEF1/C3G intronic sequences in gastrointestinal and gynecological cancer. *Int J Oncol*, **38**, 1575-1577.

Sanjay, A., Houghton, A., Neff, L., DiDomenico, E., Bardelay, C., Antoine, E., Levy, J., Gailit, J., Bowtell, D., Horne, W.C. & Baron, R. (2001) Cbl associates with Pyk2 and Src to regulate Src kinase activity, alpha(v)beta(3) integrin-mediated signaling, cell adhesion, and osteoclast motility. *J Cell Biol*, **152**, 181-195.

Sasi Kumar, K., Ramadhas, A., Nayak, S.C., Kaniyappan, S., Dayma, K. & Radha, V. (2015) C3G (RapGEF1), a regulator of actin dynamics promotes survival and myogenic differentiation of mouse mesenchymal cells. *Biochim Biophys Acta*, **1853**, 2629-2639.

Savage, J.S., Williams, C.M., Konopatskaya, O., Hers, I., Harper, M.T. & Poole, A.W. (2013) Munc13-4 is critical for thrombosis through regulating release of ADP from platelets. *J Thromb Haemost*, **11**, 771-775.

Scaife, R.M. & Langdon, W.Y. (2000) c-Cbl localizes to actin lamellae and regulates lamellipodia formation and cell morphology. *J Cell Sci*, **113 Pt 2**, 215-226.

Schafer, I.B., Hesketh, G.G., Bright, N.A., Gray, S.R., Pryor, P.R., Evans, P.R., Luzio, J.P. & Owen, D.J. (2012) The binding of Varp to VAMP7 traps VAMP7 in a closed, fusogenically inactive conformation. *Nat Struct Mol Biol*, **19**, 1300-1309.

Schindelin, J., Arganda-Carreras, I., Frise, E., Kaynig, V., Longair, M., Pietzsch, T., Preibisch, S., Rueden, C., Saalfeld, S., Schmid, B., Tinevez, J.Y., White, D.J., Hartenstein, V., Eliceiri, K., Tomancak, P. & Cardona, A. (2012) Fiji: an open-source platform for biological-image analysis. *Nat Methods*, **9**, 676-682.

Schonherr, C., Yang, H.L., Vigny, M., Palmer, R.H. & Hallberg, B. (2010) Anaplastic lymphoma kinase activates the small GTPase Rap1 via the Rap1-specific GEF C3G in both neuroblastoma and PC12 cells. *Oncogene*, **29**, 2817-2830.

Schultess, J., Danielewski, O. & Smolenski, A.P. (2005) Rap1GAP2 is a new GTPase-activating protein of Rap1 expressed in human platelets. *Blood*, **105**, 3185-3192.

Schurmans, S., Polizzi, S., Scoumanne, A., Sayyed, S. & Molina-Ortiz, P. (2015) The Ras/Rap GTPase activating protein RASA3: from gene structure to in vivo functions. *Adv Biol Regul*, **57**, 153-161.

Schurr, Y., Sperr, A., Volz, J., Beck, S., Reil, L., Kusch, C., Eiring, P., Bryson, S., Sauer, M., Nieswandt, B., Machesky, L. & Bender, M. (2019) Platelet lamellipodium formation is not required for thrombus formation and stability. *Blood*, **134**, 2318-2329.

Schwer, H.D., Lecine, P., Tiwari, S., Italiano, J.E., Jr., Hartwig, J.H. & Shivdasani, R.A. (2001) A lineage-restricted and divergent beta-tubulin isoform is essential for the biogenesis, structure and function of blood platelets. *Curr Biol*, **11**, 579-586.

Sehgal, S. & Storrie, B. (2007) Evidence that differential packaging of the major platelet granule proteins von Willebrand factor and fibrinogen can support their differential release. *J Thromb Haemost*, **5**, 2009-2016.

Selvadurai, M.V. & Hamilton, J.R. (2018) Structure and function of the open canalicular system - the platelet's specialized internal membrane network. *Platelets*, **29**, 319-325.

Senis, Y.A., Mazharian, A. & Mori, J. (2014) Src family kinases: at the forefront of platelet activation. *Blood*, **124**, 2013-2024.

Sequera, C., Bragado, P., Manzano, S., Arechederra, M., Richelme, S., Gutierrez-Uzquiza, A., Sanchez, A., Maina, F., Guerrero, C. & Porras, A. (2020) C3G Is Upregulated in Hepatocarcinoma, Contributing to Tumor Growth and Progression and to HGF/MET Pathway Activation. *Cancers (Basel)*, **12**.

Shah, B., Lutter, D., Bochenek, M.L., Kato, K., Tsytsyura, Y., Glyvuk, N., Sakakibara, A., Klingauf, J., Adams, R.H. & Puschel, A.W. (2016) C3G/Rapgef1 Is Required in Multipolar Neurons for the Transition to a Bipolar Morphology during Cortical Development. *PLoS One*, **11**, e0154174.

Sharma, S. & Lindau, M. (2018) Molecular mechanism of fusion pore formation driven by the neuronal SNARE complex. *Proc Natl Acad Sci U S A*, **115**, 12751-12756.

Shattil, S.J., Kashiwagi, H. & Pampori, N. (1998) Integrin signaling: the platelet paradigm. *Blood*, **91**, 2645-2657.

Shcherbina, A., Cooley, J., Lutskiy, M.I., Benarafa, C., Gilbert, G.E. & Remold-O'Donnell, E. (2010) WASP plays a novel role in regulating platelet responses dependent on alphaIIbbeta3 integrin outside-in signalling. *Br J Haematol*, **148**, 416-427.

Shirakawa, R., Yoshioka, A., Horiuchi, H., Nishioka, H., Tabuchi, A. & Kita, T. (2000) Small GTPase Rab4 regulates Ca2+-induced alpha-granule secretion in platelets. *J Biol Chem*, **275**, 33844-33849.

Shivakrupa, R., Radha, V., Sudhakar, C. & Swarup, G. (2003) Physical and functional interaction between Hck tyrosine kinase and guanine nucleotide exchange factor C3G results in apoptosis, which is independent of C3G catalytic domain. *J Biol Chem*, **278**, 52188-52194.

Shoji, K., Ohashi, K., Sampei, K., Oikawa, M. & Mizuno, K. (2012) Cytochalasin D acts as an inhibitor of the actin-cofilin interaction. *Biochem Biophys Res Commun*, **424**, 52-57.

Smolenski, A. (2012) Novel roles of cAMP/cGMP-dependent signaling in platelets. *J Thromb Haemost*, **10**, 167-176.

Sorrentino, S., Studt, J.D., Medalia, O. & Tanuj Sapra, K. (2015) Roll, adhere, spread and contract: structural mechanics of platelet function. *Eur J Cell Biol*, **94**, 129-138.

Stark, K. (2019) Platelet-neutrophil crosstalk and netosis. *Hemasphere*, **3**.

Stefanini, L. & Bergmeier, W. (2010) CalDAG-GEFI and platelet activation. *Platelets*, **21**, 239-243.

Stefanini, L. & Bergmeier, W. (2016) RAP1-GTPase signaling and platelet function. *J Mol Med (Berl)*, **94**, 13-19.

Stefanini, L., Boulaftali, Y., Ouellette, T.D., Holinstat, M., Desire, L., Leblond, B., Andre, P., Conley, P.B. & Bergmeier, W. (2012) Rap1-Rac1 circuits potentiate platelet activation. *Arterioscler Thromb Vasc Biol*, **32**, 434-441.

Stefanini, L., Lee, R.H., Paul, D.S., O'Shaughnessy, E.C., Ghalloussi, D., Jones, C.I., Boulaftali, Y., Poe, K.O., Piatt, R., Kechele, D.O., Caron, K.M., Hahn, K.M., Gibbins, J.M. & Bergmeier, W. (2018) Functional redundancy between RAP1 isoforms in murine platelet production and function. *Blood*, **132**, 1951-1962.

Stefanini, L., Paul, D.S., Robledo, R.F., Chan, E.R., Getz, T.M., Campbell, R.A., Kechele, D.O., Casari, C., Piatt, R., Caron, K.M., Mackman, N., Weyrich, A.S., Parrott, M.C., Boulaftali, Y., Adams, M.D., Peters, L.L. & Bergmeier, W. (2015) RASA3 is a critical inhibitor of RAP1-dependent platelet activation. *J Clin Invest*, **125**, 1419-1432.

Stefanini, L., Roden, R.C. & Bergmeier, W. (2009) CalDAG-GEFI is at the nexus of calcium-dependent platelet activation. *Blood*, **114**, 2506-2514.

Stocker, T.J., Pircher, J., Skenderi, A., Ehrlich, A., Eberle, C., Megens, R.T.A., Petzold, T., Zhang, Z., Walzog, B., Muller-Taubenberger, A., Weber, C., Massberg, S., Ishikawa-Ankerhold, H. & Schulz, C. (2018) The Actin Regulator Coronin-1A Modulates Platelet Shape Change and Consolidates Arterial Thrombosis. *Thromb Haemost*, **118**, 2098-2111.

Stork, P.J. & Dillon, T.J. (2005) Multiple roles of Rap1 in hematopoietic cells: complementary versus antagonistic functions. *Blood*, **106**, 2952-2961.

Stoter, M., Niederlein, A., Barsacchi, R., Meyenhofer, F., Brandl, H. & Bickle, M. (2013) CellProfiler and KNIME: open source tools for high content screening. *Methods Mol Biol*, **986**, 105-122.

Strehl, A., Munnix, I.C., Kuijpers, M.J., van der Meijden, P.E., Cosemans, J.M., Feijge, M.A., Nieswandt, B. & Heemskerk, J.W. (2007) Dual role of platelet protein kinase C in thrombus formation: stimulation of pro-aggregatory and suppression of procoagulant activity in platelets. *J Biol Chem*, **282**, 7046-7055.

Sudhof, T.C. & Rothman, J.E. (2009) Membrane fusion: grappling with SNARE and SM proteins. *Science*, **323**, 474-477.

Suzuki-Inoue, K., Inoue, O., Frampton, J. & Watson, S.P. (2003) Murine GPVI stimulates weak integrin activation in PLCgamma2-/- platelets: involvement of PLCgamma1 and PI3-kinase. *Blood*, **102**, 1367-1373.

Tapial Martinez, P., Lopez Navajas, P. & Lietha, D. (2020) FAK Structure and Regulation by Membrane Interactions and Force in Focal Adhesions. *Biomolecules*, **10**.

Tartoff, K.D. & Hobbs, C.A. (1987) Improved Media for Growing Plasmid and Cosmid Clones. *Bethesda Research Laboratories Focus*, **9**, 12.

Thomas, M.R. & Storey, R.F. (2015) The role of platelets in inflammation. *Thromb Haemost*, **114**, 449-458.

Thon, J.N. & Italiano, J.E. (2010) Platelet formation. *Semin Hematol*, **47**, 220-226.

Thon, J.N. & Italiano, J.E. (2012) Platelets: production, morphology and ultrastructure. *Handb Exp Pharmacol*, 3-22.

Tiedt, R., Schomber, T., Hao-Shen, H. & Skoda, R.C. (2007) Pf4-Cre transgenic mice allow the generation of lineage-restricted gene knockouts for studying megakaryocyte and platelet function in vivo. *Blood*, **109**, 1503-1506.

Tolmachova, T., Abrink, M., Futter, C.E., Authi, K.S. & Seabra, M.C. (2007) Rab27b regulates number and secretion of platelet dense granules. *Proc Natl Acad Sci U S A*, **104**, 5872-5877.

Tsuboi, S., Nonoyama, S. & Ochs, H.D. (2006) Wiskott-Aldrich syndrome protein is involved in alphaIIb beta3-mediated cell adhesion. *EMBO Rep*, **7**, 506-511.

Uemura, N. & Griffin, J.D. (1999) The adapter protein Crkl links Cbl to C3G after integrin ligation and enhances cell migration. *J Biol Chem*, **274**, 37525-37532.

Van der Meijden, P.E.J. & Heemskerk, J.W.M. (2019) Platelet biology and functions: new concepts and clinical perspectives. *Nat Rev Cardiol*, **16**, 166-179.

van Holten, T.C., Bleijerveld, O.B., Wijten, P., de Groot, P.G., Heck, A.J., Barendrecht, A.D., Merkx, T.H., Scholten, A. & Roest, M. (2014) Quantitative proteomics analysis reveals similar release profiles following specific PAR-1 or PAR-4 stimulation of platelets. *Cardiovasc Res*, **103**, 140-146.

Veltman, D.M., King, J.S., Machesky, L.M. & Insall, R.H. (2012) SCAR knockouts in Dictyostelium: WASP assumes SCAR's position and upstream regulators in pseudopods. *J Cell Biol*, **198**, 501-508.

Vishnu, V.V., Muralikrishna, B., Verma, A., Nayak, S.C., Sowpati, D.T., Radha, V. & Shekar, P.C. (2021) C3G Regulates STAT3, ERK, Adhesion Signaling, and Is Essential for Differentiation of Embryonic Stem Cells. *Stem Cell Rev Rep*, **17**, 1465-1477.

Voss, A.K., Gruss, P. & Thomas, T. (2003) The guanine nucleotide exchange factor C3G is necessary for the formation of focal adhesions and vascular maturation. *Development*, **130**, 355-367.

Voss, A.K., Krebs, D.L. & Thomas, T. (2006) C3G regulates the size of the cerebral cortex neural precursor population. *EMBO J*, **25**, 3652-3663.

Vowinkel, T., Wood, K.C., Stokes, K.Y., Russell, J., Tailor, A., Anthoni, C., Senninger, N., Krieglstein, C.F. & Granger, D.N. (2007) Mechanisms of platelet and leukocyte recruitment in experimental colitis. *Am J Physiol Gastrointest Liver Physiol*, **293**, G1054-1060.

Walsh, T.G., Li, Y., Wersall, A. & Poole, A.W. (2019) Small GTPases in platelet membrane trafficking. *Platelets*, **30**, 31-40.

Walsh, T.G., Li, Y., Williams, C.M., Aitken, E.W., Andrews, R.K. & Poole, A.W. (2021) Loss of the exocyst complex component EXOC3 promotes hemostasis and accelerates arterial thrombosis. *Blood Adv*, **5**, 674-686.

Wang, C.T., Lu, J.C., Bai, J., Chang, P.Y., Martin, T.F., Chapman, E.R. & Jackson, M.B. (2003) Different domains of

synaptotagmin control the choice between kiss-and-run and full fusion. *Nature*, **424**, 943-947.

Watson, S.P., Auger, J.M., McCarty, O.J. & Pearce, A.C. (2005) GPVI and integrin alphaIIb beta3 signaling in platelets. *J Thromb Haemost*, **3**, 1752-1762.

Wentworth, J.K., Pula, G. & Poole, A.W. (2006) Vasodilator-stimulated phosphoprotein (VASP) is phosphorylated on Ser157 by protein kinase C-dependent and -independent mechanisms in thrombin-stimulated human platelets. *Biochem J*, **393**, 555-564.

Wersall, A., Williams, C.M., Brown, E., Iannitti, T., Williams, N. & Poole, A.W. (2018) Mouse Platelet Ral GTPases Control P-Selectin Surface Expression, Regulating Platelet-Leukocyte Interaction. *Arterioscler Thromb Vasc Biol*, **38**, 787-800.

White, J.G. & Escolar, G. (1991) The blood platelet open canalicular system: a two-way street. *Eur J Cell Biol*, **56**, 233-242.

Whiteheart, S.W. (2011) Platelet granules: surprise packages. *Blood*, **118**, 1190-1191.

Williams, C.M., Li, Y., Brown, E. & Poole, A.W. (2018) Platelet-specific deletion of SNAP23 ablates granule secretion, substantially inhibiting arterial and venous thrombosis in mice. *Blood Adv*, **2**, 3627-3636.

Woo, T.H., Patel, B.K., Cinco, M., Smythe, L.D., Symonds, M.L., Norris, M.A. & Dohnt, M.F. (1998) Real-time homogeneous assay of rapid cycle polymerase chain reaction product for identification of Leptonema illini. *Anal Biochem*, **259**, 112-117.

Woronowicz, K., Dilks, J.R., Rozenvayn, N., Dowal, L., Blair, P.S., Peters, C.G., Woronowicz, L. & Flaumenhaft, R. (2010) The platelet actin cytoskeleton associates with SNAREs and participates in alpha-granule secretion. *Biochemistry*, **49**, 4533-4542.

Woulfe, D.S. (2005) Platelet G protein-coupled receptors in hemostasis and thrombosis. *J Thromb Haemost*, **3**, 2193-2200.

Wu, L.G., Hamid, E., Shin, W. & Chiang, H.C. (2014) Exocytosis and endocytosis: modes, functions, and coupling mechanisms. *Annu Rev Physiol*, **76**, 301-331.

Wu, Z., Bello, O.D., Thiyagarajan, S., Auclair, S.M., Vennekate, W., Krishnakumar, S.S., O'Shaughnessy, B. & Karatekin, E. (2017) Dilation of fusion pores by crowding of SNARE proteins. *Elife*, **6**.

Yamamoto-Furusho, J.K. & Mendieta-Escalante, E.A. (2020) Diagnostic utility of the neutrophil-platelet ratio as a novel marker of activity in patients with Ulcerative Colitis. *PLoS One*, **15**, e0231988.

Ye, S., Karim, Z.A., Al Hawas, R., Pessin, J.E., Filipovich, A.H. & Whiteheart, S.W. (2012) Syntaxin-11, but not syntaxin-2 or syntaxin-4, is required for platelet secretion. *Blood*, **120**, 2484-2492.

Zhang, G., Xiang, B., Ye, S., Chrzanowska-Wodnicka, M., Morris, A.J., Gartner, T.K., Whiteheart, S.W., White, G.C., 2nd, Smyth, S.S. & Li, Z. (2011) Distinct roles for Rap1b protein in platelet secretion

and integrin alphaIIbbeta3 outside-in signaling. *J Biol Chem*, **286**, 39466-39477.

zur Stadt, U., Rohr, J., Seifert, W., Koch, F., Grieve, S., Pagel, J., Strauss, J., Kasper, B., Nurnberg, G., Becker, C., Maul-Pavicic, A., Beutel, K., Janka, G., Griffiths, G., Ehl, S. & Hennies, H.C. (2009) Familial hemophagocytic lymphohistiocytosis type 5 (FHL-5) is caused by mutations in Munc18-2 and impaired binding to syntaxin 11. *Am J Hum Genet*, **85**, 482-492.

# ANNEXES

**Spreading C3G-wt**

https://drive.google.com/file/d/10TZ28Aluk3zHrQD58gjjciy2vDhhD4Qy/view?usp=share_link

**Spreading C3G-KO**

https://drive.google.com/file/d/1UI9NDneNQRupRjA_j7R7igH5Rfm42ho-/view?usp=share_link

**Video 1. C3G ablation delays platelet spreading.** Videos showing the spreading of C3G-wt and C3G-KO platelets on Ibi-Treat plates. The sequential formation of filopodia and lamellipodia can be distinguished in C3G-wt platelets. C3G-KO platelets only show filopodia formation for the duration of the video. The videos summarize ~9 min of spreading. See **Figure R-13** for details.

**GFP**

https://drive.google.com/file/d/1IKPSjhn-cGkDk8cVTkRQNSF_gpfdC8xl/view?usp=share_link

**C3G-wt**

https://drive.google.com/file/d/1u1-5NrkOGqo8JzyGgyCcB7hZpEU1P52v/view?usp=share_link

**C3G-Y554H**

https://drive.google.com/file/d/1xVrWUAX81JgG0eFhVwJGFA3AHWvJSRVE/view?usp=share_link

**shCT**

https://drive.google.com/file/d/1BNWVN_FSY4owBRn0gtd9ag4i3x2Pw05j/view?usp=share_link

**shC3G**

https://drive.google.com/file/d/17tqj2QBiMZxVnSdjlZXp2bdmBL3LiW6N/view?usp=share_link

**Video 2. Effect of C3G hyperactivation or silencing on the kinetics of tdOrange-NPY release in PC12 cells.** Videos showing the release of tdOrange-NPY vesicles from PC12 cells expressing GFP, C3G-wt, C3G-Y554H, shCT and shC3G, after stimulation with KCl. The release of tdOrange-NPY is visualized by an increase in the fluorescence signal. The videos are slow down to show the process of exocytosis that occurs in 12 seconds. See **Figure R-57** for details.